Title
Linear and Non-Linear Programming Techniques for System Identification and Green Engineering Applications

Author
Conner, Jeremy Alexander

Publication Date
2019

Peer reviewed|Thesis/dissertation

UNIVERSITY OF CALIFORNIA

Los Angeles

Linear and Non-Linear Programming Techniques for System Identification and Green Engineering Applications

A dissertation submitted in partial satisfaction of the requirements for the degree Doctor of Philosophy in Chemical Engineering

by

Jeremy Alexander Conner

2019

ABSTRACT OF THE DISSERTATION

Linear and Non-Linear Programming Techniques

for System Identification and

Green Engineering Applications

by

Jeremy Alexander Conner

Doctor of Philosophy in Chemical Engineering

University of California, Los Angeles, 2019

Professor Vasilios Manousiouthakis, Chair

This work focuses on linear and non-linear programming techniques for feasibility assessment, synthesis, and optimization of process networks. Analytical techniques, dimensionality reduction, convexification strategies, and functional analysis are developed to identify global optima and to enhance the efficiency of their computation. Green engineering, especially the hydrogen economy, is the primary motivation of this work. To this end, these strategies are implemented in identification of the attainable region for separator networks, optimization of compressors and coolers in series delivering hydrogen at high pressure, and minimum utility cost of an energetically-enhanced steam methane reforming process in the presence of carbon tax legislation.

Pursuant to feasibility assessment of systems with respect to delivery of pure compounds, the applicability of the Infinite DimEnsionAl State-space (IDEAS) framework is extended to attainable region (AR) identification for separator networks. The AR for a water/methanol/acetone mixture involving one network feed stream with known species molar fractions and three network outlet streams at 1 atm pressure. The binary methanol/acetone system exhibits a minimum-boiling azeotrope at 79.07% mole fraction of acetone at 328.5 K. The IDEAS-generated AR successfully identified that the binary methanol/acetone azeotrope was inside the AR, and thus demonstrated there exists a separator network that can bypass the azeotrope.

In the exploration of hydrogen as an alternative energy source, the minimum operating cost and minimum capital cost problems for a system of compressors and coolers in series that bring a gas with constant compressibility factor from a specified initial state (T0, P0) to a specified final state (T0, Pn). Through mathematical proof, the dimensionality of the optimization problems is reduced and analytical properties of the compressor outlet temperatures, when either operating costs or capital costs dominate, are established. A case study involving hydrogen compression was done to illustrate the methods, and shows the global optimum achieves cost savings of up to 13% from conventional designs.

Lastly, a novel method for solution of linear parametric programming problems is proposed based on the concept of dimensionality reduction – this allows the analytic quantification of the optimum objective function value and associated optimum variable vector. Regions in carbon/renewable utility cost coefficient ratio space are identified, in which one technology is superior over the other. EESMR is shown to be preferable in the presence of significant levels of taxation on the use of natural gas as fuel.

The dissertation of Jeremy Alexander Conner is approved.

Dante A Simonetti

Yungfeng Lu

Vwani P Roychowdhury

Vasilios Manousiouthakis, Committee Chair

University of California, Los Angeles

2019

Table of Contents

List of Figures

List of Tables

Acknowledgements

Financial support through NSF Grant NSF-CBET 0829211 for chapters 1 and 2 is gratefully acknowledged. Financial support from the U.S. Department of Energy through DOE grant DE-EE0005763 “Industrial Scale Demonstration of Smart Manufacturing Achieving Transformational Energy Productivity Gains” for chapters 2, 3, and 4 is gratefully acknowledged.

Jeremy Alexander Conner

Department of Chemical & Biomolecular Engineering
4272 Boelter Hall, University of California, Los Angeles
Los Angeles, California 90095
Cell #: (909) 800-5613
E-mail: jconner006@ucla.edu

EDUCATION

Ph.D. in Chemical Engineering (September 2019)
University of California, Los Angeles
Dissertation title: "Linear and Non-Linear Programming for System Identification and Green Engineering Applications"

M.S. in Chemical Engineering (February 2011)
University of California, Los Angeles
Master's Thesis title: "On a Sustainability Interval Index and Its Computation Through Global Optimization"

B.S. in Chemical Engineering (June 2008)
University of California, Riverside

JOURNAL PUBLICATIONS

- Al-Bassam, A.M., Conner, J.A., Manousiouthakis, V.I. (2018), "Natural gas derived hydrogen in the presence of carbon fuel taxes and concentrated solar power", *ACS Sustainable Chemistry & Engineering, 6*(3), 3029-3038.
- Conner, J.A., Manousiouthakis, V.I. (2015), "On an Interval-Analysis-Based Determination of Globally Optimal Total Annualized Cost for Compressor Sequences", *Industrial & Engineering Chemistry Research*, *54*(6), 1861-1875.
- Conner, J.A., Manousiouthakis, V.I. (2014) "Global Optimality Properties of Total Annualized and Operating Cost Problems for Compressor Sequences", *AIChE Journal*, *60*(12), 4134-4149.
- Conner, J.A., Manousiouthakis, V.I. (2014), "On the Attainable Region for Process Networks", *AIChE Journal, 60*(1), 193-212.
- Conner, J.A., Phillis, Y.A., Manousiouthakis, V.I. (2012), "On a Sustainability Interval Index and Its Computation Through Global Optimization", *AIChE Journal, 58*(9), 2743-2757.

PROFESSIONAL AND LEADERSHIP EXPERIENCE

WorleyParsons (Monrovia, CA) February 2016 – February 2017
Process Engineer I

- Involved in design and engineering of several gas compression plants
- Maintained a list of all process equipment used across all sites
- Performed hydraulic calculations on all major pipelines employed in the process
- Sized pressure vessels and centrifugal pumps based on process data and client feedback
- Communicated updates to data to employees across disciplines as they occurred

University of California, Los Angeles (Los Angeles, CA) Summer 2011, 2012, 2013
Research Lab Supervisor (UCLA High School Summer Research Program)

- Interacted with high school students daily for eight weeks
- Managed a team of high school students for sustainability data collection and survey efforts
- Assisted in development of students' literature search skills and mathematical background
- Designed surveys to educate the public on the impact of aluminum production
- Solicited public opinion on the sustainability efforts of aluminum-producing companies

TEACHING EXPERIENCE

University of California, Los Angeles (Los Angeles, CA) Winter 2014, Spring 2014
Teaching Assistant (ChE 104A – Chemical and Biomolecular Engineering Laboratory I)

- Enforced safe laboratory conduct of up to 20 undergraduate students
- Evaluated students' technical writing and oral presentation skills via post-lab reports and poster sessions

University of California, Los Angeles (Los Angeles, CA) Fall 2013
Teaching Assistant (ChE 104B – Chemical and Biomolecular Engineering Laboratory II)

- Enforced safe laboratory conduct of up to 16 undergraduate students
- Evaluated students' technical writing and oral presentation skills via pre- and post-lab reports

University of California, Los Angeles (Los Angeles, CA) Spring 2010, 2011, 2012, 2013
Teaching Assistant (ChE C119/219 – Pollution Prevention for Chemical Processes)

- Prepared and conducted bi-weekly recitations/lectures to 20-30 undergrad/grad students
- Held office hours for two hours per week
- Wrote, solved, and graded homework assignments and exams

University of California, Los Angeles (Los Angeles, CA) Winter 2013
Teaching Assistant (ChE 099 – Student Research Program)

- Enforced safe laboratory conduct of up to 12 undergraduate students developing a hydrogen-fuelled car for the AIChE ChemE Car competition

University of California, Los Angeles (Los Angeles, CA) Fall 2012
Teaching Assistant (ChE 100 – Fundamentals of Chemical and Biomolecular Engineering)

- Led two 1-hour, 30-student discussion sections each week
- Answered student questions in office hours four hours per week
- Wrote and graded homework assignments and exams for 106 undergraduate students

University of California, Los Angeles (Los Angeles, CA) Winter 2011, 2012
Teaching Assistant (ChE 102A – Thermodynamics I)

- Held office hours for homework and course content assistance four hours per week
- Led weekly discussion sections of up to 80 students per week
- Wrote, solved, and graded homeworks and exams for 119-123 students

University of California, Los Angeles (Los Angeles, CA) Fall 2009
Teaching Assistant (ChE 101A – Transport Phenomena I: Momentum Transfer)

- Graded student homework assignments and examinations
- Held office hours to answer student homework questions two hours per week
- Assisted in writing and solving midterm exams

University of California, Los Angeles (Los Angeles, CA) Spring 2009
Teaching Assistant (ChE 108B – Chemical Process Computer-Aided Design and Analysis)

- Evaluated final projects pertaining to hydrogen production plants with zero carbon emissions
- Assisted in writing and solving homework problems and midterm exams
- Held office hours to answer student questions two hours per week

University of California, Los Angeles (Los Angeles, CA) Winter 2009
Teaching Assistant (ChE 108A – Process Economics and Analysis)

- Graded student homework assignments and examinations
- Held office hours to answer student questions two hours per week
- Assisted in writing and solving homework problems and midterm exams

Chapter 1: On the Attainable Region for Process Networks

In this work the attainable region (AR) concept for process networks with outlet flowrate specifications is introduced for the first time. For process unit models to which the IDEAS conceptual framework is applicable, it is shown that identification of AR boundary membership is equivalent to feasibility assessment of an infinite linear program (ILP). A number of important AR properties are then theoretically established, including AR convexity, and representation of the AR in a concentration state space of reduced dimension. Finite dimensional approximations of the aforementioned ILP are then employed in creating increasingly accurate approximations of the AR. A case study for the vapor-liquid equilibrium-based separation of a ternary azeotropic mixture is used to illustrate the proposed method. The quantified 2- and 4-Dimensional ARs indicate that acetone mole fractions above 0.79 (acetone/methanol azeotrope) are attainable for the considered outlet flowrate ratios.

Section 1.1: Introduction

The attainable region (AR) for reactor networks has been the topic of substantial research effort, due to its effectiveness in rigorously assessing, at the early conceptual design stage, the limitations imposed on reactor network performance by the kinetic rates of the underlying reactions, the reactor network feed composition, and the properties of the underlying reactor units. The AR concept was first defined for reactor networks by Horn[1] as the complete set of points in concentration space that can be considered as product composition vectors of some steady-state reactor networks, using only processes of reaction and mixing/splitting from a given feed point. Glasser et. al.[2] and Hildebrandt et. al.[3] developed geometric methods for quantifying candidate AR's using plug-flow reactor (PFR) trajectories and continuous stirred tank reactor

(CSTR) loci. Since then, several mathematical frameworks for reactor network ARs were developed; recent works include determining AR for isothermal CSTR/PFR networks[4], non-ideal reactor networks[5], reactor networks employing variable-density fluids[6], and batch reactor networks[7]. Computational strategies for quantifying the reactor AR abound in the literature, including "outside-in" methods such as bounding hyperplanes[8] and the Shrink-Wrap method[4,9], as well as the Infinite DimEnsionAl State-space (IDEAS) framework[6,10,11,12]. Due to their vast number, we refer the reader to references within the aforementioned works for more information on AR quantification strategies.

As the reactor AR concept matured, research into coupling the reactor models with separation was carried out to identify opportunities to expand the AR for maximizing the yield of desired products. In a series of papers, Mahajani and co-workers[13,14,15,16] quantified the AR for reactive distillation networks using a generalization of the aforementioned geometric AR quantification methods. Their approach employed single-feed-single-product units termed non-azeotropic single-reactant reactive condensers/reboilers[13], azeotropic reactive rectification and reactive stripping units[14,15,16], and capitalized on the residue curve map concept formulated by Doherty et. al.[17].

Rigorous mathematical development of the AR concept for separator networks is comparatively sparse in the literature. Jobson et. al.[18] examined the feasible product regions for three configurations of two VLE flash systems: in parallel, in series, and in series with reflux. They found cases where either configuration could outperform the others in terms of attainable product purities. Nisoli et. al.[19] were the first to identify the attainable region for general hybrid separator/reactor/reactive-separator networks. They employed a reaction-separation vector for a two-product CSTR (multi-product CSTR series/PFR) model of a reactor/separator, to construct

the AR for hybrid separator/reactor/reactive-separator networks, without inlet/outlet stream flowrate specifications, by generalizing geometric methods of reactor network AR construction. In an MTBE case study, their method was able to identify that pure MTBE cannot be attained using a reactor network or a reactive-separator network. Rather, a reactor/separator or reactive-separator/separator network was shown to be required.

In this work, we introduce the attainable region (AR) concept for process networks with inlet/outlet stream flowrate specifications. This is applicable to networks with a finite number of inlets and outlets, and a possibly infinite number of process units, each of which has a finite number of inlets and outlets. The proposed process network AR concept quantifies for the first time the set of all outlet stream composition vectors that can be attained by a process network with known inlet and outlet flowrate ratios. To this end, we introduce the following definition of the process network AR:

Definition: *Consider a process network with S inlets and Q outlets whose total inlet molar flowrate sum and outlet molar flowrate sum are designated as* $\sum_{i=1}^{S} F_i^U$ *and* $\sum_{i=1}^{Q} F_i^Y$, *respectively. Let the mole fraction vector* x_i^U *and the molar flowrate ratio* $\left\{\alpha_i^U\right\}_{i=1}^{S} \triangleq \left\{F_i^U \Big/ \sum_{i=1}^{S} F_i^U\right\}_{i=1}^{S}$ *of the* i^{th} *inlet stream,* $i=1,S$ *, be known. Let also the molar flowrate ratio* $\left\{\alpha_i^Y\right\}_{i=1}^{Q} \triangleq \left\{F_i^Y \Big/ \sum_{i=1}^{Q} F_i^Y\right\}_{i=1}^{Q}$ *of the* i^{th} *outlet stream,* $i=1,Q$ *, be known. Then the process network AR, denoted* $AR_{\left\{\alpha_i^Y\right\}_{i=1}^{Q},\left\{\left(\alpha_i^U,x_i^U\right)\right\}_{i=1}^{S}}$, *is defined to be the subset of the concentration space* $\Re^{Q\cdot n}$ *consisting of all* $n\cdot Q$ *dimensional vectors consisting of the* n *dimensional outlet mole fraction vectors of the* Q *products of a realizable process network.*

This definition can be equivalently expressed in terms of either mass or molar quantities; however molar quantities are chosen to facilitate the presentation of the illustrative case study, since the associated data are given in terms of molar fractions and molar flowrates.

The rest of this chapter is structured as follows: first, the conceptual framework for $AR_{\left\{\alpha_i^Y\right\}_{i=1}^{Q},\left\{\left(\alpha_i^U,x_i^U\right)\right\}_{i=1}^{S}}$ will be presented in two parts. Part one will formulate the $AR_{\left\{\alpha_i^Y\right\}_{i=1}^{Q},\left\{\left(\alpha_i^U,x_i^U\right)\right\}_{i=1}^{S}}$ quantification problem using the IDEAS framework for process networks employing process units with multiple inlets and outlets. The properties of inlet/outlet flowrate independence, and convexity of the process network AR will then be established via rigorous mathematical proofs. Part two will show how the general formulation in part one translates to a separator network employing one inlet/two outlet VLE separators. We then test our method on two case studies involving separation of an azeotropic ternary mixture: one involving a separator network with one inlet stream and three outlet streams (4D AR), and one involving a separator network with one inlet stream and two outlet streams (2D AR). Plots demonstrating convergence of the approximated 2D ARs and visualization of both 4D and 2D ARs will be provided and discussed. Lastly, conclusions will be drawn.

Section 1.2: Conceptual Framework

IDEAS Formulation for Networks of Process units with multiple inlets/outlets

We consider an infinite network of process units possessing a finite number of network inlets (S) and network outlets (Q), with n total species among the network streams. For simplicity of notation, we consider all process units in the network to possess the same finite number of inlets (s) and outlets (q), and consider all network streams to be at the same pressure

P and to be allowed to mix. Figure 1.1 illustrates the IDEAS representation of the process network. This IDEAS representation breaks the process network into two components: the distribution network (DN), where all stream mixing, splitting, recycling and bypassing takes place, and the operator network (OP), consisting of all the network's process units.

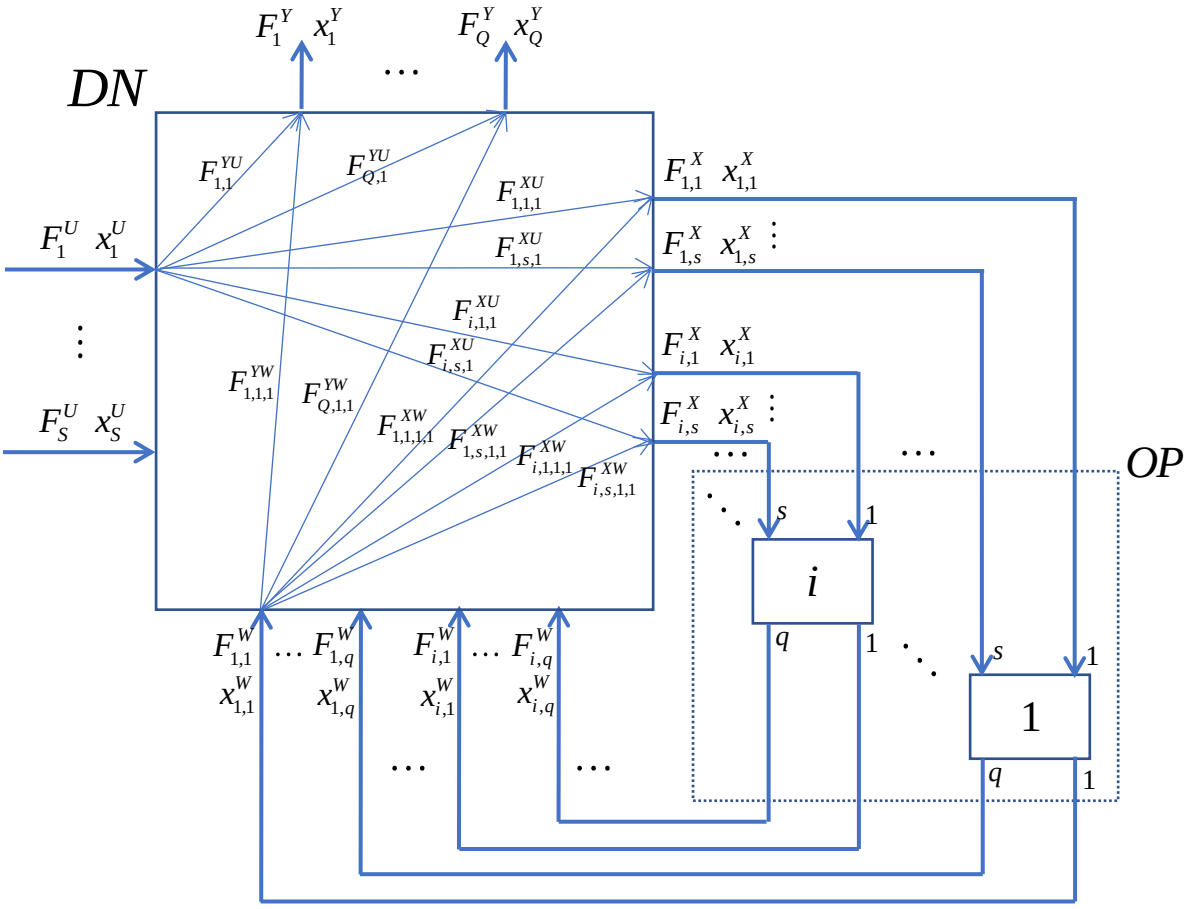

Figure 1.1: IDEAS diagram of a process network

The DN possesses four types of junctions: (1) those corresponding to the overall network inlet streams, and denoted with superscript U and indexed by subscript $j = 1, S$; (2) those corresponding to the overall network outlet streams, and denoted with superscript Y and indexed by subscript $j = 1, Q$; (3) those corresponding to the OP inlet streams, and denoted with

superscript X and indexed by subscripts (i, j) $i = 1, \infty$ $j = 1, s$; and (4) those corresponding to the OP outlet streams, and denoted with superscript W and indexed by subscripts (i, j) $i = 1, \infty$ $j = 1, q$. It should be noted that Figure 1.1 lists all mole fraction quantities as vectors in $\Re^n$. Conservation laws are enforced at all junctions, while the OP includes the models describing the process units. The IDEAS formulation characterizing $AR_{\left\{\alpha_i^Y\right\}_{i=1}^{Q},\left\{\left(\alpha_i^U, x_i^U\right)\right\}_{i=1}^{S}}$ for the diagram is described by constraints $(1)-(11)$.

Input and output flowrate ratio relations

$$F_i^U = \alpha_i^U F_{tot}^U \quad \forall i = 1, S, \ \sum_{i=1}^{S} \alpha_i^U = 1 \quad (1)$$

$$F_i^Y = \alpha_i^Y F_{tot}^Y \quad \forall i = 1, Q, \ \sum_{i=1}^{Q} \alpha_i^Y = 1 \quad (2)$$

Total mixing balances at DN junctions:

$$F_j^Y = \sum_{i=1}^{\infty} \sum_{k=1}^{q} F_{j,i,k}^{YW} + \sum_{i=1}^{S} F_{j,i}^{YU} \quad \forall j = 1, Q \quad (3)$$

$$F_{j,l}^X = \sum_{i=1}^{\infty} \sum_{k=1}^{q} F_{j,l,i,k}^{XW} + \sum_{i=1}^{S} F_{j,l,i}^{XU} \quad \forall j = 1, \infty \ \ \forall l = 1, s \quad (4)$$

Total splitting balances at DN junctions:

$$F_j^U = \sum_{i=1}^{\infty} \sum_{k=1}^{s} F_{i,k,j}^{XU} + \sum_{i=1}^{Q} F_{i,j}^{YU} \quad \forall j = 1, S \quad (5)$$

$$F_{j,l}^W = \sum_{i=1}^{\infty} \sum_{k=1}^{s} F_{i,k,j,l}^{XW} + \sum_{i=1}^{Q} F_{i,j,l}^{YW} \quad \forall j = 1, \infty \ \ \forall l = 1, q \quad (6)$$

Component mixing/ process unit balances:

$$x_j^Y F_j^Y = \sum_{i=1}^{\infty}\sum_{k=1}^{q} x_{i,k}^W F_{j,i,k}^{YW} + \sum_{i=1}^{S} x_i^U F_{j,i}^{YU} \quad \forall j = 1, Q \quad (7)$$

$$f_{j,k}^X = \sum_{i=1}^{\infty}\sum_{l=1}^{q} x_{i,l}^W F_{j,k,i,l}^{XW} + \sum_{i=1}^{S} x_i^U F_{j,k,i}^{XU}, \quad \forall j = 1, \infty \ \ \forall k = 1, s \quad (8)$$

IDEAS linear input species flowrate, input total flowrate, output total flowrate, and design variable relations for the j^{th} process unit:

$$0 = \left[R\left(\left[x_{j,1}^W \right]^{\mathrm{T}}, \cdots, \left[x_{j,q}^W \right]^{\mathrm{T}}, \left[x_{j,1}^X \right]^{\mathrm{T}}, \cdots, \left[x_{j,s}^X \right]^{\mathrm{T}}, \left[\alpha_j \right]^{\mathrm{T}} \right) \right]^{\mathrm{T}} \cdot$$
$$\left[\left[f_{j,1}^X \right]^{\mathrm{T}} \ \cdots \ \left[f_{j,s}^X \right]^{\mathrm{T}} \ F_{j,1}^X \ \cdots \ F_{j,s}^X \ F_{j,1}^W \ \cdots \ F_{j,q}^W \ \left[A_j \right]^{\mathrm{T}} \right]^{\mathrm{T}} \quad \forall j = 1, \infty \quad (9)$$

IDEAS composition, design parameter relations for the j^{th} process unit:

$$N\left(\left[x_{j,1}^W \right]^{\mathrm{T}}, \cdots, \left[x_{j,q}^W \right]^{\mathrm{T}}, \left[x_{j,1}^X \right]^{\mathrm{T}}, \cdots, \left[x_{j,s}^X \right]^{\mathrm{T}}, \left[\alpha_j \right]^{\mathrm{T}} \right) = 0 \quad \forall j = 1, \infty \quad (10)$$

The variables in the above equations must also satisfy the following positivity constraints:

$$\left\{ \begin{array}{l} F_j^Y \geq 0 \ \ \forall j = 1, Q; \ \ F_j^U \geq 0 \ \ \forall j = 1, S; \\ F_{i,j}^X \geq 0 \ \ \forall i = 1, \infty \ \ \forall j = 1, s; \ \ F_{i,j}^W \geq 0 \ \ \forall i = 1, \infty \ \forall j = 1, q; \\ F_{i,j}^{YU} \geq 0 \ \forall i = 1, Q \ \ \forall j = 1, S; \ \ F_{i,k,j}^{XU} \geq 0 \ \ \forall i = 1, \infty \ \forall k = 1, s \ \ \forall j = 1, S \\ F_{j,i,k}^{YW} \geq 0 \ \forall j = 1, Q \ \ \forall i = 1, \infty \ \ \forall k = 1, q \\ F_{j,l,i,k}^{XW} \geq 0 \ \ \forall j = 1, \infty \ \ \forall l = 1, s \ \ \forall i = 1, \infty \ \ \forall k = 1, q \\ f_{j,k}^X \geq 0 \ \ \forall j = 1, \infty \ \ \forall k = 1, s \end{array} \right\} \quad (11)$$

For a given j from 1 to ∞, Equations $(9), (10)$ capture the behavior of the j^{th} process unit. As j varies from 1 to ∞, a subvector of the vector $\left[\left[x_{j,1}^W \right]^{\mathrm{T}}, \cdots, \left[x_{j,q}^W \right]^{\mathrm{T}}, \left[x_{j,1}^X \right]^{\mathrm{T}}, \cdots, \left[x_{j,s}^X \right]^{\mathrm{T}}, \left[\alpha_j \right]^{\mathrm{T}} \right]^{\mathrm{T}}$ assumes all its possible realizable values. The structure of equations (10) is such that, for any given j, knowledge of the aforementioned subvector guarantees knowledge of the whole vector

$\left[\left[x_{j,1}^{W}\right]^{\mathrm{T}},\cdots,\left[x_{j,q}^{W}\right]^{\mathrm{T}},\left[x_{j,1}^{X}\right]^{\mathrm{T}},\cdots,\left[x_{j,s}^{X}\right]^{\mathrm{T}},\left[\alpha_{j}\right]^{\mathrm{T}}\right]^{\mathrm{T}}$. In addition, the structure of $R(\cdot)$ in (9) is such that knowledge of $\left[\left[x_{j,1}^{W}\right]^{\mathrm{T}},\cdots,\left[x_{j,q}^{W}\right]^{\mathrm{T}},\left[x_{j,1}^{X}\right]^{\mathrm{T}},\cdots,\left[x_{j,s}^{X}\right]^{\mathrm{T}},\left[\alpha_{j}\right]^{\mathrm{T}}\right]^{\mathrm{T}}$ makes $R\left(\left[x_{j,1}^{W}\right]^{\mathrm{T}},\cdots,\left[x_{j,q}^{W}\right]^{\mathrm{T}},\left[x_{j,1}^{X}\right]^{\mathrm{T}},\cdots,\left[x_{j,s}^{X}\right]^{\mathrm{T}},\left[\alpha_{j}\right]^{\mathrm{T}}\right)$ a linear operator.

It is straightforward to show using constraints $(1),(2)$, along with the total concentration balance on the process network, that an equivalent AR can be defined as a subset of $\Re^{(n-1)^2}$, with corresponding flowrate ratios and concentration vectors and flowrates $\left\{a_i^Y\right\}_{i=1}^{Q-1},\left\{\left(\alpha_i^U,x_i^U\right)\right\}_{i=1}^{S-1}$. This dimensional reduction significantly reduces the computational burden on quantification of the separation AR. Furthermore, as Theorem 1 demonstrates, the separation AR is convex for fixed network inlet mole fractions and fixed network inlet/outlet flow rate ratios. Therefore, techniques to quantify the AR can be employed focusing on quantification of the region's vertices, allowing for compact representation of the shape of the $AR_{\left\{\alpha_i^Y\right\}_{i=1}^{Q},\left\{\left(\alpha_i^U,x_i^U\right)\right\}_{i=1}^{S}}$.

Theorem 1: Let the units employed in a process network satisfy the IDEAS properties $(9),(10)$ listed above. Then for the above process network, (a) the $AR_{\left\{\alpha_i^Y\right\}_{i=1}^{Q},\left\{\left(\alpha_i^U,x_i^U\right)\right\}_{i=1}^{S}}$ does not depend on either $F_{tot}^{U}=\sum_{i=1}^{S}F_i^U$ or $F_{tot}^{Y}=\sum_{i=1}^{Q}F_i^Y$, and (b) the $AR_{\left\{\alpha_i^Y\right\}_{i=1}^{Q},\left\{\left(\alpha_i^U,x_i^U\right)\right\}_{i=1}^{S}}$ is a convex set.

Proof:

(a) Let $\left[\left[\overline{x}_1^Y\right]^{\mathrm{T}}\ \cdots\ \left[\overline{x}_Q^Y\right]^{\mathrm{T}}\right]^{\mathrm{T}}\in AR_{\left\{\alpha_i^Y\right\}_{i=1}^{Q},\left\{\left(\alpha_i^U,x_i^U\right)\right\}_{i=1}^{S}}$. Then there exists a physically realizable process network with input and output flowrate ratios $\alpha_i^U\ \ \forall i=1,S$, $\alpha_i^Y\ \ \forall i=1,Q$, design

parameters $\alpha_j \ \ \forall j = 1, \infty$, mole fractions $\bar{x}_i^Y \ \forall i = 1, Q; x_{i,k}^W \ \ \forall i = 1, \infty \ \ \forall k = 1, q; x_i^U \ \ \forall i = 1, S$,

molar flowrates $\bar{F}_{tot}^U, \bar{F}_{tot}^Y; \bar{F}_j^U \ \ \forall j = 1, S; \ \bar{F}_j^Y \ \ \forall j = 1, Q; \bar{F}_{j,i,k}^{YW} \ \ \forall j = 1, Q \ \ \forall i = 1, \infty \ \ \forall k = 1, q$,

$\bar{F}_{j,i}^{YU} \ \ \forall j = 1, Q \ \ \forall i = 1, S, \bar{F}_{j,l}^X \ \ \forall j = 1, \infty \ \ \forall l = 1, s, \bar{F}_{j,l,i,k}^{XW} \ \ \forall j = 1, \infty \ \ \forall l = 1, s \ \ \forall i = 1, \infty \ \ \forall k = 1, q$,

$\bar{F}_{j,l,i}^{XU} \ \ \forall j = 1, \infty \ \ \forall l = 1, s \ \ \forall i = 1, S, \ \bar{F}_{j,l}^W \ \ \forall j = 1, \infty \ \ \forall l = 1, q$, component molar flowrates

$\bar{f}_{j,k}^X \ \ \forall j = 1, \infty \ \ \forall k = 1, s$, and design variables $\bar{A}_j \ \ \forall j = 1, \infty$ satisfying $(1) - (11)$.

Now consider a new process network with input and output flowrate ratios $\alpha_i^U \ \ \forall i = 1, S$,

$\alpha_i^Y \ \ \forall i = 1, Q$, design parameters $\alpha_j \ \ \forall j = 1, \infty$, mole fractions $\bar{x}_i^Y \ \ \forall i = 1, Q$;

$x_{i,k}^W \ \ \forall i = 1, \infty \ \ \forall k = 1, q; x_i^U \ \ \forall i = 1, S$, molar flowrates $\lambda \bar{F}_{tot}^U, \lambda \bar{F}_{tot}^Y; \lambda \bar{F}_j^U \ \ \forall j = 1, S$;

$\lambda \bar{F}_j^Y \ \ \forall j = 1, Q; \lambda \bar{F}_{j,i,k}^{YW} \ \ \forall j = 1, Q \ \ \forall i = 1, \infty \ \ \forall k = 1, q, \lambda \bar{F}_{j,i}^{YU} \ \ \forall j = 1, Q \ \ \forall i = 1, S$,

$\lambda \bar{F}_{j,l}^X \ \ \forall j = 1, \infty \ \ \forall l = 1, s, \lambda \bar{F}_{j,l,i,k}^{XW} \ \ \forall j = 1, \infty \ \ \forall l = 1, s \ \ \forall i = 1, \infty \ \ \forall k = 1, q$,

$\lambda \bar{F}_{j,l,i}^{XU} \ \ \forall j = 1, \infty \ \ \forall l = 1, s \ \ \forall i = 1, S, \ \lambda \bar{F}_{j,l}^W \ \ \forall j = 1, \infty \ \ \forall l = 1, q$, component molar flowrates

$\lambda \bar{f}_{j,k}^X \ \ \forall j = 1, \infty \ \ \forall k = 1, s$, and design variables $\lambda \bar{A}_j \ \ \forall j = 1, \infty$, where $\lambda > 0$. Given the linearity of the operator R in (9), and the fact that (10) remains unchanged, it then holds that this new process network is also physically realizable, since $(1) - (11)$ are satisfied. Thus,

$\left[\left[\bar{x}_1^Y \right]^{\mathrm{T}} \ \ \cdots \ \ \left[\bar{x}_Q^Y \right]^{\mathrm{T}} \right]^{\mathrm{T}} \in AR_{\left\{ \alpha_i^Y \right\}_{i=1}^Q, \left\{ \left(\alpha_i^U, x_i^U \right) \right\}_{i=1}^S}$ continues to be true, even though $\bar{F}_{tot}^U$ and $\bar{F}_{tot}^Y$ have been changed to $\lambda \bar{F}_{tot}^U$ and $\lambda \bar{F}_{tot}^Y$. O.E.Δ.

(b) We proceed by contradiction. Assume that there exist two physically realizable process networks whose composite $n \cdot Q$ dimensional exit mole fraction vectors

$\left[\left[\bar{x}_1^Y\right]^{\mathrm{T}} \quad \cdots \quad \left[\bar{x}_Q^Y\right]^{\mathrm{T}}\right]^{\mathrm{T}}, \left[\left[\hat{x}_1^Y\right]^{\mathrm{T}} \quad \cdots \quad \left[\hat{x}_Q^Y\right]^{\mathrm{T}}\right]^{\mathrm{T}}$ are such that

$\left[\left[\bar{x}_1^Y\right]^{\mathrm{T}} \quad \cdots \quad \left[\bar{x}_Q^Y\right]^{\mathrm{T}}\right]^{\mathrm{T}} \in AR_{\left\{\alpha_i^Y\right\}_{i=1}^Q, \left\{\left(\alpha_i^U, x_i^U\right)\right\}_{i=1}^S}$ and $\left[\left[\hat{x}_1^Y\right]^{\mathrm{T}} \quad \cdots \quad \left[\hat{x}_Q^Y\right]^{\mathrm{T}}\right]^{\mathrm{T}} \in AR_{\left\{\alpha_i^Y\right\}_{i=1}^Q, \left\{\left(\alpha_i^U, x_i^U\right)\right\}_{i=1}^S}$. Also assume that $\exists \lambda \in (0,1): \left[\left[\lambda \bar{x}_1^Y + (1-\lambda)\hat{x}_1^Y\right]^{\mathrm{T}} \quad \cdots \quad \left[\lambda \bar{x}_Q^Y + (1-\lambda)\hat{x}_Q^Y\right]^{\mathrm{T}}\right]^{\mathrm{T}} \notin AR_{\left\{\alpha_i^Y\right\}_{i=1}^Q, \left\{\left(\alpha_i^U, x_i^U\right)\right\}_{i=1}^S}$. We will show that this leads to impossibility.

The physical realizability of the two aforementioned networks (denoted as bar and hat), combined with the lack of dependence of $AR_{\left\{\alpha_i^Y\right\}_{i=1}^Q, \left\{\left(\alpha_i^U, x_i^U\right)\right\}_{i=1}^S}$ on the total inlet and outlet network flow rate, implies that there exist input and output flowrate ratios $\alpha_i^U \left(\alpha_i^U\right) \ \forall i = 1, S$, $\alpha_i^Y \left(\alpha_i^Y\right) \ \forall i = 1, Q$, design parameters $\alpha_j \left(\alpha_j\right) \ \forall j = 1, \infty$, mole fractions $\bar{x}_i^Y \left(\hat{x}_i^Y\right) \forall i = 1, Q$; $x_{i,k}^W \left(x_{i,k}^W\right) \ \forall i = 1, \infty \ \forall k = 1, q$; $x_i^U \left(x_i^U\right) \ \forall i = 1, S$, molar flowrates $\bar{F}_{tot}^U = F_{tot}^U \left(\hat{F}_{tot}^U = F_{tot}^U\right)$, $\bar{F}_{tot}^Y = F_{tot}^Y \left(\hat{F}_{tot}^Y = F_{tot}^Y\right)$; $\bar{F}_j^U = F_j^U \left(\hat{F}_j^U = F_j^U\right) \ \forall j = 1, S$; $\bar{F}_j^Y = F_j^Y \left(\hat{F}_j^Y = F_j^Y\right) \ \forall j = 1, Q$; $\bar{F}_{j,i,k}^{YW} \left(\hat{F}_{j,i,k}^{YW}\right) \ \forall j = 1, Q \ \forall i = 1, \infty \ \forall k = 1, q$, $\bar{F}_{j,i}^{YU} \left(\hat{F}_{j,i}^{YU}\right) \ \forall j = 1, Q \ \forall i = 1, S$, $\bar{F}_{j,l}^X \left(\hat{F}_{j,l}^X\right) \ \forall j = 1, \infty \ \forall l = 1, s$, $\bar{F}_{j,l,i,k}^{XW} \left(\hat{F}_{j,l,i,k}^{XW}\right) \ \forall j = 1, \infty \ \forall l = 1, s \ \forall i = 1, \infty \ \forall k = 1, q$, $\bar{F}_{j,l,i}^{XU} \left(\hat{F}_{j,l,i}^{XU}\right) \ \forall j = 1, \infty \ \forall l = 1, s \ \forall i = 1, S$, $\bar{F}_{j,l}^W \left(\hat{F}_{j,l}^W\right) \ \forall j = 1, \infty \ \forall l = 1, q$, component molar flowrates $\bar{f}_{j,k}^X \left(\hat{f}_{j,k}^X\right) \ \forall j = 1, \infty \ \forall k = 1, s$, and design variables $\bar{A}_j \left(\hat{A}_j\right) \ \forall j = 1, \infty$ that satisfy $\left(\bar{1}\right) - \left(\overline{11}\right) \left(\left(\hat{1}\right) - \left(11\right)\right)$. As shown in part (a) above, this implies that the following networks are also physically realizable $\forall \lambda \in [0,1]$: input and output flowrate ratios $\alpha_i^U \left(\alpha_i^U\right) \ \forall i = 1, S$, $\alpha_i^Y \left(\alpha_i^Y\right) \ \forall i = 1, Q$, design parameters $\alpha_j \left(\alpha_j\right) \ \forall j = 1, \infty$, mole fractions $\bar{x}_i^Y \left(\hat{x}_i^Y\right) \forall i = 1, Q$;

$x_{i,k}^{W}\left(x_{i,k}^{W}\right)\ \forall i=1,\infty\ \ \forall k=1,q\,;x_{i}^{U}\left(x_{i}^{U}\right)\ \forall i=1,S$, molar flowrates $\lambda F_{tot}^{U}\left(\left(1-\lambda\right)F_{tot}^{U}\right)$,

$\lambda F_{tot}^{Y}\left(\left(1-\lambda\right)F_{tot}^{Y}\right);\lambda F_{j}^{U}\left(\left(1-\lambda\right)F_{j}^{U}\right)\ \forall j=1,S\,;\ \lambda F_{j}^{Y}\left(\left(1-\lambda\right)F_{j}^{Y}\right)\ \forall j=1,Q\,;$

$\lambda\bar{F}_{j,i,k}^{YW}\left(\left(1-\lambda\right)\hat{F}_{j,i,k}^{YW}\right)\ \forall j=1,Q\ \ \forall i=1,\infty\ \ \forall k=1,q$, $\lambda\bar{F}_{j,i}^{YU}\left(\left(1-\lambda\right)\hat{F}_{j,i}^{YU}\right)\ \forall j=1,Q\ \ \forall i=1,S$,

$\lambda\bar{F}_{j,l}^{X}\left(\left(1-\lambda\right)\hat{F}_{j,l}^{X}\right)\ \forall j=1,\infty\ \ \forall l=1,s$,

$\lambda\bar{F}_{j,l,i,k}^{XW}\left(\left(1-\lambda\right)\hat{F}_{j,l,i,k}^{XW}\right)\ \forall j=1,\infty\ \ \forall l=1,s\ \ \forall i=1,\infty\ \ \forall k=1,q$,

$\lambda\bar{F}_{j,l,i}^{XU}\left(\left(1-\lambda\right)\hat{F}_{j,l,i}^{XU}\right)\ \forall j=1,\infty\ \ \forall l=1,s\ \ \forall i=1,S$, $\lambda\bar{F}_{j,l}^{W}\left(\left(1-\lambda\right)\hat{F}_{j,l}^{W}\right)\ \forall j=1,\infty\ \ \forall l=1,q$,

component molar flowrates $\lambda\,\bar{f}_{j,k}^{X}\left(\left(1-\lambda\right)\,\hat{f}_{j,k}^{X}\right)\ \forall j=1,\infty\ \ \forall k=1,s$, and design variables

$\lambda\bar{A}_{j}\left(\left(1-\lambda\right)\hat{A}_{j}\right)\ \forall j=1,\infty$. But then, the following network is also physically realizable:

Input and output flowrate ratios $\alpha_{i}^{U}\ \ \forall i=1,S$, $\alpha_{i}^{Y}\ \ \forall i=1,Q$, design parameters $\alpha_{j}\ \ \forall j=1,\infty$,

mole fractions $\lambda\bar{x}_{i}^{Y}+\left(1-\lambda\right)\hat{x}_{i}^{Y}\ \ \forall i=1,Q\,;x_{i,k}^{W}\ \ \forall i=1,\infty\ \ \forall k=1,q\,;x_{i}^{U}\ \ \forall i=1,S$, molar flowrates

F_{tot}^{U} , $F_{tot}^{Y}\,;F_{j}^{U}\ \ \forall j=1,S\,;\ F_{j}^{Y}\ \ \forall j=1,Q\,;\lambda\bar{F}_{j,i,k}^{YW}+\left(1-\lambda\right)\hat{F}_{j,i,k}^{YW}\ \ \forall j=1,Q\ \ \forall i=1,\infty\ \ \forall k=1,q$,

$\lambda\bar{F}_{j,i}^{YU}+\left(1-\lambda\right)\hat{F}_{j,i}^{YU}\ \ \forall j=1,Q\ \ \forall i=1,S$, $\lambda\bar{F}_{j,l}^{X}+\left(1-\lambda\right)\hat{F}_{j,l}^{X}\ \ \forall j=1,\infty\ \ \forall l=1,s$,

$\lambda\bar{F}_{j,l,i,k}^{XW}+\left(1-\lambda\right)\hat{F}_{j,l,i,k}^{XW}\ \ \forall j=1,\infty\ \ \forall l=1,s\ \ \forall i=1,\infty\ \ \forall k=1,q$,

$\lambda\bar{F}_{j,l,i}^{XU}+\left(1-\lambda\right)\hat{F}_{j,l,i}^{XU}\ \ \forall j=1,\infty\ \ \forall l=1,s\ \ \forall i=1,S$, $\lambda\bar{F}_{j,l}^{W}+\left(1-\lambda\right)\hat{F}_{j,l}^{W}\ \ \forall j=1,\infty\ \ \forall l=1,q$,

component molar flowrates $\lambda\,\bar{f}_{j,k}^{X}+\left(1-\lambda\right)\,\hat{f}_{j,k}^{X}\ \ \forall j=1,\infty\ \ \forall k=1,s$, and design variables

$\lambda\bar{A}_{j}+\left(1-\lambda\right)\hat{A}_{j}\ \ \forall j=1,\infty$. In turn, this implies

$\forall \lambda \in [0,1]: \left[\left[\lambda \bar{x}_1^Y + (1-\lambda)\hat{x}_1^Y \right]^{\mathrm{T}} \quad \cdots \quad \left[\lambda \bar{x}_Q^Y + (1-\lambda)\hat{x}_Q^Y \right]^{\mathrm{T}} \right]^{\mathrm{T}} \in AR_{\left\{\alpha_i^Y\right\}_{i=1}^{Q}, \left\{\left(\alpha_i^U, x_i^U\right)\right\}_{i=1}^{S}}$. This is a contradiction. Thus $AR_{\left\{\alpha_i^Y\right\}_{i=1}^{Q}, \left\{\left(\alpha_i^U, x_i^U\right)\right\}_{i=1}^{S}}$ is a convex set. O.E.Δ.

IDEAS formulation for networks of vapor-liquid equilibrium separators

The advantage of IDEAS is that it overcomes the inherently nonlinear nature of process network synthesis and optimization problems, not via some kind of Taylor series approximate linearization, but rather by exploiting the decomposition and linearity properties that the process variables naturally obey. To better demonstrate the IDEAS process network AR quantification problem, and in preparation for the case study presented later, we demonstrate how constraints $(1)-(11)$ can be used to capture the behavior of a separator network separating a n species mixture , and employing vapor-liquid-equilibrium (VLE) separators, each with one input ($s=1$) and two outputs ($q=2$). The considered VLE separator model will employ the Gamma-Phi vapor liquid equilibrium formulation[20]. Equations $(1),(2)$ remain unaltered, equations $(3)-(8),(11)$ are simply specialized to $s=1,\ q=2$ and equations $(9),(10)$ become equations $(12),(13)$ below.

$$0 = \left[R\left(\left[x_{j,1}^W \right]^{\mathrm{T}}, \left[x_{j,2}^W \right]^{\mathrm{T}}, \left[x_{j,1}^X \right]^{\mathrm{T}}, \left[\alpha_j \right]^{\mathrm{T}} \right) \right]^{\mathrm{T}} \cdot \left[f_{j,1,1}^X \quad \cdots \quad f_{j,1,n}^X \quad F_{j,1}^X \quad F_{j,1}^W \quad F_{j,2}^W \right]^{\mathrm{T}} \triangleq$$

$$\triangleq \begin{bmatrix} 1 & 0 \cdots & 0 & 0 & -x_{j,1,1}^W & -x_{j,2,1}^W \\ 0 \vdots & 1 \ddots & 0 \vdots & 0 & \vdots & \vdots \\ 0 & 0 \cdots & 1 & 0 & -x_{j,1,n}^W & -x_{j,2,n}^W \\ 1 & 1 \cdots & 1 & -1 & 0 & 0 \\ 0 & 0 \cdots & 0 & 1 & -1 & -1 \end{bmatrix} \cdot \left[f_{j,1,1}^X \quad \cdots \quad f_{j,1,n}^X \quad F_{j,1}^X \quad F_{j,1}^W \quad F_{j,2}^W \right]^{\mathrm{T}} \quad \forall j = 1, \infty \quad (12)$$

$$N:\left[\left[x_{j,1}^{W}\right]^{\mathrm{T}},\left[x_{j,2}^{W}\right]^{\mathrm{T}},\left[x_{j,1}^{X}\right]^{\mathrm{T}},\left[\alpha_j\right]^{\mathrm{T}}\right]^{\mathrm{T}}\rightarrow N\left(\left[x_{j,1}^{W}\right]^{\mathrm{T}},\left[x_{j,2}^{W}\right]^{\mathrm{T}},\left[x_{j,1}^{X}\right]^{\mathrm{T}},\left[\alpha_j\right]^{\mathrm{T}}\right)\triangleq$$

$$\triangleq\begin{bmatrix} x_{j,2,1}^{W}\,\phi_1\left(\left\{x_{j,2,l}^{W}\right\}_{l=1}^{n},T_j,P\right)P-x_{j,1,1}^{W}\;\gamma_1\left(\left\{x_{j,1,l}^{W}\right\}_{l=1}^{n},T_j\right)P_1^{sat}\left(T_j\right)\\ \vdots\\ x_{j,2,n}^{W}\,\phi_n\left(\left\{x_{j,2,l}^{W}\right\}_{l=1}^{n},T_j,P\right)P-x_{j,1,n}^{W}\;\gamma_n\left(\left\{x_{j,1,l}^{W}\right\}_{l=1}^{n},T_j\right)P_n^{sat}\left(T_j\right)\\ \sum_{k=1}^{n}x_{j,1,k}^{W}-1\\ \sum_{k=1}^{n}x_{j,2,k}^{W}-1\end{bmatrix}=0\qquad\forall j=1,\infty\quad(13)$$

, where

$$\left[\alpha_j\right]^{\mathrm{T}}=\begin{bmatrix}P & T_j\end{bmatrix}\quad\forall j=1,\infty\quad(14)$$, with sub-vector $\begin{bmatrix}P & T_j & x_{j,1,1}^{W} & \cdots & x_{j,1,n-2}^{W}\end{bmatrix}\quad\forall j=1,\infty$.

A variety of thermodynamic models can be employed in quantifying the functions $\phi_k\left(\left\{x_{j,2,l}^{W}\right\}_{l=1}^{n},T_j,P\right)$, $\gamma_k\left(\left\{x_{j,1,l}^{W}\right\}_{l=1}^{n},T_j\right)$, $P_k^{sat}\left(T_j\right)\qquad\forall j=1,\infty\quad\forall k=1,n$. In this demonstration, ideal gas behavior is assumed; the Wilson equations are used to model the non-ideal liquid phase activity coefficients $\gamma_k\left(\left\{x_{i,1,l}^{W}\right\}_{l=1}^{n},T_i\right)\quad\forall i=1,\infty\quad\forall k=1,n$; and the extended Antoine equation is used to model the species vapor pressures $P_k^{sat}\left(T\right)\quad\forall k=1,n$. The relevant equations are:

$$\phi_k\left(\left\{x_{j,2,l}^{W}\right\}_{l=1}^{n},T_j,P\right)=1\quad\forall j=1,\infty\quad\forall k=1,n\quad(15)$$

$$\ln\left(\gamma_k\left(\left\{x_{j,1,l}^{W}\right\}_{l=1}^{n},T_j\right)\right)=1-\ln\left(\sum_{l=1}^{n}x_{j,1,l}^{W}\Lambda_{k,l}\left(T_j\right)\right)-\sum_{l=1}^{n}\left(\frac{x_{j,1,l}^{W}\Lambda_{l,k}\left(T_j\right)}{\sum_{i=1}^{n}x_{j,1,i}^{W}\Lambda_{l,i}\left(T_j\right)}\right)\quad\forall j=1,\infty\quad\forall k=1,n\quad(16)$$

$$\Lambda_{k,i}\left(T_j\right)=\frac{V_i^{V}}{V_k^{V}}\exp\left(\frac{-A_{k,i}}{RT_j}\right)\quad\forall j=1,\infty\quad\forall k=1,n;\quad\forall i=1,n\quad(17)$$

$$\ln\left(P_k^{sat}\left(T_j\right)\right)=A_k+\frac{B_k}{T_j+C_k}+D_k\cdot\ln\left(T_j\right)+E_k\cdot T_j^{F_k}\quad\forall i=1,\infty\quad\forall k=1,n\quad(18)$$

Section 1.3: Case Studies

We consider the isobaric separation of a water(1)/methanol(2)/acetone(3) mixture at $P = 1bar$ employing VLE separator units with one inlet ($s = 1$) and two outlets ($q = 2$). At these conditions, the binary mixture methanol/acetone exhibits a minimum boiling azeotrope at 0.2093/0.7907 mole fractions of methanol/acetone respectively. The thermodynamic behavior of both mixtures is captured by the Gamma-Phi vapor liquid equilibrium model described by $(15)-(18)$. The vapor phase is considered to be an ideal gas, while the liquid phase activity coefficients are quantified by the Wilson equations $(16),(17)$, and the vapor pressure of the various species is quantified by the Antoine equation (18). Species Wilson and Antoine coefficients for the mixture are listed in Table 1.1, Table 1.2, and Table 1.3. As an illustration of the versatility of the process network AR framework, we will pursue two examples: one involving a separator network with one inlet stream ($S = 1$) and three outlet streams ($Q = 3$) (4D AR), and one involving a separator network with one inlet stream ($S = 1$) and two outlet streams ($Q = 2$) (2D AR).

Wilson Coefficients $\left(\frac{cal}{mol}\right)$	A_{11}	A_{12}	A_{13}	A_{21}	A_{22}	A_{23}	A_{32}	A_{31}	A_{33}
W/M/A	0	469.55	1448.01	107.33	0	583.11	-161.88	291.27	0

Table 1.1: Wilson coefficients (molar energy differences) for case studies

Wilson Coefficients $\left(\frac{cm^3}{mol}\right)$	V_1	V_2	V_3
Water/Methanol/Acetone	17.88	40.76	74.47

Table 1.2: Wilson coefficients (pure species molar volumes) for case studies

Antoine Coefficients $T(K), P(bar)$	**Water/Methanol/Acetone**		
	$i=1$	$i=2$	$i=3$
A_i	65.93	59.84	71.30
B_i	-7228	-6283	-5952
C_i	0	0	0
D_i	-7.177	-6.379	-8.531
E_i	4.031e-6	4.617e-6	7.824e-6
F_i	2	2	2

Table 1.3: Antoine coefficients for case studies

Example 1:

We seek to identify the process network AR for a separation network with one inlet stream ($S=1$) and three outlet streams ($Q=3$) in which the network inlet stream has a molar flowrate of 3 mol/s and mole fractions of 0.3, 0.35, and 0.35 for species 1, 2, and 3, respectively; i.e. $F_1^U = 3\,\frac{mol}{s}$, $x_1^U = \begin{bmatrix} x_{1,1}^U & x_{1,2}^U & x_{1,3}^U \end{bmatrix}^T = \begin{bmatrix} 0.3 & 0.35 & 0.35 \end{bmatrix}^T$. We desire to separate this mixture into three outlet streams, each with molar flowrate of 1 mol/s, ($F_1^Y = F_2^Y = F_3^Y = 1\frac{mol}{s} \Rightarrow \alpha_1^Y = \alpha_2^Y = \alpha_3^Y = \frac{1}{3}$), and mole fractions $\begin{bmatrix} x_{1,1}^Y & x_{1,2}^Y & x_{1,3}^Y \end{bmatrix}^T, \begin{bmatrix} x_{2,1}^Y & x_{2,2}^Y & x_{2,3}^Y \end{bmatrix}^T, \begin{bmatrix} x_{3,1}^Y & x_{3,2}^Y & x_{3,3}^Y \end{bmatrix}^T$ to be determined.

Using the fact that all mole fractions must be in $[0,1]$, the summation property of mole fractions and the total balances on species 1 and 2, we can ease the computational burden of quantifying $AR_{\left\{\alpha_i^Y\right\}_{i=1}^Q, \left\{\left(\alpha_i^U, x_i^U\right)\right\}_{i=1}^S}$ by reducing its dimensionality from nine to four, and creating a set of conditions for identifying the initial superset containing it:

$$\left\{\begin{array}{l} 0 \le x_{1,1}^{Y} \le 1,\ 0 \le x_{1,2}^{Y} \le 1,\ 0 \le x_{1,3}^{Y} \le 1 \\ 0 \le x_{2,1}^{Y} \le 1,\ 0 \le x_{2,2}^{Y} \le 1,\ 0 \le x_{2,3}^{Y} \le 1 \\ 0 \le x_{3,1}^{Y} \le 1,\ 0 \le x_{3,2}^{Y} \le 1,\ 0 \le x_{3,3}^{Y} \le 1 \\ x_{1,1}^{Y} + x_{1,2}^{Y} + x_{1,3}^{Y} = 1 \\ x_{2,1}^{Y} + x_{2,2}^{Y} + x_{2,3}^{Y} = 1 \\ x_{3,1}^{Y} + x_{3,2}^{Y} + x_{3,3}^{Y} = 1 \\ F_1^U x_{1,1}^U = F_1^Y x_{1,1}^Y + F_2^Y x_{2,1}^Y + F_3^Y x_{3,1}^Y \\ F_1^U x_{1,2}^U = F_1^Y x_{1,2}^Y + F_2^Y x_{2,2}^Y + F_3^Y x_{3,2}^Y \end{array}\right\} \Leftrightarrow \left\{\begin{array}{l} 0 \le x_{1,1}^{Y} \le 1,\ 0 \le x_{1,2}^{Y} \le 1,\ 0 \le x_{1,3}^{Y} \le 1 \\ 0 \le x_{2,1}^{Y} \le 1,\ 0 \le x_{2,2}^{Y} \le 1,\ 0 \le x_{2,3}^{Y} \le 1 \\ 0 \le x_{3,1}^{Y} \le 1,\ 0 \le x_{3,2}^{Y} \le 1,\ 0 \le x_{3,3}^{Y} \le 1 \\ x_{1,3}^{Y} = 1 - x_{1,1}^{Y} - x_{1,2}^{Y} \\ x_{2,3}^{Y} = 1 - x_{2,1}^{Y} - x_{2,2}^{Y} \\ x_{3,3}^{Y} = 1 - x_{3,1}^{Y} - x_{3,2}^{Y} \\ x_{3,1}^{Y} = \dfrac{F_1^U}{F_3^Y} x_{1,1}^U - \dfrac{F_1^Y}{F_3^Y} x_{1,1}^Y - \dfrac{F_2^Y}{F_3^Y} x_{2,1}^Y \\ x_{3,2}^{Y} = \dfrac{F_1^U}{F_3^Y} x_{1,2}^U - \dfrac{F_1^Y}{F_3^Y} x_{1,2}^Y - \dfrac{F_2^Y}{F_3^Y} x_{2,2}^Y \end{array}\right\}$$

Substitution of $x_{1,3}^{Y}, x_{2,3}^{Y}, x_{3,1}^{Y}, x_{3,2}^{Y}, x_{3,3}^{Y}$ yields the following equivalent inequalities:

$$\left\{\begin{array}{l} 0 \le x_{1,1}^{Y} \le 1,\ 0 \le x_{1,2}^{Y} \le 1,\ 0 \le x_{2,1}^{Y} \le 1,\ 0 \le x_{2,2}^{Y} \le 1 \\ 0 \le 1 - x_{1,1}^{Y} - x_{1,2}^{Y} \le 1 \\ 0 \le 1 - x_{2,1}^{Y} - x_{2,2}^{Y} \le 1 \\ \dfrac{F_1^U}{F_3^Y} x_{1,1}^U - 1 \le \dfrac{F_1^Y}{F_3^Y} x_{1,1}^Y + \dfrac{F_2^Y}{F_3^Y} x_{2,1}^Y \le \dfrac{F_1^U}{F_3^Y} x_{1,1}^U \\ \dfrac{F_1^U}{F_3^Y} x_{1,2}^U - 1 \le \dfrac{F_1^Y}{F_3^Y} x_{1,2}^Y + \dfrac{F_2^Y}{F_3^Y} x_{2,2}^Y \le \dfrac{F_1^U}{F_3^Y} x_{1,2}^U \\ \dfrac{F_1^U}{F_3^Y}\left(x_{1,1}^U + x_{1,2}^U\right) - 1 \le \dfrac{F_1^Y}{F_3^Y}\left(x_{1,1}^Y + x_{1,2}^Y\right) + \dfrac{F_2^Y}{F_3^Y}\left(x_{2,1}^Y + x_{2,2}^Y\right) \le \dfrac{F_1^U}{F_3^Y}\left(x_{1,1}^U + x_{1,2}^U\right) \end{array}\right\} \quad (19)$$

For our known values, constraint set (19) becomes:

$$\left\{\begin{array}{l} 0 \le x_{1,1}^{Y} \le 1,\ 0 \le x_{1,2}^{Y} \le 1,\ 0 \le x_{2,1}^{Y} \le 1,\ 0 \le x_{2,2}^{Y} \le 1 \\ 0 \le 1 - x_{1,1}^{Y} - x_{1,2}^{Y} \le 1 \\ 0 \le 1 - x_{2,1}^{Y} - x_{2,2}^{Y} \le 1 \\ -0.1 \le x_{1,1}^{Y} + x_{2,1}^{Y} \le 0.9 \\ 0.05 \le x_{1,2}^{Y} + x_{2,2}^{Y} \le 1.05 \\ 0.95 \le x_{1,1}^{Y} + x_{1,2}^{Y} + x_{2,1}^{Y} + x_{2,2}^{Y} \le 1.95 \end{array}\right\} \quad (20)$$

To approximate solution of the ILP for $AR_{\left\{\alpha_i^Y\right\}_{i=1}^{Q},\left\{\left(\alpha_i^U,x_i^U\right)\right\}_{i=1}^{S}}$ quantification, we consider only a finite number of values for the network outlet mole fractions and the VLE separator sub-vector parameters. From the Gibbs phase rule, by fixing the operating pressure of the entire network, we only need to select two design parameters to fully specify a VLE separator. For our case study, we choose the i^{th} VLE separator outlet 1 species 1 and species 2 mole fractions $\left(x_{i,1,1}^W, x_{i,1,2}^W\right)$ as the two design parameters. Discretization levels of 1/16 and 1/32 for $\left(x_{i,1,1}^W, x_{i,1,2}^W\right)$ and for the network outlets $\left(x_{1,1}^Y, x_{1,2}^Y, x_{2,1}^Y, x_{2,2}^Y\right)$ will be employed. Calculation of the approximate $AR_{\left\{\alpha_i^Y\right\}_{i=1}^{Q},\left\{\left(\alpha_i^U,x_i^U\right)\right\}_{i=1}^{S}}$ for each of these discretization levels is pursued through solution of an LP feasibility problem formulation of IDEAS using a Fortran (MINOS) implementation, for all grid points in the above identified AR superset. The algorithm first generates a family of VLE separator units using the discretized sub-vector parameters and the thermodynamic model, then, for each combination of $x_{1,1}^Y, x_{1,2}^Y, x_{2,1}^Y, x_{2,2}^Y$, attempts to construct a feasible separator network using only the generated VLE separator units and interconnecting streams.

The facet-defining vertices of the 4D approximate ARs for the 1/16 and 1/32 discretization levels are shown in Tables 1.4 and 1.5. Close examination of the facet point list reveals that for any combination $\left(x_{1,1}^Y, x_{1,2}^Y, x_{2,1}^Y, x_{2,2}^Y\right)$, the combination $\left(x_{2,1}^Y, x_{2,2}^Y, x_{1,1}^Y, x_{1,2}^Y\right)$ also appears. This is a manifestation of the equal network outlet flowrate ratios, which allows for interchange of network outlet concentration combinations among the outlet streams with appropriate rearrangement of the network's VLE separator units and streams. A visual representation of the aforementioned facet-defining vertices for the 1/32 discretization level is also provided in Figure 1.2. This graphical representation illustrates each vertex point by

depicting its corresponding composition of stream 1 in one ternary diagram, and its corresponding composition of stream 2 in another ternary diagram. Since many vertices share stream 1 or stream 2 compositions, the list of vertices corresponding to a particular stream composition must be shown on the diagram. For example, from Table 1.5, the 50th vertex has coordinates $\left(x_{1,1}^{Y}, x_{1,2}^{Y}, x_{2,1}^{Y}, x_{2,2}^{Y}\right) = \left(0.125, 0.0625, 0.0313, 0.78125\right)$. It is illustrated in Figure 1.2 through its stream 1 composition $\left(x_{1,1}^{Y}, x_{1,2}^{Y}\right) = \left(0.125, 0.0625\right)$, shown in the bottom right corner of the first ternary diagram and identified through the number 50, and through its stream 2 composition $\left(x_{2,1}^{Y}, x_{2,2}^{Y}\right) = \left(0.0313, 0.78125\right)$, shown in the bottom left corner of the second ternary diagram and also identified through the number 50.

Another visual representation of the 4D approximate AR corresponding to the 1/16 discretization level is shown in Appendix 1.A. There, 2D projections of the aforementioned AR are shown for every composition of stream 1 corresponding to the composition grid generated by the 1/16 discretization level. These projections were generated by taking the convex hull of all points in $AR_{\left\{\alpha_i^Y\right\}_{i=1}^{Q}, \left\{\left(\alpha_i^U, x_i^U\right)\right\}_{i=1}^{S}}$ corresponding to each stream 1 mole fraction combination in Table 1.5

	$x_{1,1}^{Y}$	$x_{1,2}^{Y}$	$x_{2,1}^{Y}$	$x_{2,2}^{Y}$
1	0.0625	0.1875	0.125	0.6875
2	0.0625	0.1875	0.25	0.6875
3	0.0625	0.1875	0.625	0.1875
4	0.0625	0.1875	0.75	0.125
5	0.0625	0.1875	0.75	0.1875
6	0.0625	0.5625	0.625	0.3125
7	0.0625	0.625	0.75	0.1875
8	0.0625	0.6875	0.125	0.1875
9	0.0625	0.6875	0.625	0.1875
10	0.0625	0.6875	0.75	0.125
11	0.125	0.1875	0.0625	0.6875
12	0.125	0.6875	0.0625	0.1875
13	0.25	0.6875	0.0625	0.1875

14	0.25	0.6875	0.4375	0.1875
15	0.3125	0.625	0.5	0.1875
16	0.4375	0.1875	0.25	0.6875
17	0.5	0.1875	0.3125	0.625
18	0.625	0.1875	0.0625	0.1875
19	0.625	0.1875	0.0625	0.6875
20	0.625	0.3125	0.0625	0.5625
21	0.75	0.125	0.0625	0.1875
22	0.75	0.125	0.0625	0.6875
23	0.75	0.1875	0.0625	0.1875
24	0.75	0.1875	0.0625	0.625

Table 1.4: Separator AR facet-defining vertices for (1/16, 1/16) discretization

#	$x^Y_{1,1}$	$x^Y_{1,2}$	$x^Y_{2,1}$	$x^Y_{2,2}$	#	$x^Y_{1,1}$	$x^Y_{1,2}$	$x^Y_{2,1}$	$x^Y_{2,2}$
1	0.0313	0.125	0.0313	0.8125	42	0.0938	0.0938	0.75	0.21875
2	0.0313	0.125	0.0313	0.875	43	0.0938	0.84375	0.75	0.0938
3	0.0313	0.125	0.0625	0.78125	44	0.0938	0.875	0.0313	0.125
4	0.0313	0.125	0.0938	0.875	45	0.0938	0.875	0.0625	0.0938
5	0.0313	0.125	0.78125	0.0625	46	0.0938	0.875	0.125	0.0625
6	0.0313	0.125	0.8125	0.0625	47	0.0938	0.875	0.375	0.125
7	0.0313	0.125	0.8125	0.15625	48	0.0938	0.875	0.71875	0.0938
8	0.0313	0.46875	0.4375	0.53125	49	0.0938	0.875	0.75	0.0625
9	0.0313	0.78125	0.0625	0.125	50	0.125	0.0625	0.0313	0.78125
10	0.0313	0.78125	0.125	0.0625	51	0.125	0.0625	0.0313	0.90625
11	0.0313	0.78125	0.78125	0.1875	52	0.125	0.0625	0.0625	0.75
12	0.0313	0.78125	0.8125	0.15625	53	0.125	0.0625	0.0625	0.90625
13	0.0313	0.8125	0.0313	0.125	54	0.125	0.0625	0.0938	0.875
14	0.0313	0.8125	0.0625	0.0938	55	0.125	0.0625	0.6875	0.125
15	0.0313	0.84375	0.8125	0.0938	56	0.125	0.0625	0.71875	0.0938
16	0.0313	0.875	0.0313	0.125	57	0.125	0.0625	0.71875	0.25
17	0.0313	0.875	0.78125	0.0938	58	0.375	0.125	0.0938	0.875
18	0.0313	0.875	0.8125	0.0625	59	0.40625	0.0938	0.0625	0.90625
19	0.0313	0.90625	0.0625	0.0938	60	0.4375	0.0938	0.0313	0.90625
20	0.0313	0.90625	0.125	0.0625	61	0.4375	0.53125	0.0313	0.46875
21	0.0313	0.90625	0.4375	0.0938	62	0.6875	0.125	0.125	0.0625
22	0.0313	0.90625	0.78125	0.0625	63	0.71875	0.0938	0.0938	0.875
23	0.0625	0.0938	0.0313	0.8125	64	0.71875	0.0938	0.125	0.0625
24	0.0625	0.0938	0.0313	0.90625	65	0.71875	0.25	0.125	0.0625
25	0.0625	0.0938	0.0625	0.78125	66	0.75	0.0625	0.0625	0.125
26	0.0625	0.0938	0.0625	0.90625	67	0.75	0.0625	0.0625	0.90625
27	0.0625	0.0938	0.0938	0.875	68	0.75	0.0625	0.0938	0.0938
28	0.0625	0.0938	0.78125	0.0625	69	0.75	0.0625	0.0938	0.875
29	0.0625	0.0938	0.78125	0.1875	70	0.75	0.0938	0.0938	0.84375

30	0.0625	0.125	0.0313	0.78125	71	0.75	0.21875	0.0938	0.0938
31	0.0625	0.125	0.0625	0.75	72	0.78125	0.0625	0.0313	0.125
32	0.0625	0.125	0.75	0.0625	73	0.78125	0.0625	0.0313	0.90625
33	0.0625	0.75	0.0625	0.125	74	0.78125	0.0625	0.0625	0.0938
34	0.0625	0.75	0.125	0.0625	75	0.78125	0.0938	0.0313	0.875
35	0.0625	0.78125	0.0313	0.125	76	0.78125	0.1875	0.0313	0.78125
36	0.0625	0.78125	0.0625	0.0938	77	0.78125	0.1875	0.0625	0.0938
37	0.0625	0.90625	0.0625	0.0938	78	0.8125	0.0625	0.0313	0.125
38	0.0625	0.90625	0.125	0.0625	79	0.8125	0.0625	0.0313	0.875
39	0.0625	0.90625	0.40625	0.0938	80	0.8125	0.0938	0.0313	0.84375
40	0.0625	0.90625	0.75	0.0625	81	0.8125	0.15625	0.0313	0.125
41	0.0938	0.0938	0.75	0.0625	82	0.8125	0.15625	0.0313	0.78125

Table 1.5: Separator AR facet-defining vertices for 1/32 discretization

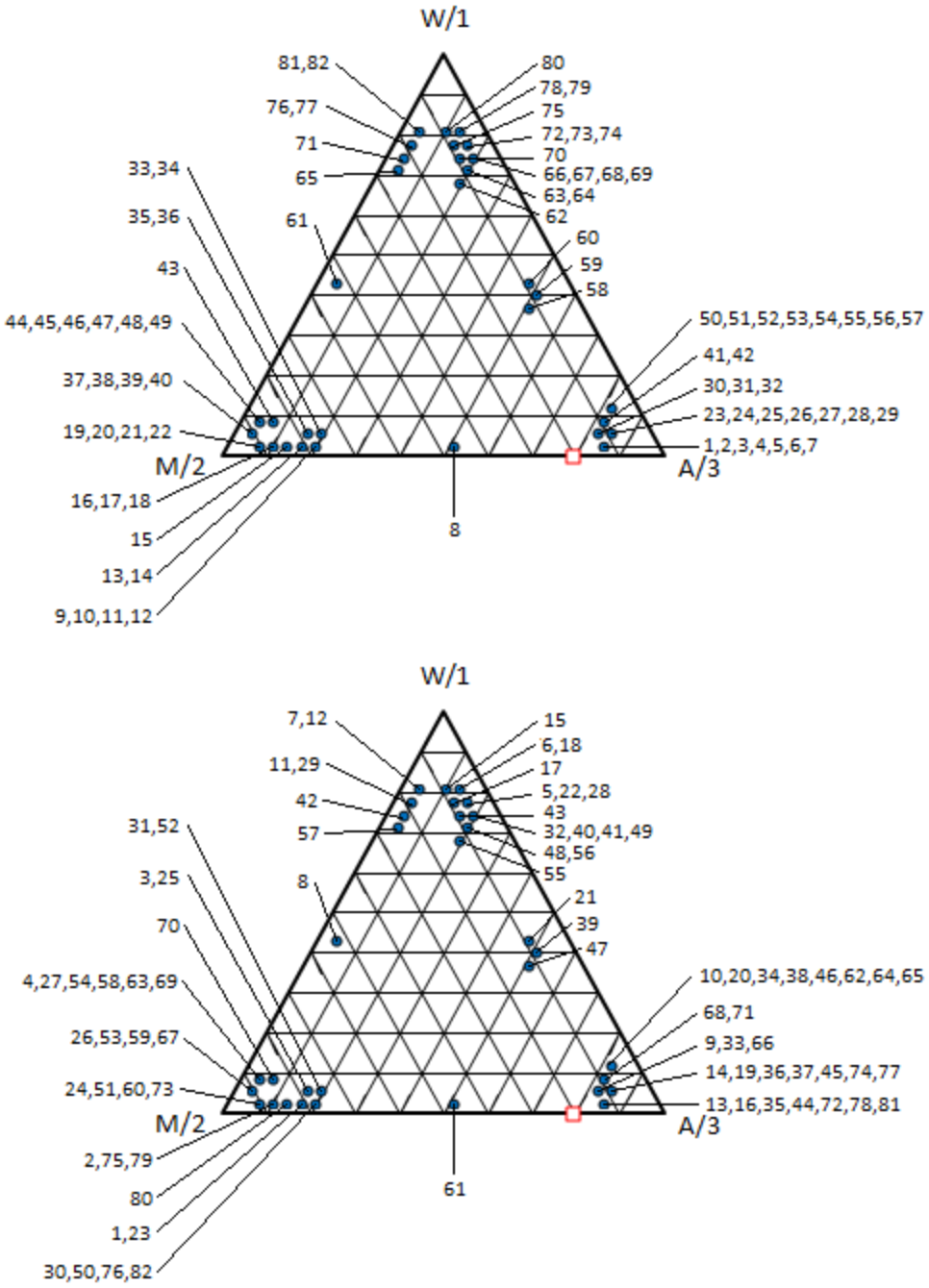

Figure 1.2: Ternary diagrams for network product streams 1 and 2

Example 2:

In this example, we seek to identify the process network AR for a separation network with one inlet stream ($S=1$) and two outlet streams ($Q=2$) in which the network inlet stream

has a molar flowrate of 3 mol/s and mole fractions of 0.3, 0.35, and 0.35 for species 1, 2, and 3, respectively; i.e. $F_1^U = 3\,\frac{mol}{s}$, $x_1^U = \begin{bmatrix} x_{1,1}^U & x_{1,2}^U & x_{1,3}^U \end{bmatrix}^T = \begin{bmatrix} 0.3 & 0.35 & 0.35 \end{bmatrix}^T$. We desire to separate this mixture into two outlet streams, one with molar flowrate of 1 mol/s, and the other with molar flowrate of 2 mol/s ($F_1^Y = 1\frac{mol}{s}, F_2^Y = 2\frac{mol}{s} \Rightarrow \alpha_1^Y = \frac{1}{3}, \alpha_2^Y = \frac{2}{3}$), and mole fractions $\begin{bmatrix} x_{1,1}^Y & x_{1,2}^Y & x_{1,3}^Y \end{bmatrix}^T$, $\begin{bmatrix} x_{2,1}^Y & x_{2,2}^Y & x_{2,3}^Y \end{bmatrix}^T$ to be determined.

As in example 1, all mole fractions must be in $[0,1]$, the summation property of mole fractions must hold, and the total balances on species 1 and 2 must also hold. Then we can ease the computational burden of quantifying $AR_{\left\{\alpha_i^Y\right\}_{i=1}^Q, \left\{\left(\alpha_i^U, x_i^U\right)\right\}_{i=1}^S}$ by reducing its dimensionality from six to two and creating a set of conditions for identifying the initial superset containing it. This is identified in a similar manner as before:

$$\left\{ \begin{array}{l} 0 \le x_{1,1}^Y \le 1 \\ 0 \le x_{1,2}^Y \le 1 \\ 0 \le 1 - x_{1,1}^Y - x_{1,2}^Y \le 1 \\ \frac{F_1^U}{F_1^Y} x_{1,1}^U \ge x_{1,1}^Y \ge \frac{F_1^U}{F_1^Y} x_{1,1}^U - \frac{F_2^Y}{F_1^Y} \\ \frac{F_1^U}{F_1^Y} x_{1,2}^U \ge x_{1,2}^Y \ge \frac{F_1^U}{F_1^Y} x_{1,2}^U - \frac{F_2^Y}{F_1^Y} \\ \frac{F_1^U}{F_1^Y} x_{1,1}^U + \frac{F_1^U}{F_1^Y} x_{1,2}^U - \frac{F_2^Y}{F_1^Y} \le x_{1,1}^Y + x_{1,2}^Y \le \frac{F_1^U}{F_1^Y} x_{1,1}^U + \frac{F_1^U}{F_1^Y} x_{1,2}^U \end{array} \right\} \quad (21)$$

For our known values $\left(F_1^U = 3, F_1^Y = 1, F_2^Y = 2, x_{1,1}^U = 0.3, x_{1,2}^U = 0.35\right)$, constraint set (21) becomes:

$$\left\{\begin{array}{l} 0 \le x_{1,1}^{Y} \le 1 \\ 0 \le x_{1,2}^{Y} \le 1 \\ 0 \le 1 - x_{1,1}^{Y} - x_{1,2}^{Y} \le 1 \\ -1.1 \le x_{1,1}^{Y} \le 0.9 \\ -0.95 \le x_{1,2}^{Y} \le 1.05 \\ -0.05 \le x_{1,1}^{Y} + x_{1,2}^{Y} \le 1.95 \end{array}\right\} \quad (22)$$

It should be noted that this 2D superset is different from the 4D superset identified earlier. In fact, the 4D superset is a subset of the 2D superset (when the latter is considered in the 4D space).

To approximate solution of the ILP for $AR_{\left\{\alpha_i^Y\right\}_{i=1}^{Q},\left\{\left(\alpha_i^U, x_i^U\right)\right\}_{i=1}^{S}}$ quantification, we consider only a finite number of values for the network outlet mole fractions and the VLE separator sub-vector parameters. Again, for the i^{th} VLE separator, outlet 1 species 1 and species 2 mole fractions $\left(x_{i,1,1}^{W}, x_{i,1,2}^{W}\right)$ are chosen as the two design parameters. Discretization levels of 1/16, 1/32, 1/64, and 1/128 for $\left(x_{i,1,1}^{W}, x_{i,1,2}^{W}\right)$ and for the network outlets $\left(x_{1,1}^{Y}, x_{1,2}^{Y}\right)$ are employed.

The 2D approximate ARs for the above discretization levels are all illustrated graphically in Figure 1.3. Additionally, the AR superset is also depicted. Table 1.6 shows the vertex points for the approximate AR corresponding to the 1/128 discretization level.

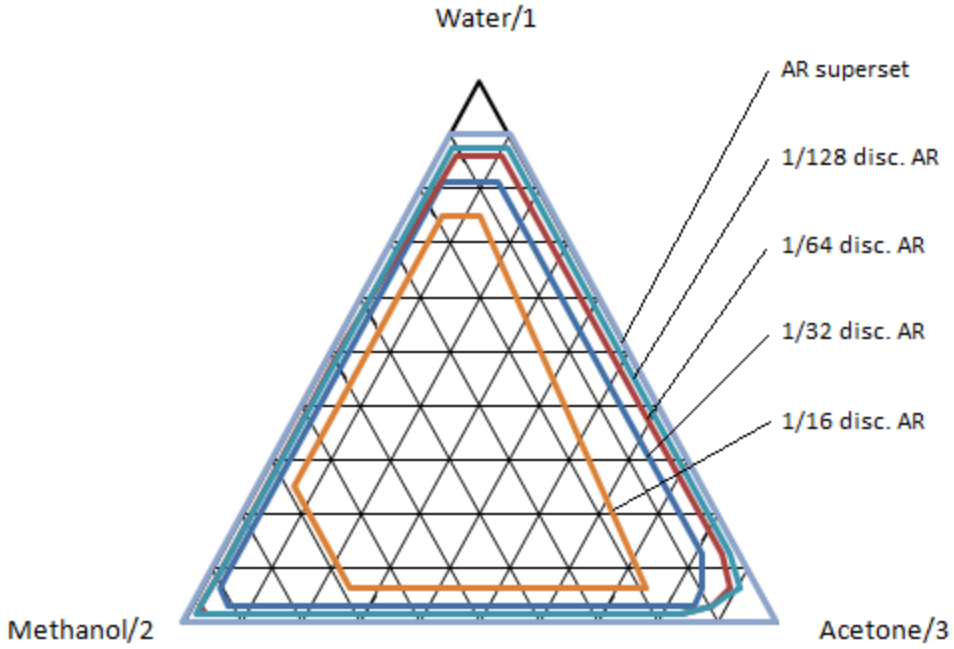

Figure 1.3: 2-D AR approximants and AR superset

#	$X^{Y}_{1,1}$	$X^{Y}_{1,2}$
1	0.015625	0.15625
2	0.015625	0.96875
3	0.03125	0.09375
4	0.03125	0.95313
5	0.046875	0.0625
6	0.0625	0.03125
7	0.09375	0.89063
8	0.125	0.015625
9	0.875	0.015625
10	0.875	0.10938

Table 1.6: AR vertices for 1/128 discretization

The boundary of the true AR is guaranteed to be within the region contained by the boundary of the aforementioned material balance derived superset, and the largest AR approximant provided by IDEAS.

Section 1.4: Discussion/Conclusions

In the 4D case study presented above, both numerical and graphical representations are shown, of a one-inlet, three-outlet VLE separator network AR. The numerical and graphical AR representations in Table 1.5 and Figure 1.2 can be utilized to rigorously address a variety of questions that a design engineer may pose.

"Is a particular combination of product compositions attainable by some one-inlet, three-outlet VLE separator network with the given flowrate specifications?" For example, consider the following product compositions: $\begin{bmatrix} x_{1,1}^{Y} & x_{1,2}^{Y} & x_{1,3}^{Y} \end{bmatrix}^{T} = \begin{bmatrix} 0.2969 & 0.3125 & 0.3906 \end{bmatrix}^{T}$,

$\begin{bmatrix} x_{2,1}^{Y} & x_{2,2}^{Y} & x_{2,3}^{Y} \end{bmatrix}^{T} = \begin{bmatrix} 0.156275 & 0.46875 & 0.374975 \end{bmatrix}^{T}$,

$\begin{bmatrix} x_{3,1}^{Y} & x_{3,2}^{Y} & x_{3,3}^{Y} \end{bmatrix}^{T} = \begin{bmatrix} 0.446825 & 0.26875 & 0.284425 \end{bmatrix}^{T}$. To answer whether a one-inlet, three-outlet VLE separator network with outlet product flowrates equal to $1 mol/s$ and these product compositions exists, one can identify using linear programming whether the point $\left(0.2969, 0.3125, 0.156275, 0.46875\right)$ under consideration can be written as a convex combination of the vertices identified in Table 1.5. For this example, this is indeed the case, since the above point can be written as an equally-weighted combination of vertices 1,8,61, and 62. Graphically, as illustrated in Figure 1.4, the point under consideration is the midpoint of the segment defined by the midpoints of the segments connecting vertices 61 and 8, and vertices 62 and 1, respectively, in each of the two ternary diagrams.

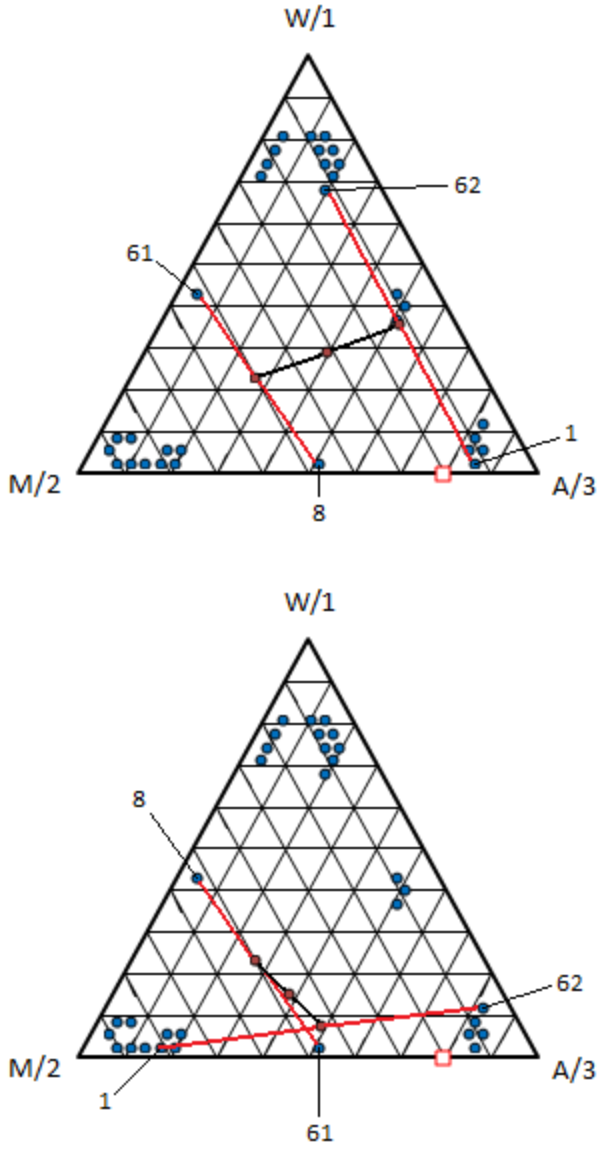

Figure 1.4: Graphical assessment of product feasibility

"What is the highest mole fraction of acetone that is attainable by some one-inlet, three-outlet VLE separator network with the given flowrate specifications?" Consulting Table 1.5 and Figure 1.2, suggests that product streams with flowrates all equal to $1 mol/s$ and compositions $\begin{bmatrix} x_{1,1}^{Y} & x_{1,2}^{Y} & x_{1,3}^{Y} \end{bmatrix}^{T} = \begin{bmatrix} 0.0313 & 0.125 & 0.8437 \end{bmatrix}^{T}$, $\begin{bmatrix} x_{2,1}^{Y} & x_{2,2}^{Y} & x_{2,3}^{Y} \end{bmatrix}^{T} = \begin{bmatrix} 0.0313 & 0.875 & 0.0937 \end{bmatrix}^{T}$, $\begin{bmatrix} x_{3,1}^{Y} & x_{3,2}^{Y} & x_{3,3}^{Y} \end{bmatrix}^{T} = \begin{bmatrix} 0.8374 & 0.05 & 0.1126 \end{bmatrix}^{T}$ are attainable. In turn, this suggests that there

exists a network that can deliver a product stream with flowrate $1 mol/s$ and an acetone mole fraction of 0.8437. This acetone mole fraction is higher than the acetone mole fraction (0.791) of the acetone/methanol binary azeotrope. The IDEAS methodology is in fact able to identify such a feasible separator network; it is presented in Tables 1.7 and 1.8 in Appendix 1.B. Table 1.7 shows all network streams, including their inlet/outlet/VLE separator destinations and sources, and each stream's flowrate. Table 1.8 lists all VLE separators employed in the network, with their operating temperatures and exit compositions. The network generated incorporates several columns of various sizes, and other complex structures. In the 2D case study presented above, Figure 1.3 shows graphical representations of one-inlet, two-outlet VLE separator network AR approximants for discretization levels of 1/16, 1/32, 1/64, and 1/128. In addition, the AR superset is also depicted. This graphical representation can be utilized to rigorously address a variety of questions that a design engineer may pose.

"Is a particular combination of product compositions attainable by some one-inlet, two-outlet VLE separator network with the given flowrate specifications?" In this case, the answer can be obtained through simple inspection as to whether the composition under consideration belongs to the AR identified in Figure 1.3.

"What is the highest mole fraction of acetone that is attainable by some one-inlet, two-outlet VLE separator network with the given flowrate specifications?" Consulting Table 1.6 and Figure 1.3, suggests that product streams with flowrates equal to $1 mol/s$ and $2 mol/s$ and compositions $\begin{bmatrix} x_{1,1}^{Y} & x_{1,2}^{Y} & x_{1,3}^{Y} \end{bmatrix}^{T} = \begin{bmatrix} 0.0625 & 0.03125 & 0.90625 \end{bmatrix}^{T}$ and $\begin{bmatrix} x_{2,1}^{Y} & x_{2,2}^{Y} & x_{2,3}^{Y} \end{bmatrix}^{T} = \begin{bmatrix} 0.41875 & 0.509375 & 0.071875 \end{bmatrix}^{T}$, respectively, are attainable. In turn, this suggests that there exists a network that can deliver a product stream with flowrate equal to $1 mol/s$ and an acetone mole fraction of 0.90625. This acetone mole fraction is higher than the

acetone mole fraction (0.791) of the acetone/methanol binary azeotrope, and is higher than the highest acetone mole fraction 0.8437 of the 4D AR. Since a simple distillation column is a one-inlet two-outlet VLE separation network, the 2D AR should contain all compositions attainable by a simple distillation column with specified top and bottom flowrate production. Indeed, an extensive parametric study was carried out in commercial simulator UNISIM by Honeywell. The results of the study are summarized in Table 1.9 in Appendix 1.C and suggest that the highest acetone mole fraction that can be attained by a conventional distillation column is 0.795. This confirms that the 2D AR encompasses all product compositions attainable by a simple distillation column.

Appendix 1.A illustrates how the 2D projections of the 4D AR evolve as the stream 1 compositions change. For example, the first nine templates of Appendix 1.A illustrate these 2D projections for the second stream outlet compositions as $x_{1,2}^{Y}$ varies from 0.1875 to 0.6875 for $x_{1,1}^{Y} = 0.0625$. As expected from physical intuition, at the endpoints of the $x_{1,2}^{Y}$ interval, the region of possible stream 2 mole fractions is smaller than those for the interval's interior points. In addition, as the value of $x_{1,2}^{Y}$ increases, the range of $x_{2,2}^{Y}$ in the 2D projection decreases, where at $x_{1,2}^{Y} = 0.6875$, $x_{2,2}^{Y}$ is effectively fixed.

The proposed process network AR framework with inlet/outlet flowrate ratio specifications is a novel concept that allows the quantification of all attainable compositions by general process networks that feature multiple inlets and outlets and possess known feed and product flowrate ratios. The aforementioned AR is shown rigorously to be a convex set in an appropriately-defined composition space. In turn, this convexity property is crucial in identifying

increasingly accurate approximants of the process network AR through application of the IDEAS conceptual framework.

Having elaborated on the novel concept of process network AR, it is important to also comment on the IDEAS conceptual framework, which plays such a key role in the quantification of the aforementioned AR. The IDEAS framework is applicable to the general process network synthesis problem. To date, we have not yet identified a single chemical process to which the framework is not applicable. The computational complexity of IDEAS grows with the number of variables needed to specify the performance of a process unit. This number is typically equal to the number of species and process unit design variables. Therefore, the approach can be effectively employed for the design of complex systems, as long as the number of species present in these systems is not large.

The IDEAS model can be written as an equation $Ax = b$ involving the linear transformation A from one infinite-dimensional space to another. The domain of A is the non-negative orthant of the space of absolutely summable sequences whose elements are the network flows. It is also true that the resulting feasible region defined by $Ax = b,\ x \geq 0$ in this infinite-dimensional space is a convex set. However, the convexity of this aforementioned feasible region has nothing to do with the convexity of the attainable region defined here, which lives in the low-dimensional space whose dimension is $\left(N_s - 1\right) \times \left(N_c - 1\right)$, where N_s is the number of network outlet streams, and N_c is the number of components (species). As various outlet concentrations are considered, the entries of b are altered, and feasibility of $Ax = b,\ x \geq 0$ is assessed. It is the union of all outlet concentrations that lead to feasible $Ax = b,\ x \geq 0$ that forms the attainable region introduced in this work and is shown to be a convex subset of $\Re^{\left(N_s - 1\right) \times \left(N_c - 1\right)}$.

Notation

Symbols

α_i^U : Molar flow rate ratio of the ith process network inlet stream, $i = 1, S$

α_i^Y : Molar flow rate ratio of the ith process network inlet stream, $i = 1, Q$

Letters

$f_{i,j}^X$: Species molar flow rate vector $\left(\left[\frac{mol\,1}{s} \quad \cdots \quad \frac{mol\,n}{s} \right]^{\mathrm{T}} \right)$ inlet to the jth inlet stream of the ith process unit in OP, $j = 1, s \quad i = 1, \infty$

F_j^U : Total molar flow rate $\left(\frac{mol}{s} \right)$ of the jth network inlet stream, $j = 1, S$

$F_{i,j}^W$: Total molar flow rate $\left(\frac{mol}{s} \right)$ of the jth outlet stream from the ith process unit in OP, $j = 1, q \quad i = 1, \infty$

$F_{i,j}^X$: Total molar flow rate $\left(\frac{mol}{s} \right)$ of the jth inlet stream to the ith process unit in OP, $j = 1, s \quad i = 1, \infty$

F_j^Y : Total molar flow rate $\left(\frac{mol}{s} \right)$ of the jth network outlet stream, $j = 1, Q$

$F_{j,i}^{YU}$: Total molar flow rate $\left(\frac{mol}{s} \right)$ to the jth network outlet stream from the ith network inlet stream, $j = 1, Q \quad i = 1, S$

$F_{j,i,k}^{YW}$: Total molar flow rate $\left(\frac{mol}{s}\right)$ to the jth network outlet stream from the kth outlet stream of the ith process unit, $j=1,Q, \quad i=1,\infty \quad k=1,q$

$F_{i,k,j}^{XU}$: Total molar flow rate $\left(\frac{mol}{s}\right)$ to the kth inlet stream of the ith process unit from the jth network inlet stream, $i=1,\infty \quad k=1,s \quad j=1,S$

$F_{j,l,i,k}^{XW}$: Total molar flow rate $\left(\frac{mol}{s}\right)$ to the lth inlet stream of the jth process unit from the kth outlet stream of the ith process unit. $j=1,\infty \quad l=1,s \quad i=1,\infty \quad k=1,q$

P : Pressure (bar)

q : Total number of outlets to each process unit in the process network

Q : Total number of outlet streams from the IDEAS process network

R : Gas constant $\left(8.314 \cdot 10^{-2} \ \frac{L \cdot bar}{mol \cdot K}\right)$

s : Total number of inlets to each process unit in the process network

S : Total number of inlet streams to the IDEAS process network

T : Temperature (K)

x_j^U : Molar fraction vector of the jth network inlet stream, $j=1,S$

$x_{i,j}^W$: Molar fraction vector of the jth liquid outlet stream from the ith process unit in OP, $j=1,q \quad i=1,\infty$

x_j^Y : Molar fraction vector of the jth network outlet stream, $j=1,Q$

$x_{i,j}^X$: Molar fraction vector of the jth inlet stream to the ith process unit in OP, $j=1,s \quad i=1,\infty$

Superscripts

U : Network inlet

X : Process unit inlet

Y : Network outlet

W : Process unit outlet

Appendix 1.A.

Figures 1.5-1.9 show 2D projections of the 4D approximate AR quantified using 1/16 discretization for $\left(x_{1,1}^{Y}, x_{1,2}^{Y}, x_{2,1}^{Y}, x_{2,2}^{Y}\right), \left(x_{i,1,1}^{W}, x_{i,1,2}^{W}\right)$.

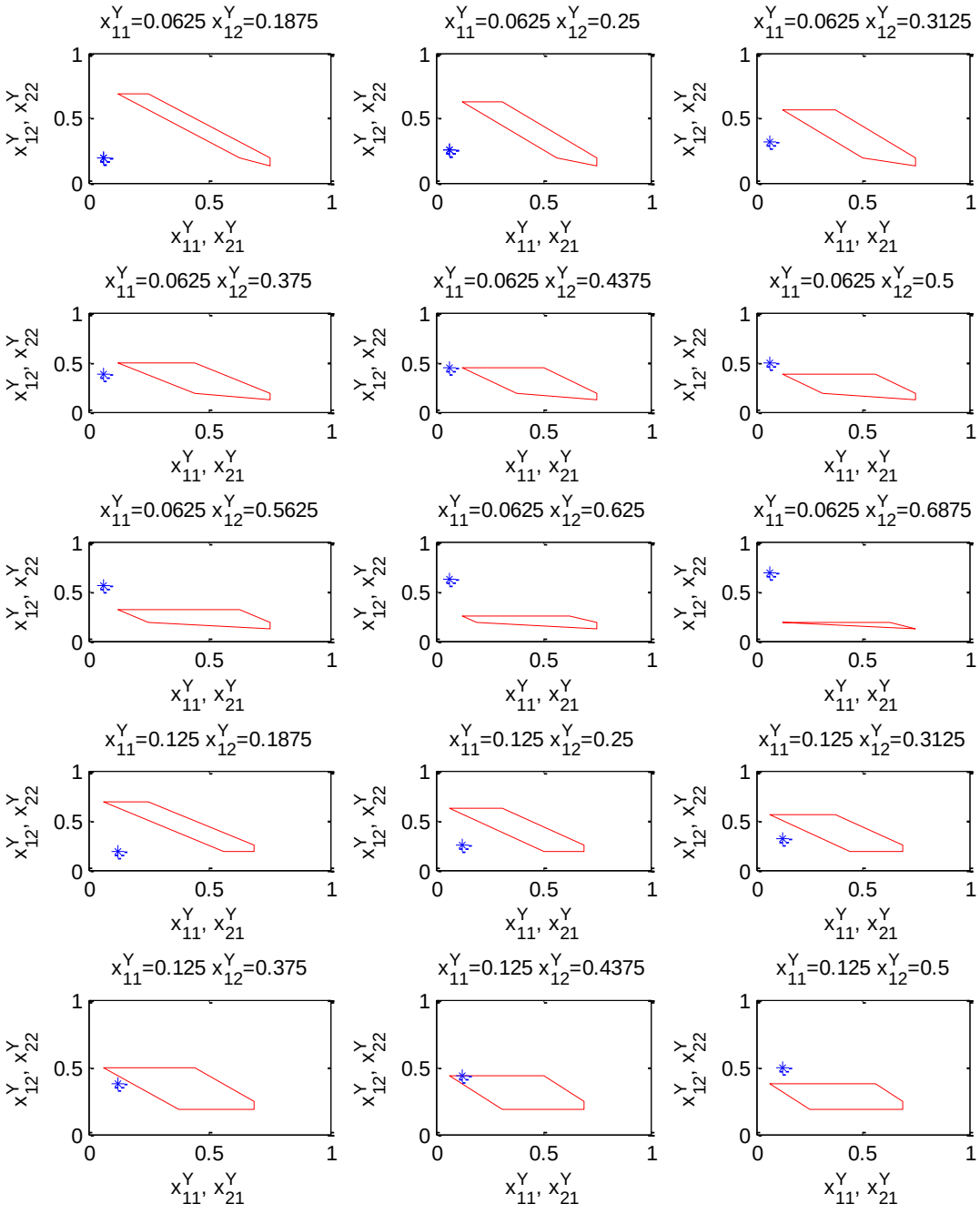

Figure 1.5: 2D projections of the 4D approximate AR quantified using 1/16 discretization (part 1 of 5)

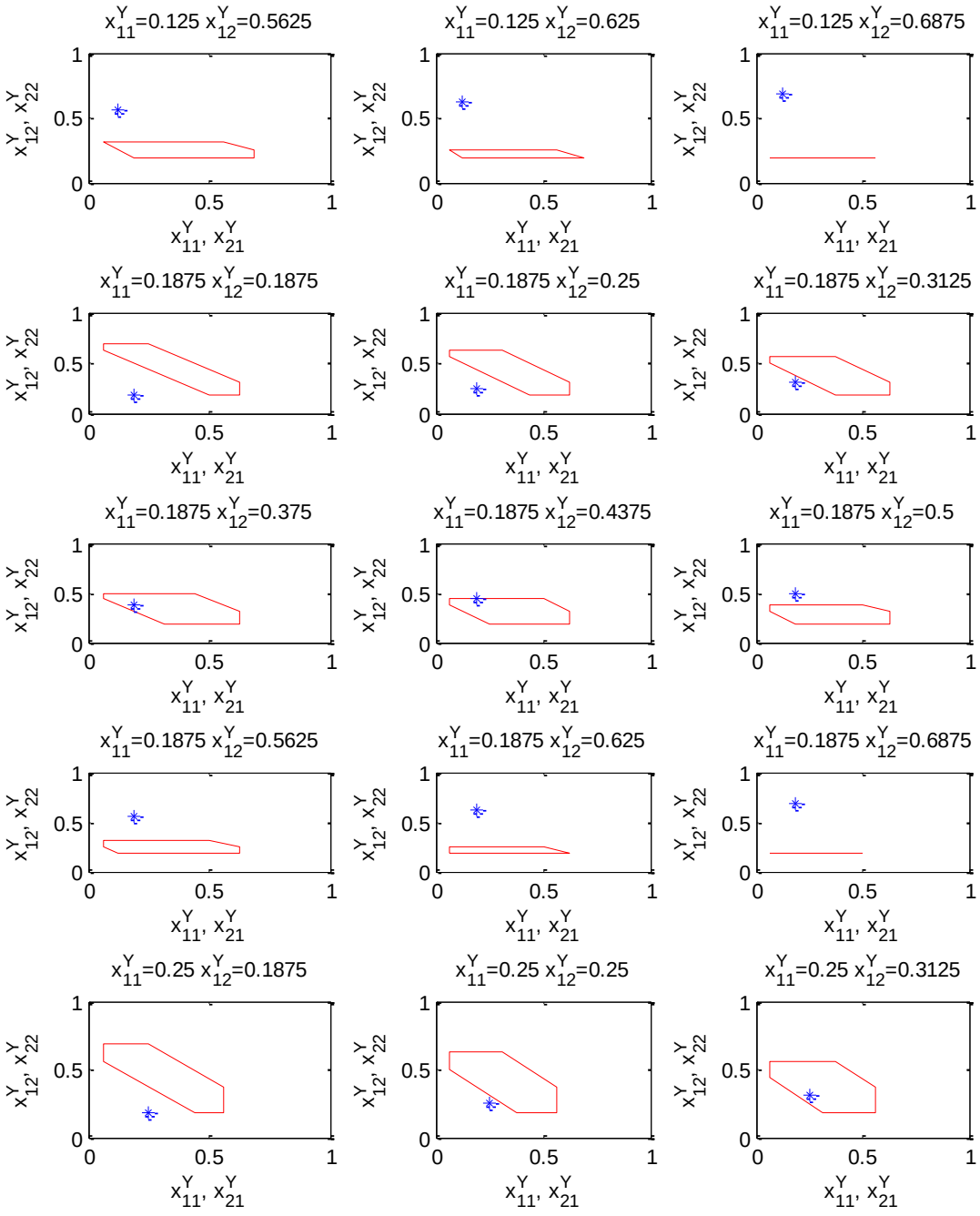

Figure 1.6: 2D projections of the 4D approximate AR quantified using 1/16 discretization (part 2 of 5)

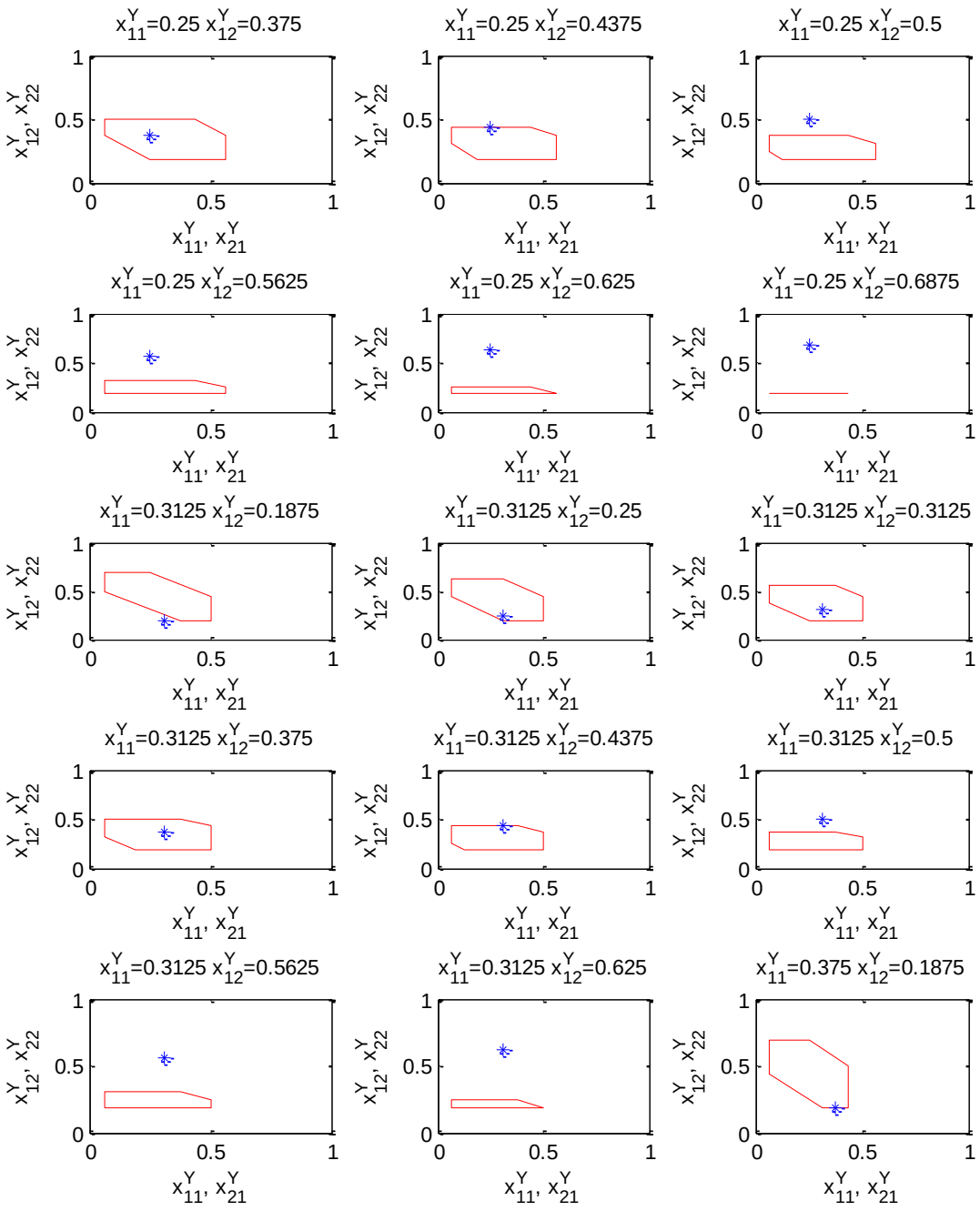

Figure 1.7: 2D projections of the 4D approximate AR quantified using 1/16 discretization (part 3 of 5)

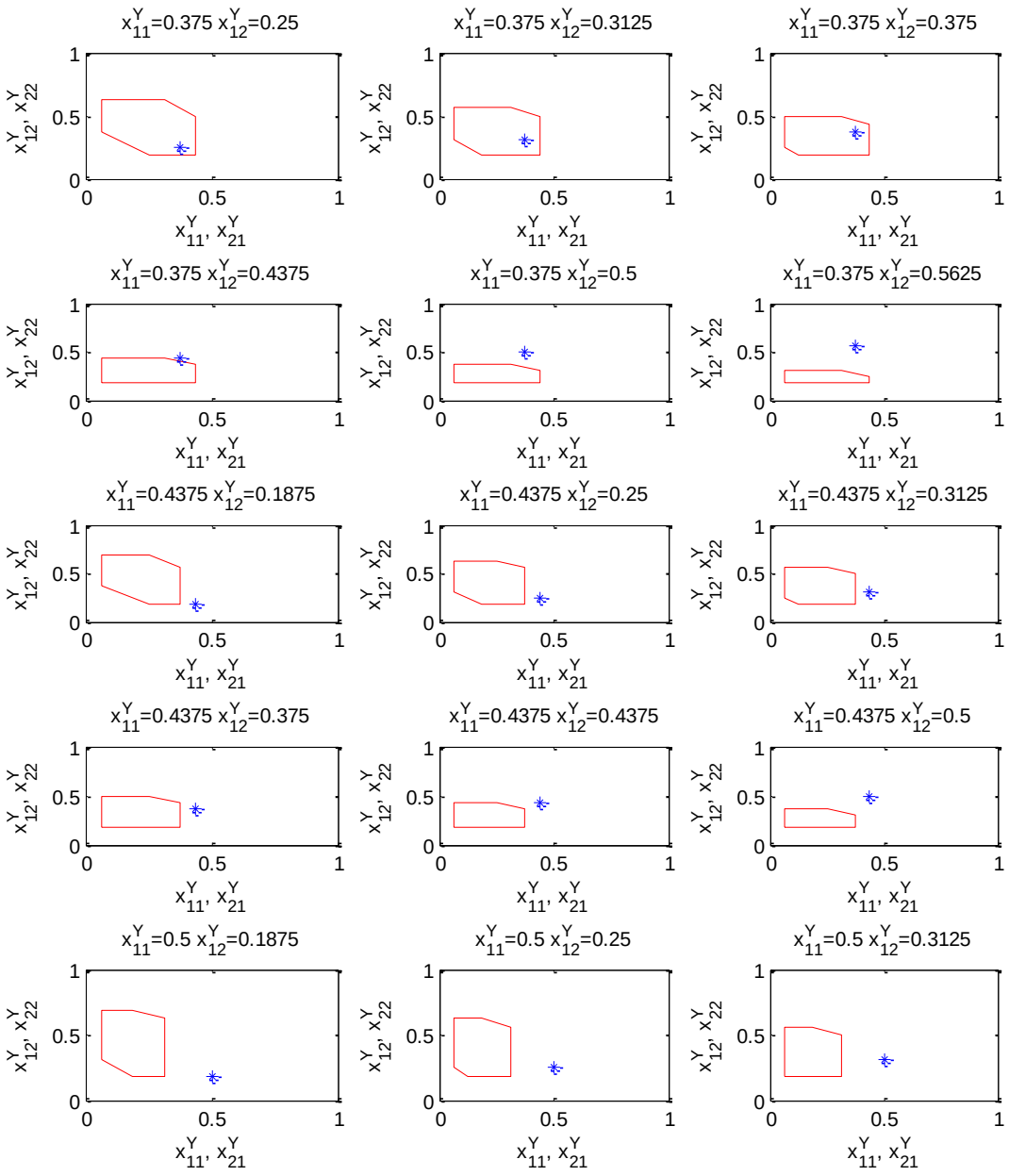

Figure 1.8: 2D projections of the 4D approximate AR quantified using 1/16 discretization (part 4 of 5)

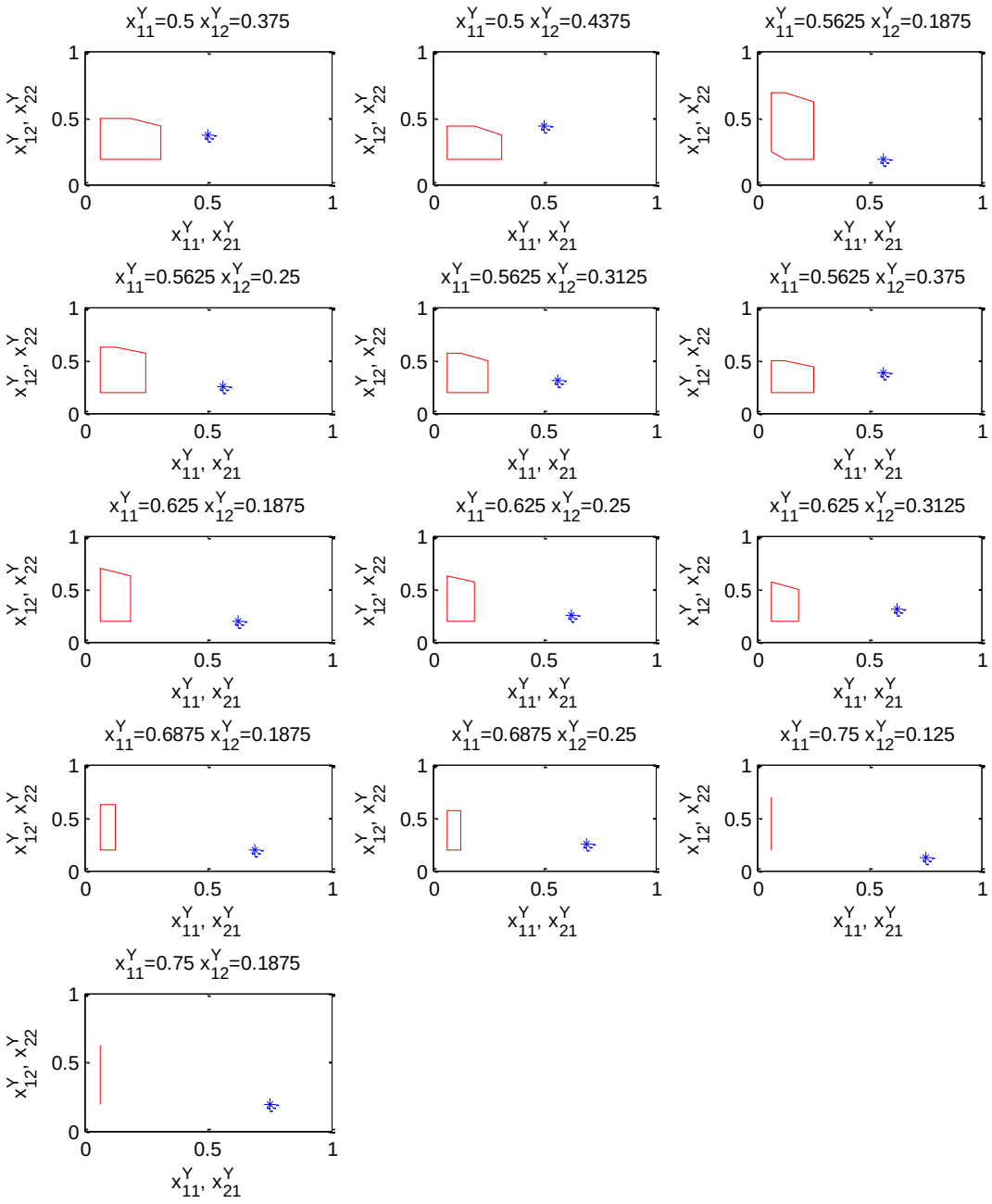

Figure 1.9: 2D projections of the 4D approximate AR quantified using 1/16 discretization (part 4 of 5)

Appendix 1.B.

Table 1.7 and Table 1.8 list an IDEAS-generated feasible VLE network configuration for the point product streams with flowrates all equal to $1 mol/s$ and compositions $\left[x_{1,1}^{Y} \quad x_{1,2}^{Y} \quad x_{1,3}^{Y}\right]^{T} = \left[0.0313 \quad 0.125 \quad 0.8437\right]^{T}$, $\left[x_{2,1}^{Y} \quad x_{2,2}^{Y} \quad x_{2,3}^{Y}\right]^{T} = \left[0.0313 \quad 0.875 \quad 0.0937\right]^{T}$, $\left[x_{3,1}^{Y} \quad x_{3,2}^{Y} \quad x_{3,3}^{Y}\right]^{T} = \left[0.8374 \quad 0.05 \quad 0.1126\right]^{T}$. Table 1.7 shows all network streams, including their inlet/outlet/VLE separator destinations and sources, and each stream's flowrate. Table 1.8 lists all VLE separators employed in the network, with their operating temperatures and exit compositions.

Stream #	Type	Dest.	Source	Flowrate	Stream #	Type	Dest.	Source	Flowrate
1	FXU	41	Inlet 1	0.025601273	177	FXW1	115	63	0.477508051
2	FXU	74	Inlet 1	1.073101297	178	FXW1	115	97	0.632153845
3	FXU	82	Inlet 1	0.505750201	179	FXW1	115	104	1.828670108
4	FXU	99	Inlet 1	0.589710595	180	FXW1	115	114	3.570144406
5	FXU	113	Inlet 1	0.80583663	181	FXW1	116	108	3.312313154
6	FYW2	Outlet1	2	0.290348384	182	FXW1	116	115	3.766865006
7	FYW2	Outlet1	19	0.419084135	183	FXW1	117	86	1.453216878
8	FYW2	Outlet1	20	0.29056748	184	FXW1	117	110	0.799170949
9	FYW1	Outlet2	17	0.996392739	185	FXW1	117	116	2.325703317
10	FYW1	Outlet2	34	0.001992062	186	FXW2	2	3	0.397021459
11	FYW2	Outlet2	33	0.0016152	187	FXW2	2	20	0.38516223
12	FYW1	Outlet3	110	0.371885657	188	FXW2	3	4	0.384044757
13	FYW1	Outlet3	116	0.228113709	189	FXW2	3	21	0.116518064
14	FYW1	Outlet3	117	0.400000634	190	FXW2	4	5	0.316227892
15	FXW1	3	2	0.491835285	191	FXW2	4	23	0.851300118
16	FXW1	7	54	0.188854384	192	FXW2	5	6	0.238451337
17	FXW1	8	7	0.882431694	193	FXW2	5	24	0.382759133
18	FXW1	9	8	1.203431356	194	FXW2	6	7	0.416086711
19	FXW1	10	9	2.010337308	195	FXW2	6	40	0.182505559
20	FXW1	11	10	1.482266564	196	FXW2	7	8	2.529760072
21	FXW1	13	11	0.395978404	197	FXW2	7	26	0.889407201
22	FXW1	14	12	0.662086058	198	FXW2	8	9	2.57829769
23	FXW1	14	13	0.023228666	199	FXW2	8	27	1.255730875
24	FXW1	15	13	0.810607318	200	FXW2	8	43	0.486323609

25	FXW1	16	14	0.68690578	201	FXW2	8	66	0.088275879
26	FXW1	16	15	0.028019254	202	FXW2	9	10	2.804739755
27	FXW1	18	17	0.426919956	203	FXW2	9	28	0.533142651
28	FXW1	20	19	0.610784287	204	FXW2	9	44	0.718685941
29	FXW1	21	3	0.595376663	205	FXW2	10	11	2.159597508
30	FXW1	21	20	1.019156895	206	FXW2	10	29	1.418995188
31	FXW1	22	21	0.852493006	207	FXW2	11	12	0.830953851
32	FXW1	23	4	0.78348326	208	FXW2	11	13	1.17098543
33	FXW1	24	5	0.304982584	209	FXW2	11	30	0.339333664
34	FXW1	24	23	0.015674673	210	FXW2	12	14	0.327253733
35	FXW1	26	7	1.422385327	211	FXW2	12	31	1.165786181
36	FXW1	27	8	1.557868352	212	FXW2	13	14	0.750018054
37	FXW1	27	26	0.408847636	213	FXW2	13	15	0.09538801
38	FXW1	28	9	0.671364681	214	FXW2	13	32	0.763436965
39	FXW1	28	27	0.242237841	215	FXW2	14	15	1.078862839
40	FXW1	29	10	1.301923728	216	FXW2	15	16	1.178602844
41	FXW1	29	28	0.066651258	217	FXW2	16	17	1.32197857
42	FXW1	30	11	0.186231173	218	FXW2	16	49	0.168211212
43	FXW1	31	11	1.081732395	219	FXW2	17	18	0.43041733
44	FXW1	31	29	0.175557522	220	FXW2	17	33	2.67460021
45	FXW1	32	30	0.087833143	221	FXW2	18	33	0.042097153
46	FXW1	33	15	0.786940053	222	FXW2	18	34	1.138255808
47	FXW1	33	16	1.026511968	223	FXW2	19	20	0.505852481
48	FXW1	34	17	0.218140596	224	FXW2	19	35	0.524015946
49	FXW1	34	18	1.176855585	225	FXW2	20	21	1.164422618
50	FXW1	36	20	0.000676911	226	FXW2	20	36	0.426209046
51	FXW1	37	21	0.418020675	227	FXW2	21	22	0.573994127
52	FXW1	38	23	1.063261653	228	FXW2	21	37	0.37073228
53	FXW1	39	24	0.459484545	229	FXW2	22	23	0.53190921
54	FXW1	41	54	0.016155129	230	FXW2	23	24	0.278711548
55	FXW1	43	42	0.141488721	231	FXW2	23	38	1.399950866
56	FXW1	44	27	0.468747254	232	FXW2	24	25	0.184208634
57	FXW1	45	28	0.31380861	233	FXW2	24	39	0.616089334
58	FXW1	45	29	0.084906636	234	FXW2	25	7	0.157618653
59	FXW1	46	29	0.442026221	235	FXW2	25	54	0.168504774
60	FXW1	47	29	0.126645492	236	FXW2	26	66	0.097971758
61	FXW1	47	30	0.197013146	237	FXW2	29	45	0.879556065
62	FXW1	48	31	0.826821833	238	FXW2	30	46	0.437948776
63	FXW1	48	32	1.042040513	239	FXW2	31	47	0.735318091
64	FXW1	49	32	0.1312026	240	FXW2	32	48	1.848846914
65	FXW1	50	33	2.180156604	241	FXW2	33	17	0.141585691
66	FXW1	50	34	0.254748314	242	FXW2	33	50	2.943431461

67	FXW1	51	35	0.342829151	243	FXW2	35	51	0.829741434
68	FXW1	52	36	0.248251537	244	FXW2	35	52	0.037103693
69	FXW1	53	21	0.007805616	245	FXW2	36	52	0.614354092
70	FXW1	54	73	0.132915213	246	FXW2	36	53	0.059429576
71	FXW1	55	64	1.002215997	247	FXW2	37	95	0.074938263
72	FXW1	57	44	0.209332649	248	FXW2	38	63	0.653537243
73	FXW1	58	45	0.496132292	249	FXW2	38	72	0.689689837
74	FXW1	59	46	0.823935433	250	FXW2	39	40	0.025283155
75	FXW1	59	47	0.008870187	251	FXW2	39	73	0.775188485
76	FXW1	60	47	0.035314391	252	FXW2	40	7	0.084311382
77	FXW1	60	48	0.018033187	253	FXW2	40	74	0.310661704
78	FXW1	61	48	0.188116707	254	FXW2	41	26	0.121727088
79	FXW1	61	49	0.056430827	255	FXW2	42	43	0.364281346
80	FXW1	61	50	0.890022633	256	FXW2	42	66	2.110303334
81	FXW1	62	116	0.000807198	257	FXW2	43	67	1.754106195
82	FXW1	63	103	0.088704947	258	FXW2	44	57	0.430342973
83	FXW1	64	6	0.360140921	259	FXW2	44	77	0.190872932
84	FXW1	64	25	0.141914789	260	FXW2	45	58	0.476245912
85	FXW1	64	73	1.813920674	261	FXW2	45	68	0.500727216
86	FXW1	65	41	0.07627014	262	FXW2	46	78	0.81985798
87	FXW1	65	74	0.064304317	263	FXW2	47	59	0.62113424
88	FXW1	66	42	0.908783791	264	FXW2	47	69	0.100897021
89	FXW1	67	43	1.044989977	265	FXW2	48	60	0.028430725
90	FXW1	68	44	0.161944564	266	FXW2	48	69	0.863622867
91	FXW1	69	59	0.516864361	267	FXW2	49	61	0.093439438
92	FXW1	69	70	0.639604747	268	FXW2	50	61	1.398549177
93	FXW1	70	47	0.266187231	269	FXW2	51	71	0.531883612
94	FXW1	70	48	0.705919111	270	FXW2	51	85	0.010686642
95	FXW1	70	60	0.024916853	271	FXW2	51	93	0.852147396
96	FXW1	70	61	0.751332768	272	FXW2	51	101	0.030580512
97	FXW1	71	51	0.938385902	273	FXW2	52	62	0.034930734
98	FXW1	71	117	0.027332904	274	FXW2	52	86	1.122435479
99	FXW1	72	38	1.006537857	275	FXW2	53	79	0.091588954
100	FXW1	72	97	0.25928816	276	FXW2	54	7	0.645187921
101	FXW1	73	39	0.643866853	277	FXW2	54	99	1.254120246
102	FXW1	73	89	0.690793749	278	FXW2	55	26	0.100375158
103	FXW1	74	40	0.187184382	279	FXW2	55	42	1.42431213
104	FXW1	74	54	0.709710703	280	FXW2	55	75	0.800573408
105	FXW1	75	55	1.482378152	281	FXW2	57	77	0.501847831
106	FXW1	76	66	2.493172893	282	FXW2	58	84	0.536195135
107	FXW1	78	58	0.556081519	283	FXW2	59	78	0.305192979
108	FXW1	78	69	1.079353838	284	FXW2	61	70	1.108751216

109	FXW1	79	53	0.039964995
110	FXW1	80	97	1.395979289
111	FXW1	81	89	0.320004513
112	FXW1	82	64	1.281182285
113	FXW1	83	65	0.121206754
114	FXW1	84	57	0.280837512
115	FXW1	84	68	0.341140608
116	FXW1	84	78	1.132184812
117	FXW1	85	117	0.00191989
118	FXW1	86	106	0.750284576
119	FXW1	87	62	0.019319768
120	FXW1	87	107	0.621656651
121	FXW1	88	115	0.201083347
122	FXW1	89	63	0.129226265
123	FXW1	89	72	0.576136175
124	FXW1	89	104	1.331669357
125	FXW1	90	73	2.510830887
126	FXW1	90	98	0.042928282
127	FXW1	91	66	0.040967426
128	FXW1	92	67	2.344483549
129	FXW1	92	77	0.412559319
130	FXW1	92	84	1.175537129
131	FXW1	93	71	0.433835189
132	FXW1	93	117	0.186175315
133	FXW1	94	110	0.279849525
134	FXW1	95	107	1.341726952
135	FXW1	96	102	2.06538789
136	FXW1	97	96	2.432527961
137	FXW1	97	115	0.00434133
138	FXW1	98	80	2.102554537
139	FXW1	99	81	0.368630887
140	FXW1	100	66	0.631025835
141	FXW1	100	76	2.119291549
142	FXW1	100	92	1.898894212
143	FXW1	101	117	0.02659968
144	FXW1	102	37	0.122226652
145	FXW1	102	79	0.808054397
146	FXW1	102	87	1.121769395
147	FXW1	102	107	1.266994637
148	FXW1	103	102	0.522760182
149	FXW1	104	88	0.592459676
150	FXW1	104	103	0.435165606
285	FXW2	62	87	0.053443302
286	FXW2	63	89	1.171566566
287	FXW2	64	41	0.087213352
288	FXW2	64	55	1.84509859
289	FXW2	64	82	0.78451215
290	FXW2	65	83	0.061034803
291	FXW2	66	76	1.014358872
292	FXW2	66	91	0.523239177
293	FXW2	66	109	3.015335268
294	FXW2	67	100	0.98904611
295	FXW2	67	105	2.0645537
296	FXW2	68	84	0.005632511
297	FXW2	68	92	0.674290749
298	FXW2	69	78	0.887404603
299	FXW2	73	54	0.948998371
300	FXW2	73	64	2.749402135
301	FXW2	73	90	1.043576949
302	FXW2	73	115	2.536186725
303	FXW2	74	65	0.080402508
304	FXW2	75	112	1.006281643
305	FXW2	76	109	0.640477521
306	FXW2	77	100	1.027374203
307	FXW2	77	105	0.077905891
308	FXW2	78	84	1.336025619
309	FXW2	78	92	0.173179414
310	FXW2	79	95	1.737067529
311	FXW2	79	117	0.477209759
312	FXW2	80	73	1.521852702
313	FXW2	80	98	0.961953875
314	FXW2	81	74	0.438145492
315	FXW2	83	112	0.003145134
316	FXW2	84	92	1.299227462
317	FXW2	85	101	0.015117104
318	FXW2	86	107	1.825367769
319	FXW2	87	102	2.346343756
320	FXW2	87	117	0.183933748
321	FXW2	88	104	0.983034553
322	FXW2	89	73	1.858116839
323	FXW2	89	81	0.206427796
324	FXW2	91	109	0.686308976
325	FXW2	92	100	0.113011839
326	FXW2	93	106	0.910335046

151	FXW1	105	75	1.688086386	327	FXW2	94	107	0.792236208
152	FXW1	105	83	0.063317083	328	FXW2	95	108	2.492081079
153	FXW1	105	91	0.204037219	329	FXW2	96	88	0.092916855
154	FXW1	105	100	2.519779444	330	FXW2	96	97	1.926679354
155	FXW1	106	85	0.006350353	331	FXW2	97	80	1.777231397
156	FXW1	106	93	0.678198154	332	FXW2	98	81	0.183091343
157	FXW1	106	117	0.137480759	333	FXW2	99	114	2.051247413
158	FXW1	107	94	0.488225049	334	FXW2	101	110	0.075813889
159	FXW1	107	116	1.826438323	335	FXW2	102	96	1.652456138
160	FXW1	108	22	0.810408087	336	FXW2	103	104	0.453357513
161	FXW1	108	87	0.290361418	337	FXW2	104	89	0.870990652
162	FXW1	108	95	2.021802148	338	FXW2	104	116	3.735997826
163	FXW1	108	111	1.730833988	339	FXW2	105	109	0.439735304
164	FXW1	109	105	2.772495876	340	FXW2	106	110	0.838590362
165	FXW1	110	52	0.754159926	341	FXW2	107	79	0.172487607
166	FXW1	110	101	0.056715953	342	FXW2	107	87	1.705679735
167	FXW1	110	117	0.970573819	343	FXW2	107	111	1.655151418
168	FXW1	112	74	1.237287353	344	FXW2	108	88	0.498741399
169	FXW1	112	82	1.002420324	345	FXW2	108	103	0.452247149
170	FXW1	112	99	1.755468668	346	FXW2	109	112	5.863701022
171	FXW1	112	109	3.854339829	347	FXW2	110	94	0.583860678
172	FXW1	113	90	1.510182236	348	FXW2	111	102	0.037009425
173	FXW1	113	112	3.320327604	349	FXW2	111	117	3.348975982
174	FXW1	114	89	1.048220886	350	FXW2	112	113	2.343939228
175	FXW1	114	98	1.280763691	351	FXW2	116	104	1.037882126
176	FXW1	114	113	3.292407242	352	FXW2	117	79	1.182111359

Table 1.7: List of streams in DN

T	VLE sep. #	$x^W_{i,1,1}$	$x^W_{i,1,2}$	$x^W_{i,2,1}$	$x^W_{i,2,2}$
55.49072	2	0.03125	0.15625	0.018231	0.159447
55.47973	3	0.03125	0.1875	0.017446	0.185926
55.5327	4	0.03125	0.25	0.016096	0.235561
55.67462	5	0.03125	0.3125	0.014986	0.282039
55.8985	6	0.03125	0.375	0.014071	0.326696
56.20333	7	0.03125	0.4375	0.013317	0.370757
56.59512	8	0.03125	0.5	0.012703	0.415463
57.08185	9	0.03125	0.5625	0.012216	0.462096
57.68052	10	0.03125	0.625	0.011847	0.512202
58.41611	11	0.03125	0.6875	0.011597	0.567714
58.84488	12	0.03125	0.71875	0.011519	0.598249
59.32162	13	0.03125	0.75	0.011473	0.631159
59.85332	14	0.03125	0.78125	0.011464	0.666939

60.446	15	0.03125	0.8125	0.011493	0.706136
61.11063	16	0.03125	0.84375	0.011566	0.749514
61.85822	17	0.03125	0.875	0.011689	0.797977
62.69976	18	0.03125	0.90625	0.011868	0.85259
55.90849	19	0.0625	0.09375	0.037328	0.099006
55.86252	20	0.0625	0.125	0.035665	0.12807
55.84353	21	0.0625	0.15625	0.034163	0.155635
55.85052	22	0.0625	0.1875	0.032805	0.18194
55.93448	23	0.0625	0.25	0.030455	0.231585
56.10538	24	0.0625	0.3125	0.028516	0.27849
56.35925	25	0.0625	0.375	0.026915	0.323965
57.12982	26	0.0625	0.5	0.024548	0.415657
57.66753	27	0.0625	0.5625	0.023731	0.464613
58.33316	28	0.0625	0.625	0.023148	0.517899
59.15671	29	0.0625	0.6875	0.022808	0.577779
59.64144	30	0.0625	0.71875	0.022738	0.611144
60.18214	31	0.0625	0.75	0.02274	0.647403
60.78881	32	0.0625	0.78125	0.022823	0.687217
63.10754	33	0.0625	0.875	0.023665	0.836459
64.09499	34	0.0625	0.90625	0.024201	0.900261
56.60311	35	0.125	0.0625	0.068274	0.064823
56.56713	36	0.125	0.09375	0.065523	0.094599
56.57113	37	0.125	0.15625	0.060753	0.150072
56.75303	38	0.125	0.25	0.055093	0.226133
56.9839	39	0.125	0.3125	0.052122	0.274147
57.30473	40	0.125	0.375	0.04969	0.321563
57.7235	41	0.125	0.4375	0.047743	0.36975
58.2562	42	0.125	0.5	0.046257	0.420262
58.92583	43	0.125	0.5625	0.045231	0.474969
59.76737	44	0.125	0.625	0.044697	0.536332
60.82879	45	0.125	0.6875	0.044722	0.607735
61.46244	46	0.125	0.71875	0.04498	0.648663
62.18105	47	0.125	0.75	0.045436	0.694207
62.9966	48	0.125	0.78125	0.046116	0.745391
63.92709	49	0.125	0.8125	0.047064	0.80363
64.9925	50	0.125	0.84375	0.048333	0.870719
57.24976	51	0.1875	0.0625	0.090843	0.062657
57.24576	52	0.1875	0.09375	0.087693	0.09179
57.26675	53	0.1875	0.125	0.084822	0.119744
58.29418	54	0.1875	0.375	0.069604	0.323178
58.82089	55	0.1875	0.4375	0.067581	0.37521
61.45544	57	0.1875	0.625	0.065925	0.567042
62.88066	58	0.1875	0.6875	0.067317	0.656033

63.75018	59	0.1875	0.71875	0.068546	0.709079
64.74963	60	0.1875	0.75	0.070225	0.769821
65.905	61	0.1875	0.78125	0.072457	0.840411
57.98435	62	0.25	0.125	0.102785	0.11811
58.4441	63	0.25	0.25	0.093449	0.223671
59.3546	64	0.25	0.375	0.08769	0.329141
60.03323	65	0.25	0.4375	0.086151	0.386521
60.91274	66	0.25	0.5	0.085624	0.450503
62.05711	67	0.25	0.5625	0.086318	0.525096
63.56329	68	0.25	0.625	0.088617	0.616485
65.57418	69	0.25	0.6875	0.093177	0.734776
66.83349	70	0.25	0.71875	0.096648	0.8091
58.55904	71	0.3125	0.0625	0.124084	0.060894
59.34061	72	0.3125	0.25	0.109352	0.226503
59.85332	73	0.3125	0.3125	0.106582	0.281723
60.53495	74	0.3125	0.375	0.104938	0.34041
61.43546	75	0.3125	0.4375	0.104595	0.405587
62.6288	76	0.3125	0.5	0.105868	0.481616
64.22592	77	0.3125	0.5625	0.109317	0.5753
66.39873	78	0.3125	0.625	0.115952	0.69816
59.44655	79	0.375	0.125	0.131528	0.118926
60.30708	80	0.375	0.25	0.124231	0.232456
60.9927	81	0.375	0.3125	0.122571	0.292548
61.91519	82	0.375	0.375	0.122513	0.358883
63.16051	83	0.375	0.4375	0.124512	0.436192
67.22128	84	0.375	0.5625	0.138584	0.659551
59.88131	85	0.4375	0.0625	0.14855	0.061927
60.03123	86	0.4375	0.09375	0.146032	0.091854
60.21712	87	0.4375	0.125	0.143868	0.121441
60.70985	88	0.4375	0.1875	0.140637	0.180736
61.39748	89	0.4375	0.25	0.13901	0.242411
62.34296	90	0.4375	0.3125	0.139323	0.309929
65.45824	91	0.4375	0.4375	0.148734	0.486182
68.03883	92	0.4375	0.5	0.161109	0.618389
60.57393	93	0.5	0.0625	0.159237	0.063535
60.78981	94	0.5	0.09375	0.1573	0.094619
61.05167	95	0.5	0.125	0.155795	0.125686
61.36549	96	0.5	0.15625	0.154754	0.157105
61.73929	97	0.5	0.1875	0.154224	0.189303
62.70576	98	0.5	0.25	0.154949	0.258098
64.06801	99	0.5	0.3125	0.158809	0.33763
68.84838	100	0.5	0.4375	0.183576	0.573957
61.32352	101	0.5625	0.0625	0.169734	0.066064

62.00614	102	0.5625	0.125	0.168181	0.13225
62.4549	103	0.5625	0.15625	0.16837	0.166597
62.9926	104	0.5625	0.1875	0.169335	0.202606
69.64394	105	0.5625	0.375	0.206022	0.525232
62.18804	106	0.625	0.0625	0.1809	0.069859
62.63979	107	0.625	0.09375	0.181205	0.105429
63.18949	108	0.625	0.125	0.182427	0.142324
70.42252	109	0.625	0.3125	0.228539	0.470884
63.27944	110	0.6875	0.0625	0.194186	0.075612
63.96806	111	0.6875	0.09375	0.196905	0.115545
75.99445	112	0.78125	0.1875	0.331237	0.412111
76.70606	113	0.8125	0.15625	0.350428	0.367799
77.47064	114	0.84375	0.125	0.371359	0.317084
78.30318	115	0.875	0.09375	0.394544	0.258123
79.22268	116	0.90625	0.0625	0.420668	0.188343
80.25911	117	0.9375	0.03125	0.450774	0.104096

Table 1.8: List of VLE separators used in the network

Section 1.5: Appendix 1.C

An extensive parametric study was carried out in commercial simulator UNISIM by Honeywell to verify that the 2D AR contains all compositions attainable by a simple distillation column with specified top and bottom flowrate production. The parameters for this study were the number of trays (25, 50, 100, 200), feed tray position (10%, 25%, 50%, 75%, and 90% of the number of trays), and reflux ratio (0, 1, 2, 3, 4). The results of the study are summarized in Table 1.9 and suggest that the highest acetone mole fraction that can be attained by a conventional distillation column is 0.795. This confirms that the 2D AR encompasses all product compositions attainable by a simple distillation column.

# Trays	Feed Tray Position	# Trays above Feed	# Trays below Feed	Reflux Ratio	Distillate Acetone Comp.
25	3	2	22	0	0.596756604
25	3	2	22	1	0.69290963
25	3	2	22	2	0.719580207
25	3	2	22	3	0.733660614
25	3	2	22	4	0.742608904
25	6	5	19	0	0.596588873

25	6	5	19	1	0.719300816
25	6	5	19	2	0.750379827
25	6	5	19	3	0.763731175
25	6	5	19	4	0.771347702
25	13	12	12	0	0.596575181
25	13	12	12	1	0.732117303
25	13	12	12	2	0.765637396
25	13	12	12	3	0.778979495
25	13	12	12	4	0.784957494
25	19	18	6	0	0.59665144
25	19	18	6	1	0.734567639
25	19	18	6	2	0.76830466
25	19	18	6	3	0.781019148
25	19	18	6	4	0.787605023
25	22	21	3	0	0.595805599
25	22	21	3	1	0.732134603
25	22	21	3	2	0.76472788
25	22	21	3	3	0.779578871
25	22	21	3	4	0.787220476
50	5	4	45	0	0.596587976
50	5	4	45	1	0.71357069
50	5	4	45	2	0.744024932
50	5	4	45	3	0.757675289
50	5	4	45	4	0.765238536
50	13	12	37	0	0.596578753
50	13	12	37	1	0.732224234
50	13	12	37	2	0.766144438
50	13	12	37	3	0.778791336
50	13	12	37	4	0.78524047
50	25	24	25	0	0.596572648
50	25	24	25	1	0.735949055
50	25	24	25	2	0.770035129
50	25	24	25	3	0.783567011
50	25	24	25	4	0.7899851
50	37	36	13	0	0.596511411
50	37	36	13	1	0.736942844
50	37	36	13	2	0.769646812
50	37	36	13	3	0.785146944
50	37	36	13	4	0.792047096
50	45	44	5	0	0.596520563
50	45	44	5	1	0.736292821
50	45	44	5	2	0.769239193
50	45	44	5	3	0.784236835

50	45	44	5	4	0.794275394
100	10	9	90	0	0.596587587
100	10	9	90	1	0.729024921
100	10	9	90	2	0.762710616
100	10	9	90	3	0.77545517
100	10	9	90	4	0.782004306
100	25	24	75	0	0.596587445
100	25	24	75	1	0.735834554
100	25	24	75	2	0.769608684
100	25	24	75	3	0.783744554
100	25	24	75	4	0.790271882
100	50	49	50	0	0.596586361
100	50	49	50	1	0.737130428
100	50	49	50	2	0.770222776
100	50	49	50	3	0.786431363
100	50	49	50	4	0.79203461
100	75	74	25	0	0.596608569
100	75	74	25	1	0.737466898
100	75	74	25	2	0.7707908
100	75	74	25	3	0.785904529
100	75	74	25	4	0.783141159
100	90	89	10	0	0.59657444
100	90	89	10	1	0.737537181
100	90	89	10	2	0.772077564
100	90	89	10	3	0.787752129
100	90	89	10	4	0.794833514
200	20	19	180	0	---
200	20	19	180	1	0.735567183
200	20	19	180	2	0.770158511
200	20	19	180	3	0.78294468
200	20	19	180	4	0.787401031
200	50	49	150	0	---
200	50	49	150	1	0.737355276
200	50	49	150	2	0.771974554
200	50	49	150	3	0.786931513
200	50	49	150	4	0.793442207
200	100	99	100	0	---
200	100	99	100	1	0.737574308
200	100	99	100	2	0.772119198
200	100	99	100	3	0.78716742
200	100	99	100	4	0.795083657
200	150	149	50	0	---
200	150	149	50	1	0.737613256

200	150	149	50	2	0.772146847
200	150	149	50	3	0.787199193
200	150	149	50	4	**0.795113556**
200	180	179	20	0	---
200	180	179	20	1	0.737625071
200	180	179	20	2	0.772160846
200	180	179	20	3	0.787865945
200	180	179	20	4	0.795099506

Table 1.9: Results of parametric studies of a simple distillation column in UNISIM

Section 1.6: References

1. Horn F. Attainable and non-attainable regions in chemical reactor technique. In *Proceedings of the Third European Symposium on Chemical Reaction Engineering* (pp. 123–138). London: Pergamon Press; 1964.

2. Glasser D, Crowe C, Hildebrandt D. A geometric approach to steady flow reactors: The attainable region and optimization in concentration space. *Industrial & engineering chemistry research*. 1987;26(9):1803-1810.

3. Hildebrandt D, Glasser D, Crowe CM. Geometry of the attainable region generated by reaction and mixing: with and without constraints. *Industrial & engineering chemistry research*. 1990;29(1):49-58.

4. Manousiouthakis V, Justanieah AM, Taylor L. The Shrink–Wrap algorithm for the construction of the attainable region: an application of the IDEAS framework. *Computers & Chemical Engineering*. 2004;28(9):1563-1575.

5. Zhou W, Manousiouthakis V. Non-ideal reactor network synthesis through IDEAS: Attainable region construction. *Chemical Engineering Science*, 2006;61(21):6936-6945.

6. Zhou W, Manousiouthakis V. Variable density fluid reactor network synthesis - Construction of the attainable region through the IDEAS approach. *Chemical Engineering Journal*. 2007;129(1-3):91-103.

7. Davis B, Taylor L, Manousiouthakis V. Identification of the attainable region for batch reactor networks. *Ind. Eng. Chem. Res.* 2008;47(10):3388-3400.

8. Abraham TK, Feinberg M. Kinetic bounds on attainability in the reactor synthesis problem. *Industrial & engineering chemistry research.* 2004;43(2):449-457.

9. Posada A, Manousiouthakis V. Multi-feed attainable region construction using the Shrink-Wrap algorithm. *Chemical Engineering Science*. 2008;63(23):5571-5592.

10. Burri JF, Wilson SD, Manousiouthakis VI. Infinite-Dimensional State-Space Approach to Reactor Network Synthesis: Application to Attainable Region Construction. *Comput. Chem. Eng.* 2002;26(6):849–862.

11. Zhou W, Manousiouthakis V. On dimensionality of attainable region construction for isothermal reactor networks. *Computers & Chemical Engineering*. 2008;32(3):439-450.

12. Zhou W, Manousiouthakis V. Automating the AR construction for non-isothermal reactor networks. *Computers & Chemical Engineering*. 2009;33(1):176-180.

13. Agarwal V, Thotla S, Mahajani SM. Attainable region of reactive distillation-Part I: Single reactant non-azeotropic systems. *Chem. Eng. Sci.* 2008;63(11):2946-2965.

14. Agarwal V, Thotla S, Kaur R, Mahajani SM. Attainable region of reactive distillation. Part II: Single reactant azeotropic systems. *Chem. Eng. Sci.* 2008;63(11):2928-2945.

15. Amte V, Nistala S, Malik R, Mahajani S. Attainable regions of reactive distillation – Part III. Complex reaction scheme: Van de Vusse reaction. *Chem. Eng. Sci.* 2011;66(11):2285-2297.

16. Amte V, Gaikwad R, Malik R, Mahajani S. Attainable region of reactive distillation-Part IV: Inclusion of multistage units for complex reaction schemes. *Chem. Eng. Sci.* 2012;68(1):166-183.

17. Doherty M, Malone M. *Conceptual Design of Distillation Systems*. New York: McGraw Hill; 2001.

18. Jobson M, Hildebrandt D, Glasser D. Attainable products for the vapour-liquid separation of homogeneous ternary mixtures. *Chemical Engineering Journal.* 1995;59:51-70.

19. Nisoli A, Malone MF, Doherty MF. Attainable Regions for Reaction with Separation. *AIChE Journal.* 1997;43(2):374-387.

20. Smith JM, Van Ness HC, Abbott MM. *Introduction to Chemical Engineering Thermodynamics, 7th ed.* New York: McGraw-Hill; 2005: p. 545.

Chapter 2: Global Optimality Properties of Total Annualized and Operating Cost Problems for Compressor Sequences

In this chapter, the minimum total annualized cost problem is studied for a series of non-isentropic compressors and coolers that brings a gas with constant compressibility factor from a specified initial pressure and temperature to a specified final pressure and the same temperature. It is established analytically that at the global optimum, the cooler outlet temperatures are equal to the minimum allowable temperature. For constant heat capacity, constant compressibility factor gases, additional properties of the globally optimal compressor sequence are analytically established for the minimum operating cost case. The aforementioned properties permit development of a solution strategy that identifies the globally-minimum operating cost. Several case studies are presented to illustrate the developed theorems and solution strategies.

Section 2.1: Introduction

According to the U.S. Energy Information Administration (EIA)[1], between 2006 and 2010, the U.S. shale gas production exhibited an average annual growth rate of 48%. In its 2013 Annual Energy Outlook for the 2010 to 2040 time period[2], the EIA predicts a 113% increase in the production of shale gas, and an annual growth rate of 11.9% for natural gas consumption for transportation. This increased natural gas production, and the need for transportation of this natural gas across the country will place increased emphasis on gas compression systems. Combined with the increased use of compressed natural gas and compressed hydrogen for automotive transportation, and the extensive use of compression systems in the process industries, a compelling case arises for the optimization of compression systems.

Compressors contribute significantly to both the operating and capital cost of processing systems in which they are employed. Since their operation often leads to a temperature increase of the gas being compressed, which in turn affects negatively compressor operation and increases power consumption, they are always operated in conjunction with a cooling system. The operating cost of each compressor is associated with its power consumption, while its capital cost is given by a power law expression of its power consumption[3]. The operating cost of the cooling system is proportional to the coolant flow rate, while its capital cost is much smaller than that of the compressor and is thus typically ignored. Given the large contribution of compressor energy consumption and operating costs to the overall energy consumption and operating cost of process plants, even small energy savings in compressor operations can have a significant beneficial impact. As an example, substitution of low efficiency with high efficiency compressors can reduce power consumption by over 5%[4].

Minimization of Total Annualized Cost (TAC) is a challenging problem with few global optimality results available in the literature. Martin and Manousiouthakis[5], established rigorous optimality properties for the heat exchanger network TAC problem. Zhou and Manousiouthakis[6] provided converging upper and lower bounds to the minimum TAC problem for reactor networks within the IDEAS framework. Motivated by this problem formulation, Manousiouthakis et. al.[7] developed a branch-and-bound-based method that can identify in a finite number of steps the global minimum of a concave power law objective function over a system of linear constraints. Concave power law objective functions with rational exponents can be transformed to rationally constrained rational programs, which Manousiouthakis et. al.[8] demonstrated how to solve globally by first transforming them to convex, quadratically

constrained quadratic programs with an additional separable concave constraint, and then solving using branch and bound[9] or Generalized Benders Decomposition[10,11] methods.

The behavior of compressors and coolers is captured through models well-established in the literature[12,13,14,15]. Elrod[16], Happel[13], and Aris et. al.[17] presented the solution to the steady-state, work (power) minimization problem, for two, three and a sequence respectively, of isentropic compressors and intermediate coolers, that brings an ideal gas from an initial temperature and pressure to a desired final pressure and a final temperature equal to the initial temperature. The optimal works of the compressors are shown to be equal at the optimum. Wang and Fan[18] showed that the multistage, isentropic compression of ideal gas is part of a class of so called one dimensional multistage processes, whose common characteristic is that they optimally require equal amounts of control action in each stage.

In this work, the minimum total annualized cost and minimum operating cost problems are formulated, for a sequence of compressors and coolers that brings a gas with constant compressibility factor from a specified initial state (T_0, P_0) to a specified final state (T_0, P_n). Using a constant compressibility factor other than unity is a common approach to accounting for gas non-idealities. In particular, using an average compressibility factor value between the values at (T_0, P_0), and (T_0, P_n) is common industrial practice[19]. To establish a range of variation for the compressibility factor of various gases, first methane is considered. The compressibility factor Z for methane varies between 0.70 and 1.05 for pressures between 0 psia (0 bar) and 3500 psia (241 bar), and temperatures between 32 ºF (0 ºC) and 400 ºF (204 ºC)[12]. For hydrogen which is the focus of our case study, the compressibility factor at the temperatures $T = 300\,K$, $T = 400\,K$ and for pressures such that $700\ bar \geq P \geq 1\ bar$ is such that $1.45 \geq Z \geq 1$ and $1.34 \geq Z \geq 1$ respectively[20]. For general gases, a popular compressibility factor correlation that exhibits errors

of 2% to 3% for nonpolar/slightly polar gases (though larger errors for polar/associative gases) is the Pitzer correlation $Z = Z^0 + \omega Z^1$ [12]. Values for the acentric factor ω typically range in the 0.1 to 0.7 range (methane 0.012, hydrogen -0.216)[12]. Ranges for $Z^0\left(T_r, P_r\right)$, $Z^1\left(T_r, P_r\right)$ can be determined from ranges for the reduced temperature and pressure T_r, P_r of the considered gas from the Lee/Kesler tables[12]:

$$\left\{\begin{matrix} 4.00 \geq T_r \geq 1.15 \\ 1.00 \geq P_r \geq 0.01 \end{matrix}\right\} \Rightarrow \left\{\begin{matrix} 1.0115 \geq Z^0\left(T_r, P_r\right) \geq 0.7443 \\ 0.0864 \geq Z^1\left(T_r, P_r\right) \geq 0.0002 \end{matrix}\right\}.$$

In turn this implies that within the above identified reduced temperature and pressure ranges, the compressibility factor for most gases is between 0.70 and 1.05.

The rest of the paper is structured as follows: First, thermodynamic and economic models for the compression of a constant compressibility factor gas are developed. Second, it is established analytically that at the TAC problem's global minimum, the cooler outlet temperatures are equal to the minimum allowable temperature. For constant heat capacity, constant compressibility factor gases, additional properties of the globally optimal compressor sequence are analytically established for the minimum operating cost case. The aforementioned properties permit development of analytical formulas that enable the global solution of the minimum operating cost problem. Two case studies are presented to illustrate the developed theorems and solution strategies. Lastly, conclusions are drawn.

Section 2.2: Conceptual Framework

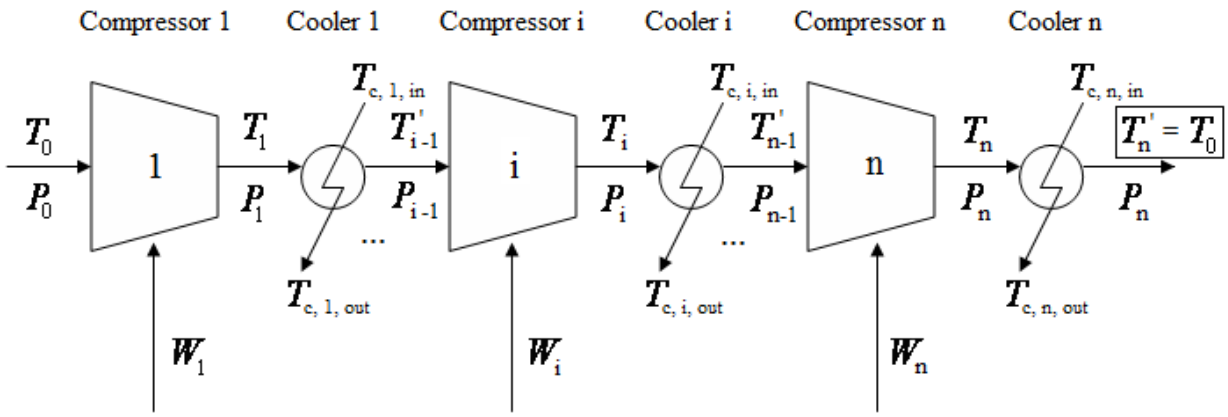

Figure 2.1: Process flowsheet for n compressors and n intermediate coolers

Preliminaries

In this work the minimum cost problem is considered, for a sequence of compressors and isobaric coolers that brings a gas with constant compressibility factor Z from a specified initial state (T_0, P_0) to a specified final state (T_0, P_n). The inlet and outlet temperatures for any compressor in the series must be above T_0 and below $T_{\max}$, the maximum allowable operating temperature for all compressors, respectively. The following are considered to hold:

1. The compressors operate with isentropic efficiency $\eta \in (0,1)$ (i.e. not isentropically)
2. The coolant inlet and outlet temperatures are considered fixed and known for all coolers. They are defined such that $T_{c,i,in} \le T_{c,i,out} \le T_0$, $i = 1, n$.

Thermodynamic Relations

Lemma:

(a) The changes in molar enthalpy and molar entropy of a real fluid from the state (T^o, P^o) to the state (T, P) are:

$$H(T,P)-H(T^o,P^o)=\left[\begin{array}{l}\int_{P^R}^{P} V(T,P')\left(1-\beta(T,P')T\right)dP'+\int_{T^o}^{T} C_p\left(T',P^R\right)dT'+\\ +\int_{P^o}^{P^R} V\left(T^o,P'\right)\left(1-\beta\left(T^o,P'\right)T^o\right)dP'\end{array}\right] \quad (1)$$

$$S(T,P)-S(T^o,P^o)=\left[\begin{array}{l}-\int_{P^R}^{P} \beta(T,P')V(T,P')dP'+\int_{T^o}^{T}\frac{C_p\left(T',P^R\right)}{T'}dT'+\\ -\int_{P^o}^{P^R} \beta\left(T^o,P'\right)V\left(T^o,P'\right)dP'\end{array}\right] \quad (2)$$

where $\left(T^R,P^R\right)$ denotes a reference state where $P^R\to 0$ (ideal gas state),

$$\beta(T,P)\hat{=}\frac{1}{V(T,P)}\frac{\partial V(T,P)}{\partial T},\kappa(T,P)\hat{=}-\frac{1}{V(T,P)}\frac{\partial V(T,P)}{\partial P},$$

$C_p\left(T,P^R\right)\hat{=}C_p(T)\geq 0\ \ \forall T\in\mathbb{R}^+$ is the molar, constant pressure $P^R\to 0$, ideal gas, heat capacity of a fluid, that is only a function of temperature.

(b) A gas featuring a constant compressibility factor satisfies the following:

$$\boxed{Z(T,P)\hat{=}\frac{PV(T,P)}{RT}=Z=constant} \quad (3)$$

$$\boxed{\beta(T,P)=\beta(T)=\frac{1}{T},\ \kappa(T,P)=\kappa(P)=\frac{1}{P}} \quad (4)$$

$$\boxed{H(T,P)-H(T^o,P^o)=\int_{T^o}^{T} C_p\left(T',P^R\right)dT'} \quad (5)$$

$$\boxed{S(T,P)-S(T^o,P^o)=\int_{T^o}^{T}\frac{C_p\left(T',P^R\right)}{T'}dT'-ZR\ln\left(\frac{P}{P^o}\right)} \quad (6)$$

$$\boxed{C_p(T,P)-C_v(T,P)=RZ} \quad (7)$$

(c) Consider a constant compressibility factor gas compressed through a reversible adiabatic (ideal) compressor, with inlet and outlet temperatures and pressures T_{in}, T'_{out} and P_{in}, P_{out} respectively. The compressor consumes the following amount of molar work, and satisfies the following isentropic requirement across its inlet and outlet:

$$\boxed{W_{id} = R\frac{H\left(T'_{out}, P_{out}\right) - H\left(T_{in}, P_{in}\right)}{R} = R\int_{T_{in}}^{T'_{out}} \frac{C_p\left(T'\right)}{R} dT'} \quad (8)$$

$$\boxed{S\left(T'_{out}, P_{out}\right) = S\left(T_{in}, P_{in}\right) \Leftrightarrow \int_{T_{in}}^{T'_{out}} \frac{C_p\left(T'\right)}{RT'} dT' = Z\ln\left(\frac{P_{out}}{P_{in}}\right)} \quad (9)$$

(d) Consider a constant compressibility factor gas compressed through an adiabatic (real) compressor with known efficiency $\eta \in (0,1)$, and inlet and outlet temperatures and pressures T_{in}, T_{out} and P_{in}, P_{out} respectively. The compressor consumes the following amount of molar work, and satisfies the following efficiency relations with the ideal compressor:

$$\boxed{W_r = R\frac{H\left(T_{out}, P_{out}\right) - H\left(T_{in}, P_{in}\right)}{R} = R\int_{T_{in}}^{T_{out}} \frac{C_p\left(T'\right)}{R} dT'} \quad (10)$$

$$\boxed{\eta_i = \frac{W_{id}}{W_r} = \frac{H\left(T'_{out}, P_{out}\right) - H\left(T_{in}, P_{in}\right)}{H\left(T_{out}, P_{out}\right) - H\left(T_{in}, P_{in}\right)} = \frac{\int_{T_{in}}^{T'_{out}} C_p\left(T'\right) dT'}{\int_{T_{in}}^{T_{out}} C_p\left(T'\right) dT'}} \quad (11)$$

(e) The changes in molar enthalpy and molar entropy of a constant compressibility factor gas with a temperature-independent (constant), constant-pressure, ideal gas, heat capacity $C_p\left(T, P^R\right) \triangleq C_p\left(T\right) = C_p = constant$, from the state $\left(T^o, P^o\right)$ to the state $\left(T, P\right)$ are:

$$\boxed{\frac{H\left(T,P\right) - H\left(T^o, P^o\right)}{R} = \frac{C_p}{R}\left(T - T^o\right)} \quad (12)$$

$$\boxed{\frac{S(T,P)-S^{o}\left(T^{o},P^{o}\right)}{R}=\frac{C_{p}}{R}\ln\left(\frac{T}{T^{o}}\right)-Z\ln\left(\frac{P}{P^{o}}\right)} \quad (13)$$

(f) Let this gas be compressed through an adiabatic ideal compressor, and through an adiabatic real compressor with known efficiency $\eta\in(0,1)$. Let the inlet temperatures, and inlet and outlet pressures T_{in},P_{in},P_{out} to both compressors be the same, and let the outlet temperatures be denoted as T'_{out},T_{out}, respectively. Then the following relations hold:

$$\boxed{W_{id}=ZR\frac{k}{k-1}T_{in}\left(\left(\frac{P_{out}}{P_{in}}\right)^{\frac{k-1}{k}}-1\right),W_{r}=\frac{1}{\eta}ZR\frac{k}{k-1}T_{in}\left(\left(\frac{P_{out}}{P_{in}}\right)^{\frac{k-1}{k}}-1\right)} \quad (14)$$

$$\boxed{T'_{out}=T_{in}\left(\frac{P_{out}}{P_{in}}\right)^{\frac{k-1}{k}},T_{out}=T_{in}\left(1+\frac{\left(\frac{P_{out}}{P_{in}}\right)^{\frac{k-1}{k}}-1}{\eta}\right)} \quad (15)$$

Proof: See Appendix 2.A.

The above thermodynamic properties are employed in establishing a monotonicity property regarding the behavior of a real compressor.

Theorem 1:

Consider the compression of a gas with constant compressibility factor $Z>0$, by an ideal compressor and by a real compressor with known efficiency η. Let the gas inlet temperature T_{in}, the gas inlet pressure P_{in}, and the compression ratio $\frac{P_{out}}{P_{in}}>1$ be the same for both compressors.

Finally, let the outlet temperatures of the ideal compressor and the real compressor be denoted as T'_{out} and T_{out} respectively. Then:

(1) Let the compression ratio $\frac{P_{out}}{P_{in}} > 1$ be known, and $\int_{T_{in}}^{T'_{out}} \frac{C_p(T')}{T'} dT'$ be equal to the positive constant $ZR \ln\left(\frac{P_{out}}{P_{in}}\right) > 0$. Then, there exists a function $f : \mathbb{R}^+ \to \mathbb{R}^+,\ f : T_{in} \to T'_{out} = f(T_{in})$. In addition, the function f is differentiable and monotonically increasing with derivative

$$\frac{df(T_{in})}{dT_{in}} = \frac{C_p(T_{in})}{T_{in}} \frac{f(T_{in})}{C_p(f(T_{in}))} = \frac{C_p(T_{in})}{T_{in}} \frac{T'_{out}}{C_p(T'_{out})} > 0 \quad \forall T_{in} > 0. \quad (16)$$

(2) Let the compression ratio $\frac{P_{out}}{P_{in}} > 1$ be known, and $\int_{T_{in}}^{T'_{out}} \frac{C_p(T')}{T'} dT'$ be equal to the positive constant $ZR \ln\left(\frac{P_{out}}{P_{in}}\right) > 0$. Then the function

$$\Delta H : \mathbb{R}^+ \to \mathbb{R}^+,\ \Delta H : T_{in} \to \Delta H(T_{in}) \hat{=} H(T'_{out}, P_{out}) - H(T_{in}, P_{in}) =$$
$$= H(f(T_{in}), P_{out}) - H(T_{in}, P_{in}) = \int_{T_{in}}^{T'_{out}} C_p(T') dT'$$

is differentiable and monotonically increasing with derivative

$$\frac{d(\Delta H(T_{in}))}{dT_{in}} = C_p(T_{in})\left(\frac{f(T_{in})}{T_{in}} - 1\right) = C_p(T_{in})\left(\frac{T'_{out}}{T_{in}} - 1\right) > 0 \quad \forall T_{in} > 0. \quad (17)$$

Proof: See Appendix 2.A.

Section 2.3: Mathematical Problem Formulation

The optimization problem considered in this work is the minimization of an objective function that reflects the total annualized cost of the compressor/cooler sequence, subject to a number of constraints that capture the behavior of the sequence units, and the operating requirements on these units. The general mathematical formulation of the problem is:

$$
\begin{aligned}
\nu = \min_{\substack{\{W_i\}_{i=1}^{n} \\ \{\dot{n}_{c,i}\}_{i=1}^{n} \\ \{P_i, T_i, T_i', T_i''\}_{i=1}^{n}}} & \sum_{i=1}^{n}\left[FC_{compr.}^{cap.}\left(W_i \cdot \dot{n}\right)^{a} + C_{compr.}^{oper.}\left(W_i \cdot \dot{n}\right) + C_{cooler}^{oper.}\left(\dot{n}_{c,i}\right)\right] \\
s.t. & \\
W_i = R\int_{T_{i-1}'}^{T_i} \frac{C_p\left(T'\right)}{R} dT' &= \frac{R}{\eta_i}\int_{T_{i-1}'}^{T_i''} \frac{C_p\left(T'\right)}{R} dT',\ i = 1, n \\
Z \ln\left(\frac{P_i}{P_{i-1}}\right) &= \int_{T_{i-1}'}^{T_i''} \frac{C_p\left(T'\right)}{RT'} dT',\ i = 1, n;\ \frac{P_n}{P_0}\ known \\
\dot{n}_{c,i} &= \frac{\dot{n} \cdot R\int_{T_i'}^{T_i} \frac{C_p\left(T'\right)}{R} dT'}{C_{p,c}\left(T_{c,out} - T_{c,in}\right)},\ i = 1, n \\
\eta_i &= \frac{\int_{T_{i-1}'}^{T_i''} \frac{C_p\left(T'\right)}{R} dT'}{\int_{T_{i-1}'}^{T_i} \frac{C_p\left(T'\right)}{R} dT'},\ i = 1, n \\
T_{i-1}' \le T_i'' \le T_i \le T_{\max} < \infty, i = 1, n;\ T_0' &= T_0 \\
0 < T_0 \le T_i' \le T_i \quad , i = 1, n-1;\ T_n' &= T_0
\end{aligned}
\qquad (18)
$$

The objective function is a finite sum of terms that reflect the total annualized cost associated with the compressor/cooler units. Each term of this sum consists of three components: the ith compressor's annualized capital cost, the ith compressor's annual operating cost, and the ith cooler's annual operating cost. The capital cost of coolers is considered to be small compared to that of compressors and is thus not incorporated in the problem formulation. The capital cost of each compressor is considered to be given by a power law expression of its power consumption. The operating cost of the compressor is considered proportional to its power consumption, while the operating cost of the cooler is proportional to its coolant flow rate.

The first equality constraint quantifies the work consumed by the ith real compressor, in terms of the inlet and outlet temperatures of the ith real and ith ideal (isentropic) compressor respectively. The second equality constraint is derived based on the isentropic requirement for an ideal compressor and quantifies the relationship between the inlet and outlet pressures and

temperatures of an ideal (isentropic) compressor. It also states the requirement that the compressor sequence's overall compression ratio $\frac{P_n}{P_0}$ is known. The third equality constraint is based on the 1st law of thermodynamics for the ith cooler, equating the coolant and compressed gas heat loads in the ith cooler. The fourth equality constraint relates the efficiency of the ith real compressor to the molar enthalpy changes across the ith ideal and real compressors.

The first set of inequalities stipulates that the ith (ideal or real) compressor's inlet temperature must be below the ith ideal compressor's outlet temperature, which must be below the ith real compressor's outlet temperature, which must be below the maximum allowable temperature. The second set of inequalities imposes the restriction that the outlet gas temperature of the ith cooler should be below the ith real compressor's outlet temperature and above the compressor sequence's inlet and outlet temperature T_0.

The first and third sets of equality constraints can be used to substitute for W_i and $\dot{n}_{c,i}$ in the objective function. In addition, the second set of equality constraints can be substituted by a single equality constraint involving only the known overall compression ratio $\frac{P_n}{P_0}$. Then, the above optimization problem (18) becomes:

$$\nu = \min_{\{T_i, T_i', T_i''\}_{i=1}^{n}} \sum_{i=1}^{n} \left[\begin{array}{l} FC_{compr.}^{cap.} \left(\dfrac{\dot{n} \cdot R}{\eta_i} \int_{T_{i-1}'}^{T_i''} \dfrac{C_p(T')}{R} dT' \right)^a + C_{compr.}^{oper.} \left(\dfrac{\dot{n} \cdot R}{\eta_i} \int_{T_{i-1}'}^{T_i''} \dfrac{C_p(T')}{R} dT' \right) + \\ + C_{cooler}^{oper.} \left(\dfrac{\dot{n} \cdot R \int_{T_i'}^{T_i} \dfrac{C_p(T')}{R} dT'}{C_{p,c}\left(T_{c,out} - T_{c,in}\right)} \right) \end{array} \right]$$

s.t.

$$Z \ln\left(\frac{P_n}{P_0}\right) = \sum_{i=1}^{n} \int_{T_{i-1}'}^{T_i''} \frac{C_p(T')}{RT'} dT'$$

$$0 < \eta_i = \frac{\int_{T_{i-1}'}^{T_i''} \frac{C_p(T')}{R} dT'}{\int_{T_{i-1}'}^{T_i} \frac{C_p(T')}{R} dT'} < 1, \; i = 1, n$$

$$T_{i-1}' \le T_i'' \le T_i \le T_{\max} < \infty, i = 1, n; \; T_0' = T_0$$

$$0 < T_0 \le T_i' \le T_i \quad , i = 1, n-1; \; T_n' = T_0 \qquad (19)$$

Next, it is shown that the optimization problem (19) possesses the following optimality property, allowing for significant reduction of dimensionality of the problem:

Theorem 2: $T_{i-1}' = T_0$ for $i = 2, n$ at the global optimum of (19).

Proof: See Appendix 2.A.

In light of Theorem 2, we can now replace all T_{i-1}' terms in our problem with T_0. Our resulting problem is:

$$\nu = \min_{\{T_i, T_i''\}_{i=1}^n} \sum_{i=1}^{n} \left[\begin{array}{l} FC_{compr.}^{cap.} \left(\dfrac{\dot{n} \cdot R}{\eta_i} \int_{T_0}^{T_i''} \dfrac{C_p(T')}{R} dT' \right)^a + C_{compr.}^{oper.} \left(\dfrac{\dot{n} \cdot R}{\eta_i} \int_{T_0}^{T_i''} \dfrac{C_p(T')}{R} dT' \right) + \\ + C_{cooler}^{oper.} \left(\dfrac{\dot{n} \cdot R \int_{T_0}^{T_i} \dfrac{C_p(T')}{R} dT'}{C_{p,c}\left(T_{c,out} - T_{c,in}\right)} \right) \end{array} \right]$$

s.t.

$$Z \ln\left(\frac{P_n}{P_0}\right) = \sum_{i=1}^{n} \int_{T_0}^{T_i''} \frac{C_p(T')}{RT'} dT' \qquad (20)$$

$$\eta_i = \frac{\int_{T_0}^{T_i''} \dfrac{C_p(T')}{R} dT'}{\int_{T_0}^{T_i} \dfrac{C_p(T')}{R} dT'}, \; i = 1, n$$

$$0 < T_0 \le T_i'' \le T_i \le T_{\max} < \infty, \quad i = 1, n$$

Constant Heat Capacity Formulation

Compressor sequences employ intercoolers so that compressor exit temperatures are not allowed to rise significantly. This suggests as a reasonable approximation the use of a temperature-independent, constant pressure, ideal gas heat capacity with values equal to the average value of the temperature dependent, constant pressure, ideal gas heat capacity over the temperature interval of the minimum and maximum allowable compressor outlet temperatures.

When C_p is constant (or equivalently $k \triangleq \dfrac{C_p}{C_v} = constant$), problem (20) becomes:

$$\nu = \left\{ \begin{array}{l} \min\limits_{\{w_i\}_{i=1}^n} A \sum\limits_{i=1}^{n} \dfrac{1}{\eta_i} \cdot w_i + B \sum\limits_{i=1}^{n} \left(\dfrac{1}{\eta_i} \right)^a \cdot (w_i)^a \\ s.t. \\ \prod\limits_{i=1}^{n} (w_i + 1) - C = 0 \\ 0 \le w_i \le \eta_i D, \quad i = 1, n \end{array} \right\} \qquad (21)$$

where, $A \triangleq \left(C_{compr.}^{oper.} \cdot \dot{n} \cdot C_p + \frac{C_{cooler}^{oper.} \cdot \dot{n} \cdot C_p}{C_{p,c}\left(T_{c,out} - T_{c,in}\right)} \right) T_0 \geq 0$, $B \triangleq FC_{compr.}^{cap.} \dot{n}^a \cdot \left(C_p\right)^a \left(T_0\right)^a \geq 0$,

$C \triangleq \left(\frac{P_n}{P_0} \right)^{\left(\frac{ZR}{C_p} \right)} > 1$, $D \triangleq \frac{T_{\max} - T_0}{T_0} > 0$, and $w_i \triangleq \frac{T_i'' - T_0}{T_0} \Leftrightarrow T_i'' = w_i \cdot T_0 + T_0 = T_0 \cdot \left(w_i + 1\right)$.

Theorem 3:

Let $D > 0,\ C > 1,\ \eta_i \in (0,1]\ \forall i = 1,n$. Then the optimization problem (21) is feasible iff

$C \leq \prod_{i=1}^{n} \left(\eta_i D + 1\right)$.

Proof: See Appendix 2.A.

Operating Costs Only

Define the sets $S_D^w \triangleq \left\{ i = 1,n : w_i = \eta_i D \right\}$ (compressors operating at maximum allowable outlet temperature), $S_0^w \triangleq \left\{ i = 1,n : w_i = 0 \right\}$ (compressors not in use), and $S_I^w \triangleq \left\{ \{1,\cdots,n\} - S_D^w - S_0^w \right\}$ (compressors in use and operating below maximum allowable outlet temperature) with cardinalities N_D^w, N_0^w, N_I^w, respectively. Then $N_I^w \triangleq n - N_D^w - N_0^w$. If $N_I^w = 0$, it is clear that $N_D^w \geq 1$, otherwise the compression level C could not be attained. In this case, straightforward combinatorial calculations, on which compressors belong to S_D^w, can be carried out to identify the global minimum without any need of the optimality conditions. Thus in the Theorem below, it is considered that $N_I^w \geq 1$.

Theorem 4:

Let $A > 0,\ B = 0,\ D > 0,\ 1 < C \leq \prod_{i=1}^{n} \left(\eta_i D + 1\right),\ \eta_i \in (0,1]\ \forall i = 1,n,\ N_I^w \geq 1$ and consider the problem

$$\nu = A \cdot \left\{ \begin{array}{l} \min\limits_{\{w_i\}_{i=1}^n} \sum\limits_{i=1}^{n} \dfrac{1}{\eta_i} \cdot w_i \\ s.t. \\ \prod\limits_{i=1}^{n} \left(w_i + 1\right) - C = 0 \\ 0 \le w_i \le \eta_i D, \quad i = 1, n \end{array} \right\}.$$

Then, the optimum objective function value is

$$\boxed{\nu = A \cdot \left[N_I^w \frac{C^{\frac{1}{N_I^w}}}{\left(\prod\limits_{l \in S_I^w} \eta_l \right)^{\frac{1}{N_I^w}} \cdot \left(\prod\limits_{m \in S_D^w} \left(\eta_m D + 1\right) \right)^{\frac{1}{N_I^w}}} - \sum_{k \in S_I^w} \frac{1}{\eta_k} + N_D^w \cdot D \right]} \quad (22),$$

the optimum variable values are

$$w_k = \left[\eta_k \left[\frac{C}{\left(\prod\limits_{l \in S_I^w} \eta_l \right) \left(\prod\limits_{m \in S_D^w} \left(\eta_m D + 1\right) \right)} \right]^{\frac{1}{N_I^w}} - 1 \right] \in \left(0, \eta_k D\right) \quad \forall k \in S_I^w$$

$$w_i = 0 \qquad \forall i \in S_0^w$$

$$w_j = \eta_j D \qquad \forall j \in S_D^w$$

and the following four conditions must be satisfied by the global minimum

$$\boxed{\begin{array}{l} \max\left(\left(D + \dfrac{1}{\min\limits_{j \in S_D^w} \eta_j} \right)^{N_I^w}, \left(\dfrac{1}{\min\limits_{k \in S_I^w} \eta_k} \right)^{N_I^w} \right) \le \dfrac{C}{\left(\prod\limits_{l \in S_I^w} \eta_l \right) \cdot \left(\prod\limits_{m \in S_D^w} \left(\eta_m D + 1\right) \right)} \le \\ \le \min\left(\left(\dfrac{1}{\max\limits_{i \in S_0^w} \eta_i} \right)^{N_I^w}, \left(D + \dfrac{1}{\max\limits_{k \in S_I^w} \eta_k} \right)^{N_I^w} \right) \quad if \;\; N_0^w \ne 0 \wedge N_D^w \ne 0 \end{array}}$$

$$\max\left(\left(D+\frac{1}{\min\limits_{j\in S_D^w}\eta_j}\right)^{N_I^w},\left(\frac{1}{\min\limits_{k\in S_I^w}\eta_k}\right)^{N_I^w}\right)\le\frac{C}{\left(\prod\limits_{l\in S_I^w}\eta_l\right)\cdot\left(\prod\limits_{m\in S_D^w}\left(\eta_m D+1\right)\right)}\le$$
$$\le\left(D+\frac{1}{\max\limits_{k\in S_I^w}\eta_k}\right)^{N_I^w}\quad if\ \ N_0^w=0\wedge N_D^w\neq 0$$

$$\left(\frac{1}{\min\limits_{k\in S_I^w}\eta_k}\right)^{N_I^w}\le\frac{C}{\left(\prod\limits_{l\in S_I^w}\eta_l\right)}\le\min\left(\left(\frac{1}{\max\limits_{i\in S_0^w}\eta_i}\right)^{N_I^w},\left(D+\frac{1}{\max\limits_{k\in S_I^w}\eta_k}\right)^{N_I^w}\right)\ \ if\ \ N_0^w\neq 0\wedge N_D^w=0$$

$$\left(\frac{1}{\min\limits_{k\in S_I^w}\eta_k}\right)^{n}\le\frac{C}{\left(\prod\limits_{l\in S_I^w}\eta_l\right)}\le\left(D+\frac{1}{\max\limits_{k\in S_I^w}\eta_k}\right)^{n}\quad if\ \ N_0^w=0\wedge N_D^w=0\quad(23)$$

Proof: See Appendix 2.A.

Theorem 4 suggests the following compressor efficiency related properties must hold for the three defined sets S_D^w, S_0^w, S_I^w:

$$\max\left(\left(D+\frac{1}{\min\limits_{j\in S_D^w}\eta_j}\right)^{N_I^w},\left(\frac{1}{\min\limits_{k\in S_I^w}\eta_k}\right)^{N_I^w}\right)\le\frac{C}{\left(\prod\limits_{l\in S_I^w}\eta_l\right)\cdot\left(\prod\limits_{m\in S_D^w}\left(\eta_m D+1\right)\right)}\le$$
$$\le\min\left(\left(\frac{1}{\max\limits_{i\in S_0^w}\eta_i}\right)^{N_I^w},\left(D+\frac{1}{\max\limits_{k\in S_I^w}\eta_k}\right)^{N_I^w}\right)\ \ if\ \ N_0^w\neq 0\wedge N_D^w\neq 0$$

1. The maximum compressor efficiency in the set of unused compressors has to be less than or equal to the minimum compressor efficiency in the set of compressors used below capacity.

2. The sum of the temperature defined bound D and the inverse of the maximum compressor efficiency in the set of compressors used below capacity has to be greater than or equal to the inverse of the minimum compressor efficiency in the set of compressors used below capacity.
3. The inverse of the maximum compressor efficiency in the set of unused compressors has to be greater than or equal to the sum of the temperature defined bound D and the inverse of the minimum compressor efficiency in the set of compressors used at capacity.
4. The maximum compressor efficiency in the set of compressors used below capacity has to be less than or equal to the minimum compressor efficiency in the set of compressors used at capacity.

When a set's cardinality is zero, the above criteria involving that set should be ignored. In particular, $N_0^w = 0$ implies that criteria 1, 3 should be ignored; $N_I^w = 0$ implies that criteria 1,2,4 should be ignored; and finally $N_D^w = 0$ implies that criteria 3,4 should be ignored.

The above suggest the following procedure to identify the global minimum:

1. Rank from lowest to highest the inverses of the compressor efficiencies.
2. Select a combination of cardinalities N_D^w, N_I^w for the sets S_D^w, S_I^w respectively, possibly starting from zero and such that $N_D^w + N_I^w \le n$. If all combinations of cardinalities have been considered, then go to step 5.
3. Consider that the N_D^w compressors with the highest efficiencies belong to S_D^w, the N_I^w compressors with the next highest efficiencies belong to S_I^w, and the remaining $N_0^w = n - N_D^w - N_I^w$ compressors belong to S_0^w

4. Verify that the four aforementioned compressor efficiency related properties of S_D^w, S_0^w, S_I^w (which are independent of the value of C) are satisfied. If not, then declare the combination infeasible, go to step 2 and consider another cardinality $N_D^w,\ N_I^w$ combination. If yes, then store this combination in a feasible candidate combination list.
5. For a given value of C, and for each combination of cardinalities $N_D^w,\ N_I^w$ in the feasible candidate combination list, verify that the necessary conditions of optimality (23) are satisfied. If no, then go to the next combination of cardinalities $N_D^w,\ N_I^w$ in the feasible candidate combination list and repeat. If yes, then evaluate ν using equation (22) and store it in a candidate optimum list. Then go to the next combination of cardinalities $N_D^w,\ N_I^w$ in the feasible candidate combination list and repeat until the list is exhausted.
6. Select the minimum value of ν from the candidate optimum list. This is the global minimum ν.

Section 2.4: Discussion

The above global optimum solution procedure requires that a number of cases be considered depending on the three cardinalities N_0^w, N_D^w, N_I^w, which must also satisfy $N_0^w + N_D^w + N_I^w = n$. Thus the number of cases that must be considered grows at most quadratically with the number of compressors n. For each of these cases, the efficiency-related optimality criteria of Theorem 4 significantly reduce the number of alternatives that need to be considered. The above facts make the solution procedure effective, even for large numbers of compressors.

Theorem 4 and the solution procedure discussed in the previous section simplify greatly for the case of compressors of equal efficiency, i.e. for the case $\eta_i = \eta \ \forall i = 1, n$. Then Theorem 4 implies that the optimum objective function value is:

$$\nu = A \cdot \left[\frac{N_I^w}{\eta} \left(\left(\frac{C}{(\eta D + 1)^{N_D^w}} \right)^{\frac{1}{N_I^w}} - 1 \right) + N_D^w \cdot D \right]$$

, the optimal variable values are

$$w_k = \left[\left[\frac{C}{(\eta D + 1)^{N_D^w}} \right]^{\frac{1}{N_I^w}} - 1 \right] \in (0, \eta D) \quad \forall k \in S_I^w$$

$$w_i = 0 \qquad \forall i \in S_0^w$$

$$w_j = \eta_j D \qquad \forall j \in S_D^w$$

and the necessary optimality conditions for $N_I^w \geq 1$become

$$\left(D + \frac{1}{\eta} \right)^{N_I^w} \leq \frac{C}{\eta^{N_I^w} (\eta D + 1)^{N_D^w}} \leq \left(\frac{1}{\eta} \right)^{N_I^w} \quad if \ \ N_0^w \neq 0 \wedge N_D^w \neq 0$$

$$\left(D + \frac{1}{\eta} \right)^{N_I^w} = \frac{C}{\eta^{N_I^w} (\eta D + 1)^{N_D^w}} \quad if \ \ N_0^w = 0 \wedge N_D^w \neq 0$$

$$\left(\frac{1}{\eta} \right)^{N_I^w} = \frac{C}{\eta^{N_I^w}} \quad if \ \ N_0^w \neq 0 \wedge N_D^w = 0$$

$$\left(\frac{1}{\eta} \right)^{n} \leq \frac{C}{\eta^{n}} \leq \left(D + \frac{1}{\eta} \right)^{n} \quad if \ \ N_0^w = 0 \wedge N_D^w = 0$$

It becomes obvious from the above that for the case of equal efficiency compressors, and when $N_I^w \geq 1$, then the case $N_0^w \neq 0 \wedge N_D^w \neq 0$ is impossible. Also that, at the optimum, all used

compressors whose outlet temperature is below the maximum operating temperature must have equal power consumption and equal exit temperature.

Section 2.5: Case Studies

We now present two case studies involving compression of a gas with compressibility factor equal to one, from the initial state $(T_0, P_0) = (298\,K, 101.325\ kPa)$ to the final state $(T_n, P_n) = (T_0, P_n) = (298\,K, P_n)$, where P_n varies. In both cases, the parameters shown in Table 2.1 are fixed.

Parameter (Units)	Value	Parameter (Units)	Value
$T_0\ (K)$	298	$P_0\,(kPa)$	101.325
$T_{\max}\,(K)$	405	$C_p\left(\frac{J}{mol \cdot K}\right)$	28.85
$R\left(\frac{J}{mol \cdot K}\right)$	8.314	Z	1

Table 2.1: Fixed parameters for case study

The first case study considers compressors of equal efficiency and examines how the globally minimum operating cost value changes with the number of available compressors and with varying final pressures P_n. In this case, the total number of available compressors to be studied will be one, two, and three.

The second case study considers compressors of unequal efficiencies and examines how the globally minimum operating cost value changes with the final pressure P_n. In this case, the total number of available compressors to be studied is always four. However, the optimal sequence may not necessarily employ all of them.

Both case studies are solved using the solution procedure suggested following Theorem 4 in the previous section.

Case Study 1: Operating cost minimization, compressors with equal efficiencies

For this case study, we consider compressors with the same efficiency $\eta = 1$. Figure 2.2 and Figure 2.3 illustrate the objective function values for one, two, and three compressors of equal efficiencies in series. Figure 2.3 is a magnification of region 1 to emphasize the differences in the objective function values for each of the compressor systems considered. For all desired outlet pressures in which one compressor is feasible (region 1), and those in which two compressors are feasible (regions 1 and 2), the objective value corresponding to the three equal compressors is the lowest. This is in agreement with Theorem 4, which suggests that when $N_I^w \geq 1$, then all compressors operating below the maximum operating temperature must be equal, and that it is impossible to have $N_0^w \neq 0 \wedge N_D^w \neq 0$.

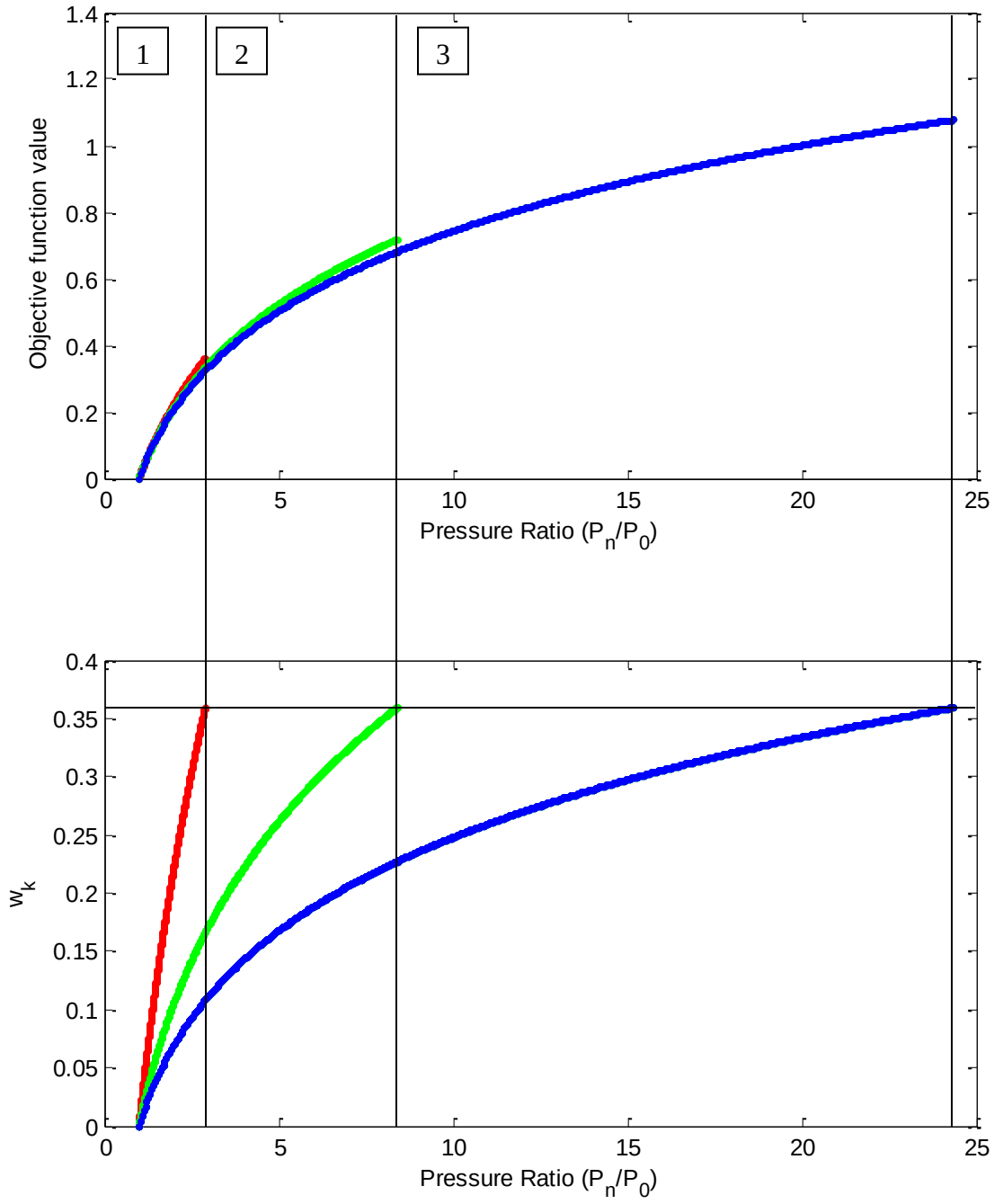

Figure 2.2: Global optima for Example 1

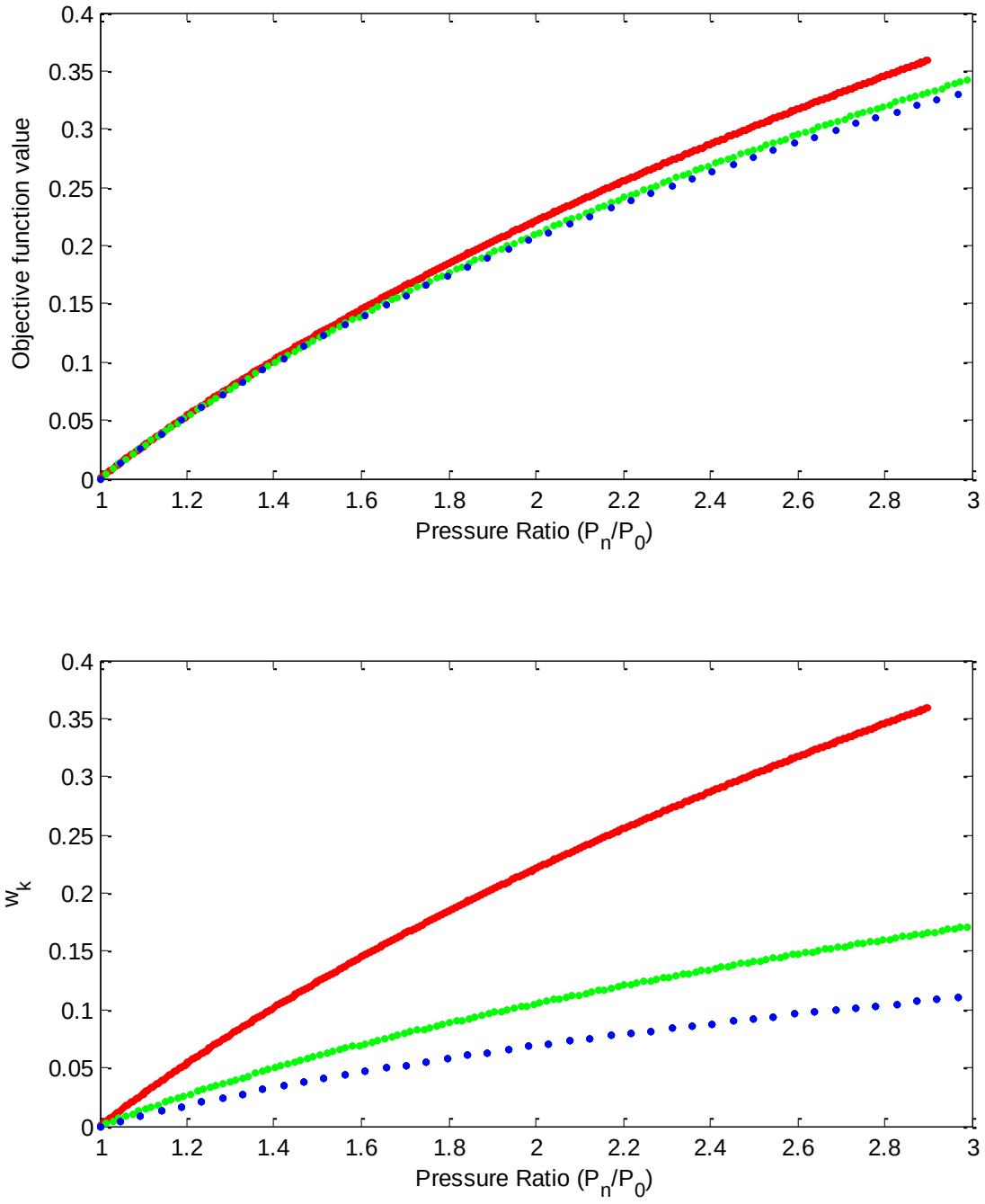

Figure 2.3: Zoom-in of objective function values and outlet temperature ratios in region 1

Case Study 2: Operating cost minimization, compressors with unequal efficiencies

For this case, we considered a system utilizing four compressors of unequal efficiencies ($\eta_1 = 1, \eta_2 = 0.9, \eta_3 = 0.8, \eta_4 = 0.7$) to explore how the global optimum prioritizes their use. Figure 4 illustrates the globally optimal objective function values and temperature ratios $\{w_i\}_{i=1}^{4}$ for this system identified via the solution method from Theorem 4. Vertical lines identify pressure ratios at which either one compressor begins to be used, or when one compressor reaches capacity; i.e., when the cardinalities N_D^w, N_0^w, N_I^w of the global optimum change. Table 2.2 depicts how much energy savings is achieved by switching from a system employing all four compressors with equal duties to the identified globally-optimal configuration.

From Figure 2.4, we can see that this collection of compressors in series can deliver compressed gas at pressures up to 40 times the initial pressure P_0. As the pressure ratio increases, the global optimum begins employing the compressor with the highest efficiency ($\eta_1 = 1$) first, with the other compressors following in descending order of efficiency.

For a given pressure ratio, both the temperature ratios and slopes of the temperature ratio curves decrease with decreasing efficiency. These results are in line with intuition: given a set of compressors of varying efficiencies, it is best to allocate the bulk of the necessary work to the most efficient compressor, saving the other compressors for higher work demands. However the number of compressors to be used at each pressure ratio is not straightforward to identify. It is also important to emphasize that, unlike the equal efficiency case, there are pressure ratio ranges for which it is not optimal to use all available compressors. As can be seen in Figure 2.4, below a pressure ratio of about 10, it is not optimal to use all four available compressors. In fact, below a value of 3.3 it is optimal to use only two compressors, and below a value of 1.4 it is optimal to

use only one compressor. This behavior is completely different from the equal efficiency compressor case, where for all pressure ratios it is optimal to use all available compressors.

It is also important to emphasize that the energy savings that stem from using the optimal compressor sequence over a conventional design, such as a compressor sequence where all compressor outlet temperatures are equal, are not insignificant, especially for small pressure ratios for a given number of compressors. Table 2.2 summarizes these savings, which can be as high as 12.868%.

P_0/P_n	$W_{tot,eq}\left(J/mol\right)$	$W_{tot,opt}\left(J/mol\right)$	$W_{savings}\left(\%\right)$
1.00	0	0	N/A
1.25	655	571	12.868
1.50	1198	1065	11.105
1.75	1661	1497	9.887
2.00	2064	1879	8.988
2.25	2435	2221	8.781
2.50	2762	2533	8.300
2.75	3060	2819	7.884
3.00	3334	3084	7.513
3.25	3588	3330	7.195
3.50	3829	3560	7.034
3.75	4045	3776	6.651
4.00	4252	3979	6.416
4.25	4447	4171	6.199
4.50	4631	4353	5.995
4.75	4805	4526	5.801
5.00	4979	4691	5.770
5.25	5139	4849	5.638
5.50	5292	5000	5.515
5.75	5439	5145	5.402
6.00	5580	5285	5.295
6.25	5716	5419	5.195
6.50	5847	5549	5.101
6.75	5973	5674	5.012
7.00	6095	5795	4.928
7.25	6213	5912	4.847
7.50	6327	6025	4.770
7.75	6438	6136	4.697

8.00	6545	6243	4.626
8.50	6751	6448	4.485
9.00	6946	6644	4.347
9.50	7131	6831	4.211
10.00	7307	7009	4.077
10.50	7475	7180	3.947
11.00	7636	7344	3.819
11.50	7789	7502	3.695
12.00	7943	7653	3.651
12.50	8086	7799	3.548
13.00	8224	7940	3.452
13.50	8357	8076	3.360
14.00	8485	8207	3.273
14.50	8609	8335	3.190
15.00	8730	8458	3.110
15.50	8846	8578	3.033
16.00	8959	8694	2.956
16.50	9069	8808	2.881
17.00	9176	8919	2.807
17.50	9280	9027	2.734
18.00	9382	9132	2.662
18.50	9480	9235	2.591
19.00	9577	9335	2.522
19.50	9671	9433	2.454
20.00	9758	9529	2.341
20.50	9848	9623	2.283
21.00	9937	9715	2.225
21.50	10023	9806	2.168
22.00	10107	9894	2.110
22.50	10190	9981	2.053
23.00	10271	10066	1.995
23.50	10350	10150	1.938
24.00	10428	10232	1.881
24.50	10504	10312	1.824
25.00	10578	10391	1.767
25.50	10649	10469	1.692
26.00	10723	10546	1.654
26.50	10794	10621	1.598
27.00	10863	10695	1.542
27.50	10931	10768	1.486
28.00	10997	10840	1.430
28.50	11063	10911	1.373
29.00	11127	10981	1.315

29.50	11190	11050	1.255
30.00	11253	11118	1.194
30.50	11314	11186	1.132
31.00	11374	11253	1.069
31.50	11433	11319	1.005
32.00	11497	11384	0.984
32.50	11555	11448	0.925
33.00	11613	11512	0.865
33.50	11669	11575	0.805
34.00	11725	11638	0.745
34.50	11780	11699	0.684
35.00	11834	11761	0.623
35.50	11888	11821	0.562
36.00	11941	11881	0.501
36.50	11993	11940	0.439
37.00	12045	11999	0.378
37.50	12096	12057	0.316
38.00	12146	12115	0.254
38.50	12196	12172	0.192
39.00	12245	12229	0.130
39.50	12293	12285	0.068
40.00	12341	12341	0.006

Table 2.2: Energy savings switching from a sequence of equal-duty compressors to the identified optimal sequence

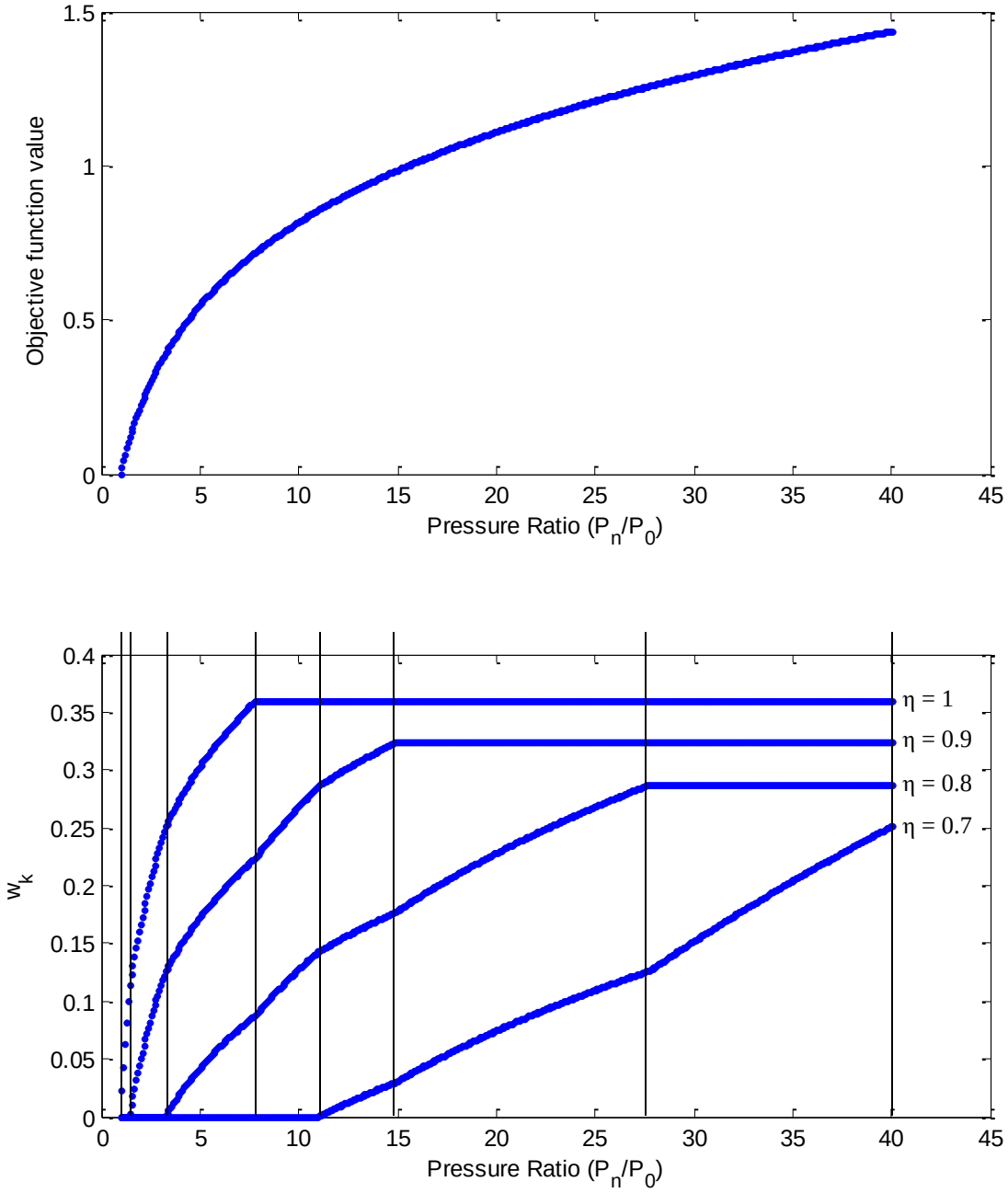

Figure 2.4: Global optima for Example 2 (Unequal Compressors)

Section 2.6: Conclusions

In this work we studied both the total annualized cost and the minimum operating cost problems for a system of compressors and coolers in series bringing a gas with constant compressibility factor from a specified initial state (T_0, P_0) to a specified final state (T_0, P_n). We established analytically that at the global optimum of the general TAC problem, the cooler outlet temperatures are equal to the minimum allowable temperature. For constant heat capacity, constant compressibility factor gases, additional properties of the globally optimal compressor sequence are analytically established for the minimum operating cost case. The aforementioned properties permitted development of an analytical solution methodology that can identify the globally-minimum operating cost for any number of compressors of possibly different efficiencies. Two case studies are presented to illustrate the developed theorems and solution strategies. It is shown that the globally minimum cost for sequences of compressors with unequal efficiencies may correspond to a sequence that does not employ all available compressors. Energy savings of up to 12.868% are identified over conventional designs.

Appendix 2.A.

Proof of Lemma:

(a): The changes in molar enthalpy and molar entropy of a real fluid from the state (T^o, P^o) to the state (T, P) are derived from the exact differentials of molar enthalpy and molar entropy in (T, P) space[12]:

$$\begin{Bmatrix} dH = C_p(T,P)\,dT + V(T,P)\left(1-\beta(T,P)T\right)dP \\ dS = \dfrac{C_p(T,P)}{T}\,dT - \beta(T,P)V(T,P)\,dP \end{Bmatrix}$$

where $\beta(T,P) \hat{=} \dfrac{1}{V(T,P)}\dfrac{\partial V(T,P)}{\partial T}$, $\kappa(T,P) \hat{=} -\dfrac{1}{V(T,P)}\dfrac{\partial V(T,P)}{\partial P}$.

Consider the reference state $\left(T^R, P^R\right)$ where $P^R \to 0$. Since H, S are state functions, it then holds:

$$H\left(T,P\right)-H\left(T^o,P^o\right)=\left[\begin{array}{l}\left[H\left(T,P\right)-H\left(T,P^R\right)\right]+\left[H\left(T,P^R\right)-H\left(T^R,P^R\right)\right]+\\ \left[H\left(T^R,P^R\right)-H\left(T^o,P^R\right)\right]+\left[H\left(T^o,P^R\right)-H\left(T^o,P^o\right)\right]\end{array}\right]\Rightarrow$$

$$H\left(T,P\right)-H\left(T^o,P^o\right)=\left[\begin{array}{l}\int_{P^R}^{P}V\left(T,P'\right)\left(1-\beta\left(T,P'\right)T\right)dP'+\int_{T^R}^{T}C_p\left(T',P^R\right)dT'+\\ +\int_{T^o}^{T^R}C_p\left(T',P^R\right)dT'+\int_{P^o}^{P^R}V\left(T^o,P'\right)\left(1-\beta\left(T^o,P'\right)T^o\right)dP'\end{array}\right]\Rightarrow$$

$$H\left(T,P\right)-H\left(T^o,P^o\right)=\left[\begin{array}{l}\int_{P^R}^{P}V\left(T,P'\right)\left(1-\beta\left(T,P'\right)T\right)dP'+\int_{T^o}^{T}C_p\left(T',P^R\right)dT'+\\ +\int_{P^o}^{P^R}V\left(T^o,P'\right)\left(1-\beta\left(T^o,P'\right)T^o\right)dP'\end{array}\right]$$

$$S\left(T,P\right)-S\left(T^o,P^o\right)=\left[\begin{array}{l}\left[S\left(T,P\right)-S\left(T,P^R\right)\right]+\left[S\left(T,P^R\right)-S\left(T^R,P^R\right)\right]+\\ \left[S\left(T^R,P^R\right)-S\left(T^o,P^R\right)\right]+\left[S\left(T^o,P^R\right)-S\left(T^o,P^o\right)\right]\end{array}\right]\Rightarrow$$

$$S\left(T,P\right)-S\left(T^o,P^o\right)=\left[\begin{array}{l}-\int_{P^R}^{P}\beta\left(T,P'\right)V\left(T,P'\right)dP'+\int_{T^R}^{T}\frac{C_p\left(T',P^R\right)}{T'}dT'+\\ +\int_{T^o}^{T^R}\frac{C_p\left(T',P^R\right)}{T'}dT'-\int_{P^o}^{P^R}\beta\left(T^o,P'\right)V\left(T^o,P'\right)dP'\end{array}\right]\Rightarrow$$

$$S\left(T,P\right)-S\left(T^o,P^o\right)=\left[\begin{array}{l}-\int_{P^R}^{P}\beta\left(T,P'\right)V\left(T,P'\right)dP'+\int_{T^o}^{T}\frac{C_p\left(T',P^R\right)}{T'}dT'+\\ -\int_{P^o}^{P^R}\beta\left(T^o,P'\right)V\left(T^o,P'\right)dP'\end{array}\right]$$

(b) Equation (3) holds by assumption of constant compressibility factor. The proof for equations $(4)-(6)$ is straightforward. To establish (7) we proceed as follows:

The constant-pressure and constant-volume heat capacities are related as follows:

$$C_p(T,P)-C_v(T,P)-\frac{\beta(T,P)^2}{\kappa(T,P)}TV=0.$$

For a gas with a constant compressibility factor Z, by equation (4) it holds:

$\beta(T,P)=\beta(T)=\frac{1}{T}$, $\kappa(T,P)=\kappa(P)=\frac{1}{P}$. Then, the above relation becomes:

$$C_p(T,P)-C_v(T,P)-\frac{PV}{T}=0 \overset{Z=\frac{PV}{RT}}{\Leftrightarrow} C_p(T,P)-C_v(T,P)=RZ.$$

(c) The inlet and outlet molar entropies of a reversible adiabatic (ideal) compressor of a gas featuring a constant compressibility factor are equal to one another. Thus, considering the ideal compressor's inlet and outlet temperatures and pressures to be T_{in}, T'_{out} and P_{in}, P_{out} respectively, equation (6) yields the following:

$$S(T'_{out},P_{out})=S(T_{in},P_{in}) \Leftrightarrow \int_{T_{in}}^{T'_{out}}\frac{C_p(T')}{RT'}dT'=Z\ln\left(\frac{P_{out}}{P_{in}}\right)$$

An energy balance for the ideal compressor, combined with its adiabatic nature yields:

$W_{id}=H(T'_{out},P_{out})-H(T_{in},P_{in})$. By equation (5), it then holds $W_{id}=R\int_{T_{in}}^{T'_{out}}\frac{C_p(T')}{R}dT'$.

(d) An energy balance for the real compressor, combined with its adiabatic nature yields:

$W_r=H(T_{out},P_{out})-H(T_{in},P_{in})$. By equation (5), it then holds $W_r=R\int_{T_{in}}^{T_{out}}\frac{C_p(T')}{R}dT'$.

By the definition of compressor efficiency, it holds: $\eta = \frac{W_{id}}{W_r}$. Then, the work equations developed in part (c) and in the earlier part of (d) yield:

$$\eta = \frac{H\left(T'_{out}, P_{out}\right) - H\left(T_{in}, P_{in}\right)}{H\left(T_{out}, P_{out}\right) - H\left(T_{in}, P_{in}\right)} = \frac{\int_{T_{in}}^{T'_{out}} C_p\left(T'\right) dT'}{\int_{T_{in}}^{T_{out}} C_p\left(T'\right) dT'}$$

(e) Straightforward.

(f) Consider a constant compressibility factor gas with a temperature-independent (constant), constant-pressure, ideal gas, heat capacity $C_p\left(T, P^R\right) \hat{=} C_p\left(T\right) = C_p = constant$. Let this gas be compressed through an adiabatic ideal compressor, and through an adiabatic real compressor with known efficiency $\eta \in (0,1)$. Let the inlet temperatures, and inlet and outlet pressures T_{in}, P_{in}, P_{out} to both compressors be the same, and let the outlet temperatures be denoted as T'_{out}, T_{out}, respectively. Combining equations $(7),(8)$, and the fact that $C_p = constant$ yields:

$$\left\{\begin{array}{l} W_{id} = \int_{T_{in}}^{T'_{out}} C_p dT' \\ ZR\ln\left(\frac{P_{out}}{P_{in}}\right) = \int_{T_{in}}^{T'_{out}} \frac{C_p}{T'} dT' \end{array}\right\} \overset{C_p = constant}{\Leftrightarrow} \left\{\begin{array}{l} W_{id} = C_p\left(T'_{out} - T_{in}\right) \\ ZR\ln\left(\frac{P_{out}}{P_{in}}\right) = C_p \ln\left(\frac{T'_{out}}{T_{in}}\right) \end{array}\right\} \overset{\substack{C_p - C_v = RZ \\ \Leftrightarrow \\ k \hat{=} \frac{C_p}{C_v}}}{}$$

$$\left\{\begin{array}{l} W_{id} = C_p\left(T'_{out} - T_{in}\right) \\ \frac{k-1}{k}\ln\left(\frac{P_{out}}{P_{in}}\right) = \ln\left(\frac{T'_{out}}{T_{in}}\right) \end{array}\right\} \Leftrightarrow \left\{\begin{array}{l} W_{id} = ZR\frac{k}{k-1}T_{in}\left(\left(\frac{P_{out}}{P_{in}}\right)^{\frac{k-1}{k}} - 1\right) \\ T'_{out} = T_{in}\left(\frac{P_{out}}{P_{in}}\right)^{\frac{k-1}{k}} \end{array}\right\}$$

The work of the real compressor and its outlet temperature then become

$$W_r = \frac{W_{id}}{\eta} = \frac{1}{\eta} ZR \frac{k}{k-1} T_{in} \left(\left(\frac{P_{out}}{P_{in}} \right)^{\frac{k-1}{k}} - 1 \right)$$

$$\eta = \frac{W_{id}}{W_r} = \frac{C_p\left(T'_{out} - T_{in}\right)}{C_p\left(T_{out} - T_{in}\right)} = \frac{\left(T'_{out} - T_{in}\right)}{\left(T_{out} - T_{in}\right)} \Rightarrow T_{out} = T_{in} + \frac{\left(T'_{out} - T_{in}\right)}{\eta} = T_{in} \left(1 + \frac{\left(\frac{P_{out}}{P_{in}} \right)^{\frac{k-1}{k}} - 1}{\eta} \right) \text{ O.E.Δ.}$$

Proof of Theorem 1:

(1): The compression ratio $\frac{P_{out}}{P_{in}} > 1$ is known. Let

$C_p : \mathbb{R}^+ \to \mathbb{R}^+, \quad C_p : T \to C_p(T) \hat{=} C_p\left(T, P^o\right) \geq 0 \quad \forall T \in \mathbb{R}^+$. Then, equation (8) implies

$\int_{T_{in}}^{T'_{out}} \frac{C_p(T')}{T'} dT' = ZR \ln\left(\frac{P_{out}}{P_{in}} \right) > 0$. Since $C_p(T) > 0 \quad \forall T \in \left[T_{in}, T'_{out}\right] \wedge T_{in} > 0$, it then holds

$\frac{C_p(T)}{T} > 0 \quad \forall T \in \left[T_{in}, T'_{out}\right]$. Then, since $Z > 0$ and $\frac{P_{out}}{P_{in}} > 1$, it holds

$0 < ZR \ln\left(\frac{P_{out}}{P_{in}} \right) = \int_{T_{in}}^{T'_{out}} \frac{C_p(T')}{T'} dT' \Rightarrow T'_{out} > T_{in}$. Consider now, for any arbitrary but fixed $T_{in} > 0$,

that $\exists\left(T'_{out,a}, T'_{out,b}\right) : T'_{out,a} > T'_{out,b} > T_{in} \ \wedge \ ZR \ln\left(\frac{P_{out}}{P_{in}} \right) = \int_{T_{in}}^{T'_{out,a}} \frac{C_p(T')}{T'} dT' = \int_{T_{in}}^{T'_{out,b}} \frac{C_p(T')}{T'} dT'$. Then,

$\int_{T_{in}}^{T'_{out,b}} \frac{C_p(T')}{T'} dT' - \int_{T_{in}}^{T'_{out,a}} \frac{C_p(T')}{T'} dT' = 0 \Rightarrow \int_{T'_{out,a}}^{T'_{out,b}} \frac{C_p(T')}{T'} dT' = 0 \overset{\frac{C_p(T')}{T'} > 0 \ \forall T' > 0}{\Leftrightarrow} T'_{out,a} = T'_{out,b}$. This is a

contradiction. Therefore, each T_{in} maps to a unique corresponding T'_{out}. In turn, this implies that

there exists a function $f : \mathbb{R}^+ \to \mathbb{R}^+, \ f : T_{in} \to T'_{out} = f\left(T_{in}\right)$.

It was established above that $\int_{T_{in}}^{T'_{out}} \frac{C_p(T')}{T'} dT' = \int_{T_{in}}^{f(T_{in})} \frac{C_p(T')}{T'} dT' = ZR \ln\left(\frac{P_{out}}{P_{in}}\right) > 0 \ \ \forall T_{in} > 0$

establishes the existence of a function $f : \mathbb{R}^+ \to \mathbb{R}^+, \ f : T_{in} \to T'_{out} = f(T_{in})$. Then

$$\frac{d\left(\int_{T_{in}}^{f(T_{in})} \frac{C_p(T')}{T'} dT'\right)}{dT_{in}} = \frac{d\left(ZR \ln\left(\frac{P_{out}}{P_{in}}\right)\right)}{dT_{in}} = 0 \ \ \forall T_{in} > 0 \Rightarrow$$

$$\int_{T_{in}}^{f(T_{in})} \frac{\partial\left(\frac{C_p(T')}{T'}\right)}{\partial T_{in}} dT' + \frac{C_p(f(T_{in}))}{f(T_{in})} \frac{df(T_{in})}{dT_{in}} - \frac{C_p(T_{in})}{T_{in}} \frac{dT_{in}}{dT_{in}} = 0 \ \ \forall T_{in} > 0 \Rightarrow$$

$$\frac{df(T_{in})}{dT_{in}} = \frac{C_p(T_{in})}{T_{in}} \frac{f(T_{in})}{C_p(f(T_{in}))} = \frac{C_p(T_{in})}{T_{in}} \frac{T'_{out}}{C_p(T'_{out})} > 0 \ \ \forall T_{in} > 0 \,. \text{O.E.}\Delta.$$

(2): In part (1) of Theorem 1, it was shown that the relation

$\int_{T_{in}}^{T'_{out}} \frac{C_p(T')}{T'} dT' = ZR \ln\left(\frac{P_{out}}{P_{in}}\right) > 0$ establishes the existence of a function

$f : \mathbb{R}^+ \to \mathbb{R}^+, \ f : T_{in} \to T'_{out} = f(T_{in})$ with derivative

$\frac{df(T_{in})}{dT_{in}} = \frac{C_p(T_{in})}{T_{in}} \frac{f(T_{in})}{C_p(f(T_{in}))} = \frac{C_p(T_{in})}{T_{in}} \frac{T'_{out}}{C_p(T'_{out})} > 0 \ \ \forall T_{in} > 0$. Then, the function

$\Delta H : \mathbb{R}^+ \to \mathbb{R}^+, \Delta H : T_{in} \to \Delta H(T_{in}) \doteq \int_{T_{in}}^{T'_{out}} C_p(T') dT' = \int_{T_{in}}^{f(T_{in})} C_p(T') dT'$ is differentiable $\forall T_{in} > 0$,

with derivative

$$\frac{d\left(\Delta H\left(T_{in}\right)\right)}{dT_{in}}=\frac{d\left(\int_{T_{in}}^{f(T_{in})}C_p\left(T'\right)dT'\right)}{dT_{in}}=\int_{T_{in}}^{f(T_{in})}\frac{\partial\left(C_p\left(T'\right)\right)}{\partial T_{in}}dT'+C_p\left(f\left(T_{in}\right)\right)\frac{df\left(T_{in}\right)}{dT_{in}}-C_p\left(T_{in}\right)\frac{dT_{in}}{dT_{in}}=$$

$$=C_p\left(f\left(T_{in}\right)\right)\frac{df\left(T_{in}\right)}{dT_{in}}-C_p\left(T_{in}\right)=C_p\left(f\left(T_{in}\right)\right)\frac{C_p\left(T_{in}\right)}{T_{in}}\frac{f\left(T_{in}\right)}{C_p\left(f\left(T_{in}\right)\right)}-C_p\left(T_{in}\right)=$$

$$=C_p\left(T_{in}\right)\left(\frac{f\left(T_{in}\right)}{T_{in}}-1\right)=C_p\left(T_{in}\right)\left(\frac{T'_{out}}{T_{in}}-1\right)\ \forall T_{in}>0$$

Based on the above, $\frac{d\left(\Delta H\left(T_{in}\right)\right)}{dT_{in}}>0\Leftrightarrow C_p\left(T_{in}\right)\left(\frac{T'_{out}}{T_{in}}-1\right)>0\overset{C_p(T_{in})>0\ \forall T_{in}>0}{\Leftrightarrow}$

$\frac{T'_{out}}{T_{in}}-1>0\Leftrightarrow T'_{out}>T_{in}$, which is true by the proof of (1). Thus ΔH is a monotonically increasing function of T_{in}. O.E.Δ.

Proof of Theorem 2:

The sequential nature of a compressor/cooler sequence allows an embedded representation of the considered optimization problem. In the interior optimization problem, all temperatures can be considered fixed, but unknown, at arbitrary (feasible) values, except for T'_{k-1},T''_k,T_k, which are the interior optimization problem's variables. Then problem (19) can be rewritten as:

$$
\nu = \min_{\substack{\{T_i, T_i''\}_{\substack{i=1 \\ i\neq k}}^{n} \\ \{T_i'\}_{\substack{i=1 \\ i\neq k-1}}^{n}}}
\left[
\begin{array}{l}
\displaystyle\sum_{\substack{i=1 \\ i\neq k}}^{n}\left[FC_{compr.}^{cap.}\left(\frac{\dot{n}\cdot R}{\eta_i}\int_{T_{i-1}'}^{T_i''}\frac{C_p(T')}{R}dT' \right)^{a} + C_{compr.}^{oper.}\left(\frac{\dot{n}\cdot R}{\eta_i}\int_{T_{i-1}'}^{T_i''}\frac{C_p(T')}{R}dT' \right)\right] \\
\displaystyle + \sum_{\substack{i=1 \\ i\neq k,k-1}}^{n} C_{cooler}^{oper.}\left(\frac{\dot{n}\cdot R\int_{T_i'}^{T_i}\frac{C_p(T')}{R}dT'}{C_{p,c}\left(T_{c,out}-T_{c,in}\right)} \right) \\
\displaystyle + \min_{T_k, T_{k-1}', T_k''}\left[
\begin{array}{l}
\displaystyle FC_{compr.}^{cap.}\left(\frac{\dot{n}\cdot R}{\eta_k}\int_{T_{k-1}'}^{T_k''}\frac{C_p(T')}{R}dT' \right)^{a} + C_{compr.}^{oper.}\left(\frac{\dot{n}\cdot R}{\eta_k}\int_{T_{k-1}'}^{T_k''}\frac{C_p(T')}{R}dT' \right) \\
\displaystyle + C_{cooler}^{oper.}\left(\frac{\dot{n}\cdot R\int_{T_k'}^{T_k}\frac{C_p(T')}{R}dT'}{C_{p,c}\left(T_{c,out}-T_{c,in}\right)} \right) + C_{cooler}^{oper.}\left(\frac{\dot{n}\cdot R\int_{T_{k-1}'}^{T_{k-1}}\frac{C_p(T')}{R}dT'}{C_{p,c}\left(T_{c,out}-T_{c,in}\right)} \right)
\end{array}
\right]
\end{array}
\right]
$$

s.t.

$$
Z\ln\left(\frac{P_n}{P_0}\right) = \int_{T_{k-1}'}^{T_k''}\frac{C_p(T')}{RT'}dT' + \sum_{\substack{i=1 \\ i\neq k}}^{n}\int_{T_{i-1}'}^{T_i''}\frac{C_p(T')}{RT'}dT'
$$

$$
0<\eta_k = \frac{\displaystyle\int_{T_{k-1}'}^{T_k''}\frac{C_p(T')}{R}dT'}{\displaystyle\int_{T_{k-1}'}^{T_k}\frac{C_p(T')}{R}dT'} < 1,\ \ 0<\eta_i = \frac{\displaystyle\int_{T_{i-1}'}^{T_i''}\frac{C_p(T')}{R}dT'}{\displaystyle\int_{T_{i-1}'}^{T_i}\frac{C_p(T')}{R}dT'} < 1,\ i=1,n;\ i\neq k \qquad (24)
$$

$$
T_{k-1}' \le T_k'' \le T_k \le T_{\max}
$$

$$
T_0 \le T_k' \le T_k,\ \ T_0 \le T_{k-1}' \le T_{k-1}
$$

$$
T_{i-1}' \le T_i'' \le T_i \le T_{\max} < \infty,\ \ i=1,n;\ i\neq k,\ T_0' = T_0
$$

$$
0 < T_0 \le T_i' \le T_i \quad ,i=1,n-1;\ i\neq k,k-1,\ \ T_n' = T_0
$$

The inner level of the above embedded optimization problem can then be stated as follows:

$$\min_{T_k,T'_{k-1},T''_k}\left[\begin{array}{l} FC^{cap.}_{compr.}\left(\dfrac{\dot{n}\cdot R}{\eta_k}\int_{T'_{k-1}}^{T''_k}\dfrac{C_p(T')}{R}dT'\right)^a + C^{oper.}_{compr.}\left(\dfrac{\dot{n}\cdot R}{\eta_k}\int_{T'_{k-1}}^{T''_k}\dfrac{C_p(T')}{R}dT'\right) \\ +C^{oper.}_{cooler}\left(\dfrac{\dot{n}\cdot R\int_{T'_k}^{T_k}\dfrac{C_p(T')}{R}dT'}{C_{p,c}\left(T_{c,out}-T_{c,in}\right)}\right)+C^{oper.}_{cooler}\left(\dfrac{\dot{n}\cdot R\int_{T'_{k-1}}^{T_{k-1}}\dfrac{C_p(T')}{R}dT'}{C_{p,c}\left(T_{c,out}-T_{c,in}\right)}\right)\end{array}\right]$$

s.t.

$$0<\left[Z\ln\left(\frac{P_n}{P_0}\right)-\sum_{\substack{i=1\\ i\neq k}}^{n}\int_{T'_{i-1}}^{T''_i}\frac{C_p(T')}{RT'}dT'\right]=\int_{T'_{k-1}}^{T''_k}\frac{C_p(T')}{RT'}dT'$$

$$0<\eta_k=\frac{\int_{T'_{k-1}}^{T''_k}\frac{C_p(T')}{R}dT'}{\int_{T'_{k-1}}^{T_k}\frac{C_p(T')}{R}dT'}\le 1$$

$$T'_{k-1}\le T''_k\le T_k\le T_{\max} \qquad (25)$$

$$T_0\le T'_k\le T_k,\ T_0\le T'_{k-1}\le T_{k-1}$$

However,

$$\int_{T'_{k-1}}^{T_k}\frac{C_p(T')}{R}dT'=\frac{1}{\eta_k}\int_{T'_{k-1}}^{T''_k}\frac{C_p(T')}{R}dT'\Rightarrow$$

$$\int_{T'_k}^{T_k}\frac{C_p(T')}{R}dT'=\int_{T'_{k-1}}^{T_k}\frac{C_p(T')}{R}dT'+\int_{T'_k}^{T'_{k-1}}\frac{C_p(T')}{R}dT'=\frac{1}{\eta_k}\int_{T'_{k-1}}^{T''_k}\frac{C_p(T')}{R}dT'+\int_{T'_k}^{T'_{k-1}}\frac{C_p(T')}{R}dT'.$$

The objective function of problem (25) then becomes:

$$FC^{cap.}_{compr.}\left(\frac{\dot{n}\cdot R}{\eta_k}\int_{T'_{k-1}}^{T''_k}\frac{C_p(T')}{R}dT'\right)^a+C^{oper.}_{compr.}\left(\frac{\dot{n}\cdot R}{\eta_k}\int_{T'_{k-1}}^{T''_k}\frac{C_p(T')}{R}dT'\right)+$$

$$+C^{oper.}_{cooler}\left(\frac{\dot{n}\cdot R\left(\frac{1}{\eta_k}\int_{T'_{k-1}}^{T''_k}\frac{C_p(T')}{R}dT'+\int_{T'_k}^{T'_{k-1}}\frac{C_p(T')}{R}dT'\right)}{C_{p,c}\left(T_{c,out}-T_{c,in}\right)}\right)+C^{oper.}_{cooler}\left(\frac{\dot{n}\cdot R\int_{T'_{k-1}}^{T_{k-1}}\frac{C_p(T')}{R}dT'}{C_{p,c}\left(T_{c,out}-T_{c,in}\right)}\right)=$$

$$FC_{compr.}^{cap.}\left(\frac{\dot{n}\cdot R}{\eta_k}\int_{T'_{k-1}}^{T''_k}\frac{C_p(T')}{R}dT'\right)^a+\left(C_{compr.}^{oper.}+\frac{C_{cooler}^{oper.}}{C_{p,c}\left(T_{c,out}-T_{c,in}\right)}\right)\frac{\dot{n}\cdot R}{\eta_k}\int_{T'_{k-1}}^{T''_k}\frac{C_p(T')}{R}dT'+C_{cooler}^{oper.}\frac{\dot{n}\cdot R\int_{T'_k}^{T_{k-1}}\frac{C_p(T')}{R}dT'}{C_{p,c}\left(T_{c,out}-T_{c,in}\right)}$$

Since T'_k, T_{k-1} are considered fixed but unknown, the optimization problem (25) can be rewritten as:

$$C_{cooler}^{oper.}\frac{\dot{n}\cdot R\int_{T'_k}^{T_{k-1}}\frac{C_p(T')}{R}dT'}{C_{p,c}\left(T_{c,out}-T_{c,in}\right)}+\min_{T_k,T'_{k-1},T''_k}FC_{compr.}^{cap.}\left(\frac{\dot{n}\cdot R}{\eta_k}\int_{T'_{k-1}}^{T''_k}\frac{C_p(T')}{R}dT'\right)^a+\left(C_{compr.}^{oper.}+\frac{C_{cooler}^{oper.}}{C_{p,c}\left(T_{c,out}-T_{c,in}\right)}\right)\frac{\dot{n}\cdot R}{\eta_k}\int_{T'_{k-1}}^{T''_k}\frac{C_p(T')}{R}dT'$$

s.t.

$$0<\left[Z\ln\left(\frac{P_n}{P_0}\right)-\sum_{\substack{i=1\\ i\neq k}}^{n}\int_{T'_{i-1}}^{T''_i}\frac{C_p(T')}{RT'}dT'\right]=\int_{T'_{k-1}}^{T''_k}\frac{C_p(T')}{RT'}dT'$$

$$0<\eta_k=\frac{\int_{T'_{k-1}}^{T''_k}\frac{C_p(T')}{R}dT'}{\int_{T'_{k-1}}^{T_k}\frac{C_p(T')}{R}dT'}\le 1$$

$$T'_{k-1}\le T''_k\le T_k\le T_{\max}$$

$$T_0\le T'_k\le T_k,\ T_0\le T'_{k-1}\le T_{k-1}$$

The constraint $0<\left[Z\ln\left(\frac{P_n}{P_0}\right)-\sum_{\substack{i=1\\ i\neq k}}^{n}\int_{T'_{i-1}}^{T''_i}\frac{C_p(T')}{RT'}dT'\right]=\int_{T'_{k-1}}^{T''_k}\frac{C_p(T')}{RT'}dT'$ and part (2) of Theorem 1 suggest that $\int_{T'_{k-1}}^{T''_k}\frac{C_p(T')}{R}dT'$ is a monotonically increasing function of T'_{k-1}. Since the objective function is a positive weighted combination of $\int_{T'_{k-1}}^{T''_k}\frac{C_p(T')}{R}dT'$ and its a^{th} power, its global optimum occurs at the minimum possible value of T'_{k-1}. Examination of the problem's constraints suggests that this value is T_0. Thus, at the global optimum it holds $T'_{k-1}=T_0$. Repeating this process for all compressors establishes the theorem's claim. O.E.Δ.

Proof of Theorem 3:

$(\Leftarrow)$ Let $C \le \prod_{i=1}^{n}(\eta_i D+1)$. Define $w_i \triangleq \phi\eta_i D, \quad \forall i=1,n$, where $\phi \in [0,1]$ is such that

$C = \prod_{i=1}^{n}(\phi\eta_i D+1)$. Such a $\phi \in [0,1]$ exists, since the function

$g:[0,1]\to\mathbb{R},\ g:\phi \to g(\phi) \triangleq C - \prod_{i=1}^{n}(\phi\eta_i D+1)$ is continuous on $[0,1]$, and has values

$g(0) \triangleq C-1>0 \ \wedge\ g(1) \triangleq C - \prod_{i=1}^{n}(\eta_i D+1) \le 0$. Then, the variable vector $\{w_i\}_1^n \triangleq \{\phi\eta_i D\}_1^n$,

where $\phi \in [0,1]$ is such that $C = \prod_{i=1}^{n}(\phi\eta_i D+1)$, is a feasible point for ν.

$(\Rightarrow)$ Let ν be feasible. For any feasible variable vector $\{w_i\}_1^n$, it holds

$$\left\{\prod_{i=1}^{n}(w_i+1)-C=0 \ \wedge\ 0\le w_i\le \eta_i D, \quad i=1,n\right\} \Rightarrow 1 \le \prod_{i=1}^{n}(w_i+1)=C\le\prod_{i=1}^{n}(\eta_i D+1).$$ O.E.Δ.

Proof of Theorem 4:

It is easy to establish that the above optimization problem's feasible region (which is nonempty) is closed, and bounded, that its objective function and constraint defining functions are all differentiable throughout the feasible region, and that all its feasible points are regular. Then the problem's optimum exists and the following first-order necessary optimality conditions are defined based on the Lagrangian

$L(w,\lambda,\mu,\nu) \triangleq \sum_{i=1}^{n}\frac{1}{\eta_i}\cdot w_i + \lambda\cdot\left(\prod_{i=1}^{n}(w_i+1)-C\right)+\sum_{i=1}^{n}\mu_i\cdot(-w_i)+\sum_{i=1}^{n}\nu_i\cdot(w_i-\eta_i D)$. They are:

$$\left\{\begin{array}{l}\dfrac{\partial L(w,\lambda,\mu,\nu)}{\partial w_k}=\dfrac{1}{\eta_k}+\lambda\cdot\prod\limits_{\substack{i=1\\ i\neq k}}^{n}(w_i+1)-\mu_k+\nu_k=0 \qquad \forall k=1,n \\ \prod\limits_{i=1}^{n}(w_i+1)-C=0,\ \ 0\le w_i\le\eta_i D \ \ \forall i=1,n \\ \mu_i\ge 0 \ \ \forall i=1,n,\ \ \nu_i\ge 0 \ \ \forall i=1,n,\ \ \mu_i w_i=0 \ \ \forall i=1,n,\ \ \nu_i(w_i-\eta_i D)=0 \ \ \forall i=1,n, \end{array}\right\} \overset{w_k+1\ge 1\ \forall k=1,n}{\Leftrightarrow}$$

$$\left\{\begin{array}{l}\dfrac{1}{\eta_k}(w_k+1)+\lambda\cdot C=0 \qquad \forall k\in S_I^w \\ \left(\dfrac{1}{\eta_i}-\mu_i\right)+\lambda\cdot C=0 \qquad \forall i\in S_0^w \\ \left(\dfrac{1}{\eta_j}+\nu_j\right)(\eta_j D+1)+\lambda\cdot C=0 \qquad \forall j\in S_D^w \\ \prod\limits_{l\in S_I^w}[-\lambda\eta_l C]\prod\limits_{m\in S_D^w}(\eta_m D+1)-C=0 \\ 0<w_k<\eta_k D \qquad \forall k\in S_I^w \\ \mu_i\ge 0 \qquad \forall i\in S_0^w,\ \ \nu_j\ge 0 \qquad \forall j\in S_D^w \end{array}\right\}\Leftrightarrow$$

$$\left\{\begin{array}{ll}
0 < w_k = \eta_k \left[\dfrac{C}{\left(\prod_{l\in S_I^w} \eta_l\right)\left(\prod_{m\in S_D^w} (\eta_m D+1)\right)} \right]^{\frac{1}{N_I^w}} - 1 < \eta_k D & \forall k \in S_I^w \\
\mu_i = \dfrac{1}{\eta_i} - \left[\dfrac{C}{\left(\prod_{l\in S_I^w} \eta_l\right)\left(\prod_{m\in S_D^w} (\eta_m D+1)\right)} \right]^{\frac{1}{N_I^w}} \geq 0 & \forall i \in S_0^w \\
\nu_j = \left[\dfrac{C}{\left(\prod_{l\in S_I^w} \eta_l\right)\left(\prod_{m\in S_D^w} (\eta_m D+1)\right)} \right]^{\frac{1}{N_I^w}} \dfrac{1}{(\eta_j D+1)} - \dfrac{1}{\eta_j} \geq 0 & \forall j \in S_D^w \\
\lambda = \dfrac{-1}{C} \left[\dfrac{C}{\left(\prod_{l\in S_I^w} \eta_l\right)\left(\prod_{m\in S_D^w} (\eta_m D+1)\right)} \right]^{\frac{1}{N_I^w}} < 0 &
\end{array}\right.$$

The associated objective function value is:

$$\boxed{\nu = A \cdot \left[N_I^w \left[\frac{C}{\left(\prod_{l\in S_I^w} \eta_l\right)\left(\prod_{m\in S_D^w} (\eta_m D+1)\right)} \right]^{\frac{1}{N_I^w}} - \sum_{k\in S_I^w} \frac{1}{\eta_k} + N_D^w \cdot D \right]}$$

The above necessary optimality conditions then imply:

$$\left\{ \begin{array}{l} \boxed{\begin{array}{ll} w_k = \left[\eta_k \left[\dfrac{C}{\left(\prod\limits_{l \in S_I^w} \eta_l \right) \left(\prod\limits_{m \in S_D^w} (\eta_m D + 1) \right)} \right]^{\frac{1}{N_I^w}} - 1 \right] \in (0, \eta_k D) & \forall k \in S_I^w \\ w_i = 0 & \forall i \in S_0^w \\ w_j = \eta_j D & \forall j \in S_D^w \end{array}} \wedge \\ \left\{ \begin{array}{ll} \left(\dfrac{1}{\eta_k} \right)^{N_I^w} < \dfrac{C}{\left(\prod\limits_{l \in S_I^w} \eta_l \right) \cdot \left(\prod\limits_{m \in S_D^w} (\eta_m D + 1) \right)} < \left(D + \dfrac{1}{\eta_k} \right)^{N_I^w} & \forall k \in S_I^w \\ \left(\dfrac{1}{\eta_i} \right)^{N_I^w} \geq \dfrac{C}{\left(\prod\limits_{l \in S_I^w} \eta_l \right) \cdot \left(\prod\limits_{m \in S_D^w} (\eta_m D + 1) \right)} & \forall i \in S_0^w \\ \dfrac{C}{\left(\prod\limits_{l \in S_I^w} \eta_l \right) \cdot \left(\prod\limits_{m \in S_D^w} (\eta_m D + 1) \right)} \geq \left(D + \dfrac{1}{\eta_j} \right)^{N_I^w} & \forall j \in S_D^w \end{array} \right. \end{array} \right. \Rightarrow$$

$$\left\{ \begin{array}{l} \max\limits_{k \in S_I^w} \left(\dfrac{1}{\eta_k} \right)^{N_I^w} < \dfrac{C}{\left(\prod\limits_{l \in S_I^w} \eta_l \right) \cdot \left(\prod\limits_{m \in S_D^w} (\eta_m D + 1) \right)} < \min\limits_{k \in S_I^w} \left(D + \dfrac{1}{\eta_k} \right)^{N_I^w} \\ \min\limits_{i \in S_0^w} \left(\dfrac{1}{\eta_i} \right)^{N_I^w} \geq \dfrac{C}{\left(\prod\limits_{l \in S_I^w} \eta_l \right) \cdot \left(\prod\limits_{m \in S_D^w} (\eta_m D + 1) \right)} \\ \dfrac{C}{\left(\prod\limits_{l \in S_I^w} \eta_l \right) \cdot \left(\prod\limits_{m \in S_D^w} (\eta_m D + 1) \right)} \geq \max\limits_{j \in S_D^w} \left(D + \dfrac{1}{\eta_j} \right)^{N_I^w} \end{array} \right. \Rightarrow$$

$$\max\left(\left(D+\frac{1}{\min\limits_{j\in S_D^w}\eta_j}\right)^{N_I^w},\left(\frac{1}{\min\limits_{k\in S_I^w}\eta_k}\right)^{N_I^w}\right)\le\frac{C}{\left(\prod\limits_{l\in S_I^w}\eta_l\right)\cdot\left(\prod\limits_{m\in S_D^w}\left(\eta_m D+1\right)\right)}\le$$
$$\le\min\left(\left(\frac{1}{\max\limits_{i\in S_0^w}\eta_i}\right)^{N_I^w},\left(D+\frac{1}{\max\limits_{k\in S_I^w}\eta_k}\right)^{N_I^w}\right)\ \ if\ \ N_0^w\neq 0\ \wedge\ N_D^w\neq 0$$

The remaining conditions are straightforward to establish. O.E.Δ.

Notation

Greek Letters:

β: Volume expansivity $\left(1/K\right)$

η_i: Efficiency of compressor i

κ: Isothermal compressibility $\left(1/kPa\right)$

ν: Objective function value

Letters:

A: Operating cost coefficient; $A\doteq\left(C_{compr.}^{oper.}\cdot\dot{n}\cdot C_p+\frac{C_{cooler}^{oper.}\cdot\dot{n}\cdot C_p}{C_{p,c}\left(T_{c,out}-T_{c,in}\right)}\right)T_0\ \left(\$\right)$

B: Capital cost coefficient; $B\doteq FC_{compr.}^{cap.}\dot{n}^a\cdot\left(C_p\right)^a\left(T_0\right)^a\ \ \left(\$\right)$

C: Modified pressure ratio; $C\doteq\left(\frac{P_n}{P_0}\right)^{\left(\frac{ZR}{C_p}\right)}$

C_p: Constant-pressure molar heat capacity of gas $\left(J/mol\cdot K\right)$

$C_{p,c}$: Constant-pressure molar heat capacity of coolant $\left(J/mol\cdot K\right)$

C_v : Constant-volume molar heat capacity of gas $\left(J/mol \cdot K\right)$

$C_{compr.}^{cap.}$: Capital cost coefficient of compression $\left(\$/\left(watt\right)^a\right)$

$C_{compr.}^{oper.}$: Operating cost coefficient of compression $\left(\$/J\right)$

$C_{cooler}^{oper.}$: Operating cost coefficient of cooling $\left(\$/mol\right)$

D:Maximum normalized compressor outlet temperature; $D \triangleq \frac{T_{\max} - T_0}{T_0}$

F : Annualization factor $\left(1/s\right)$

H : Molar enthalpy of fluid stream $\left(J\right)$

$\dot{n}$: Molar flow rate of gas stream $\left(mol/s\right)$

$\dot{n}_{c,i}$: Molar flow rate of coolant stream through cooler i $\left(mol/s\right)$

P_0 : Inlet pressure of gas stream to compressor/cooler system $\left(kPa\right)$

P_i : Outlet pressure of gas stream from compressor i $\left(kPa\right)$

P_n : Outlet pressure of gas stream from compressor/cooler system $\left(kPa\right)$

R : Universal gas constant $\left(J/mol \cdot K\right)$

S : Molar entropy of fluid stream $\left(J/K\right)$

T_0 : Inlet temperature of gas stream to compressor/cooler system $\left(K\right)$

$T_{c,i,in}$: Inlet temperature of coolant to cooler i $\left(K\right)$

$T_{c,i,out}$: Outlet temperature of coolant from cooler i $\left(K\right)$

T_i : Outlet temperature of gas stream from compressor i (K)

T'_{i-1} : Outlet temperature of gas stream from cooler $i-1$ to compressor i (K)

T''_i : Outlet temperature of gas stream from hypothetical isentropic compressor i (K)

$T_{\max}$: Maximum allowable operating temperature for all compressors (K)

T_n : Outlet temperature of gas stream from compressor/cooler system (K)

w_i : Normalized ideal compressor outlet temperature; $w_i \triangleq \frac{T''_i - T_0}{T_0}$

W_i : Work done by compressor i (J/mol)

W^i : Work done by a hypothetical isentropic compressor (J/mol)

Z : Compressibility factor

Subscripts:

id : Ideal (isentropic) compressor

in : Inlet stream to process unit

out : Outlet stream to process unit

r : Real compressor

Superscripts:

i : Ideal (isentropic) compressor case

o : Initial state of fluid stream

R : Reference state of fluid stream

Section 2.7: References

1. Annual Energy Outlook 2011 Reference Case. U.S. Department of Energy, U.S. Energy Information Administration, Office of Integrated and International Energy Analysis, Washington, DC, U.S., 2011.

2. Annual Energy Outlook 2013 with Projections to 2040. U.S. Department of Energy, U.S. Energy Information Administration, Office of Integrated and International Energy Analysis, Washington, 2013; http://www.eia.gov/forecasts/aeo/pdf/0383(2013).pdf.

3. Peters MS, Timmerhaus KD, West RE. Plant Design and Economics for Chemical Engineers, 5th Edition. New York: McGraw-Hill; 2003

4. Kaya, D., Phelan, P., Chau, D., & Ibrahim Sarac, H. (2002). Energy conservation in compressed-air systems. *International Journal of Energy Research*, 26(9), 837-849

5. Martin LL, Manousiouthakis VI. Total annualized cost optimality properties of state space models for mass and heat exchanger networks. *Chemical Engineering Science*. 2001;56(20): 5835-5851

6. Zhou W, Manousiouthakis VI. Global capital/total annualized cost minimization of homogeneous and isothermal reactor networks. *Industrial & Engineering Chemistry Research*. 2008;47(10): 3771-3782

7. Manousiouthakis VI, Thomas N, Justanieah AM. On a Finite Branch and Bound Algorithm for the Global Minimization of a Concave Power Law Over a Polytope. *Journal of Optimization Theory and Applications*. 2011;151(1): 121-134

8. Manousiouthakis V, Sourlas D. (1992) A global optimization approach to rationally constrained rational programming. *Chemical Engineering Communications.* 1992;115(1): 127-147.

9. Falk JE, Soland RM. An Algorithm for Separable Nonconvex Programming Problems. *Management Science* 1969, 15, 550-569.

10. Geoffrion AM. Generalized Benders Decomposition. *Journal of Optimization Theory and Applications.* 1972;10(4): 237-260.

11. Bagajewicz MJ, Manousiouthakis, V. On the Generalized Benders Decomposition. *Computers & Chemical Engineering*. 1991;15(10) 691-700.

12. Smith JM, Van Ness HC, Abbott MM. Introduction to Chemical Engineering Thermodynamics, 7th Edition. New York: McGraw-Hill; 2005: pp. 127, 199-208, 273-280.

13. Happel, J., Chemical Process Economics, John Wiley & Sons, 1958, New York, ch. 3.

14. Edgar TF, Himmelblau DM. Optimization of Chemical Processes. New York: McGraw-Hill; 1988.

15. Seider WD, Seader JD, Lewin DR. Process Design Principles: synthesis, analysis, and evaluation. 1999: John Wiley and Sons, Inc, New York, NY

16. Elrod HG Jr, Minimum Work in Multistage Compression, *Industrial Engineering Chemistry*, Vol37, No8, 1945, pp.789-790

17. Aris R., Bellman, R., Kalaba R., Some optimization problems in chemical engineering, *Chem. Eng. Prog. Symp. Ser*., 56, 31, (1960), pp. 95-102

18. Wang C-S, Fan L-T, Optimization of one-dimensional multistage linear processes, *Applied Scientific Research, Section B*, Vol. 11, 1965, pp. 321-334.

19. Engineering Data Book, Gas Processors Suppliers Association, Tulsa, OK, 2006

20. Linstrom PJ, Mallard WG, Eds., NIST Chemistry WebBook, NIST Standard Reference Database Number 69, National Institute of Standards and Technology, Gaithersburg MD, http://webbook.nist.gov, (retrieved June 24, 2014).

Chapter 3: Global Minimization of an Infinite Collection of Instances of the Total Annualized Cost Problem for Compressor Sequences

In this work, a novel hybrid method is proposed for the global solution of an infinite collection of instances of the minimum total annualized cost (TAC) problem for a series of gas compressors and coolers, that brings a gas from a given pressure and temperature to a specified final pressure and the same temperature. The gas is considered to possess a constant compressibility factor, and a constant, ideal gas, constant pressure, heat capacity. The collection of TAC problem instances considered is parameterized by the overall compression ratio. The proposed method combines the TAC problem's first and second order necessary conditions of optimality with interval analysis, to determine converging upper and lower bounds to the globally optimal solution and associated optimal solution vector components, for all considered instances of the TAC problem. Two case studies are presented to illustrate the novel solution method, and the impact of economies of scale on the global optimum.

Section 3.1: Introduction

As the energy picture in the US evolves to increased natural gas production (48% annual growth rate of shale gas production between 2006 and 2010[1]), the transportation of this natural gas across the country will place increased emphasis on gas compression systems. According to the U.S. Energy Information Administration (EIA)[2], this trend will not abate for at least the next twenty-five years with predicted annual growth rates of 11.9% for natural gas consumption in transportation. Combined with the increased use of compressed natural gas and compressed

hydrogen for automotive transportation, and the extensive use of compression systems in the process industries, a compelling case arises for the optimization of gas compression systems. As an example, even the simple substitution of low efficiency with high efficiency compressors can reduce overall plant power consumption by over 5%[3].

Gas compression is typically carried out industrially via sequences of compressors with intermediate coolers, which are placed at the exit of each compressor to ameliorate the gas temperature increases associated with gas compression. These compressor-cooler sequences typically constitute a significant portion of a process plant's Total Annualized cost (TAC). The operating cost component of the TAC of a compressor/cooler sequence is associated with the compressors' power consumption and the coolers' cooling costs. The annualized capital cost component of the TAC of a compressor/cooler sequence is largely associated with only the compressors' capital cost, which is significantly higher than the coolers' capital cost.

The capital cost of a compressor is typically correlated to the compressor's power consumption. Peters et. al.[4] (figure 12-28, p.531) present linear correlations on a log-log plot of compressor purchased cost $K(\$)$ as a function of consumed power $W(kW)$, thus suggesting that the compressor capital cost obeys the relation $K(\$) = K_1(\$)\left(\frac{W(kW)}{W_1(kW)}\right)^a$ with power law exponent, a, values ranging from 0.65 to 0.95. These correlations capture the economies of scale expected with the purchase of larger sized equipment.

Biegler et. al.[5] also employ the same correlation (Table 4.12, p. 134) with $K_1(\$) = 23{,}000(\$)$, $W_1(hp) = 100(hp)$ and $a = 0.77$. Similar correlations are also given by Seider et. al.[6] (figure 16.9, p.521) for

$$\text{centrifugal}\left[\frac{K_1}{(W_1)^a}\left(\frac{\$}{(hp)^a}\right)=\exp[7.2223]\left(\frac{\$}{(hp)^a}\right),\ W(hp),\ a=0.80\right],$$

$$\text{reciprocating}\left[\frac{K_1}{(W_1)^a}\left(\frac{\$}{(hp)^a}\right)=\exp[7.6084]\left(\frac{\$}{(hp)^a}\right),\ W(hp),\ a=0.80\right], \text{ and}$$

$$\text{screw}\left[\frac{K_1}{(W_1)^a}\left(\frac{\$}{(hp)^a}\right)=\exp[7.7661]\left(\frac{\$}{(hp)^a}\right),\ W(hp),\ a=0.7243\right] \text{compressors.}$$

The inherently non-convex nature of the Total Annualized Cost (TAC) minimization problem, due to the incorporation of the aforementioned economies of scale, makes it a challenging problem with few global optimality results available in the literature. Manousiouthakis and coworkers[7,8,9], studied the TAC problem for heat exchanger networks, reactor networks, and compressor sequences respectively. Motivated by the reactor network problem formulation within the IDEAS framework [8], Manousiouthakis et. al.[10] developed a branch-and-bound-based method that can identify in a finite number of steps the global minimum of a concave power law over a system of linear constraints. Concave power law objective functions with rational exponents can be transformed to rationally constrained rational programs, which Manousiouthakis et. al.[11] demonstrated how to solve globally by first transforming them to convex, quadratically constrained quadratic programs with an additional separable concave quadratic constraint, and then solving using branch and bound[12] or Generalized Benders Decomposition[13,14] methods.

The behavior of compressors and coolers is captured through models well-established in the literature[15]. Elrod[16], Happel[17], and Aris et. al.[18] presented the solution to the steady-state, work (power) minimization problem, for two, three and a sequence respectively, of isentropic compressors and intermediate coolers, that brings an ideal gas from an initial temperature and

pressure to a desired final pressure and a final temperature equal to the initial temperature. The optimal works of the compressors are shown to be equal at the optimum. Wang and Fan[19] showed that the multistage, isentropic compression of ideal gas is part of a class of so called one dimensional multistage processes, whose common characteristic is that they optimally require equal amounts of control action in each stage. The minimization of consumed work for general compressor/cooler sequences can be found in the textbooks by Edgar and Himmelblau[20] and by Seader et al[21]. More recently, Conner and Manousiouthakis[9] established optimality properties for TAC minimization of a series of non-isentropic compressors and coolers that brings a constant compressibility factor gas from a specified initial pressure and temperature to a specified final pressure and the same temperature. For constant heat capacity, constant compressibility factor gases, they also presented a solution method for the globally minimum operating cost problem.

In this work, the TAC minimization of a series of non-isentropic compressors and coolers that brings a constant compressibility factor, and constant heat capacity gas from a specified initial temperature and pressure to the same final temperature and a parametrized final pressure belonging to a known interval. Consider for example the compression of hydrogen gas from room temperature and pressure to a pressure that may be employed in hydrogen fuel cell vehicle storage tanks. It is desired to know the number and associated workloads of compressors needed to minimize the TAC for this operation. Clearly, the TAC optimum depends parametrically on the sequence's overall compression ratio and it is desirable to identify it as a function of that ratio. The theoretical developments that follow will allow the quantification of the aforementioned optimum TAC versus overall compression ratio function.

The rest of the paper is structured as follows: First, the TAC problem considered in this work and associated background material are introduced. Second, our mathematical framework

is briefly reviewed and the notion of optimization problem instances is defined. Our new theoretical developments are then presented establishing first and second order necessary conditions of optimality for the considered TAC problem. Then a novel hybrid method is presented which combines the aforementioned conditions of optimality with interval analysis (see Manousiouthakis et. al.[21] and references therein), to determine converging upper and lower bounds to the globally optimal solution and associated optimal solution vector components, for all considered instances of the TAC problem. Two case studies are presented to illustrate the developed theorems and solution strategies. Lastly, conclusions are drawn.

Section 3.2: Conceptual Framework

Preliminaries

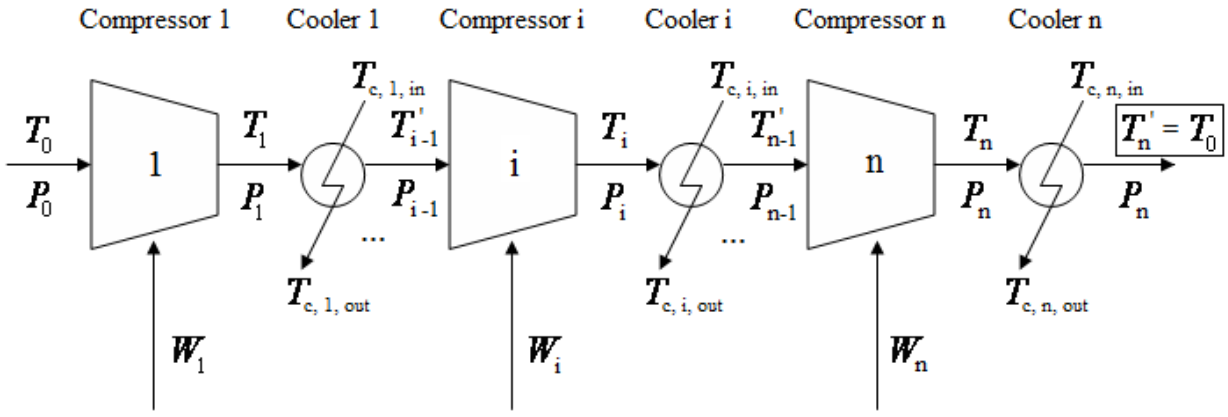

Figure 3.1: Process flowsheet for n compressors and n intermediate coolers

In this work, the minimum total annualized cost (TAC) problem is considered, for a sequence of n non-isentropic compressors and isobaric coolers (see Figure 3.1) that brings a gas with constant compressibility factor Z, and constant, ideal gas, constant pressure, heat capacity C_p, from a specified initial state (T_0, P_0) to a specified final state (T_0, P_n). The inlet and outlet

temperatures for any compressor in the series must be above T_0 and below $T_{\max}$, the maximum allowable operating temperature for all compressors, respectively. Each compressor has a known, constant, isentropic efficiency $\eta_i \in (0,1] \ \forall i = 1,n$. The coolant inlet and outlet temperatures are considered fixed and known for all coolers. They are defined such that $T_{c,i,in} \le T_{c,i,out} \le T_0,\ i = 1,n$.

In our earlier work[9], the following were established for a gas featuring a constant compressibility factor Z, and a constant, ideal gas, constant pressure, heat capacity C_p:

1. $$\boxed{Z = \frac{PV}{RT}} \quad (1)$$
$$\boxed{\beta = \frac{1}{T},\ \kappa = \frac{1}{P}} \quad (2)$$
$$\boxed{H(T,P) - H\left(T^o,P^o\right) = C_p\left(T - T^o\right)} \quad (3)$$
$$\boxed{S(T,P) - S^o\left(T^o,P^o\right) = C_p \ln\left(\frac{T}{T^o}\right) - RZ\ln\left(\frac{P}{P^o}\right)} \quad (4)$$
$$\boxed{C_p - C_v = RZ} \quad (5)$$
$$\boxed{k \triangleq \frac{C_p}{C_v} = \frac{C_p}{C_p - RZ},\ \frac{k-1}{k} = \frac{RZ}{C_p}} \quad (6)$$

2. Consider that the aforementioned gas is compressed through an adiabatic ideal compressor, and through an adiabatic real compressor with known, constant, efficiency $\eta \in (0,1]$. Let the inlet temperatures, and inlet and outlet pressures T_{in}, P_{in}, P_{out} to both compressors be the same, and let the outlet temperatures be denoted as T''_{out}, T_{out}, respectively. Then the following relations hold:
$$\boxed{T''_{out} = T_{in}\left(\frac{P_{out}}{P_{in}}\right)^{\frac{k-1}{k}},\ T_{out} = T_{in}\left(1 + \frac{\left(\frac{P_{out}}{P_{in}}\right)^{\frac{k-1}{k}} - 1}{\eta}\right)} \quad (7)$$

$$W_{id} = C_p\left(T''_{out} - T_{in}\right) = ZR\frac{k}{k-1}T_{in}\left(\left(\frac{P_{out}}{P_{in}}\right)^{\frac{k-1}{k}} - 1\right) \quad (8)$$

$$W_r = C_p\left(T_{out} - T_{in}\right) = \frac{1}{\eta}ZR\frac{k}{k-1}T_{in}\left(\left(\frac{P_{out}}{P_{in}}\right)^{\frac{k-1}{k}} - 1\right) \quad (9)$$

3. At the global optimum of the TAC problem for the aforementioned gas, the cooler outlet temperatures are equal to the minimum allowable temperature, i.e. $T'_{i-1} = T_0$ for $i = 2, n$ (see Figure 1).

4. The resulting TAC problem for the aforementioned gas can be formulated as:

$$\nu = \begin{Bmatrix} \min\limits_{\{w_i\}_{i=1}^n} A\sum\limits_{i=1}^{n}\frac{1}{\eta_i}\cdot w_i + B\sum\limits_{i=1}^{n}\left(\frac{1}{\eta_i}\right)^a\cdot\left(w_i\right)^a \\ s.t. \\ \prod\limits_{i=1}^{n}\left(w_i+1\right) - C = 0 \\ 0 \le w_i \le \eta_i D, \quad i = 1, n \end{Bmatrix} \quad (10)$$

where $A\left(\frac{\$}{s}\right) \triangleq \left(C^{oper.}_{compr.}\cdot\dot{n}\cdot C_p + \frac{C^{oper.}_{cooler}\cdot\dot{n}\cdot C_p}{C_{p,c}\left(T_{c,out} - T_{c,in}\right)}\right)T_0 \ge 0$,

$B\left(\frac{\$}{s}\right) \triangleq FC^{cap.}_{compr.}\dot{n}^a\cdot\left(C_p\right)^a\left(T_0\right)^a \ge 0$, $C \triangleq \left(\frac{P_n}{P_0}\right)^{\left(\frac{ZR}{C_p}\right)} > 1$, $D \triangleq \frac{T_{\max} - T_0}{T_0} > 0$,

$\eta_i = \frac{T''_i - T_0}{T_i - T_0} \in (0,1] \;\; \forall i = 1, n$ and $w_i \triangleq \frac{W_{id,i}}{C_p T_0} = \frac{T''_i - T_0}{T_0} = \frac{\eta_i\left(T_i - T_0\right)}{T_0} = \frac{\eta_i W_i}{C_p T_0} \quad i = 1, n$.

The first cost coefficient $A\left(\frac{\$}{s}\right)$ captures the compressor and cooler operating cost (electrical work consumed by the compressors and cooling water cost for the coolers); the second cost coefficient $B\left(\frac{\$}{s}\right)$ captures the annualized compressor capital cost (the cooler capital cost is ignored, as it is much smaller than that of the compressor); the third dimensionless parameter C is the compressor sequence's compression ratio raised to a dimensionless power proportional to the ratio of the gas' compressibility factor over the gas' ideal gas, constant pressure heat capacity ratio; the fourth dimensionless parameter D captures the maximum temperature allowed at the exit of each compressor. Finally,

$\eta_i \;\; i=1,n$ are dimensionless parameters denoting the efficiency of each compressor, and $w_i \;\; i=1,n$ are dimensionless variables proportional to each compressor's ideal work.

5. The TAC problem (10) for the aforementioned gas is feasible iff $C \le \prod_{i=1}^{n}(\eta_i D+1)$. The feasibility condition $C \le \prod_{i=1}^{n}(\eta_i D+1)$ is the direct result of the outlet temperature limitation for every real compressor, namely that $T_i \le T_{\max} \;\; \forall i=1,n$. Indeed the above limitation can be equivalently stated as follows:
Each real compressor must be such that $T_i \le T_{\max} \;\; \forall i=1,n \Leftrightarrow$
$T_i - T_0 \le T_{\max} - T_0 \;\; \forall i=1,n \Leftrightarrow T_i - T_0 \le DT_0 \;\; \forall i=1,n \Leftrightarrow$
$\eta_i (T_i - T_0) \le \eta_i DT_0 \;\; \forall i=1,n \Leftrightarrow T_i'' - T_0 \le \eta_i DT_0 \;\; \forall i=1,n \Leftrightarrow \frac{T_i''}{T_0} \le \eta_i D+1 \;\; \forall i=1,n \Leftrightarrow$
$\left(\frac{P_i}{P_{i-1}}\right)^{\frac{RZ}{C_p}} \le \eta_i D+1 \;\; \forall i=1,n$. This implies $\left(\frac{P_n}{P_0}\right)^{\frac{RZ}{C_p}} \le \prod_{i=1}^{n}(\eta_i D+1) \Leftrightarrow C \le \prod_{i=1}^{n}(\eta_i D+1)$.
Therefore, the feasibility statement simply ensures that the compressor sequence's overall compression ratio is such that the outlet temperatures of all real compressors are all below the maximum allowable temperature.

6. The optimal solution of the Operating cost (OC) problem, (10) *with* $B=0,\; N_I^w \ge 1$, satisfies the following:

$$v = A \cdot \left[N_I^w \frac{C^{\frac{1}{N_I^w}}}{\left(\prod_{l\in S_I^w}\eta_l\right)^{\frac{1}{N_I^w}} \cdot \left(\prod_{m\in S_D^w}(\eta_m D+1)\right)^{\frac{1}{N_I^w}}} - \sum_{k\in S_I^w}\frac{1}{\eta_k} + N_D^w \cdot D \right]$$

$$w_k = \left[\eta_k \left[\frac{C}{\left(\prod_{l\in S_I^w}\eta_l\right)\left(\prod_{m\in S_D^w}(\eta_m D+1)\right)} \right]^{\frac{1}{N_I^w}} - 1 \right] \in (0, \eta_k D) \;\; \forall k \in S_I^w; \; \begin{Bmatrix} w_i = 0 \;\; \forall i \in S_0^w \\ w_j = \eta_j D \;\; \forall j \in S_D^w \end{Bmatrix}$$

$$\max\left(\left(D + \frac{1}{\min_{j\in S_D^w}\eta_j}\right), \left(\frac{1}{\min_{k\in S_I^w}\eta_k}\right) \right) \le \left[\frac{C}{\left(\prod_{l\in S_I^w}\eta_l\right)\cdot\left(\prod_{m\in S_D^w}(\eta_m D+1)\right)} \right]^{\frac{1}{N_I^w}} \le \min\left(\left(\frac{1}{\max_{i\in S_0^w}\eta_i}\right), \left(D + \frac{1}{\max_{k\in S_I^w}\eta_k}\right) \right)$$

where $S_D^w \triangleq \{i = 1, n : w_i = \eta_i D\}$ (compressors operating at maximum allowable outlet temperature), $S_0^w \triangleq \{i = 1, n : w_i = 0\}$ (compressors not in use), $S_I^w \triangleq \{i = 1, n : 0 < w_i < \eta_i D\}$ (compressors in use and operating below maximum allowable outlet temperature) with cardinalities N_D^w, N_0^w, N_I^w, respectively, and all min and max operators are taken over non-empty sets, otherwise the associated actions are omitted.

Section 3.3: Mathematical Problem Formulation

In this section, first a brief review is provided of optimization problem instances, and the concept of solving a collection of instances of an optimization problem is formalized. Second, the TAC minimization problem (10) is infinitesimally altered to yield TAC minimization problem (11), which possesses desirable differentiability properties. Third, the instance related concepts of (11) considered in this work are clearly defined. Fourth, the first and second order optimality conditions of (11) are presented. Finally, these are combined with interval analysis to develop a novel, hybrid, global solution methodology for the considered infinite collection of TAC problem instances, parameterized by the overall compression ratio.

An optimization problem Q can be considered as the 4-tuple $\langle I_Q, S_Q, f_Q, opt_Q \rangle$ [21], where I_Q is the set of *instances*; S_Q is the function that maps each $x \in I_Q$ to the set $S_Q(x)$ of *feasible solutions* corresponding to $x \in I_Q$; f_Q is the *objective function* that maps each pair $(x, y) \in (I_Q, S_Q(x))$ to the *objective function value* $f_Q(x, y)$ corresponding to that *instance* x and that *feasible solution* $y \in S_Q(x)$; $opt_Q \in \{\min, \max\}$ is a linguistic variable that determines whether the *minimum* or the *maximum* of the objective function is to be identified.

In this work, the 4-tuple defined above is used to quantify the function Z_Q, as the function that maps each $x \in I_Q$ to the set $Z_Q(x)$ of *optimum feasible solutions* corresponding to $x \in I_Q$, and the function F_Q, as the function that maps each $x \in I_Q$ to the *optimum objective function value* $F_Q(x) \triangleq f_Q(x,z) \ \forall z \in Z_Q(x)$ corresponding to $x \in I_Q$.

Solving the optimization problem Q can then be defined as follows: Given an *instance* $x \in I_Q$, identify the set of *optimum feasible solutions* $Z_Q(x) \subset S_Q(x)$ such that $\forall z \in Z_Q(x)$ the *optimum objective function value* $F_Q(x) \triangleq f_Q(x,z) \ \forall z \in Z_Q(x)$ is the *minimum* (or the *maximum* depending on opt_Q) among all *objective function values* $f_Q(x,y)$ corresponding to the *instance* x and all *feasible solutions* $y \in S_Q(x)$.

However, as Birattari[22] points out in his text, it seems advisable to recognize that different specific problems have some common structure and can be profitably considered as different instances of the same problem. In this work, we further advance the above idea by formalizing the concept of solving a *collection of instances of the optimization problem* Q as follows: Given the 4-tuple $\langle I_Q, S_Q, f_Q, opt_Q \rangle$, and a *subset* $X_Q \subset I_Q$ of the set of *instances* I_Q, identify the graphs of the restrictions $Z_Q \mid X_Q$ and $F_Q \mid X_Q$ of the functions Z_Q and F_Q respectively to the subset X_Q, which quantify the *set of optimal solutions corresponding* to X_Q, and the *set of optimum objective function values corresponding* to X_Q, as functions of X_Q.

Having briefly reviewed the concept of optimization problem instances and having formalized the concept of solving a collection of instances of an optimization problem, our

attention turns to TAC problem (10), whose objective function is not differentiable over its feasible region. Thus, the following TAC problem with an infinitesimally smaller region is introduced. Let $\varepsilon \in \left(0, \dfrac{\min\limits_{i=1,n} \eta_i}{\max\limits_{i=1,n} \eta_i} D\right)$; $\varepsilon \simeq 0$, and define

$$\nu_\varepsilon \triangleq A \left\{ \begin{array}{l} \min\limits_{\{w_i\}_{i=1}^n} \sum\limits_{i=1}^n \dfrac{1}{\eta_i} \cdot w_i + \dfrac{B}{A} \sum\limits_{i=1}^n \left(\dfrac{1}{\eta_i}\right)^a \cdot (w_i)^a \\ s.t. \\ \prod\limits_{i=1}^n (w_i + 1) - C = 0 \\ \eta_i \varepsilon \le w_i \le \eta_i D, \quad i = 1, n \end{array} \right\} (11)$$

Denoting the above defined problem (11) as Q, leads to the following definitions for the 4-tuple $\langle I_Q, S_Q, f_Q, opt_Q \rangle$, and the associated Z_Q, F_Q

$$I_Q \triangleq \left\{ \left(\frac{B}{A}, C, D, \{\eta_i\}_{i=1}^n \right) \in \mathbb{R}^+ \times \mathbb{R}^+ \times \mathbb{R}^+ \times \mathbb{R}^n : 1 < C \le \prod_{i=1}^n (\eta_i D + 1),\ \eta_i \in (0,1] \ \ \forall i = 1, n \right\},$$

$S_Q : I_Q \to \mathbb{R}^n$, $S_Q : x \to S_Q(x)$, where

$$x = \left(\frac{B}{A}, C, D, \{\eta_i\}_{i=1}^n \right) \in I_Q, \quad S_Q(x) \triangleq \left\{ \{y_i\}_{i=1}^n \in \mathbb{R}^n : \left[\begin{array}{l} y_i \in [\eta_i \varepsilon, \eta_i D] \ \ \forall i = 1, n \\ \prod\limits_{i=1}^n (y_i + 1) = C \end{array} \right] \right\};$$

$f_Q : I_Q \times S_Q(x) \to \mathbb{R}$, $f_Q : (x, y) \to f_Q(x, y) \triangleq \left[\sum\limits_{i=1}^n \dfrac{1}{\eta_i} \cdot y_i + \dfrac{B}{A} \sum\limits_{i=1}^n \left(\dfrac{1}{\eta_i}\right)^a \cdot (y_i)^a \right] \in \mathbb{R}$, where

$$x = \left(\frac{B}{A}, C, D, \{\eta_i\}_{i=1}^n \right) \in I_Q, \ y = \{y_i\}_{i=1}^n \in S_Q(x); \ opt_Q \triangleq \min$$

$Z_Q : I_Q \to \mathbb{R}^n$, $Z_Q : x \to Z_Q(x)$, and $F_Q : I_Q \to \mathbb{R}$, $F_Q : x \to F_Q(x)$, where

$$x = \left(\frac{B}{A}, C, D, \{\eta_i\}_{i=1}^{n} \right) \in I_Q ,$$

$$Z_Q(x) \triangleq \left\{ \{z_i\}_{i=1}^{n} \in S_Q(x) : \left\{ \begin{bmatrix} \sum_{i=1}^{n} \frac{1}{\eta_i} \cdot z_i + \frac{B}{A} \sum_{i=1}^{n} \left(\frac{1}{\eta_i} \right)^a \cdot (z_i)^a \end{bmatrix} \leq \right. \right.$$
$$\left. \left. \begin{bmatrix} \sum_{i=1}^{n} \frac{1}{\eta_i} \cdot y_i + \frac{B}{A} \sum_{i=1}^{n} \left(\frac{1}{\eta_i} \right)^a \cdot (y_i)^a \end{bmatrix} \ \forall \{y_i\}_{i=1}^{n} \in S_Q(x) \right\} \right\}$$

$$F_Q(x) \triangleq \left\{ \begin{bmatrix} \sum_{i=1}^{n} \frac{1}{\eta_i} \cdot z_i + \frac{B}{A} \sum_{i=1}^{n} \left(\frac{1}{\eta_i} \right)^a \cdot (z_i)^a \end{bmatrix} \in \mathbb{R} : \left\{ \begin{bmatrix} \sum_{i=1}^{n} \frac{1}{\eta_i} \cdot z_i + \frac{B}{A} \sum_{i=1}^{n} \left(\frac{1}{\eta_i} \right)^a \cdot (z_i)^a \end{bmatrix} \leq \right. \right.$$
$$\left. \left. \begin{bmatrix} \sum_{i=1}^{n} \frac{1}{\eta_i} \cdot y_i + \frac{B}{A} \sum_{i=1}^{n} \left(\frac{1}{\eta_i} \right)^a \cdot (y_i)^a \end{bmatrix} \ \forall \{y_i\}_{i=1}^{n} \in S_Q(x) \right\} \right\}$$

The infinite collection of instances $X_Q \subset I_Q$ considered in this work is:

$$X_Q \triangleq \left\{ \left(\frac{B}{A}, C, D, \{\eta_i\}_{i=1}^{n} \right) \in \mathbb{R}^+ \times \mathbb{R}^+ \times \mathbb{R}^+ \times \mathbb{R}^n : \begin{bmatrix} \eta_i \in (0,1] \ \ \forall i = 1, n \\ \left(\frac{B}{A}, D, \{\eta_i\}_{i=1}^{n} \right) \textit{is known} \\ C \in \left(1, \prod_{i=1}^{n} (\eta_i D + 1) \right] \end{bmatrix} \right\} \subset I_Q$$

It is easy to see from the above definition, that the infinite collection of instances X_Q can be parameterized, in terms of the single parameter C.

Having defined X_Q for TAC(11), we now present Theorem 1, which quantifies optimality properties for TAC(11). To this end, let $\{w_i^*\}_{i=1}^{n}$ be a globally optimum variable vector of ν_ε, and define the associated sets $S_D^{w*} \triangleq \{i = 1, n : w_i^* = \eta_i D\}$ (compressors operating at maximum temperature at the optimum), $S_\varepsilon^{w*} \triangleq \{i = 1, n : w_i^* = \eta_i \varepsilon\}$ (compressors practically not in

use at the optimum), and $S_I^{w*} \triangleq \left\{ i = 1, n : \eta_i \varepsilon < w_i^* < \eta_i D \right\} = \left\{ \{1, \cdots, n\} - S_\varepsilon^{w*} - S_D^{w*} \right\}$ (compressors in use and operating below maximum temperature at the optimum) with cardinalities $N_D^{w*}, N_\varepsilon^{w*}, N_I^{w*}$, respectively. Then $N_I^{w*} = n - N_D^{w*} - N_\varepsilon^{w*}$.

If $N_I^{w*} = 0$, it must then hold that $N_D^{w*} \geq 1$, otherwise the compression level C could not be attained. In this case, straightforward combinatorial calculations, on which compressors belong to S_D^{w*}, can be carried out to identify the global minimum without any need of the optimality conditions. Thus in Theorems 1 and 2, it is considered that $N_I^{w*} \geq 1$.

Theorem 1:

Let $A > 0,\ B > 0,\ D > 0,\ 1 < C \leq \prod_{i=1}^{n} \left(\eta_i D + 1 \right),\ \eta_i \in (0,1]\ \ \forall i = 1, n$ and consider the problem TAC(11), where $\varepsilon \in \left(0, \dfrac{\min\limits_{i=1,n} \eta_i}{\max\limits_{i=1,n} \eta_i} D \right)$; $\varepsilon \simeq 0$.

Then

a. $1 \leq N_D^{w*} < n$ implies $\min\limits_{i \in S_D^{w*}} \eta_i \geq \max\limits_{i \in S_I^{w*} \cup S_\varepsilon^{w*}} \eta_i$

b. $1 \leq N_\varepsilon^{w*}$ implies $\max\limits_{i \in S_\varepsilon^{w*}} \eta_i \leq \min\limits_{i \in S_I^{w*} \cup S_D^{w*}} \eta_i$

One should rank order all considered compressors according to their efficiency (highest efficiency ranked first). Then Theorem 1 establishes that at the global optimum of the TAC problem considered in this work, the first N_D^w compressors in the above ranked list should be in the on-saturated category, the next N_I^w compressors should be in the on-interior category, and

the last N_{ε}^{w} should be in the off category. Then the sets $S_D^w, S_I^w, S_{\varepsilon}^w$ are:

$$S_D^w \triangleq \{1,\ldots,N_D^w\},\ S_I^w \triangleq \{N_D^w+1,\ldots,N_D^w+N_I^w\},\ S_{\varepsilon}^w \triangleq \{N_D^w+N_I^w,\ldots,n\}.$$

Theorem 2:

Consider the optimization problem TAC(11), with $\varepsilon \in \left(0, \dfrac{\min\limits_{i=1,n} \eta_i}{\max\limits_{i=1,n} \eta_i} D\right)$; $\varepsilon \simeq 0$,

$A>0,\ B>0,\ D>0,\ 1<C\le \prod_{i=1}^{n}(\eta_i D+1),\ \eta_i \in (0,1]\ \ \forall i=1,n,\ \ N_I^w \ge 1$. Let $\{w_i\}_{i=1}^{n}$ be a

feasible variable vector of ν_{ε}, and define the corresponding sets $S_D^w \triangleq \{i=1,n : w_i = \eta_i D\}$

(compressors operating at maximum temperature at the optimum), $S_{\varepsilon}^w \triangleq \{i=1,n : w_i = \eta_i \varepsilon\}$

(compressors practically not in use at the optimum), and

$S_I^w \triangleq \{i=1,n : \eta_i \varepsilon < w_i < \eta_i D\} = \{\{1,\cdots,n\} - S_D^w - S_0^w\}$ (compressors in use and operating below

maximum temperature at the optimum) with cardinalities $N_D^w, N_{\varepsilon}^w, N_I^w$, respectively, where

$N_I^w \triangleq n - N_D^w - N_{\varepsilon}^w$.

Then, if $\{w_i\}_{i=1}^{n}$ is to be a globally optimum variable vector of ν_{ε}, the following must be satisfied:

$$\left\{\begin{array}{l}
\left(\dfrac{1}{\eta_k}+a\dfrac{B}{A}\left(\dfrac{1}{\eta_k}\right)^{a}\left(w_k\right)^{a-1}\right)\left(w_k+1\right)+\lambda C=0 \qquad \forall k\in S_I^w \\
\mu_i=\dfrac{1}{\eta_i}+a\dfrac{B}{A}\dfrac{1}{\eta_i}\varepsilon^{a-1}+\dfrac{\lambda C}{\left(\eta_i\varepsilon+1\right)}\geq 0 \qquad \forall i\in S_\varepsilon^w \\
\nu_j=\dfrac{-\lambda C}{\left(\eta_j D+1\right)}-\left(\dfrac{1}{\eta_j}+a\dfrac{B}{A}\dfrac{1}{\eta_j}D^{a-1}\right)\geq 0 \qquad \forall j\in S_D^w \\
\left[\begin{array}{cccc}
E_{N_D^w+1}+E_{N_D^w+N_I^w} & E_{N_D^w+N_I^w} & \cdots & E_{N_D^w+N_I^w} \\
E_{N_D^w+N_I^w} & E_{N_D^w+2}+E_{N_D^w+N_I^w} & \cdots & E_{N_D^w+N_I^w} \\
\vdots & \vdots & \ddots & \vdots \\
E_{N_D^w+N_I^w} & E_{N_D^w+N_I^w} & \cdots & E_{N_D^w+N_I^w-1}+E_{N_D^w+N_I^w}
\end{array}\right] \text{ is psd on } \mathbb{R}^{N_I^w-1} \\
\prod_{o\in S_\varepsilon^w}\left(\eta_o\varepsilon+1\right)\prod_{l\in S_I^w}\left(w_l+1\right)\prod_{m\in S_D^w}\left(\eta_m D+1\right)-C=0,\ 0<\eta_k\varepsilon<w_k<\eta_k D \qquad \forall k\in S_I^w \\
w_i=\eta_i\varepsilon \ \ \forall i\in S_\varepsilon^w,\ \ w_j=\eta_j D \ \ \forall j\in S_D^w
\end{array}\right\}$$

where $E_i \triangleq \dfrac{a\left(a-1\right)B}{AC}\left(\dfrac{1}{\eta_i}\right)^{a}\dfrac{\left(w_i+1\right)^2}{\left(w_i\right)^{2-a}}-\lambda \ \ \forall i\in\left\{N_D^w+1,\cdots,N_D^w+N_I^w\right\}$, and *psd* means positive semi-definite.

Given the above, it is straightforward to establish that the optimum objective function value must satisfy

$$\nu_\varepsilon = A\left\{\left(D+\frac{B}{A}D^a\right)N_D^w+\left(\varepsilon+\frac{B}{A}\varepsilon^a\right)N_\varepsilon^w+\inf_{\{w_i\}_{i\in S_I^w}}\left[\sum_{i\in S_I^w}\frac{1}{\eta_i}w_i+\frac{B}{A}\sum_{i\in S_I^w}\left(\frac{1}{\eta_i}\right)^a\left(w_i\right)^a\right]\right\}$$

$$\begin{array}{l}
\textit{s.t.} \\
\prod_{i\in S_\varepsilon^w}\left(\eta_i\varepsilon+1\right)\prod_{i\in S_I^w}\left(w_i+1\right)\prod_{i\in S_D^w}\left(\eta_i D+1\right)-C=0 \\
\eta_i\varepsilon<w_i<\eta_i D, \ \ \forall i\in S_I^w
\end{array}$$

As the parameter C varies over the interval $\left(1,\prod_{i=1}^{n}\left(\eta_i D+1\right)\right]$, the infinite collection of instances X_Q is generated. Having defined X_Q for TAC(11), optimality properties for each instance of

TAC (11) were presented in Theorems 1 and 2. What is important to point out to the reader, is that all but one of these properties can be enforced without the parameter C having to be specified. In turn, this allows the creation of a solution procedure which creates an enclosure of upper and lower bounds on the graphs of the restrictions $Z_Q \big| X_Q$ and $F_Q \big| X_Q$ of the functions Z_Q and F_Q respectively to the subset X_Q. In other terms, this allows the creation of upper and lower bounds on the globally optimum objective function value, and on the associated globally optimum variable values of TAC (11), corresponding to each possible value of the parameter C in the interval $\left(1, \prod_{i=1}^{n} (\eta_i D + 1)\right]$. Indeed, from Theorem 2, it holds

$\left(\frac{1}{\eta_k} + a\frac{B}{A}\left(\frac{1}{\eta_k}\right)^a (w_k)^{a-1}\right)(w_k + 1) + \lambda C = 0 \qquad \forall k \in S_I^w$. This can be equivalently written as

$\left(\frac{1}{\eta_k} + a\frac{B}{A}\left(\frac{1}{\eta_k}\right)^a (w_k)^{a-1}\right)(w_k + 1) = \left(\frac{1}{\eta_{N_D^w+1}} + a\frac{B}{A}\left(\frac{1}{\eta_{N_D^w+1}}\right)^a \left(w_{N_D^w+1}\right)^{a-1}\right)\left(w_{N_D^w+1} + 1\right) \qquad \forall k \in S_I^w$, and

$\lambda C = -\left(\frac{1}{\eta_{N_D^w+1}} + a\frac{B}{A}\left(\frac{1}{\eta_{N_D^w+1}}\right)^a \left(w_{N_D^w+1}\right)^{a-1}\right)\left(w_{N_D^w+1} + 1\right)$. Clearly the first of the above statements does not depend on the parameter C. This argument can be similarly used for all but one of the other conditions identified in Theorem 2, including the matrix condition

$$\begin{bmatrix} E_{N_D^w+1} + E_{N_D^w+N_I^w} & E_{N_D^w+N_I^w} & \cdots & E_{N_D^w+N_I^w} \\ E_{N_D^w+N_I^w} & E_{N_D^w+2} + E_{N_D^w+N_I^w} & \cdots & E_{N_D^w+N_I^w} \\ \vdots & \vdots & \ddots & \vdots \\ E_{N_D^w+N_I^w} & E_{N_D^w+N_I^w} & \cdots & E_{N_D^w+N_I^w-1} + E_{N_D^w+N_I^w} \end{bmatrix} \text{ is psd on } \mathbb{R}^{N_I^w-1},$$ which is

equivalent to $C\begin{bmatrix} E_{N_D^w+1}+E_{N_D^w+N_I^w} & E_{N_D^w+N_I^w} & \cdots & E_{N_D^w+N_I^w} \\ E_{N_D^w+N_I^w} & E_{N_D^w+2}+E_{N_D^w+N_I^w} & \cdots & E_{N_D^w+N_I^w} \\ \vdots & \vdots & \ddots & \vdots \\ E_{N_D^w+N_I^w} & E_{N_D^w+N_I^w} & \cdots & E_{N_D^w+N_I^w-1}+E_{N_D^w+N_I^w} \end{bmatrix}$ *is psd on* $\mathbb{R}^{N_I^w-1}$,

and which only seemingly depends on C. The only condition that really depends on C is $\prod_{o\in S_\varepsilon^w}(\eta_o\varepsilon+1)\prod_{l\in S_I^w}(w_l+1)\prod_{m\in S_D^w}(\eta_m D+1)-C=0$, and this is the condition used for the evaluation of C.

The above optimality conditions motivate that the behavior of the following functions be studied.

$$f_k:(0,+\infty)\to(0,+\infty),\quad f_k:w_k\to f_k(w_k)\triangleq\left[\frac{1}{\eta_k}+a\cdot\frac{B}{A}\left(\frac{1}{\eta_k}\right)^a\cdot(w_k)^{a-1}\right](w_k+1)\ \ \forall k\in N_I^w$$

Their first and second derivatives are:

$$\dot f_k:(0,+\infty)\to(0,+\infty),\quad \dot f_k:w_k\to \dot f_k(w_k)\triangleq\left[\frac{1}{\eta_k}+a(a-1+aw_k)\frac{B}{A}\left(\frac{1}{\eta_k}\right)^a\cdot(w_k)^{a-2}\right]\ \ \forall k\in N_I^w$$

$$\ddot f_k:(0,+\infty)\to(0,+\infty),\quad \ddot f_k:w_k\to \ddot f_k(w_k)\triangleq a(a-1)\frac{B}{A}\left(\frac{1}{\eta_k}\right)^a\cdot(w_k)^{a-3}\left[aw_k+a-2\right]\ \ \forall k\in N_I^w$$

Then

$$w_k>\frac{1-a}{a}\Rightarrow \dot f_k(w_k)>0$$

$$\ddot f_k(w_k)\underset{<}{\overset{>}{=}}0\Leftrightarrow a(a-1)\frac{B}{A}\left(\frac{1}{\eta_k}\right)^a\cdot(w_k)^{a-3}\left[aw_k+a-2\right]\underset{<}{\overset{>}{=}}0\Leftrightarrow \boxed{\frac{2-a}{a}\underset{<}{\overset{>}{=}}w_k\Leftrightarrow \ddot f_k(w_k)\underset{<}{\overset{>}{=}}0}$$

The above imply that f_k is convex and $\dot{f}_k$ is monotonically increasing in $\left(0, \frac{2-a}{a}\right)$, and f_k is concave and $\dot{f}_k$ is monotonically decreasing in $\left(\frac{2-a}{a}, +\infty\right)$. In addition, f_k is monotonically increasing in $\left(\frac{1-a}{a}, +\infty\right)$.

It also holds:

$$\lim_{w_k \to 0^+} f_k(w_k) = +\infty, \lim_{w_k \to +\infty} f_k(w_k) = +\infty, f_k\left(\frac{1-a}{a}\right) \triangleq \left[\frac{1}{\eta_k} + a \cdot \frac{B}{A}\left(\frac{1}{\eta_k}\right)^a \cdot \left(\frac{1-a}{a}\right)^{a-1}\right]\frac{1}{a} > 0,$$

$$f_k\left(\frac{2-a}{a}\right) = \left[\frac{1}{\eta_k} + a \cdot \frac{B}{A}\left(\frac{1}{\eta_k}\right)^a \cdot \left(\frac{2-a}{a}\right)^{a-1}\right]\frac{2}{a} > 0, f_k(\eta_k D) \triangleq \left[1 + a \cdot \frac{B}{A} D^{\alpha-1}\right]\left(D + \frac{1}{\eta_k}\right) > 0$$

$$\lim_{w_k \to 0^+} \dot{f}_k(w_k) = -\infty, \lim_{w_k \to +\infty} \dot{f}_k(w_k) = 0^+, \dot{f}_k\left(\frac{2-a}{a}\right) \triangleq \left[\frac{1}{\eta_k} + a\frac{B}{A}\left(\frac{1}{\eta_k}\right)^a \cdot \left(\frac{2-a}{a}\right)^{a-2}\right] > 0,$$

$$\dot{f}_k\left(\frac{1-a}{a}\right) \triangleq \left[\frac{1}{\eta_k}\right] > 0.$$

Since $\dot{f}_k$ is monotonically increasing in $\left(0, \frac{2-a}{a}\right)$, $\lim_{w_k \to 0^+} \dot{f}_k(w_k) = -\infty$, $\dot{f}_k\left(\frac{1-a}{a}\right) \triangleq \left[\frac{1}{\eta_k}\right] > 0$, and $\frac{1-a}{a} < \frac{2-a}{a}$, it then holds that there exists only a unique root $\rho_k \in \left(0, \frac{1-a}{a}\right)$: $\dot{f}_k(\rho_k) = 0$.

In addition, since $\dot{f}_k$ is monotonically increasing in $\left(0, \frac{2-a}{a}\right)$, $\dot{f}_k\left(\frac{1-a}{a}\right) \triangleq \left[\frac{1}{\eta_k}\right] > 0$,

$\dot{f}_k\left(\frac{2-a}{a}\right) \triangleq \left[\frac{1}{\eta_k} + a\frac{B}{A}\left(\frac{1}{\eta_k}\right)^a \cdot \left(\frac{2-a}{a}\right)^{a-2}\right] > 0$, and $\frac{1-a}{a} < \frac{2-a}{a}$,it then holds

$\dot{f}_k(w_k) > 0 \ \ \forall w_k \in \left(\frac{1-a}{a}, \frac{2-a}{a}\right)$. Since $\dot{f}_k$ is monotonically decreasing in $\left(\frac{2-a}{a}, +\infty\right)$,

$\dot{f}_k\left(\frac{2-a}{a}\right) \triangleq \left[\frac{1}{\eta_k} + a\frac{B}{A}\left(\frac{1}{\eta_k}\right)^a \cdot \left(\frac{2-a}{a}\right)^{a-2}\right] > 0$, and $\lim_{w_k \to +\infty} \dot{f}_k(w_k) = 0^+$, it then holds

$\dot{f}_k(w_k) > 0 \ \ \forall w_k \in \left(\frac{2-a}{a}, +\infty\right)$. Since $\dot{f}_k$ is monotonically increasing in $\left(0, \frac{2-a}{a}\right)$, there exists only a unique root $\rho_k \in \left(0, \frac{1-a}{a}\right)$: $\dot{f}_k(\rho_k) = 0$, $\lim_{w_k \to 0^+} \dot{f}_k(w_k) = -\infty$, it then holds

$\dot{f}_k(w_k) > 0 \ \ \forall w_k \in \left(\rho_k, \frac{1-a}{a}\right)$, $\dot{f}_k(\rho_k) = 0$, $\dot{f}_k(w_k) < 0 \ \ \forall w_k \in (0, \rho_k)$.

In turn, the above imply that f_k has a unique minimum at $\rho_k \in \left(0, \frac{1-a}{a}\right)$, that f_k is monotonically decreasing in $(0, \rho_k)$, and that f_k is monotonically increasing in $(\rho_k, +\infty)$.

In turn, this implies that left and right inverse functions of f_k can be defined as follows:

$$f_k^L : (0, \rho_k] \to (0, +\infty), \ \ f_k^L : w_k \to f_k^L(w_k) \triangleq \left[\frac{1}{\eta_k} + a \cdot \frac{B}{A}\left(\frac{1}{\eta_k}\right)^a \cdot (w_k)^{a-1}\right](w_k + 1) \ \ \forall k \in S_I^w$$

$$f_k^R : [\rho_k, +\infty) \to (0, +\infty), \ \ f_k^R : w_k \to f_k^R(w_k) \triangleq \left[\frac{1}{\eta_k} + a \cdot \frac{B}{A}\left(\frac{1}{\eta_k}\right)^a \cdot (w_k)^{a-1}\right](w_k + 1) \ \ \forall k \in S_I^w,$$

which $\forall k \in S_I^w$ admit the inverse functions

$$\left(f_k^L\right)^{-1} : [f_k(\rho_k), +\infty) \to (0, \rho_k]$$

$$\left(f_k^L\right)^{-1} : y_k \triangleq \left[\frac{1}{\eta_k} + a \cdot \frac{B}{A}\left(\frac{1}{\eta_k}\right)^a \cdot (w_k)^{a-1}\right](w_k + 1) \to \left(f_k^L\right)^{-1}(y_k) \triangleq w_k \in (0, \rho_k],$$

$$\left(f_k^R\right)^{-1} : [f_k(\rho_k), +\infty) \to [\rho_k, +\infty),$$

$$\left(f_k^R\right)^{-1} : y_k \triangleq \left[\frac{1}{\eta_k} + a \cdot \frac{B}{A}\left(\frac{1}{\eta_k}\right)^a \cdot (w_k)^{a-1}\right](w_k + 1) \to \left(f_k^R\right)^{-1}(y_k) \triangleq w_k \in [\rho_k, +\infty)$$

respectively.

Having established the behavior of f_k over $(0,+\infty)$, we now restate the first order necessary conditions of optimality in terms of f_k.

$$\left\{\begin{array}{l} f_k(w_k) = -\lambda C \qquad \forall k \in S_I^w \\ f_k(w_k) \le (\eta_i \varepsilon + 1)\left(\dfrac{1}{\eta_i} + a\dfrac{B}{A}\dfrac{1}{\eta_i}\varepsilon^{a-1}\right) \qquad \forall k \in S_I^w,\ \forall i \in S_\varepsilon^w \\ \left(D + \dfrac{1}{\eta_j}\right)\left(1 + a\dfrac{B}{A}D^{a-1}\right) \le f_k(w_k) \qquad \forall k \in S_I^w,\ \forall j \in S_D^w \\ \displaystyle\prod_{l \in S_I^w}(w_l + 1) = \frac{C}{\displaystyle\prod_{o \in S_\varepsilon^w}(\eta_o \varepsilon + 1)\prod_{m \in S_D^w}(\eta_m D + 1)} \\ 0 < \eta_k \varepsilon < w_k < \eta_k D \qquad \forall k \in S_I^w,\ w_i = \eta_i \varepsilon \ \ \forall i \in S_\varepsilon^w,\ \ w_j = \eta_j D \ \ \forall j \in S_D^w \end{array}\right\}$$

Previously, we established that for any given value of λ, each equation

$$f_k(w_k) + \lambda C = 0 \ \ has \left\{\begin{array}{l} no\ roots\ iff\ -\lambda C < f_k(\rho_k) \\ one\ root\left(\rho_k^1 = \rho_k^2 = \rho_k\right)\ iff\ -\lambda C = f_k(\rho_k) \\ two\ roots\left(\rho_k^1 < \rho_k < \rho_k^2\right) iff\ -\lambda C > f_k(\rho_k) \end{array}\right\} k \in S_I^w .$$

Designating as $w_{N_D^w+1}$ the optimization variable corresponding to the first element of S_I^w, then the above equations can be written as $f_k(w_k) = f_{N_D^w+1}\left(w_{N_D^w+1}\right)\ \forall k \in S_I^w$. Then for any fixed value of $w_{N_D^w+1}$, each of these equations can have

$$\left\{\begin{array}{l} no\ roots\ iff\ \ f_{N_D^w+1}\left(w_{N_D^w+1}\right) < f_k(\rho_k) \\ one\ root\left(w_k = \rho_k^1 = \rho_k^2 = \rho_k\right)\ \ iff\ \ f_{N_D^w+1}\left(w_{N_D^w+1}\right) = f_k(\rho_k) \\ two\ roots\left(w_k = \rho_k^1\ \vee\ w_k = \rho_k^2\right) iff\ \ f_{N_D^w+1}\left(w_{N_D^w+1}\right) > f_k(\rho_k) \end{array}\right\}$$, where $\dot{f}_k(\rho_k) = 0$. Figure 3.2 shows an example graph for $f_k(w_k)$.

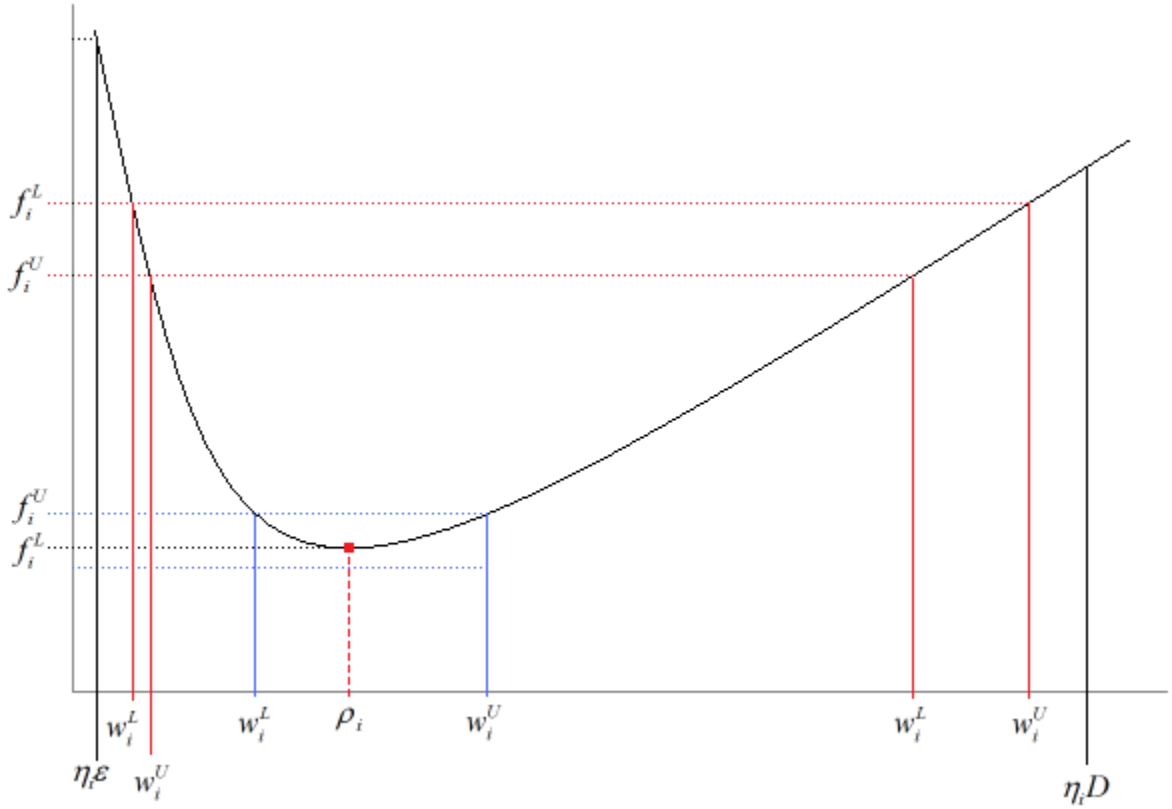

Figure 3.2: Example graph of an arbitrary f(w_i)

TAC(11) is not amenable to an analytical solution like the operating cost problem solved in our previous work[9]. Nevertheless Theorems 1 and 2 significantly reduce the combinatorial nature of the problem, since only combinations of feasible cardinalities $N_D^w, N_I^w, N_\varepsilon^w$ need be considered, rather than combinations of individual compressors. The employed combinatorial analysis only relies on the parameters on the number of off/on-interior/on-saturated compressors $N_\varepsilon^w, N_I^w, N_D^w$. The developed theory allows theoretical determination of which compressors belong to which class once only the cardinality of each class is specified. This reduces significantly the number of combinations that need to be considered.

The necessary optimality conditions presented in Theorems 1 and 2 are employed in the development of an interval analysis-based algorithm that can provide upper and lower bounds of any desired accuracy to the optimum objective function values and associated optimum variable values for an infinite collection of instances of TAC(11) that is parameterized by the compression ratio related parameter C. The algorithm proceeds as follows:

1. Assume a combination of feasible cardinalities $N_D^w, N_I^w, N_\varepsilon^w$ from the list of cardinality combinations that have not yet been considered. Based on Theorem 1, the compressor efficiencies η_i corresponding to each set $S_D^w, S_I^w, S_\varepsilon^w$ are then known.
2. For given $a, \frac{B}{A}, \eta_i \quad \forall i = N_D^w + 1, \ldots, N_D^w + N_I^w$, determine the unique roots $\rho_i \in \left(0, \frac{1-a}{a}\right): \ \dot{f}_i(\rho_i) = 0 \ \ \forall i = N_D^w + 1, \ldots, N_D^w + N_I^w$.
3. Given that $w_{N_D^w+1} \in \left(\eta_{N_D^w+1}\varepsilon, \eta_{N_D^w+1}D\right)$, discretize $\left[\eta_{N_D^w+1}\varepsilon, \eta_{N_D^w+1}D\right]$ into a number $p_{N_D^w+1}$ of equal intervals $\left[w^L_{N_D^w+1,j}, w^U_{N_D^w+1,j}\right] \quad \forall j = 1, p_{N_D^w+1}$ with $w^L_{N_D^w+1,1} = \eta_{N_D^w+1}\varepsilon, \ w^U_{N_D^w+1,j} = w^L_{N_D^w+1,j+1} \ \ \forall j = 1, p_{N_D^w+1} - 1, \ w^U_{N_D^w+1,p_{N_D^w+1}} = \eta_{N_D^w+1}D$.
4. For each interval $\left[w^L_{N_D^w+1,j}, w^U_{N_D^w+1,j}\right] \quad \forall j = 1, p_{N_D^w+1}$, the following holds. These are the $f_{N_D^w+1}\left(w_{N_D^w+1}\right)$ intervals shown in Figure 3.2:

$$\left\{\left\{w_{N_D^w+1}\in\left[\,w^L_{N_D^w+1,j},w^U_{N_D^w+1,j}\,\right]\right\}\wedge\left\{f_{N_D^w+1}\left(w_{N_D^w+1}\right)\in\left[\begin{array}{l}\max\limits_{j\in S_D^w}\left[\left(D+\dfrac{1}{\eta_j}\right)\left(1+a\dfrac{B}{A}D^{a-1}\right)\right],\\ \min\limits_{i\in S_\varepsilon^w}\left[\left(\varepsilon+\dfrac{1}{\eta_i}\right)\left(1+a\dfrac{B}{A}\varepsilon^{a-1}\right)\right]\end{array}\right]\right\}\right\}\Rightarrow$$

$$f_{N_D^w+1}\left(w_{N_D^w+1}\right)\in\left[\,f^L_{N_D^w+1,j},f^U_{N_D^w+1,j}\,\right]\triangleq\left\{\begin{array}{ll}\left[\begin{array}{l}\left[\,f_{N_D^w+1}\left(w^U_{N_D^w+1,j}\right),f_{N_D^w+1}\left(w^L_{N_D^w+1,j}\right)\right]\cap\\ \left[\begin{array}{l}\max\limits_{j\in S_D^w}\left[\left(D+\dfrac{1}{\eta_j}\right)\left(1+a\dfrac{B}{A}D^{a-1}\right)\right],\\ \min\limits_{i\in S_\varepsilon^w}\left[\left(\varepsilon+\dfrac{1}{\eta_i}\right)\left(1+a\dfrac{B}{A}\varepsilon^{a-1}\right)\right]\end{array}\right]\end{array}\right] & if\ \ w^U_{N_D^w+1,j}\le\rho_{N_D^w+1}\\ \left[\begin{array}{l}\left[\begin{array}{l}f_{N_D^w+1}\left(\rho_{N_D^w+1}\right),\\ \max\left(\begin{array}{l}f_{N_D^w+1}\left(w^L_{N_D^w+1,j}\right),\\ f_{N_D^w+1}\left(w^U_{N_D^w+1,j}\right)\end{array}\right)\end{array}\right]\cap\\ \left[\begin{array}{l}\max\limits_{j\in S_D^w}\left[\left(D+\dfrac{1}{\eta_j}\right)\left(1+a\dfrac{B}{A}D^{a-1}\right)\right],\\ \min\limits_{i\in S_\varepsilon^w}\left[\left(\varepsilon+\dfrac{1}{\eta_i}\right)\left(1+a\dfrac{B}{A}\varepsilon^{a-1}\right)\right]\end{array}\right]\end{array}\right] & if\ \ w^L_{N_D^w+1,j}<\rho_{N_D^w+1}<w^U_{N_D^w+1,j}\\ \left[\begin{array}{l}\left[\,f_{N_D^w+1}\left(w^L_{N_D^w+1,j}\right),f_{N_D^w+1}\left(w^U_{N_D^w+1,j}\right)\right]\cap\\ \left[\begin{array}{l}\max\limits_{j\in S_D^w}\left[\left(D+\dfrac{1}{\eta_j}\right)\left(1+a\dfrac{B}{A}D^{a-1}\right)\right],\\ \min\limits_{i\in S_\varepsilon^w}\left[\left(\varepsilon+\dfrac{1}{\eta_i}\right)\left(1+a\dfrac{B}{A}\varepsilon^{a-1}\right)\right]\end{array}\right]\end{array}\right] & if\ \ \rho_{N_D^w+1}\le w^L_{N_D^w+1,j}\end{array}\right\}$$

5. For each interval $\left[\,w^L_{N_D^w+1,j},w^U_{N_D^w+1,j}\,\right]\quad j=1,p_{N_D^w+1}$ such that $\left[\,f^L_{N_D^w+1,j},f^U_{N_D^w+1,j}\,\right]\neq\varnothing$, and $\forall i=N_D^w+2,\ldots,N_D^w+N_I^w$ it holds:

$$\left\{\begin{array}{l}w_{N_D^w+1}\in\left[\,w^L_{N_D^w+1,j},w^U_{N_D^w+1,j}\,\right]\wedge\\ f_{N_D^w+1}\left(w_{N_D^w+1}\right)\in\left[\begin{array}{l}\max\limits_{j\in S_D^w}\left[\left(D+\dfrac{1}{\eta_j}\right)\left(1+a\dfrac{B}{A}D^{a-1}\right)\right],\\ \min\limits_{i\in S_\varepsilon^w}\left[\left(\varepsilon+\dfrac{1}{\eta_i}\right)\left(1+a\dfrac{B}{A}\varepsilon^{a-1}\right)\right]\end{array}\right]\wedge w_i\in\left(\eta_i\varepsilon,\eta_i D\right)\end{array}\right\}\Rightarrow$$

$$\left\{ f_{N_D^w+1}\left(w_{N_D^w+1}\right) \in \left[f^L_{N_D^w+1,j},\, f^U_{N_D^w+1,j} \right] \wedge w_i \in (\eta_i \varepsilon, \eta_i D) \right\} \Rightarrow$$

$$w_i \in W_{i,j} \triangleq \begin{Bmatrix} \varnothing & \text{if } \; f^U_{N_D^w+1,j} < f_i(\rho_i) \\ \left[\left(f_i^L\right)^{-1}\left(f^U_{N_D^w+1,j}\right), \left(f_i^R\right)^{-1}\left(f^U_{N_D^w+1,j}\right) \right] \cap (\eta_i \varepsilon, \eta_i D) & \text{if } \; f^L_{N_D^w+1,j} < f_i(\rho_i) \le f^U_{N_D^w+1,j} \\ \left\{ \begin{matrix} \left[\left(f_i^L\right)^{-1}\left(f^U_{N_D^w+1,j}\right), \left(f_i^L\right)^{-1}\left(f^L_{N_D^w+1,j}\right) \right] \cup \\ \left[\left(f_i^R\right)^{-1}\left(f^L_{N_D^w+1,j}\right), \left(f_i^R\right)^{-1}\left(f^U_{N_D^w+1,j}\right) \right] \end{matrix} \right\} \cap (\eta_i \varepsilon, \eta_i D) & \text{if } \; f_i(\rho_i) \le f^L_{N_D^w+1,j} \end{Bmatrix}$$

6. For each interval $\left[w^L_{N_D^w+1,j}, w^U_{N_D^w+1,j} \right] \quad j = 1, p_{N_D^w+1}$, such that $\left\{ \left[f^L_{N_D^w+1,j},\, f^U_{N_D^w+1,j} \right] \neq \varnothing \right\} \wedge \left\{ W_{i,j} \neq \varnothing \;\; \forall i = N_D^w + 2, \ldots, N_D^w + N_I^w \right\}$, use interval analysis to evaluate intervals (or unions of intervals) first for the variables $E_i \triangleq \dfrac{a(a-1)B}{AC}\left(\dfrac{1}{\eta_i}\right)^a \dfrac{\left(w_i+1\right)^2}{\left(w_i\right)^{2-a}} - \lambda \;\; \forall i \in \left\{ N_D^w + 1, \cdots, N_D^w + N_I^w \right\}$ appearing in the second order necessary condition of optimality presented in Theorem 2, and subsequently for all the principal minors which are required to be non-negative for the aforementioned necessary condition to be satisfied. If any interval (or interval union) of any principal minor has an empty intersection with $[0, +\infty)$, then the corresponding interval $\left[w^L_{N_D^w+1,j}, w^U_{N_D^w+1,j} \right]$ is eliminated from further consideration. Otherwise, include the interval $\left[w^L_{N_D^w+1,j}, w^U_{N_D^w+1,j} \right]$ in the candidate optimal interior interval list, and proceed to the next step.

7. For each interval $\left[w^L_{N_D^w+1,j}, w^U_{N_D^w+1,j} \right]$ in the candidate optima interior interval list, and each corresponding interval (or union of intervals) $\left\{ W_{i,j} \neq \varnothing \;\; \forall i = N_D^w + 2, \ldots, N_D^w + N_I^w \right\}$, identify the corresponding interval (or union of intervals) for the objective function $\left(D + \dfrac{B}{A} D^a \right) N_D^w + \left(\varepsilon + \dfrac{B}{A} \varepsilon^a \right) N_\varepsilon^w + \left[\displaystyle\sum_{i \in N_I^w} \frac{1}{\eta_i} w_i + \frac{B}{A} \sum_{i \in N_I^w} \left(\frac{1}{\eta_i} \right)^a \left(w_i \right)^a \right]$ and for the expression $\displaystyle\prod_{i \in S_D^w} (\eta_i D + 1) \prod_{i \in S_I^w} (w_i + 1) \prod_{i \in S_\varepsilon^w} (\eta_i \varepsilon + 1)$ which must contain the compression ratio related parameter C. All interval calculations associated with the considered combination $N_D^w, N_I^w, N_\varepsilon^w$ are incorporated in the candidate optima interval list. The resulting rectangles (boxes) in the objective function versus parameter C plane, are guaranteed to contain the graph of the candidate optimum objective function, associated with the considered combination $N_D^w, N_I^w, N_\varepsilon^w$, as a function of the parameter C.

8. If there are combinations of feasible cardinalities $N_D^w, N_I^w, N_\varepsilon^w$ that have not yet been considered, return to Step 1. Otherwise, proceed to the next step.
9. The union of all intervals (or unions of intervals), over all cardinality combinations, in the candidate optima interval list, for the expression $\prod_{i \in S_D^w} (\eta_i D + 1) \prod_{i \in S_I^w} (w_i + 1) \prod_{i \in S_\varepsilon^w} (\eta_i \varepsilon + 1)$, must be the interval $\left[\prod_{i=1,n} (\eta_i \varepsilon + 1), \prod_{i=1,n} (\eta_i D + 1) \right]$. The piecewise constant function defined in the objective function versus parameter C plane, via the lowest lower bounds on objective function values over all rectangles (boxes) identified in Step 7 for all combinations of $N_D^w, N_I^w, N_\varepsilon^w$, provides lower bounds to the globally optimum objective function values for all instances of v_ε parameterized by the parameter C. The upper bounds of the intervals whose lower bounds form the aforementioned function, form another piecewise constant function, which provides upper bounds to the globally optimum objective function values for all instances of v_ε parameterized by the parameter C. These bounds are illustrated in Figure 3.3. The intervals on the variables $\{w_i\}_{i=1}^n$ corresponding to the aforementioned objective function intervals, similarly define two piecewise constant functions in the n variable $\{w_i\}_{i=1}^n$ versus parameter C planes, which bound below and above the globally optimal values of these variables as a function of the parameter C.
10. If the optimum objective function values, and/or the optimum variable values are identified as a function of the parameter C, without satisfactory accuracy, then the number of intervals $p_{N_D^w+1}$ is doubled, and the algorithm is repeated. Otherwise, the algorithm is terminated.

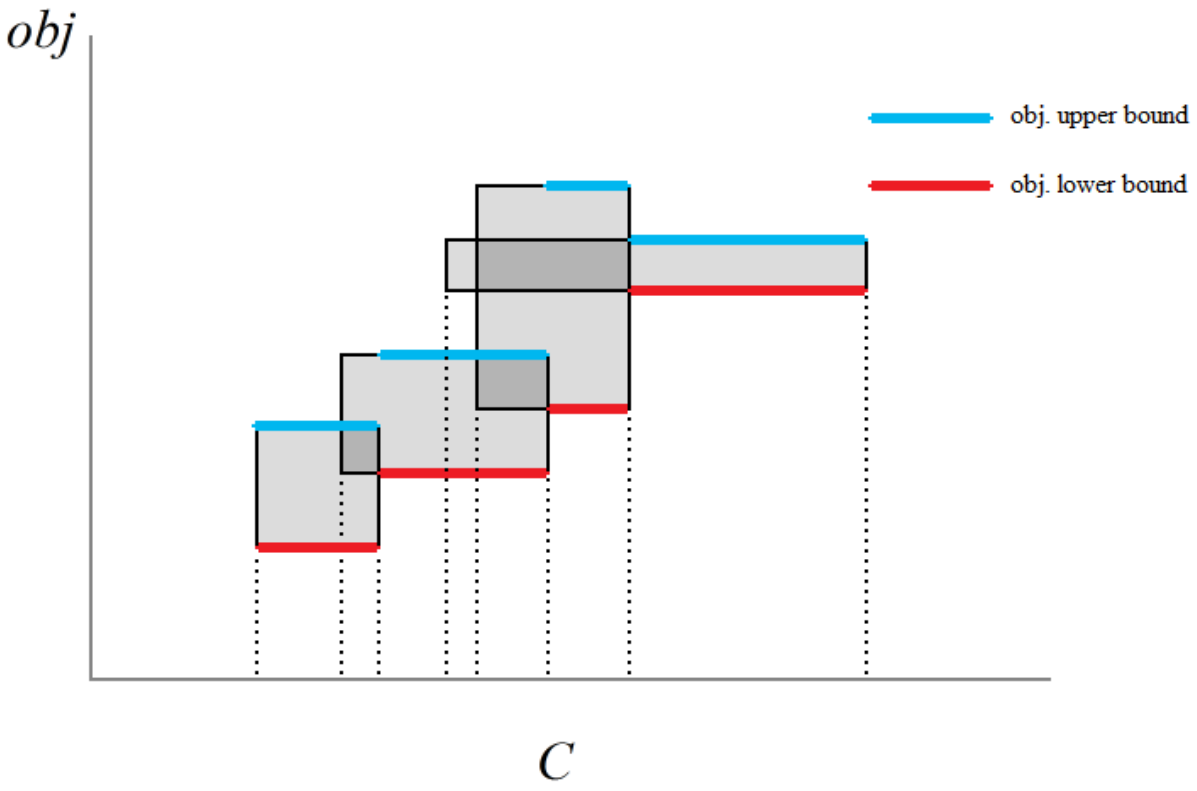

Figure 3.3: Identification of objective function interval

Section 3.4: Case studies

To illustrate the power of the proposed methodology, we present two case studies seeking to identify the global minimum for an infinite collection of instances of the minimum-TAC problem for a compressor/cooler sequence involving at most four compressors and associated coolers, $(n=4)$. In both case studies, the sequence compresses a gas with compressibility factor equal to one, from the initial state $(T_0, P_0) = (298\,K, 101.325\ kPa)$ to the final state $(T_n, P_n) = (T_0, P_n) = (298\,K, P_n)$, where P_n varies so as to generate all TAC problem instances of interest. The parameters in Table 3.1 are considered fixed in both case studies.

Parameter (Units)	Value	Parameter (Units)	Value

$T_0\,(K)$	298	$P_0\,(kPa)$	101.325
α	0.67	$C_p\left(\frac{J}{mol\cdot K}\right)$	28.85
Z	1	η_1	1
η_2	0.9	η_3	0.8
η_4	0.7		

Table 3.1: Parameters considered fixed for both case studies

Table 3.2 lists all possible combinations of cardinalities $N_D^w, N_I^w, N_\varepsilon^w$ for this four compressor sequence, using Theorem 1 to determine corresponding $\eta's$. For combinations 1-5 (i.e. when $N_I^w = 0$), all compressor outlets are fully determined and yield a single objective value. For combinations 6-9, since $N_I^w - 1 = 0$, the condition of positive semi-definiteness in Theorem 2 is trivially satisfied.

Combination	N_D^w	N_I^w	N_ε^w	$\eta\left(S_D^w\right)$	$\eta\left(S_I^w\right)$	$\eta\left(S_\varepsilon^w\right)$
1	4	0	0	1,0.9,0.8,0.7	-	-
2	3	0	1	1,0.9,0.8	-	0.7
3	2	0	2	1,0.9	-	0.8,0.7
4	1	0	3	1	-	0.9,0.8,0.7
5	0	0	4	-	-	1,0.9,0.8,0.7
6	0	1	3	-	1	0.9,0.8,0.7
7	1	1	2	1	0.9	0.8,0.7
8	2	1	1	1,0.9	0.8	0.7
9	3	1	0	1,0.9,0.8	0.7	-
10	0	2	2	-	1,0.9	0.8,0.7
11	1	2	1	1	0.9,0.8	0.7
12	2	2	0	1,0.9	0.8,0.7	-
13	0	3	1	-	1,0.9,0.8	0.7
14	1	3	0	1	0.9,0.8,0.7	-
15	0	4	0	-	1,0.9,0.8,0.7	-

Table 3.2: Possible cardinality combinations for the considered four compressor sequence

The remaining combinations 10-15 must satisfy the first-order and second-order necessary conditions identified in Theorem 2. In particular, the condition

$$\begin{bmatrix} E_{N_D^w+1}+E_{N_D^w+N_I^w} & E_{N_D^w+N_I^w} & \cdots & E_{N_D^w+N_I^w} \\ E_{N_D^w+N_I^w} & E_{N_D^w+2}+E_{N_D^w+N_I^w} & \cdots & E_{N_D^w+N_I^w} \\ \vdots & \vdots & \ddots & \vdots \\ E_{N_D^w+N_I^w} & E_{N_D^w+N_I^w} & \cdots & E_{N_D^w+N_I^w-1}+E_{N_D^w+N_I^w} \end{bmatrix} \text{ is psd on } \mathbb{R}^{N_I^w-1} \text{ becomes}$$

Combination 10: $\left(N_D^w, N_I^w, N_\varepsilon^w\right)=(0,2,2): E_1+E_2\geq 0$

Combination 11: $\left(N_D^w, N_I^w, N_\varepsilon^w\right)=(1,2,1): E_2+E_3\geq 0$

Combination 12: $\left(N_D^w, N_I^w, N_\varepsilon^w\right)=(2,2,0): E_3+E_4\geq 0$

Combination 13: $\left(N_D^w, N_I^w, N_\varepsilon^w\right)=(0,3,1): \begin{Bmatrix} E_1+E_3\geq 0 \\ E_1E_2+E_1E_3+E_2E_3\geq 0 \end{Bmatrix}$

Combination 14: $\left(N_D^w, N_I^w, N_\varepsilon^w\right)=(1,3,0): \begin{Bmatrix} E_2+E_4\geq 0 \\ E_2E_3+E_2E_4+E_3E_4\geq 0 \end{Bmatrix}$

Combination 15: $\left(N_D^w, N_I^w, N_\varepsilon^w\right)=(0,4,0): \begin{Bmatrix} E_1+E_4\geq 0 \\ E_1E_2+E_1E_4+E_2E_4\geq 0 \\ E_1E_2E_3+E_1E_2E_4+E_1E_3E_4+E_2E_3E_4\geq 0 \end{Bmatrix}$

A discretization of 0.001 in $w_{N_D^w+1}$ was chosen for both case studies.

Section 3.5: Results/Discussion

Case Study 1

This case study intends to verify the presented globally optimal solution method through reproduction of the operating cost results in our previous work[9]. To this end, we choose $A=3,\ B=0.0001,\ T_{\max}=405$, since the presented theory assumes $B>0$. Figures 3.4 and 3.5 illustrate the intervals containing the globally optimal TAC objective function values, and the

associated globally optimal variable $w_1,...,w_4$ values, respectively. Regions in C delineating different sets of optimal combinations are shown in Figure 3.5 and listed in Table 3.3.

There are several intervals in C where the algorithm switches between two different cardinality combinations; for example, in region 10, the algorithm identifies optimizers $w_1,...,w_4$ corresponding to both configuration 9 and 12 as the candidate global optima. This situation arises whenever the optimum objective function values for two different combinations are too close to be distinguished for the chosen $w_1,...,w_4$ discretization, as illustrated in Figure 3.4. In this sense, the proposed interval analysis algorithm can serve the dual purpose of identifying the global optima for infinite instances of the TAC problem and qualitatively showing intervals in C for which the identified global optimum does not confer much savings from one or more alternative designs.

Figures 3.6 and 3.7 are the same graphs presented in Figures 3.4 and 3.5, superimposed over a set of points (displayed as crosses) corresponding to the global optima identified analytically in our previous work[9]. The analytical method's points show excellent agreement with both the optimal objective function intervals identified by the algorithm in Figure 3.6, and the optimizers $w_1,...,w_4$ identified by the algorithm in Figure 3.7, validating the proposed interval analysis algorithm. Furthermore, the combination of points and boxes in Figure 3.7 shows precisely where a globally optimal design is only marginally better than another suboptimal design. This lends greater insight into the behavior and sensitivity of the TAC problem optimum for all attainable network outlet pressures.

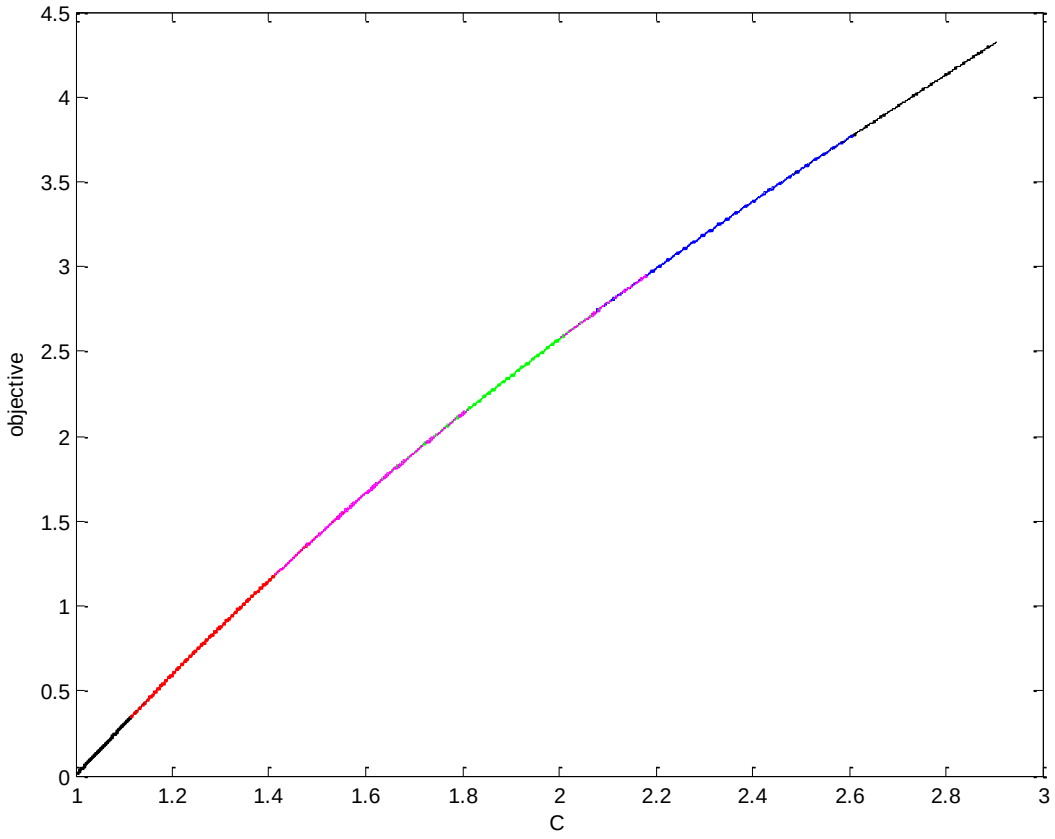

Figure 3.4: Upper/lower bounds for optimum objective function values of case study 1

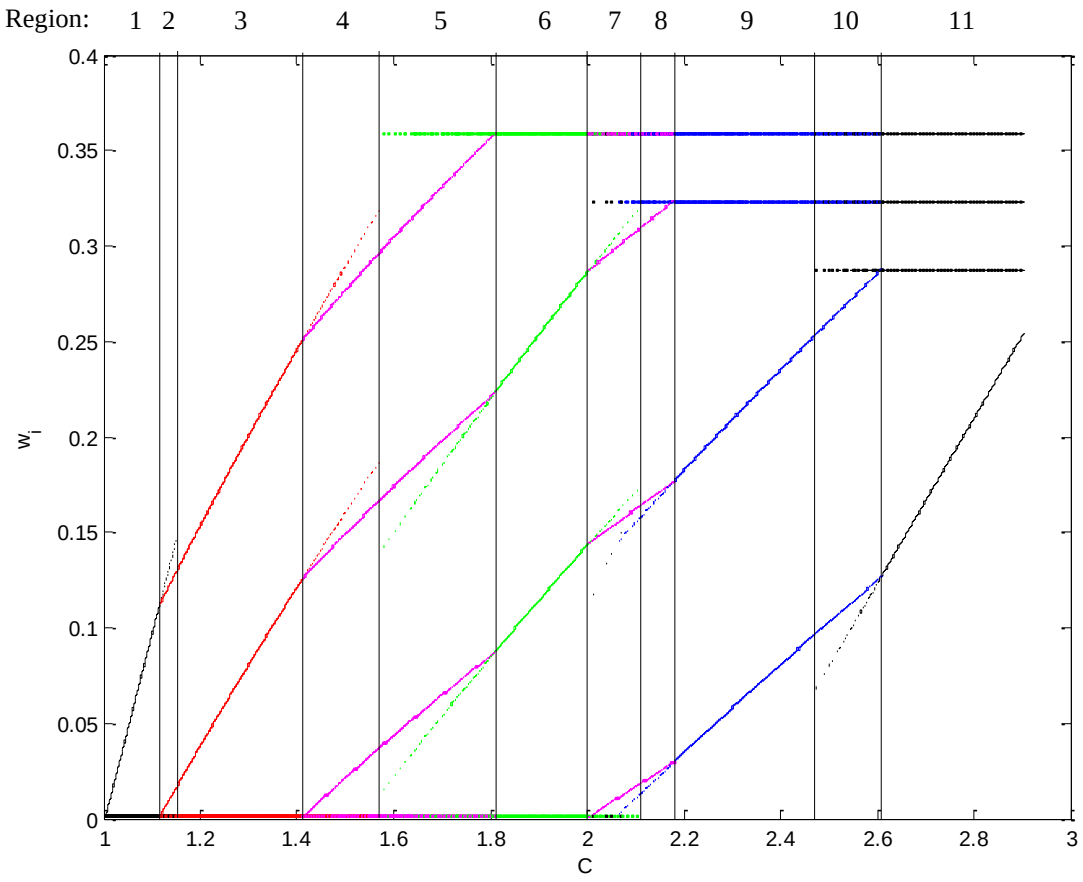

Figure 3.5: Upper/lower bounds for optimum variable w1-w4 values of case study 1

Region	Configurations
1	6
2	6, 10
3	10
4	10, 13
5	13, 11
6	11
7	11, 14, 12
8	14, 12
9	12
10	9, 12
11	9

Table 3.3: Combinations identified as candidate global optima for each region in Figure 3.5

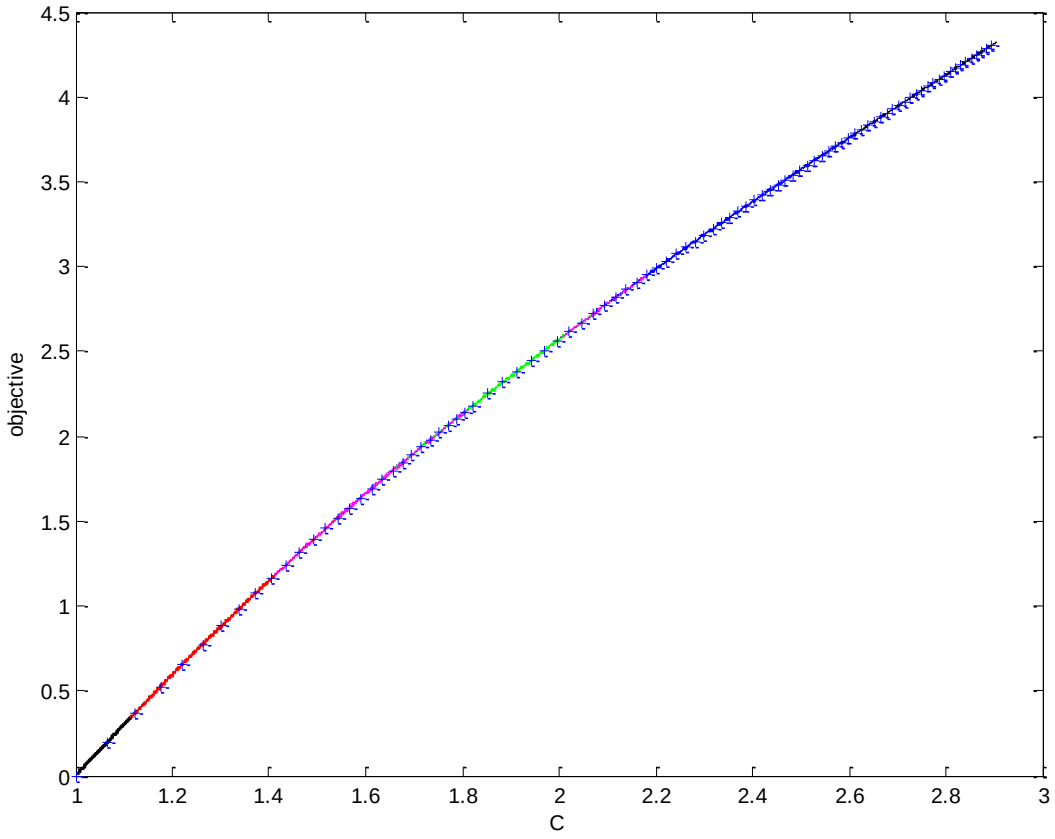

Figure 3.6: Upper/lower bounds and analytical solution for optimum objective function values of case study 1

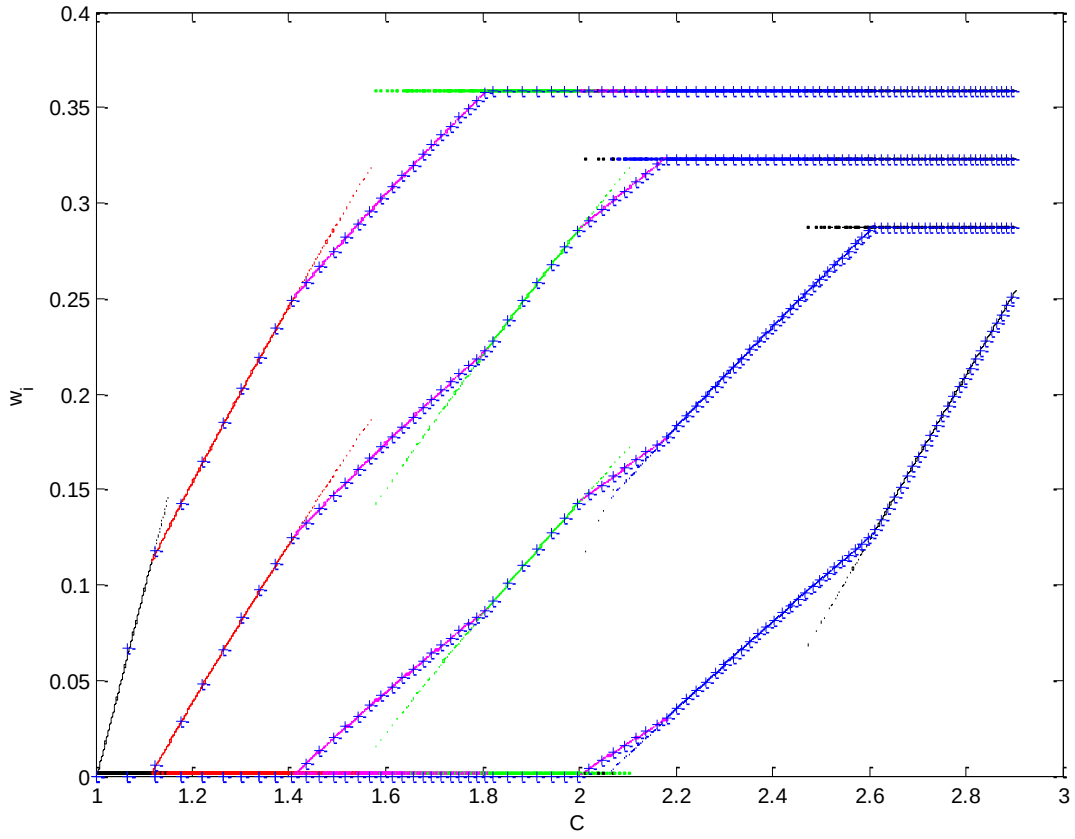

Figure 3.7: Upper/lower bounds and analytical solution for optimum variables w1-w4 of case study 1

Case Study 2

This case study explores how the power-law based capital cost component of the TAC objective function affects the nature of the solution of the TAC global minimization problem. To this end, we choose $A=3,\ B=1,\ T_{\max}=700$. The higher $T_{\max}$ chosen in this case study, allows for the possibility of combination 15, $\left(N_D^w, N_I^w, N_\varepsilon^w\right)=(0,4,0)$, to be identified as a candidate global minimum. Figures 3.8 and 3.9 illustrate the intervals containing the globally optimal TAC objective function values, and the associated globally optimal variable $w_1,...,w_4$ values, respectively.

Similarly to case study 1, Figure 3.9 shows that, for the employed $w_1,...,w_4$ discretization, there are several intervals in C in which the algorithm identifies two different compressor combinations as the candidate global optimum. Nevertheless, as can be seen from Figure 3.8, the identified objective function intervals are practically indistinguishable, throughout the entire C range.

A striking aspect of Figure 3.9 is seen in the approximate optimizers $w_1,...,w_4$ for the region $1 < C < 5$. As C increases, the optimum compressor sequence: (1) begins to use compressor 2 at a load much greater than zero and reduces the load of compressor 1; (2) begins to use compressor 3 at a load much greater than zero and reduces the load of both compressors 1 and 2; and (3) begins to use compressor 4 at a load much greater than zero and reduces the loads of compressors 1, 2, and 3. This stands in sharp contrast to the solution of the operating cost (OC) minimization problem studied in Case Study 1. In that case (Figure 3.6), both the sets of intervals identified by the algorithm and the analytical solutions identified in our previous work[9] suggest that for increasing values of C, the values of $w_1,...,w_4$ are non-decreasing. This discrepancy in the behavior of the optimal solutions for the OC and TAC problems, can be attributed to the presence of economies of scale in the TAC problem. Indeed, for small values of each compressor's consumed work, its capital cost rises rapidly because the derivative of the power law function near zero is nearly infinite. Thus, the optimization finds it beneficial to decrease the work load of a more efficient compressor and increase the work load of an inefficient one because in this manner it avoids the high slope capital cost region of the power law component of the objective function. Clearly, such behavior is directly influenced by the ratio of the capital over operating cost coefficients $\frac{B}{A}$ and the economy of scale exponent α, and

it may be expected to be more pronounced for large values of the former and small values of the latter.

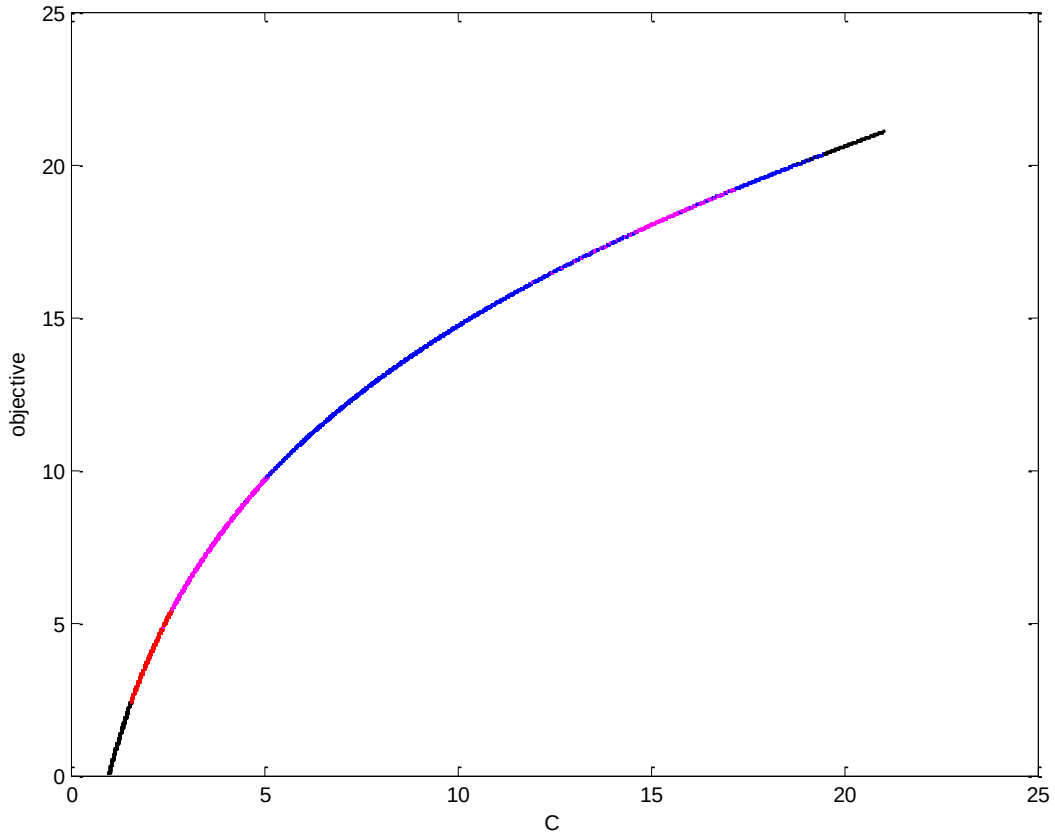

Figure 3.8: Upper/lower bounds for optimum objective function values of case study 2

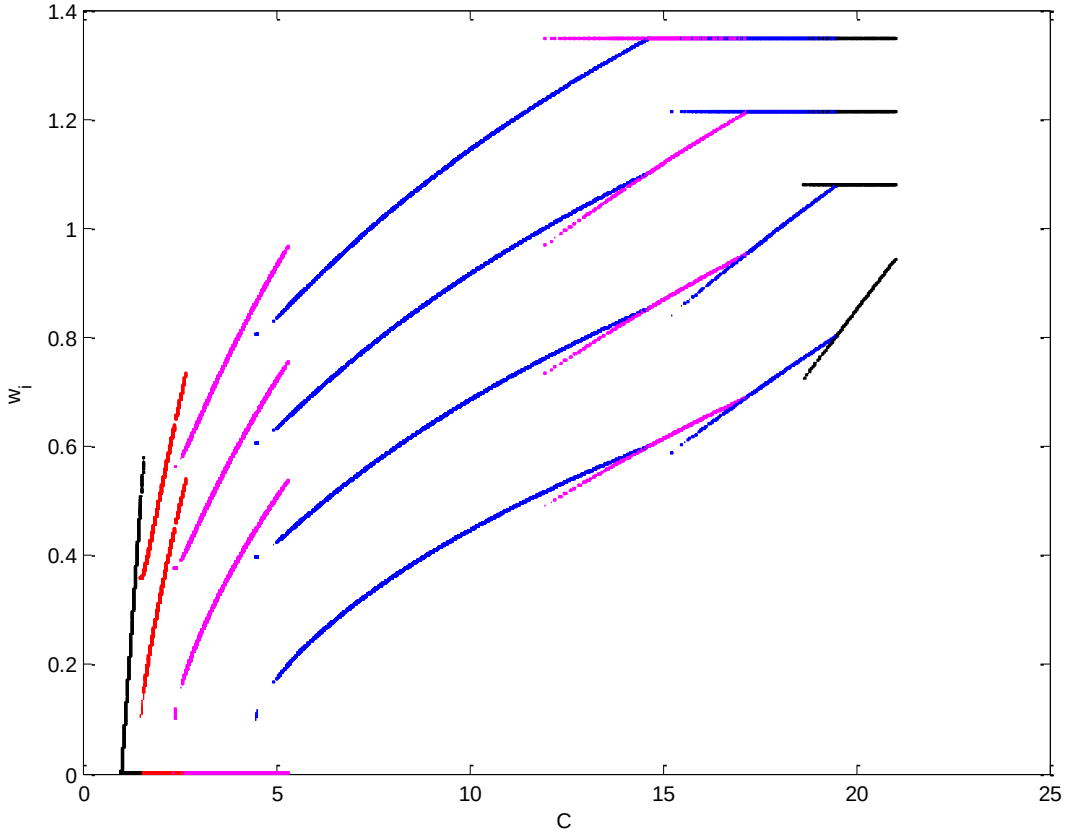

Figure 3.9: Upper/lower bounds for optimum variable w1-w4 values of case study 2

Another interesting behavior illustrated in Figure 3.9 is the appearance of discontinuities and multi-valued function behavior near the transition points where new compressors are incorporated into the optimal compressor sequence. Figure 3.9 depicts all of the w_i interval combinations yielding the lowest objective function interval lower bounds. Since interval analysis constructs intervals containing the w_i optimal values, and the C value based on an interval of $w_{N_D^w+1}$, there are cases where the algorithm will select one compressor combination to be the optimum for an interval of $w_{N_D^w+1}$ and another combination to be the optimum for an adjacent or nearby interval of $w_{N_D^w+1}$. This will have an effect on the other w_i intervals containing

the optimal w_i values and the C intervals. This phenomenon is manifested near compression ratios C where a new compressor is activated at the TAC optimum.

Section 3.6: Conclusions

In this work we identified the globally optimal solution of an infinite collection of instances of the minimum total annualized cost (TAC) problem for a series of gas compressors and coolers, parameterized by the overall compression ratio. In two theorems, we identified first- and second-order necessary conditions for optimality of the compressor/cooler sequence that minimizes TAC. A novel, hybrid algorithm was then presented that employs these optimality conditions with interval analysis, to determine converging upper and lower bounds to the globally optimal solution and associated optimal solution vector components, for all considered instances of the TAC problem. Two case studies illustrated the proposed method and identified important and non-intuitive characteristics of the optimal solutions, arising from the economies of scale characteristics of the capital cost component of the TAC objective function. Indeed, the presence of economies of scale in the TAC problem results in solutions where reducing the load of a more efficient compressor and increasing the load of a less efficient compressor actually yields a lower TAC than just increasing the load on the former compressor. This goes against conventional wisdom that would suggest always placing the highest demand on the most efficient compressor.

The proposed method serves a dual purpose; not only can it identify the global optimum for infinite instances of the TAC problem, it can also identify intervals in C for which the identified global optimum is only marginally better than one or more alternative designs. This information is often of use to the designer during the planning phase of high-pressure gas delivery projects. As the number of compressors n increases, the amount of compressor

combinations that need to be considered by the proposed method does not increase exponentially, but rather quadratically, thus making the method practical for the optimal design of compressor sequences featuring a large number of compressors.

Notation

Greek Letters:

β: Volume expansivity $\left(1/K\right)$

η_i: Efficiency of compressor i

κ: Isothermal compressibility $\left(1/kPa\right)$

ν: Objective function value

Letters:

A: Operating cost coefficient; $A \triangleq \left(C_{compr.}^{oper.} \cdot \dot{n} \cdot C_p + \frac{C_{cooler}^{oper.} \cdot \dot{n} \cdot C_p}{C_{p,c}\left(T_{c,out} - T_{c,in}\right)} \right) T_0 \left(\$\right)$

B: Capital cost coefficient; $B \triangleq F C_{compr.}^{cap.} \dot{n}^a \cdot \left(C_p\right)^a \left(T_0\right)^a \ \left(\$\right)$

C: Modified pressure ratio; $C \triangleq \left(\frac{P_n}{P_0} \right)^{\left(\frac{ZR}{C_p}\right)}$

C_p: Constant-pressure molar heat capacity of gas $\left(J/mol \cdot K\right)$

$C_{p,c}$: Constant-pressure molar heat capacity of coolant $\left(J/mol \cdot K\right)$

C_v: Constant-volume molar heat capacity of gas $\left(J/mol \cdot K\right)$

$C_{compr.}^{cap.}$: Capital cost coefficient of compression $\left(\$/\left(watt\right)^a\right)$

$C_{compr.}^{oper.}$: Operating cost coefficient of compression $\left(\$/J\right)$

$C_{cooler}^{oper.}$: Operating cost coefficient of cooling $(\$/mol)$

D:Maximum normalized compressor outlet temperature; $D \triangleq \frac{T_{\max} - T_0}{T_0}$

f_Q: The objective function that maps each pair $(x, y) \in (I_Q, S_Q(x))$ to the *objective function value* $f_Q(x, y)$ corresponding to that *instance* x and that *feasible solution* $y \in S_Q(x)$

F : Annualization factor $(1/s)$

F_Q: The function that maps each $x \in I_Q$ to the *optimum objective function value*

$F_Q(x) \triangleq f_Q(x, z) \ \forall z \in Z_Q(x)$ corresponding to $x \in I_Q$.

H : Molar enthalpy of fluid stream (J)

I_Q: The set of instances of the optimization problem Q

$k = \frac{C_p}{C_v}$: Ratio of constant-pressure and constant-volume molar heat capacities

K : Compressor purchased cost $(\$)$

$\dot{n}$: Molar flow rate of gas stream (mol/s)

$\dot{n}_{c,i}$: Molar flow rate of coolant stream through cooler i (mol/s)

N_0^w: Cardinality of set S_0^w

N_D^w: Cardinality of set S_D^w

N_I^w: Cardinality of set S_I^w

$opt_Q \in \{\min, \max\}$: A linguistic variable that determines whether the *minimum* or the *maximum* of the objective function is to be identified.

P_0: Inlet pressure of gas stream to compressor/cooler system (kPa)

P_i: Outlet pressure of gas stream from compressor i (kPa)

P_n: Outlet pressure of gas stream from compressor/cooler system (kPa)

Q: Optimization problem, considered as the 4-tuple $\langle I_Q, S_Q, f_Q, opt_Q \rangle$.

R: Universal gas constant $(J/mol \cdot K)$

S: Molar entropy of fluid stream (J/K)

S_0^w: The set of compressors not in use in a network; $S_0^w \triangleq \{i = 1, n : w_i = 0\}$

S_D^w: The set of compressors operating at maximum allowable outlet temperature in a network;

$S_D^w \triangleq \{i = 1, n : w_i = \eta_i D\}$

S_I^w: The set of compressors in use and operating below maximum allowable outlet temperature;

$S_I^w \triangleq \{i = 1, n : 0 < w_i < \eta_i D\}$

S_Q: The function that maps each $x \in I_Q$ to the set $S_Q(x)$ of feasible solutions corresponding to

$x \in I_Q$

T_0: Inlet temperature of gas stream to compressor/cooler system (K)

$T_{c,i,in}$: Inlet temperature of coolant to cooler i (K)

$T_{c,i,out}$: Outlet temperature of coolant from cooler i (K)

T_i: Outlet temperature of gas stream from compressor i (K)

T'_{i-1}: Outlet temperature of gas stream from cooler $i-1$ to compressor i (K)

T_i'' : Outlet temperature of gas stream from hypothetical isentropic compressor i (K)

$T_{\max}$: Maximum allowable operating temperature for all compressors (K)

T_n : Outlet temperature of gas stream from compressor/cooler system (K)

w_i : Normalized ideal compressor outlet temperature; $w_i \triangleq \frac{T_i'' - T_0}{T_0}$

W : Consumed power (kW)

W_i : Work done by compressor i (J/mol)

w^i : Work done by a hypothetical isentropic compressor (J/mol)

X_Q : The infinite collection of instances $X_Q \subset I_Q$ considered in this work;

$$X_Q \triangleq \left\{ \left(\frac{B}{A}, C, D, \{\eta_i\}_{i=1}^n \right) \in \mathbb{R}^+ \times \mathbb{R}^+ \times \mathbb{R}^+ \times \mathbb{R}^n : \begin{bmatrix} \eta_i \in (0,1] \ \ \forall i = 1,n \\ \left(\frac{B}{A}, D, \{\eta_i\}_{i=1}^n \right) \text{is known} \\ C \in \left(1, \prod_{i=1}^n (\eta_i D + 1) \right] \end{bmatrix} \right\} \subset I_Q$$

Z : Compressibility factor

Z_Q : The function that maps each $x \in I_Q$ to the set $Z_Q(x)$ of *optimum feasible solutions* corresponding to $x \in I_Q$

Subscripts:

id : Ideal (isentropic) compressor

in : Inlet stream to process unit

out : Outlet stream to process unit

r : Real compressor

Superscripts:

i : Ideal (isentropic) compressor case

o : Initial state of fluid stream

R : Reference state of fluid stream

Section 3.7: References

1. U.S. Department of Energy, U.S. Energy Information Administration, Office of Integrated and International Energy Analysis, Washington, DC. U.S. Annual Energy Outlook 2011 Reference Case, 2011.

2. U.S. Department of Energy, U.S. Energy Information Administration, Office of Integrated and International Energy Analysis, Washington, DC. Annual Energy Outlook 2013 with Projections to 2040, 2013.

3. Kaya, D.; Phelan, P.; Chau, D.; Sarac, H. I. Energy conservation in compressed-air systems. *Int. J. Energ. Res*. **2002**, *26* (9), 837.

4. Peters, M. S.; Timmerhaus, K. D.; West, R. E. *Plant Design and Economics for Chemical Engineers, 5th Edition*; McGraw-Hill: New York, 2003.

5. Biegler, L. T.; Grossmann, I. E.; Westerberg A. W. *Systematic Methods of Chemical Process Design*; Prentice Hall: New Jersey, 1997.

6. Seider, W. D.; Seader, J. D.; Lewin, D. R. *Product and Process Design Principles; Synthesis, Analysis, and Evaluation, 2nd Edition*; John Wiley & Sons: New York, 2004.

7. Martin, L. L.; Manousiouthakis, V. I. Total Annualized Cost Optimality Properties of State Space Models for Mass and Heat Exchanger Networks. *Chem. Eng. Sci*. **2001**, *56* (20), 5835.

8. Zhou, W.; Manousiouthakis, V. I. Global Capital/Total Annualized Cost Minimization of Homogeneous and Isothermal Reactor Networks. *Ind. Eng. Chem. Res*. **2008**, *47* (10), 3771.

9. Conner, J. A.; Manousiouthakis, V. I. Global Optimality Properties of Total Annualized and Operating Cost Problems for Compressor Sequences. *AIChE J.*, in press.

10. Manousiouthakis, V. I.; Thomas, N.; Justanieah, A. M. On a Finite Branch and Bound Algorithm for the Global Minimization of a Concave Power Law Over a Polytope. *J. Optim. Theory Appl.* **2011**, *151* (1), 121.

11. Manousiouthakis, V.; Sourlas, D. A Global Optimization Approach to Rationally Constrained Rational Programming. *Chem. Eng. Commun.* **1992**, *115* (1), 127.

12. Falk, J. E.; Soland, R. M. An Algorithm for Separable Nonconvex Programming Problems. *Manage. Sci.* **1969**, *15*, 550.

13. Geoffrion, A. M. Generalized Benders Decomposition. *J. Optim. Theory Appl.* **1972**, *10* (4), 237.

14. Bagajewicz, M. J.; Manousiouthakis, V. On the Generalized Benders Decomposition. *Comput. Chem. Eng.* **1991**, *15* (10), 691.

15. Smith, J. M.; Van Ness, H. C.; Abbott, M. M. *Introduction to Chemical Engineering Thermodynamics, 7th Edition*; McGraw-Hill: New York, 2005.

16. Elrod Jr., H. G. Minimum Work in Multistage Compression, *Ind. Eng. Chem.* **1945**, *37* (8), 789.

17. Happel, J. *Chemical Process Economics*; John Wiley & Sons: New York, 1958.

18. Aris, R.; Bellman, R.; Kalaba, R. Some Optimization Problems in Chemical Engineering. *Chem. Engng. Prog. Symp. Ser.* **1960**, *56* (31), 95.

19. Wang, C. S.; Fan, L. T. Optimization of One-Dimensional Multistage Linear Processes. *Appl. Sci. Res.* **1965**, Section B, Vol. 11, 321.

20. Edgar, T. F.; Himmelblau, D. M. *Optimization of Chemical Processes*; McGraw-Hill: New York, 2001.

21. Han, Ju Ran, Vasilios Manousiouthakis, and Soo Hyoung Choi. "Global optimization of chemical processes using the interval analysis." Korean journal of chemical engineering 14.4 (1997): 270-276.

22. Chen, J. Introduction to Tractability and Approximability of Optimization Problems. http://faculty.cs.tamu.edu/chen/notes/opt.pdf (accessed September 2014).

23. Birattari, M. *Tuning Metaheuristics: A Machine Learning Perspective*; Springer: Berlin-Heidelberg, 2009.

Appendix 3.A.

Proof of Theorem 1:

a. We proceed by contradiction. Assume that $\min_{i\in S_D^{w*}} \eta_i < \max_{i\in S_I^{w*}\cup S_\varepsilon^{w*}} \eta_i$. This implies that

$\exists (k,l) \in \left(S_I^{w*} \cup S_\varepsilon^{w*}\right) \times S_D^{w*} : \eta_k > \eta_l$. Two cases are then considered:

Case 1: $\exists(k,l) \in S_I^{w*} \times S_D^{w*} : \eta_k > \eta_l$

It is easy to verify that since $\varepsilon \in \left(0, \frac{\min\limits_{i=1,n} \eta_i}{\max\limits_{i=1,n} \eta_i} D\right)$; $\varepsilon \simeq 0$ and $\eta_k > \eta_l$, it then holds

$$\{0 < \eta_k - \eta_l \wedge 0 < \varepsilon < D\} \Rightarrow \{0 < (\eta_k - \eta_l)(D - \varepsilon) \wedge \varepsilon < D\} \Leftrightarrow$$

$$\{0 < (\eta_k - \eta_l)(D - \varepsilon) \wedge \eta_l \varepsilon(\eta_k D + 1) < \eta_l D(\eta_k D + 1)\} \Leftrightarrow$$

$$\{\eta_k \varepsilon(\eta_l D + 1) < \eta_l \varepsilon(\eta_k D + 1) + (\eta_k - \eta_l) D \wedge \eta_l \varepsilon(\eta_k D + 1) + (\eta_k - \eta_l) D < \eta_k D(\eta_l D + 1)\} \Leftrightarrow$$

$$\eta_k \varepsilon(\eta_l D + 1) < \eta_l \varepsilon(\eta_k D + 1) + (\eta_k - \eta_l) D < \eta_k D(\eta_l D + 1) \Leftrightarrow$$

$$\eta_k \varepsilon < \eta_l \varepsilon \frac{(\eta_k D + 1)}{(\eta_l D + 1)} + \frac{(\eta_k - \eta_l) D}{(\eta_l D + 1)} < \eta_k D$$

Two subcases are now considered:

Case 1a: $\exists(k,l) \in S_I^{w*} \times S_D^{w*} : \left\{\eta_k > \eta_l \wedge \eta_k \varepsilon < \eta_l \varepsilon \frac{(\eta_k D + 1)}{(\eta_l D + 1)} + \frac{(\eta_k - \eta_l) D}{(\eta_l D + 1)} \le w_k^* < \eta_k D\right\}$

Consider the vector $\{\hat{w}_i\}_{i=1}^n$ where

$$\hat{w}_i \triangleq w_i^* \quad \forall i \in \{i = 1,n : i \neq k \wedge i \neq l\},\ \hat{w}_k \triangleq \eta_k D,\ \hat{w}_l \triangleq \frac{(\eta_l D + 1)}{(\eta_k D + 1)}(w_k^* + 1) - 1$$

It is easy to verify that $\prod_{i=1}^n (\hat{w}_i + 1) - C = \prod_{i=1}^n (w_i^* + 1) - C = 0$. In addition

$$\eta_l \varepsilon \le \hat{w}_l \le \eta_l D \Leftrightarrow \eta_l \varepsilon \le \frac{(\eta_l D + 1)}{(\eta_k D + 1)}(w_k^* + 1) - 1 \le \eta_l D \Leftrightarrow$$

$$(\eta_l \varepsilon + 1)(\eta_k D + 1) \le (\eta_l D + 1)(w_k^* + 1) \le (\eta_l D + 1)(\eta_k D + 1) \Leftrightarrow$$

$$\frac{(\eta_l \varepsilon + 1)(\eta_k D + 1)}{(\eta_l D + 1)} \le (w_k^* + 1) \le (\eta_k D + 1) \Leftrightarrow \frac{(\eta_l \varepsilon + 1)(\eta_k D + 1)}{(\eta_l D + 1)} - 1 \le w_k^* \le \eta_k D \Leftrightarrow$$

$\eta_l \varepsilon \frac{(\eta_k D+1)}{(\eta_l D+1)} + \frac{(\eta_k - \eta_l) D}{(\eta_l D+1)} \le w_k^* \le \eta_k D$, which is true by the conditions constituting Case 1a.

Thus all constraints of ν are satisfied and $\{\hat{w}_i\}_{i=1}^n$ is a feasible point of ν.

Let Δ be defined as:

$$\Delta \triangleq \left[\sum_{i=1}^{n} \frac{1}{\eta_i} w_i^* + \frac{B}{A}\sum_{i=1}^{n}\left(\frac{1}{\eta_i}\right)^a \left(w_i^*\right)^a\right] - \left[\sum_{i=1}^{n} \frac{1}{\eta_i} \hat{w}_i + \frac{B}{A}\sum_{i=1}^{n}\left(\frac{1}{\eta_i}\right)^a \left(\hat{w}_i\right)^a\right] \Leftrightarrow$$

$$\Delta = \left(\frac{1}{\eta_k} w_k^* + \frac{1}{\eta_l} w_l^* - \frac{1}{\eta_k}\hat{w}_k - \frac{1}{\eta_l}\hat{w}_l\right) + \frac{B}{A}\left(\left(\frac{1}{\eta_k}\right)^\alpha \left(w_k^*\right)^\alpha + \left(\frac{1}{\eta_l}\right)^\alpha \left(w_l^*\right)^\alpha - \left(\frac{1}{\eta_k}\right)^\alpha \left(\hat{w}_k\right)^\alpha - \left(\frac{1}{\eta_l}\right)^\alpha \left(\hat{w}_l\right)^\alpha\right) \Leftrightarrow$$

$$\Delta = \left[\begin{array}{l} \left(\frac{1}{\eta_k} w_k^* + \frac{1}{\eta_l}\eta_l D - \frac{1}{\eta_k}\eta_k D - \frac{1}{\eta_l}\left(\frac{(\eta_l D+1)}{(\eta_k D+1)}\left(w_k^*+1\right)-1\right)\right) + \\ + \frac{B}{A}\left(\left(\frac{1}{\eta_k}\right)^\alpha \left(w_k^*\right)^\alpha + \left(\frac{1}{\eta_l}\right)^\alpha (\eta_l D)^\alpha - \left(\frac{1}{\eta_k}\right)^\alpha (\eta_k D)^\alpha - \left(\frac{1}{\eta_l}\right)^\alpha \left(\frac{(\eta_l D+1)}{(\eta_k D+1)}\left(w_k^*+1\right)-1\right)^\alpha\right) \end{array}\right] \Leftrightarrow$$

$$\Delta = \left[\begin{array}{l} \left(\frac{w_k^*\eta_l(\eta_k D+1) - \eta_k(\eta_l D+1)\left(w_k^*+1\right) + \eta_k(\eta_k D+1)}{\eta_k\eta_l(\eta_k D+1)}\right) + \\ + \frac{B}{A}\left(\left(\frac{w_k^*\eta_l(\eta_k D+1)}{\eta_k\eta_l(\eta_k D+1)}\right)^\alpha - \left(\frac{\eta_k(\eta_l D+1)\left(w_k^*+1\right) - \eta_k(\eta_k D+1)}{\eta_k\eta_l(\eta_k D+1)}\right)^\alpha\right) \end{array}\right] \Leftrightarrow$$

$$\Delta = \left[\begin{array}{l} \left(\frac{w_k^*(\eta_l - \eta_k) - \eta_k(\eta_l D+1) + \eta_k(\eta_k D+1)}{\eta_k\eta_l(\eta_k D+1)}\right) + \\ + \frac{B}{A}\left(\left(\frac{w_k^*\eta_l(\eta_k D+1)}{\eta_k\eta_l(\eta_k D+1)}\right)^\alpha - \left(\frac{\eta_k(\eta_l D+1)\left(w_k^*+1\right) - \eta_k(\eta_k D+1)}{\eta_k\eta_l(\eta_k D+1)}\right)^\alpha\right) \end{array}\right] \Leftrightarrow$$

$$\Delta = \left[\begin{array}{l} \left(\frac{\left(w_k^* - \eta_k D\right)(\eta_l - \eta_k)}{\eta_k\eta_l(\eta_k D+1)}\right) + \\ + \frac{B}{A}\frac{1}{\left(\eta_k\eta_l(\eta_k D+1)\right)^\alpha}\left(\left(w_k^*\eta_l(\eta_k D+1)\right)^\alpha - \left(\eta_k\eta_l D w_k^* + \eta_k w_k^* + \eta_k\eta_l D - \eta_k\eta_k D\right)^\alpha\right) \end{array}\right]$$

Since $(k,l) \in S_I^{w*} \times S_D^{w*} : \eta_k > \eta_l$, it holds $\varepsilon < w_k^* < \eta_k D$. Then $\left(w_k^* - \eta_k D\right)\left(\eta_l - \eta_k\right) > 0$. In addition,

$$\left(w_k^* \eta_l \left(\eta_k D + 1\right)\right)^{\alpha} > \left(\eta_k \eta_l D w_k^* + \eta_k w_k^* + \eta_k \eta_l D - \eta_k \eta_k D\right)^{\alpha} \Leftrightarrow$$

$$w_k^* \eta_l \left(\eta_k D + 1\right) > \eta_k \eta_l D w_k^* + \eta_k w_k^* + \eta_k \eta_l D - \eta_k \eta_k D \Leftrightarrow$$

$\left(w_k^* - \eta_k D\right)\left(\eta_l - \eta_k\right) > 0$ which is shown above to be true. Thus, $\Delta > 0$. In turn this implies that $\{\hat{w}_i\}_{i=1}^n$ is a feasible point of ν_ε with corresponding objective function value that is strictly lower than ν_ε. This is impossible. Thus $\min_{i \in S_D^{w*}} \eta_i \geq \max_{i \in S_I^{w*}} \eta_i$ O.E.Δ.

Case 1b: $\exists (k,l) \in S_I^{w*} \times S_D^{w*} : \left\{ \eta_k > \eta_l \wedge \eta_k \varepsilon < w_k^* < \eta_l \varepsilon \frac{\left(\eta_k D + 1\right)}{\left(\eta_l D + 1\right)} + \frac{\left(\eta_k - \eta_l\right) D}{\left(\eta_l D + 1\right)} < \eta_k D \right\}$

Consider the vector $\{\hat{w}_i\}_{i=1}^n$ where

$$\hat{w}_i \triangleq w_i^* \quad \forall i \in \{i = 1, n : i \neq k \wedge i \neq l\},\ \hat{w}_k \triangleq \frac{\left(\eta_l D + 1\right)}{\left(\eta_l \varepsilon + 1\right)}\left(w_k^* + 1\right) - 1,\ \hat{w}_l \triangleq \eta_l \varepsilon$$

It is easy to verify that $\prod_{i=1}^n \left(\hat{w}_i + 1\right) - C = \prod_{i=1}^n \left(w_i^* + 1\right) - C = 0$. In addition

$$\eta_k \varepsilon \leq \hat{w}_k \leq \eta_k D \Leftrightarrow \eta_k \varepsilon \leq \frac{\left(\eta_l D + 1\right)}{\left(\eta_l \varepsilon + 1\right)}\left(w_k^* + 1\right) - 1 \leq \eta_k D \Leftrightarrow$$

$$\left(\eta_k \varepsilon + 1\right)\left(\eta_l \varepsilon + 1\right) \leq \left(\eta_l D + 1\right)\left(w_k^* + 1\right) \leq \left(\eta_k D + 1\right)\left(\eta_l \varepsilon + 1\right) \Leftrightarrow$$

$$\frac{\left(\eta_k \varepsilon + 1\right)\left(\eta_l \varepsilon + 1\right)}{\left(\eta_l D + 1\right)} - 1 \leq w_k^* \leq \frac{\left(\eta_k D + 1\right)}{\left(\eta_l D + 1\right)}\left(\eta_l \varepsilon + 1\right) - 1 \Leftrightarrow$$

$$\left\{\frac{(\eta_k\varepsilon+1)(\eta_l\varepsilon+1)}{(\eta_l D+1)}-1\le w_k^{\ *}\ \wedge\ w_k^{\ *}\le\eta_l\varepsilon\frac{(\eta_k D+1)}{(\eta_l D+1)}+\frac{(\eta_k-\eta_l)D}{(\eta_l D+1)}\right\}\Leftrightarrow$$

$$\left\{\frac{(\eta_l\varepsilon+1)}{(\eta_l D+1)}\le\frac{(w_k^{\ *}+1)}{(\eta_k\varepsilon+1)}\wedge\ w_k^{\ *}\le\eta_l\varepsilon\frac{(\eta_k D+1)}{(\eta_l D+1)}+\frac{(\eta_k-\eta_l)D}{(\eta_l D+1)}\right\}$$

which is true by the conditions constituting Case 1b, and the fact that $\varepsilon\in\left(0,\frac{\min\limits_{i=1,n}\eta_i}{\max\limits_{i=1,n}\eta_i}D\right)$; $\varepsilon\simeq 0$.

Let again Δ be defined as:

$$\Delta\triangleq\left[\sum_{i=1}^{n}\frac{1}{\eta_i}w_i^{\ *}+\frac{B}{A}\sum_{i=1}^{n}\left(\frac{1}{\eta_i}\right)^a\left(w_i^{\ *}\right)^a\right]-\left[\sum_{i=1}^{n}\frac{1}{\eta_i}\hat{w}_i+\frac{B}{A}\sum_{i=1}^{n}\left(\frac{1}{\eta_i}\right)^a\left(\hat{w}_i\right)^a\right]\Leftrightarrow$$

$$\Delta=\left(\frac{1}{\eta_k}w_k^{\ *}+\frac{1}{\eta_l}w_l^{\ *}-\frac{1}{\eta_k}\hat{w}_k-\frac{1}{\eta_l}\hat{w}_l\right)+\frac{B}{A}\left(\left(\frac{1}{\eta_k}\right)^\alpha\left(w_k^{\ *}\right)^\alpha+\left(\frac{1}{\eta_l}\right)^\alpha\left(w_l^{\ *}\right)^\alpha-\left(\frac{1}{\eta_k}\right)^\alpha\left(\hat{w}_k\right)^\alpha-\left(\frac{1}{\eta_l}\right)^\alpha\left(\hat{w}_l\right)^\alpha\right)\Leftrightarrow$$

$$\Delta=\left[\begin{array}{l}\left(\frac{1}{\eta_k}w_k^{\ *}+\frac{1}{\eta_l}(\eta_l D)-\frac{1}{\eta_k}\left(\frac{(\eta_l D+1)}{(\eta_l\varepsilon+1)}\left(w_k^{\ *}+1\right)-1\right)-\frac{1}{\eta_l}\eta_l\varepsilon\right)+\\ +\frac{B}{A}\left(\left(\frac{1}{\eta_k}\right)^\alpha\left(w_k^{\ *}\right)^\alpha+\left(\frac{1}{\eta_l}\right)^\alpha(\eta_l D)^\alpha-\left(\frac{1}{\eta_k}\right)^\alpha\left(\frac{(\eta_l D+1)}{(\eta_l\varepsilon+1)}\left(w_k^{\ *}+1\right)-1\right)^\alpha-\left(\frac{1}{\eta_l}\right)^\alpha(\eta_l\varepsilon)^\alpha\right)\end{array}\right]\Leftrightarrow$$

$$\Delta=\left[\begin{array}{l}\left(\frac{1}{\eta_k}w_k^{\ *}+D-\frac{1}{\eta_k}\left(\frac{(\eta_l D+1)}{(\eta_l\varepsilon+1)}\left(w_k^{\ *}+1\right)-1\right)-\varepsilon\right)+\\ +\frac{B}{A}\left(\left(\frac{1}{\eta_k}\right)^\alpha\left(w_k^{\ *}\right)^\alpha+D^\alpha-\left(\frac{1}{\eta_k}\right)^\alpha\left(\frac{(\eta_l D+1)}{(\eta_l\varepsilon+1)}\left(w_k^{\ *}+1\right)-1\right)^\alpha-\varepsilon^\alpha\right)\end{array}\right]\Leftrightarrow$$

$$\Delta=\left[\begin{array}{l}\left(\frac{1}{\eta_k}\right)\left(\left[w_k^{\ *}-\eta_k\varepsilon\right]+\left[\eta_k D-\left(\frac{(\eta_l D+1)}{(\eta_l\varepsilon+1)}\left(w_k^{\ *}+1\right)-1\right)\right]\right)+\\ +\frac{B}{A}\left(\frac{1}{\eta_k}\right)^\alpha\left(\left[\left(w_k^{\ *}\right)^\alpha-(\eta_k\varepsilon)^\alpha\right]+\left[(\eta_k D)^\alpha-\left(\frac{(\eta_l D+1)}{(\eta_l\varepsilon+1)}\left(w_k^{\ *}+1\right)-1\right)^\alpha\right]\right)\end{array}\right]$$

Based on the conditions of Case 1b the following hold:

$$\eta_k\varepsilon < w_k^* < \eta_l\varepsilon\frac{(\eta_k D+1)}{(\eta_l D+1)} + \frac{(\eta_k-\eta_l)D}{(\eta_l D+1)} \Leftrightarrow \eta_k\varepsilon+1 < w_k^*+1 < (\eta_l\varepsilon+1)\frac{(\eta_k D+1)}{(\eta_l D+1)} \Leftrightarrow$$

$$\frac{(\eta_l D+1)}{(\eta_l\varepsilon+1)}(\eta_l\varepsilon+1) < \frac{(\eta_l D+1)}{(\eta_l\varepsilon+1)}(w_k^*+1) < \frac{(\eta_l D+1)}{(\eta_l\varepsilon+1)}(\eta_l\varepsilon+1)\frac{(\eta_k D+1)}{(\eta_l D+1)} \Leftrightarrow$$

$$(\eta_l D+1) < \frac{(\eta_l D+1)}{(\eta_l\varepsilon+1)}(w_k^*+1) < (\eta_k D+1) \Leftrightarrow \eta_l D < \frac{(\eta_l D+1)}{(\eta_l\varepsilon+1)}(w_k^*+1) - 1 < \eta_k D.$$

Furthermore $\eta_k\varepsilon < w_k^* \Rightarrow (w_k^*)^\alpha > (\eta_k\varepsilon)^\alpha$, and $\frac{(\eta_l D+1)}{(\eta_l\varepsilon+1)}(w_k^*+1) - 1 < \eta_k D \Rightarrow$

$$(\eta_k D)^\alpha > \left(\frac{(\eta_l D+1)}{(\eta_l\varepsilon+1)}(w_k^*+1) - 1\right)^\alpha.$$

Thus $\Delta > 0$. In turn this implies that $\{\hat{w}_i\}_{i=1}^n$ is a feasible point of ν_ε with corresponding objective function value that is strictly lower than ν_ε. This is impossible. Thus $\min_{i\in S_D^{w*}} \eta_i \geq \max_{i\in S_I^{w*}} \eta_i$ O.E.Δ.

Case 2. $\exists(k,l) \in S_\varepsilon^{w*} \times S_D^{w*} : \eta_k > \eta_l$

Consider the following vector:

$\{\hat{w}_i\}_{i=1}^n$ where $\hat{w}_i \triangleq w_i^* \quad \forall i \in \{i = 1,n : i \neq k \wedge i \neq l\}$, $\hat{w}_k \triangleq \eta_l D$, $\hat{w}_l \triangleq \eta_k\varepsilon$

It is easy to verify that

$$\prod_{i=1}^n (\hat{w}_i + 1) - C = \prod_{i=1}^n (w_i^* + 1) - C = 0.$$

Since $\varepsilon \in \left(0, \frac{\min_{i=1,n} \eta_i}{\max_{i=1,n} \eta_i} D\right)$; $\varepsilon \simeq 0$ and $\eta_k > \eta_l$, it then holds $\eta_l\varepsilon < \eta_k\varepsilon \triangleq \hat{w}_l$, $\hat{w}_k \triangleq \eta_l D < \eta_k D$. Thus all constraints of ν are satisfied and $\{\hat{w}_i\}_{i=1}^n$ is a feasible point of ν.

Let Δ be defined as:

$$\Delta \hat{=} \left[\sum_{i=1}^{n} \frac{1}{\eta_i} w_i^* + \frac{B}{A} \sum_{i=1}^{n} \left(\frac{1}{\eta_i} \right)^a \left(w_i^* \right)^a \right] - \left[\sum_{i=1}^{n} \frac{1}{\eta_i} \hat{w}_i + \frac{B}{A} \sum_{i=1}^{n} \left(\frac{1}{\eta_i} \right)^a \left(\hat{w}_i \right)^a \right] \Leftrightarrow$$

$$\Delta = \left(\frac{1}{\eta_k} w_k^* + \frac{1}{\eta_l} w_l^* - \frac{1}{\eta_k} \hat{w}_k - \frac{1}{\eta_l} \hat{w}_l \right) + \frac{B}{A} \left(\left(\frac{1}{\eta_k} \right)^\alpha \left(w_k^* \right)^\alpha + \left(\frac{1}{\eta_l} \right)^\alpha \left(w_l^* \right)^\alpha - \left(\frac{1}{\eta_k} \right)^\alpha \left(\hat{w}_k \right)^\alpha - \left(\frac{1}{\eta_l} \right)^\alpha \left(\hat{w}_l \right)^\alpha \right) \Leftrightarrow$$

$$\Delta = \left[\begin{array}{l} \left(\frac{1}{\eta_k} \eta_k \varepsilon + \frac{1}{\eta_l} \eta_l D - \frac{1}{\eta_k} \eta_l D - \frac{1}{\eta_l} \eta_k \varepsilon \right) + \\ + \frac{B}{A} \left(\left(\frac{1}{\eta_k} \right)^\alpha \left(\eta_k \varepsilon \right)^\alpha + \left(\frac{1}{\eta_l} \right)^\alpha \left(\eta_l D \right)^\alpha - \left(\frac{1}{\eta_k} \right)^\alpha \left(\eta_l D \right)^\alpha - \left(\frac{1}{\eta_l} \right)^\alpha \left(\eta_k \varepsilon \right)^\alpha \right) \end{array} \right] \Leftrightarrow$$

$$\Delta = \left(\eta_l D - \eta_k \varepsilon \right) \left(\frac{1}{\eta_l} - \frac{1}{\eta_k} \right) + \frac{B}{A} \left(\left(\eta_l D \right)^\alpha - \left(\eta_k \varepsilon \right)^\alpha \right) \left(\left(\frac{1}{\eta_l} \right)^\alpha - \left(\frac{1}{\eta_k} \right)^\alpha \right)$$

Since $(k,l) \in S_\varepsilon^{w*} \times S_D^{w*} : \eta_k > \eta_l$, and $\varepsilon \in \left(0, \frac{\min\limits_{i=1,n} \eta_i}{\max\limits_{i=1,n} \eta_i} D \right)$; $\varepsilon \simeq 0$ it holds $\Delta > 0$. In turn this implies that $\{\hat{w}_i\}_{i=1}^n$ is a feasible point of ν_ε with corresponding objective function value that is strictly lower than ν_ε. This is impossible. Thus $\min\limits_{i \in S_D^{w*}} \eta_i \geq \max\limits_{i \in S_\varepsilon^{w*}} \eta_i$ O.E.Δ.

b. We again proceed by contradiction. Assume that $\max\limits_{i \in S_\varepsilon^{w*}} \eta_i > \min\limits_{i \in S_I^{w*} \cup S_D^{w*}} \eta_i$. This implies that $\exists (k,l) \in \left(S_I^{w*} \cup S_D^{w*} \right) \times S_\varepsilon^{w*} : \eta_k < \eta_l$. Two cases are then considered.

Case 1. $\exists (k.l) \in S_I^{w*} \times S_\varepsilon^{w*} : \eta_k < \eta_l$

Consider the following vector:

$\{\hat{w}_i\}_{i=1}^n$ where $\hat{w}_i \triangleq w_i^* \quad \forall i \in \{i = 1,n : i \neq k \wedge i \neq l\}$, $\hat{w}_k \triangleq \eta_k \varepsilon$, $\hat{w}_l \triangleq \dfrac{(w_k^* + 1)(\eta_l \varepsilon + 1)}{(\eta_k \varepsilon + 1)} - 1$

It is easy to verify that

$$\prod_{i=1}^{n} (\hat{w}_i + 1) - C = \prod_{i=1}^{n} (w_i^* + 1) - C = 0 .$$

In addition

$$\eta_l \varepsilon \leq \frac{(w_k^* + 1)(\eta_l \varepsilon + 1)}{(\eta_k \varepsilon + 1)} - 1 \leq \eta_l D \Leftrightarrow (\eta_l \varepsilon + 1) \leq \frac{(w_k^* + 1)(\eta_l \varepsilon + 1)}{(\eta_k \varepsilon + 1)} \leq (\eta_l D + 1) \Leftrightarrow$$

$$\eta_k \varepsilon \leq w_k^* \leq \frac{(\eta_l D + 1)}{(\eta_l \varepsilon + 1)}(\eta_k \varepsilon + 1) - 1 \Leftrightarrow \eta_k \varepsilon \leq w_k^* \leq \eta_k D + \frac{(\eta_l D + 1)}{(\eta_l \varepsilon + 1)}(\eta_k \varepsilon + 1) - (\eta_k D + 1) \Leftrightarrow$$

$$\eta_k \varepsilon \leq w_k^* \leq \eta_k D + \frac{(\eta_l D + 1)(\eta_k \varepsilon + 1) - (\eta_k D + 1)(\eta_l \varepsilon + 1)}{(\eta_l \varepsilon + 1)} \Leftrightarrow$$

$\eta_k \varepsilon \leq w_k^* \leq \eta_k D + \dfrac{(\eta_l - \eta_k)(D - \varepsilon)}{(\eta_l \varepsilon + 1)}$, which is true, since $0 < \eta_k \varepsilon < w_k^* < \eta_k D$, $\eta_l > \eta_k$, and

$\varepsilon \in \left(0, \dfrac{\min\limits_{i=1,n} \eta_i}{\max\limits_{i=1,n} \eta_i} D\right)$; $\varepsilon \simeq 0$. Thus all constraints of ν_ε are satisfied and $\{\hat{w}_i\}_{i=1}^n$ is a feasible point of

ν_ε.

Let Δ be defined as:

$$\Delta \triangleq \left[\sum_{i=1}^{n} \frac{1}{\eta_i} w_i^* + \frac{B}{A} \sum_{i=1}^{n} \left(\frac{1}{\eta_i}\right)^a (w_i^*)^a\right] - \left[\sum_{i=1}^{n} \frac{1}{\eta_i} \hat{w}_i + \frac{B}{A} \sum_{i=1}^{n} \left(\frac{1}{\eta_i}\right)^a (\hat{w}_i)^a\right] \Leftrightarrow$$

$$\Delta = \left(\frac{1}{\eta_k} w_k^* + \frac{1}{\eta_l} w_l^* - \frac{1}{\eta_k} \hat{w}_k - \frac{1}{\eta_l} \hat{w}_l\right) + \frac{B}{A}\left(\left(\frac{1}{\eta_k}\right)^\alpha (w_k^*)^\alpha + \left(\frac{1}{\eta_l}\right)^\alpha (w_l^*)^\alpha - \left(\frac{1}{\eta_k}\right)^\alpha (\hat{w}_k)^\alpha - \left(\frac{1}{\eta_l}\right)^\alpha (\hat{w}_l)^\alpha\right) \Leftrightarrow$$

$$\Delta = \left[\begin{array}{l} \left(\frac{1}{\eta_k} w_k^{\,*} + \frac{1}{\eta_l}(\eta_l \varepsilon) - \frac{1}{\eta_k}(\eta_k \varepsilon) - \frac{1}{\eta_l}\left(\frac{\left(w_k^{\,*}+1\right)\left(\eta_l \varepsilon + 1\right)}{\left(\eta_k \varepsilon + 1\right)} - 1 \right) \right) + \\ + \frac{B}{A}\left(\left(\frac{1}{\eta_k}\right)^{\alpha} \left(w_k^{\,*}\right)^{\alpha} + \left(\frac{1}{\eta_l}\right)^{\alpha} (\eta_l \varepsilon)^{\alpha} - \left(\frac{1}{\eta_k}\right)^{\alpha} (\eta_k \varepsilon)^{\alpha} - \left(\frac{1}{\eta_l}\right)^{\alpha} \left(\frac{\left(w_k^{\,*}+1\right)\left(\eta_l \varepsilon + 1\right)}{\left(\eta_k \varepsilon + 1\right)} - 1 \right)^{\alpha} \right) \end{array} \right] \Leftrightarrow$$

$$\Delta = \left[\begin{array}{l} \left(\frac{1}{\eta_k} w_k^{\,*} - \frac{1}{\eta_l}\left(\frac{\left(w_k^{\,*}+1\right)\left(\eta_l \varepsilon + 1\right)}{\left(\eta_k \varepsilon + 1\right)} - 1 \right) \right) + \\ + \frac{B}{A}\left(\left(\frac{1}{\eta_k}\right)^{\alpha} \left(w_k^{\,*}\right)^{\alpha} - \left(\frac{1}{\eta_l}\right)^{\alpha} \left(\frac{\left(w_k^{\,*}+1\right)\left(\eta_l \varepsilon + 1\right)}{\left(\eta_k \varepsilon + 1\right)} - 1 \right)^{\alpha} \right) \end{array} \right]$$

However

$$w_k^{\,*} > \eta_k \varepsilon \overset{\eta_l > \eta_k}{\Leftrightarrow} \left(w_k^{\,*}+1\right)\left(\frac{\eta_l - \eta_k}{\eta_l} \right) > \left(\eta_k \varepsilon + 1\right)\left(\frac{\eta_l - \eta_k}{\eta_l} \right) \Leftrightarrow$$

$$\left(w_k^{\,*}+1\right)\left(1 - \frac{\eta_k}{\eta_l}\frac{\left(\eta_l \varepsilon + 1\right)}{\left(\eta_k \varepsilon + 1\right)} \right) > \left(\frac{\eta_l - \eta_k}{\eta_l} \right) \Leftrightarrow w_k^{\,*} + 1 > \frac{\eta_k}{\eta_l}\frac{\left(w_k^{\,*}+1\right)\left(\eta_l \varepsilon + 1\right)}{\left(\eta_k \varepsilon + 1\right)} - \frac{\eta_k}{\eta_l} + 1 \Leftrightarrow$$

$$\frac{1}{\eta_k} w_k^{\,*} > \frac{1}{\eta_l}\left(\frac{\left(w_k^{\,*}+1\right)\left(\eta_l \varepsilon + 1\right)}{\left(\eta_k \varepsilon + 1\right)} - 1 \right) \Rightarrow \left(\frac{1}{\eta_k}\right)^{\alpha} \left(w_k^{\,*}\right)^{\alpha} > \left(\frac{1}{\eta_l}\right)^{\alpha} \left(\frac{\left(w_k^{\,*}+1\right)\left(\eta_l \varepsilon + 1\right)}{\left(\eta_k \varepsilon + 1\right)} - 1 \right)^{\alpha}$$

It then holds $\Delta > 0$. In turn this implies that $\left\{\hat{w}_i\right\}_{i=1}^{n}$ is a feasible point of ν_ε with corresponding objective function value that is strictly lower than ν_ε. This is impossible. Thus

$$\max_{i \in S_\varepsilon^{w*}} \eta_i \leq \min_{i \in S_I^{w*}} \eta_i \quad \text{O.E.}\Delta.$$

Case 2. $\exists (k,l) \in S_D^{w*} \times S_\varepsilon^{w*} : \eta_k < \eta_l$

Consider the following vector:

$\left\{\hat{w}_i\right\}_{i=1}^{n}$ where $\hat{w}_i \triangleq w_i^{\,*} \quad \forall i \in \left\{ i = 1, n : i \neq k \wedge i \neq l \right\},\ \hat{w}_k \triangleq \eta_l \varepsilon,\ \hat{w}_l \triangleq \eta_k D$

It is easy to verify that

$$\prod_{i=1}^{n}(\hat{w}_i+1)-C=\prod_{i=1}^{n}\left(w_i^*+1\right)-C=0.$$

It also holds

$0<\eta_k\varepsilon<\eta_l\varepsilon\triangleq\hat{w}_k<\eta_k D$, and $0<\eta_k\varepsilon<\eta_l\varepsilon<\eta_k D\triangleq\hat{w}_l<\eta_k D<\eta_l D$, since $\eta_k<\eta_l$, and

$\varepsilon\in\left(0,\dfrac{\min\limits_{i=1,n}\eta_i}{\max\limits_{i=1,n}\eta_i}D\right)$; $\varepsilon\simeq 0$. Thus all constraints of ν_ε are satisfied and $\{\hat{w}_i\}_{i=1}^{n}$ is a feasible point of ν_ε.

Let Δ be defined as:

$$\Delta\triangleq\left[\sum_{i=1}^{n}\frac{1}{\eta_i}w_i^*+\frac{B}{A}\sum_{i=1}^{n}\left(\frac{1}{\eta_i}\right)^a\left(w_i^*\right)^a\right]-\left[\sum_{i=1}^{n}\frac{1}{\eta_i}\hat{w}_i+\frac{B}{A}\sum_{i=1}^{n}\left(\frac{1}{\eta_i}\right)^a\left(\hat{w}_i\right)^a\right]\Leftrightarrow$$

$$\Delta=\left(\frac{1}{\eta_k}w_k^*+\frac{1}{\eta_l}w_l^*-\frac{1}{\eta_k}\hat{w}_k-\frac{1}{\eta_l}\hat{w}_l\right)+\frac{B}{A}\left(\left(\frac{1}{\eta_k}\right)^\alpha\left(w_k^*\right)^\alpha+\left(\frac{1}{\eta_l}\right)^\alpha\left(w_l^*\right)^\alpha-\left(\frac{1}{\eta_k}\right)^\alpha\left(\hat{w}_k\right)^\alpha-\left(\frac{1}{\eta_l}\right)^\alpha\left(\hat{w}_l\right)^\alpha\right)\Leftrightarrow$$

$$\Delta=\left[\begin{array}{l}\left(\dfrac{1}{\eta_k}\eta_k D+\dfrac{1}{\eta_l}\eta_l\varepsilon-\dfrac{1}{\eta_k}\eta_l\varepsilon-\dfrac{1}{\eta_l}\eta_k D\right)+\\+\dfrac{B}{A}\left(\left(\dfrac{1}{\eta_k}\right)^\alpha\left(\eta_k D\right)^\alpha+\left(\dfrac{1}{\eta_l}\right)^\alpha\left(\eta_l\varepsilon\right)^\alpha-\left(\dfrac{1}{\eta_k}\right)^\alpha\left(\eta_l\varepsilon\right)^\alpha-\left(\dfrac{1}{\eta_l}\right)^\alpha\left(\eta_k D\right)^\alpha\right)\end{array}\right]\Leftrightarrow$$

$$\Delta=\left[\begin{array}{l}\left(\dfrac{1}{\eta_k}-\dfrac{1}{\eta_l}\right)\left(\eta_k D-\eta_l\varepsilon\right)+\\+\dfrac{B}{A}\left(\left(\dfrac{1}{\eta_k}\right)^\alpha-\left(\dfrac{1}{\eta_l}\right)^\alpha\right)\left(\left(\eta_k D\right)^\alpha-\left(\eta_l\varepsilon\right)^\alpha\right)\end{array}\right]$$

Since $\eta_k < \eta_l$, and $\varepsilon \in \left(0, \frac{\min\limits_{i=1,n} \eta_i}{\max\limits_{i=1,n} \eta_i} D\right)$; $\varepsilon \simeq 0$, it holds $\Delta > 0$. In turn this implies that $\{\hat{w}_i\}_{i=1}^n$ is a feasible point of ν_ε with corresponding objective function value that is strictly lower than ν_ε. This is impossible. Thus $\max\limits_{i \in S_\varepsilon^{w*}} \eta_i \leq \min\limits_{i \in S_D^{w*}}$ O.E.Δ.

Proof of Theorem 2:

It is easy to establish that ν_ε has a feasible region that is nonempty, closed, and bounded, an objective function and constraint defining functions that are all twice differentiable throughout the feasible region, and feasible points that are all regular (i.e. the gradients of all constraints that are active at each feasible point are all linearly independent).

Considering that the compressors are ranked according to efficiency (first compressor has the highest efficiency), then based on Theorem 1, if $\{w_i\}_{i=1}^n$ is to be a globally optimum variable vector of ν_ε, the sets $S_D^w, S_I^w, S_\varepsilon^w$ must be:

$$S_D^w \triangleq \{1, \ldots, N_D^w\},\ S_I^w \triangleq \{N_D^w + 1, \ldots, N_D^w + N_I^w\},\ S_\varepsilon^w \triangleq \{N_D^w + N_I^w, \ldots, n\}.$$

Then the problem's optimum exists and the following first order, and second order necessary optimality conditions are defined based on the Lagrangian

$$L(w, \lambda, \mu, \nu) \triangleq \left[\begin{array}{l} \sum_{i=1}^n \frac{1}{\eta_i} \cdot w_i + \frac{B}{A} \sum_{i=1}^n \left(\frac{1}{\eta_i}\right)^a \cdot (w_i)^a + \lambda \cdot \left(\prod_{i=1}^n (w_i + 1) - C\right) + \\ + \sum_{i=1}^n \mu_i \cdot (\eta_i \varepsilon - w_i) + \sum_{i=1}^n \nu_i \cdot (w_i - \eta_i D) \end{array}\right]$$

They are:

$$
\left\{
\begin{array}{l}
\dfrac{\partial L(w,\lambda,\mu,\nu)}{\partial w_k} \triangleq \dfrac{1}{\eta_k} + a\cdot\dfrac{B}{A}\left(\dfrac{1}{\eta_k}\right)^{a}\cdot\left(w_k\right)^{a-1} + \lambda\cdot\prod_{\substack{i=1\\ i\neq k}}^{n}\left(w_i+1\right) - \mu_k + \nu_k = 0 \qquad \forall k = 1,n \\
\dfrac{\partial^2 L(w,\lambda,\mu,\nu)}{\partial w^2} \triangleq \begin{bmatrix}
a(a-1)\dfrac{B}{A}\left(\dfrac{1}{\eta_1}\right)^{a}\cdot\left(w_1\right)^{a-2} & \dfrac{\lambda C}{(w_1+1)(w_2+1)} & \cdots & \dfrac{\lambda C}{(w_1+1)(w_n+1)} \\
\dfrac{\lambda C}{(w_2+1)(w_1+1)} & a(a-1)\dfrac{B}{A}\left(\dfrac{1}{\eta_1}\right)^{a}\cdot\left(w_1\right)^{a-2} & \cdots & \dfrac{\lambda C}{(w_2+1)(w_n+1)} \\
\vdots & \vdots & \ddots & \vdots \\
\dfrac{\lambda C}{(w_n+1)(w_1+1)} & \dfrac{\lambda C}{(w_n+1)(w_2+1)} & \cdots & a(a-1)\dfrac{B}{A}\left(\dfrac{1}{\eta_1}\right)^{a}\cdot\left(w_1\right)^{a-2}
\end{bmatrix} \\
is\ \ psd\ \ \forall z \triangleq \begin{bmatrix} z_1 \\ \vdots \\ z_{N_D^w} \\ z_{N_D^w+1} \\ \vdots \\ z_{N_D^w+N_I^w} \\ z_{N_D^w+N_I^w+1} \\ \vdots \\ z_n \end{bmatrix} \in \mathbb{R}^n : \begin{bmatrix} \dfrac{\partial\left[\prod_{i=1}^{n}(w_i+1)-C\right]}{\partial w} \\ \dfrac{\partial\left[w_1-\eta_1 D\right]}{\partial w} \\ \vdots \\ \dfrac{\partial\left[w_{N_D^w}-\eta_{N_D^w} D\right]}{\partial w} \\ \dfrac{\partial\left[\eta_{N_D^w+N_I^w+1}\varepsilon - w_{N_D^w+N_I^w+1}\right]}{\partial w} \\ \vdots \\ \dfrac{\partial\left[\eta_n\varepsilon - w_n\right]}{\partial w} \end{bmatrix}^{\mathrm{T}} \cdot z = \begin{bmatrix} \sum_{i=1}^{n}\dfrac{Cz_i}{(w_i+1)} \\ z_1 \\ \vdots \\ z_{N_D^w} \\ -z_{N_D^w+N_I^w+1} \\ \vdots \\ -z_n \end{bmatrix} = 0; \begin{bmatrix} S_D^w \triangleq \{1,\ldots,N_D^w\}; \\ S_\varepsilon^w \triangleq \{N_D^w+N_I^w+1,\ldots,n\} \end{bmatrix} \\
\prod_{i=1}^{n}(w_i+1) - C = 0,\ \ 0 < \eta_i\varepsilon \le w_i \le \eta_i D\ \ \forall i = 1,n \\
\mu_i \ge 0\ \ \forall i = 1,n,\ \ \nu_i \ge 0\ \ \forall i = 1,n,\ \ \mu_i\left(\eta_i\varepsilon - w_i\right) = 0\ \ \forall i = 1,n,\ \ \nu_i\left(w_i - \eta_i D\right) = 0\ \ \forall i = 1,n
\end{array}
\right\}
\overset{w_k+1\ge 1\ \forall k=1,n}{\Leftrightarrow}
$$

$$
\left\{
\begin{array}{l}
\left(\frac{1}{\eta_k}+a\cdot\frac{B}{A}\left(\frac{1}{\eta_k}\right)^{a}\cdot\left(w_k\right)^{a-1}\right)\left(w_k+1\right)+\lambda C=0 \qquad \forall k\in S_I^w \\
\left(\frac{1}{\eta_i}+a\cdot\frac{B}{A}\left(\frac{1}{\eta_i}\right)^{a}\cdot\left(\eta_i\varepsilon\right)^{a-1}-\mu_i\right)\left(\eta_i\varepsilon+1\right)+\lambda C=0 \qquad \forall i\in S_\varepsilon^w \\
\left(\frac{1}{\eta_j}+a\cdot\frac{B}{A}\left(\frac{1}{\eta_j}\right)^{a}\cdot\left(\eta_j D\right)^{a-1}+\nu_j\right)\left(\eta_j D+1\right)+\lambda C=0 \qquad \forall j\in S_D^w \\
\left[\begin{array}{cccc}
a\left(a-1\right)\frac{B}{A}\left(\frac{1}{\eta_1}\right)^{a}\cdot\left(w_1\right)^{a-2} & \frac{\lambda C}{\left(w_1+1\right)\left(w_2+1\right)} & \cdots & \frac{\lambda C}{\left(w_1+1\right)\left(w_n+1\right)} \\
\frac{\lambda C}{\left(w_2+1\right)\left(w_1+1\right)} & a\left(a-1\right)\frac{B}{A}\left(\frac{1}{\eta_1}\right)^{a}\cdot\left(w_1\right)^{a-2} & \cdots & \frac{\lambda C}{\left(w_2+1\right)\left(w_n+1\right)} \\
\vdots & \vdots & \ddots & \vdots \\
\frac{\lambda C}{\left(w_n+1\right)\left(w_1+1\right)} & \frac{\lambda C}{\left(w_n+1\right)\left(w_2+1\right)} & \cdots & a\left(a-1\right)\frac{B}{A}\left(\frac{1}{\eta_1}\right)^{a}\cdot\left(w_1\right)^{a-2}
\end{array}\right] \Leftrightarrow \\
is\ \ psd\ \ \forall z\in\mathbb{R}^n:\left[\begin{array}{c}
\sum_{i=1}^{n}\frac{z_i}{\left(w_i+1\right)} \\
z_1 \\
\vdots \\
z_{N_D^w} \\
z_{N_D^w+N_I^w+1} \\
\vdots \\
z_n
\end{array}\right]=0; S_D^w\triangleq\left\{1,\ldots,N_D^w\right\};\ S_\varepsilon^w\triangleq\left\{N_D^w+N_I^w+1,\ldots,n\right\} \\
\prod_{o\in S_\varepsilon^w}\left(\eta_o\varepsilon+1\right)\prod_{l\in S_I^w}\left(w_l+1\right)\prod_{m\in S_D^w}\left(\eta_m D+1\right)-C=0,\ \ 0<\eta_k\varepsilon<w_k<\eta_k D \qquad \forall k\in S_I^w \\
\mu_i\geq 0\ \ \forall i\in S_\varepsilon^w,\ \ \nu_j\geq 0\ \ \forall j\in S_D^w,\ \ w_i=\eta_i\varepsilon\ \ \forall i\in S_\varepsilon^w,\ \ w_j=\eta_j D\ \ \forall j\in S_D^w
\end{array}
\right.
$$

$$
\left\{
\begin{array}{l}
\left(\frac{1}{\eta_k}+a\cdot\frac{B}{A}\left(\frac{1}{\eta_k}\right)^a\cdot\left(w_k\right)^{a-1}\right)\left(w_k+1\right)+\lambda C=0 \qquad \forall k\in S_I^w \\
\mu_i=\frac{1}{\eta_i}+a\cdot\frac{B}{A}\left(\frac{1}{\eta_i}\right)^a\cdot\left(\eta_i\varepsilon\right)^{a-1}+\frac{\lambda C}{\left(\eta_i\varepsilon+1\right)}\geq 0 \qquad \forall i\in S_\varepsilon^w \\
\nu_j=\frac{-\lambda C}{\left(\eta_j D+1\right)}-\left(\frac{1}{\eta_j}+a\cdot\frac{B}{A}\left(\frac{1}{\eta_j}\right)^a\cdot\left(\eta_j D\right)^{a-1}\right)\geq 0 \qquad \forall j\in S_D^w \\
\left[
\begin{array}{cccc}
a\left(a-1\right)\frac{B}{A}\left(\frac{1}{\eta_1}\right)^a\cdot\left(w_1\right)^{a-2} & \frac{\lambda C}{\left(w_1+1\right)\left(w_2+1\right)} & \cdots & \frac{\lambda C}{\left(w_1+1\right)\left(w_n+1\right)} \\
\frac{\lambda C}{\left(w_2+1\right)\left(w_1+1\right)} & a\left(a-1\right)\frac{B}{A}\left(\frac{1}{\eta_1}\right)^a\cdot\left(w_1\right)^{a-2} & \cdots & \frac{\lambda C}{\left(w_2+1\right)\left(w_n+1\right)} \\
\vdots & \vdots & \ddots & \vdots \\
\frac{\lambda C}{\left(w_n+1\right)\left(w_1+1\right)} & \frac{\lambda C}{\left(w_n+1\right)\left(w_2+1\right)} & \cdots & a\left(a-1\right)\frac{B}{A}\left(\frac{1}{\eta_1}\right)^a\cdot\left(w_1\right)^{a-2}
\end{array}
\right] \\
\text{is psd } \forall z\in\mathbb{R}^n:\left[
\begin{array}{c}
\sum_{i=1}^{n}\frac{z_i}{\left(w_i+1\right)} \\
z_1 \\
\vdots \\
z_{N_D^w} \\
z_{N_D^w+N_I^w+1} \\
\vdots \\
z_n
\end{array}
\right]=0; S_D^w\triangleq\left\{1,\ldots,N_D^w\right\};\ S_\varepsilon^w\triangleq\left\{N_D^w+N_I^w+1,\ldots,n\right\} \\
\prod_{o\in S_\varepsilon^w}\left(\eta_o\varepsilon+1\right)\prod_{l\in S_I^w}\left(w_l+1\right)\prod_{m\in S_D^w}\left(\eta_m D+1\right)-C=0,\ 0<\eta_k\varepsilon<w_k<\eta_k D \qquad \forall k\in S_I^w \\
w_i=\eta_i\varepsilon\ \ \forall i\in S_\varepsilon^w,\ \ w_j=\eta_j D\ \ \forall j\in S_D^w
\end{array}
\right\}\Leftrightarrow
$$

$$
\left\{
\begin{array}{l}
\left(\frac{1}{\eta_k}+a\frac{B}{A}\left(\frac{1}{\eta_k}\right)^{a}\left(w_k\right)^{a-1}\right)\left(w_k+1\right)+\lambda C=0 \qquad \forall k\in S_I^w \\
\mu_i=\frac{1}{\eta_i}+a\frac{B}{A}\frac{1}{\eta_i}\varepsilon^{a-1}+\frac{\lambda C}{\left(\eta_i\varepsilon+1\right)}\geq 0 \qquad \forall i\in S_\varepsilon^w \\
\nu_j=\frac{-\lambda C}{\left(\eta_j D+1\right)}-\left(\frac{1}{\eta_j}+a\frac{B}{A}\frac{1}{\eta_j}D^{a-1}\right)\geq 0 \qquad \forall j\in S_D^w \\
\left[
\begin{array}{cccc}
a\left(a-1\right)\frac{B}{AC}\left(\frac{1}{\eta_1}\right)^{a}\cdot\left(w_1\right)^{a-2} & \frac{\lambda}{\left(w_1+1\right)\left(w_2+1\right)} & \cdots & \frac{\lambda}{\left(w_1+1\right)\left(w_n+1\right)} \\
\frac{\lambda}{\left(w_2+1\right)\left(w_1+1\right)} & a\left(a-1\right)\frac{B}{AC}\left(\frac{1}{\eta_1}\right)^{a}\cdot\left(w_1\right)^{a-2} & \cdots & \frac{\lambda}{\left(w_2+1\right)\left(w_n+1\right)} \\
\vdots & \vdots & \ddots & \vdots \\
\frac{\lambda}{\left(w_n+1\right)\left(w_1+1\right)} & \frac{\lambda}{\left(w_n+1\right)\left(w_2+1\right)} & \cdots & a\left(a-1\right)\frac{B}{AC}\left(\frac{1}{\eta_1}\right)^{a}\cdot\left(w_1\right)^{a-2}
\end{array}
\right] \\
\text{is psd } \forall z\in\mathbb{R}^n:\begin{bmatrix}\sum_{i=1}^{n}\frac{z_i}{\left(w_i+1\right)} \\ z_1 \\ \vdots \\ z_{N_D^w} \\ z_{N_D^w+N_I^w+1} \\ \vdots \\ z_n\end{bmatrix}=0 \\
\prod_{o\in S_\varepsilon^w}\left(\eta_o\varepsilon+1\right)\prod_{l\in S_I^w}\left(w_l+1\right)\prod_{m\in S_D^w}\left(\eta_m D+1\right)-C=0,\ 0<\eta_k\varepsilon<w_k<\eta_k D \qquad \forall k\in S_I^w \\
w_i=\eta_i\varepsilon \ \ \forall i\in S_\varepsilon^w,\ \ w_j=\eta_j D \ \ \forall j\in S_D^w
\end{array}
\right\}\Leftrightarrow
$$

$$
\left\{
\begin{array}{l}
\left(\dfrac{1}{\eta_k}+a\dfrac{B}{A}\left(\dfrac{1}{\eta_k}\right)^{a}\left(w_k\right)^{a-1}\right)\left(w_k+1\right)+\lambda C=0 \qquad \forall k\in S_I^w \\
\mu_i=\dfrac{1}{\eta_i}+a\dfrac{B}{A}\dfrac{1}{\eta_i}\varepsilon^{a-1}+\dfrac{\lambda C}{\left(\eta_i\varepsilon+1\right)}\geq 0 \qquad \forall i\in S_\varepsilon^w \\
\nu_j=\dfrac{-\lambda C}{\left(\eta_j D+1\right)}-\left(\dfrac{1}{\eta_j}+a\dfrac{B}{A}\dfrac{1}{\eta_j}D^{a-1}\right)\geq 0 \qquad \forall j\in S_D^w \\
\begin{bmatrix} z_1 \\ z_2 \\ \vdots \\ z_n \end{bmatrix}^{\mathrm{T}}\begin{bmatrix} \dfrac{1}{\left(w_1+1\right)} & 0 & \cdots & 0 \\ 0 & \dfrac{1}{\left(w_2+1\right)} & \cdots & 0 \\ \vdots & \vdots & \ddots & \vdots \\ 0 & 0 & \cdots & \dfrac{1}{\left(w_n+1\right)} \end{bmatrix}\cdot \\
\left\{\begin{bmatrix} \dfrac{a\left(a-1\right)B}{AC}\left(\dfrac{1}{\eta_1}\right)^{a}\dfrac{\left(w_1+1\right)^2}{\left(w_1\right)^{2-a}} & \lambda & \cdots & \lambda \\ \lambda & \dfrac{a\left(a-1\right)B}{AC}\left(\dfrac{1}{\eta_2}\right)^{a}\dfrac{\left(w_2+1\right)^2}{\left(w_2\right)^{2-a}} & \cdots & \lambda \\ \vdots & \vdots & \ddots & \vdots \\ \lambda & \lambda & \cdots & \dfrac{a\left(a-1\right)B}{AC}\left(\dfrac{1}{\eta_n}\right)^{a}\dfrac{\left(w_n+1\right)^2}{\left(w_n\right)^{2-a}} \end{bmatrix}\right\}\cdot \Leftrightarrow \\
\cdot\begin{bmatrix} \dfrac{1}{\left(w_1+1\right)} & 0 & \cdots & 0 \\ 0 & \dfrac{1}{\left(w_2+1\right)} & \cdots & 0 \\ \vdots & \vdots & \ddots & \vdots \\ 0 & 0 & \cdots & \dfrac{1}{\left(w_n+1\right)} \end{bmatrix}\begin{bmatrix} z_1 \\ z_2 \\ \vdots \\ z_n \end{bmatrix}\geq 0 \;\; \forall z=\begin{bmatrix} z_1 \\ z_2 \\ \vdots \\ z_n \end{bmatrix}\in\mathbb{R}^n : \begin{bmatrix} \displaystyle\sum_{i=1}^{n}\dfrac{z_i}{\left(w_i+1\right)} \\ z_1 \\ \vdots \\ z_{N_D^w} \\ z_{N_D^w+N_I^w+1} \\ \vdots \\ z_n \end{bmatrix}=0 \\
\displaystyle\prod_{o\in S_\varepsilon^w}\left(\eta_o\varepsilon+1\right)\prod_{l\in S_I^w}\left(w_l+1\right)\prod_{m\in S_D^w}\left(\eta_m D+1\right)-C=0,\;\; 0<\eta_k\varepsilon<w_k<\eta_k D \qquad \forall k\in S_I^w \\
w_i=\eta_i\varepsilon \;\; \forall i\in S_\varepsilon^w,\;\; w_j=\eta_j D \;\; \forall j\in S_D^w
\end{array}
\right\}
$$

$$
\left\{
\begin{array}{l}
\left(\dfrac{1}{\eta_k}+a\dfrac{B}{A}\left(\dfrac{1}{\eta_k}\right)^{a}\left(w_k\right)^{a-1}\right)\left(w_k+1\right)+\lambda C=0 \qquad \forall k\in S_I^w \\
\mu_i=\dfrac{1}{\eta_i}+a\dfrac{B}{A}\dfrac{1}{\eta_i}\varepsilon^{a-1}+\dfrac{\lambda C}{\left(\eta_i\varepsilon+1\right)}\geq 0 \qquad \forall i\in S_\varepsilon^w \\
\nu_j=\dfrac{-\lambda C}{\left(\eta_j D+1\right)}-\left(\dfrac{1}{\eta_j}+a\dfrac{B}{A}\dfrac{1}{\eta_j}D^{a-1}\right)\geq 0 \qquad \forall j\in S_D^w \\
\left[\dfrac{1}{\left(w_1+1\right)}z_1 \quad \dfrac{1}{\left(w_2+1\right)}z_2 \quad \cdots \quad \dfrac{1}{\left(w_n+1\right)}z_n\right]\cdot \\
\left[\begin{array}{cccc}
\dfrac{a\left(a-1\right)B}{AC}\left(\dfrac{1}{\eta_1}\right)^{a}\dfrac{\left(w_1+1\right)^2}{\left(w_1\right)^{2-a}} & \lambda & \cdots & \lambda \\
\lambda & \dfrac{a\left(a-1\right)B}{AC}\left(\dfrac{1}{\eta_2}\right)^{a}\dfrac{\left(w_2+1\right)^2}{\left(w_2\right)^{2-a}} & \cdots & \lambda \\
\vdots & \vdots & \ddots & \vdots \\
\lambda & \lambda & \cdots & \dfrac{a\left(a-1\right)B}{AC}\left(\dfrac{1}{\eta_n}\right)^{a}\dfrac{\left(w_n+1\right)^2}{\left(w_n\right)^{2-a}}
\end{array}\right]\cdot \\
\cdot\left[\dfrac{1}{\left(w_1+1\right)}z_1 \quad \dfrac{1}{\left(w_2+1\right)}z_2 \quad \cdots \quad \dfrac{1}{\left(w_n+1\right)}z_n\right]^{\mathrm{T}}\geq 0 \;\; \forall z=\begin{bmatrix}z_1\\z_2\\\vdots\\z_n\end{bmatrix}\in\mathbb{R}^n : \begin{bmatrix}\sum_{i=1}^{n}\dfrac{z_i}{\left(w_i+1\right)}\\z_1\\\vdots\\z_{N_D^w}\\z_{N_D^w+N_I^w+1}\\\vdots\\z_n\end{bmatrix}=0 \\
\prod_{o\in S_\varepsilon^w}\left(\eta_o\varepsilon+1\right)\prod_{l\in S_I^w}\left(w_l+1\right)\prod_{m\in S_D^w}\left(\eta_m D+1\right)-C=0,\;\; 0<\eta_k\varepsilon<w_k<\eta_k D \qquad \forall k\in S_I^w \\
w_i=\eta_i\varepsilon \;\; \forall i\in S_\varepsilon^w,\;\; w_j=\eta_j D \;\; \forall j\in S_D^w
\end{array}
\right\}\cdot
\begin{array}{l}
x_i\triangleq\frac{1}{\left(w_i+1\right)}z_i \;\; \forall i=1,n \\
\Leftrightarrow \\
w_k+1\geq 1 \;\forall k=1,n
\end{array}
$$

$$
\left\{
\begin{array}{l}
\left(\dfrac{1}{\eta_k}+a\dfrac{B}{A}\left(\dfrac{1}{\eta_k}\right)^{a}\left(w_k\right)^{a-1}\right)\left(w_k+1\right)+\lambda C=0 \qquad \forall k\in S_I^w \\
\mu_i=\dfrac{1}{\eta_i}+a\dfrac{B}{A}\dfrac{1}{\eta_i}\varepsilon^{a-1}+\dfrac{\lambda C}{\left(\eta_i\varepsilon+1\right)}\geq 0 \qquad \forall i\in S_\varepsilon^w \\
\nu_j=\dfrac{-\lambda C}{\left(\eta_j D+1\right)}-\left(\dfrac{1}{\eta_j}+a\dfrac{B}{A}\dfrac{1}{\eta_j}D^{a-1}\right)\geq 0 \qquad \forall j\in S_D^w \\
\begin{bmatrix}x_1 & x_2 & \cdots & x_n\end{bmatrix}\cdot
\begin{bmatrix}
\dfrac{a\left(a-1\right)B}{AC}\left(\dfrac{1}{\eta_1}\right)^{a}\dfrac{\left(w_1+1\right)^2}{\left(w_1\right)^{2-a}} & \lambda & \cdots & \lambda \\
\lambda & \dfrac{a\left(a-1\right)B}{AC}\left(\dfrac{1}{\eta_2}\right)^{a}\dfrac{\left(w_2+1\right)^2}{\left(w_2\right)^{2-a}} & \cdots & \lambda \\
\vdots & \vdots & \ddots & \vdots \\
\lambda & \lambda & \cdots & \dfrac{a\left(a-1\right)B}{AC}\left(\dfrac{1}{\eta_n}\right)^{a}\dfrac{\left(w_n+1\right)^2}{\left(w_n\right)^{2-a}}
\end{bmatrix}\cdot \\
\cdot\begin{bmatrix}x_1 & x_2 & \cdots & x_n\end{bmatrix}^{\mathrm{T}}\geq 0\ \forall x=\begin{bmatrix}x_1\\x_2\\\vdots\\x_n\end{bmatrix}\in\mathbb{R}^n:\begin{bmatrix}\sum_{i=1}^{n}x_i\\x_1\\\vdots\\x_{N_D^w}\\x_{N_D^w+N_I^w+1}\\\vdots\\x_n\end{bmatrix}=0 \\
\prod_{o\in S_\varepsilon^w}\left(\eta_o\varepsilon+1\right)\prod_{l\in S_I^w}\left(w_l+1\right)\prod_{m\in S_D^w}\left(\eta_m D+1\right)-C=0,\ \ 0<\eta_k\varepsilon<w_k<\eta_k D \qquad \forall k\in S_I^w \\
w_i=\eta_i\varepsilon\ \ \forall i\in S_\varepsilon^w,\ \ w_j=\eta_j D\ \ \forall j\in S_D^w
\end{array}
\right\}\Leftrightarrow
$$

$$
\left\{
\begin{array}{l}
\left(\dfrac{1}{\eta_k}+a\dfrac{B}{A}\left(\dfrac{1}{\eta_k}\right)^{a}\left(w_k\right)^{a-1}\right)\left(w_k+1\right)+\lambda C=0 \qquad \forall k\in S_I^w \\
\mu_i=\dfrac{1}{\eta_i}+a\dfrac{B}{A}\dfrac{1}{\eta_i}\varepsilon^{a-1}+\dfrac{\lambda C}{\left(\eta_i\varepsilon+1\right)}\geq 0 \qquad \forall i\in S_\varepsilon^w \\
\nu_j=\dfrac{-\lambda C}{\left(\eta_j D+1\right)}-\left(\dfrac{1}{\eta_j}+a\dfrac{B}{A}\dfrac{1}{\eta_j}D^{a-1}\right)\geq 0 \qquad \forall j\in S_D^w \\
\begin{bmatrix} x_1 & x_2 & \cdots & x_n \end{bmatrix}\cdot\begin{bmatrix}
\dfrac{a\left(a-1\right)B}{AC}\left(\dfrac{1}{\eta_1}\right)^{a}\dfrac{\left(w_1+1\right)^2}{\left(w_1\right)^{2-a}}x_1+\lambda x_2+\cdots\lambda x_n \\
\lambda x_1+\dfrac{a\left(a-1\right)B}{AC}\left(\dfrac{1}{\eta_2}\right)^{a}\dfrac{\left(w_2+1\right)^2}{\left(w_2\right)^{2-a}}x_2+\cdots\lambda x_n \\
\vdots \\
\lambda x_1+\lambda x_2+\cdots+\dfrac{a\left(a-1\right)B}{AC}\left(\dfrac{1}{\eta_n}\right)^{a}\dfrac{\left(w_n+1\right)^2}{\left(w_n\right)^{2-a}}x_n
\end{bmatrix}\geq 0 \\
\forall x=\begin{bmatrix} x_1 \\ x_2 \\ \vdots \\ x_n \end{bmatrix}\in\mathbb{R}^n:\begin{bmatrix}
\sum_{i=1}^{n}x_i \\ x_1 \\ \vdots \\ x_{N_D^w} \\ x_{N_D^w+N_I^w+1} \\ \vdots \\ x_n
\end{bmatrix}=0 \\
\prod_{o\in S_\varepsilon^w}\left(\eta_o\varepsilon+1\right)\prod_{l\in S_I^w}\left(w_l+1\right)\prod_{m\in S_D^w}\left(\eta_m D+1\right)-C=0,\ \ 0<\eta_k\varepsilon<w_k<\eta_k D \qquad \forall k\in S_I^w \\
w_i=\eta_i\varepsilon\ \ \forall i\in S_\varepsilon^w,\ \ w_j=\eta_j D\ \ \forall j\in S_D^w
\end{array}
\right\}
\overset{w_k+1\geq 1\ \forall k=1,n}{\Leftrightarrow}
$$

$$
\left\{
\begin{array}{l}
\left(\frac{1}{\eta_k}+a\frac{B}{A}\left(\frac{1}{\eta_k}\right)^{a}\left(w_k\right)^{a-1}\right)\left(w_k+1\right)+\lambda C=0 \qquad \forall k\in S_I^w \\
\mu_i=\frac{1}{\eta_i}+a\frac{B}{A}\frac{1}{\eta_i}\varepsilon^{a-1}+\frac{\lambda C}{\left(\eta_i\varepsilon+1\right)}\geq 0 \qquad \forall i\in S_\varepsilon^w \\
\nu_j=\frac{-\lambda C}{\left(\eta_j D+1\right)}-\left(\frac{1}{\eta_j}+a\frac{B}{A}\frac{1}{\eta_j}D^{a-1}\right)\geq 0 \qquad \forall j\in S_D^w \\
\sum_{i=1}^{n}\left[\left(\frac{a\left(a-1\right)B}{AC}\left(\frac{1}{\eta_i}\right)^{a}\frac{\left(w_i+1\right)^2}{\left(w_i\right)^{2-a}}-\lambda\right)x_i^{\,2}\right]\geq 0 \;\; \forall x=\begin{bmatrix}x_1\\x_2\\\vdots\\x_n\end{bmatrix}\in\mathbb{R}^n : \begin{bmatrix}\sum_{i=1}^{n}x_i\\x_1\\\vdots\\x_{N_D^w}\\x_{N_D^w+N_I^w+1}\\\vdots\\x_n\end{bmatrix}=0 \\
\prod_{o\in S_\varepsilon^w}\left(\eta_o\varepsilon+1\right)\prod_{l\in S_I^w}\left(w_l+1\right)\prod_{m\in S_D^w}\left(\eta_m D+1\right)-C=0,\;\; 0<\eta_k\varepsilon<w_k<\eta_k D \qquad \forall k\in S_I^w \\
w_i=\eta_i\varepsilon \;\; \forall i\in S_\varepsilon^w,\;\; w_j=\eta_j D \;\; \forall j\in S_D^w
\end{array}
\right\}\Leftrightarrow
$$

$$\left\{\begin{array}{l}
\left(\dfrac{1}{\eta_k}+a\dfrac{B}{A}\left(\dfrac{1}{\eta_k}\right)^a\left(w_k\right)^{a-1}\right)\left(w_k+1\right)+\lambda C=0 \qquad \forall k\in S_I^w \\
\mu_i=\dfrac{1}{\eta_i}+a\dfrac{B}{A}\dfrac{1}{\eta_i}\varepsilon^{a-1}+\dfrac{\lambda C}{\left(\eta_i\varepsilon+1\right)}\geq 0 \qquad \forall i\in S_\varepsilon^w \\
\nu_j=\dfrac{-\lambda C}{\left(\eta_j D+1\right)}-\left(\dfrac{1}{\eta_j}+a\dfrac{B}{A}\dfrac{1}{\eta_j}D^{a-1}\right)\geq 0 \qquad \forall j\in S_D^w \\
\sum\limits_{i=N_D^w+1}^{N_D^w+N_I^w}\left[\left(\dfrac{a\left(a-1\right)B}{AC}\left(\dfrac{1}{\eta_i}\right)^a\dfrac{\left(w_i+1\right)^2}{\left(w_i\right)^{2-a}}-\lambda\right)x_i^{\,2}\right]\geq 0 \;\; \forall\begin{bmatrix} x_{N_D^w+1} \\ \vdots \\ x_{N_D^w+N_I^w}\end{bmatrix}\in\mathbb{R}^{N_I^w} : \sum\limits_{i=N_D^w+1}^{N_D^w+N_I^w}x_i=0 \\
\prod\limits_{o\in S_\varepsilon^w}\left(\eta_o\varepsilon+1\right)\prod\limits_{l\in S_I^w}\left(w_l+1\right)\prod\limits_{m\in S_D^w}\left(\eta_m D+1\right)-C=0,\;\; 0<\eta_k\varepsilon<w_k<\eta_k D \qquad \forall k\in S_I^w \\
w_i=\eta_i\varepsilon \;\; \forall i\in S_\varepsilon^w,\;\; w_j=\eta_j D \;\; \forall j\in S_D^w
\end{array}\right\}\Leftrightarrow$$

$$\left\{\begin{array}{l}
\left(\dfrac{1}{\eta_k}+a\dfrac{B}{A}\left(\dfrac{1}{\eta_k}\right)^a\left(w_k\right)^{a-1}\right)\left(w_k+1\right)+\lambda C=0 \qquad \forall k\in S_I^w \\
\mu_i=\dfrac{1}{\eta_i}+a\dfrac{B}{A}\dfrac{1}{\eta_i}\varepsilon^{a-1}+\dfrac{\lambda C}{\left(\eta_i\varepsilon+1\right)}\geq 0 \qquad \forall i\in S_\varepsilon^w \\
\nu_j=\dfrac{-\lambda C}{\left(\eta_j D+1\right)}-\left(\dfrac{1}{\eta_j}+a\dfrac{B}{A}\dfrac{1}{\eta_j}D^{a-1}\right)\geq 0 \qquad \forall j\in S_D^w \\
\left[\begin{array}{l}
\displaystyle\sum_{i=N_D^w+1}^{N_D^w+N_I^w-1}\left[\left(\dfrac{a\left(a-1\right)B}{AC}\left(\dfrac{1}{\eta_i}\right)^a\dfrac{\left(w_i+1\right)^2}{\left(w_i\right)^{2-a}}-\lambda\right)x_i^{\,2}\right]+ \\
+\left(\dfrac{a\left(a-1\right)B}{AC}\left(\dfrac{1}{\eta_{N_D^w+N_I^w}}\right)^a\dfrac{\left(w_{N_D^w+N_I^w}+1\right)^2}{\left(w_{N_D^w+N_I^w}\right)^{2-a}}-\lambda\right)\left(\displaystyle\sum_{i=N_D^w+1}^{N_D^w+N_I^w-1}x_i\right)^2
\end{array}\right]\geq 0 \;\; \forall\begin{bmatrix} x_{N_D^w+1} \\ \vdots \\ x_{N_D^w+N_I^w-1}\end{bmatrix}\in\mathbb{R}^{N_I^w-1} \\
\prod\limits_{o\in S_\varepsilon^w}\left(\eta_o\varepsilon+1\right)\prod\limits_{l\in S_I^w}\left(w_l+1\right)\prod\limits_{m\in S_D^w}\left(\eta_m D+1\right)-C=0,\;\; 0<\eta_k\varepsilon<w_k<\eta_k D \qquad \forall k\in S_I^w \\
w_i=\eta_i\varepsilon \;\; \forall i\in S_\varepsilon^w,\;\; w_j=\eta_j D \;\; \forall j\in S_D^w
\end{array}\right\}\Leftrightarrow$$

Define $E_i \triangleq \frac{a(a-1)B}{AC}\left(\frac{1}{\eta_i}\right)^a \frac{(w_i+1)^2}{(w_i)^{2-a}} - \lambda \quad \forall i \in \left\{N_D^w+1,\cdots,N_D^w+N_I^w\right\}$ Then the above necessary optimality conditions are equivalent to:

$$\left\{\begin{array}{l}
\left(\frac{1}{\eta_k}+a\frac{B}{A}\left(\frac{1}{\eta_k}\right)^a(w_k)^{a-1}\right)(w_k+1)+\lambda C=0 \qquad \forall k\in S_I^w \\
\mu_i=\frac{1}{\eta_i}+a\frac{B}{A}\frac{1}{\eta_i}\varepsilon^{a-1}+\frac{\lambda C}{(\eta_i\varepsilon+1)}\geq 0 \qquad \forall i\in S_\varepsilon^w \\
\nu_j=\frac{-\lambda C}{(\eta_j D+1)}-\left(\frac{1}{\eta_j}+a\frac{B}{A}\frac{1}{\eta_j}D^{a-1}\right)\geq 0 \qquad \forall j\in S_D^w \\
\sum_{i=N_D^w+1}^{N_D^w+N_I^w-1}\left[E_i x_i^{\,2}\right]+E_{N_D^w+N_I^w}\left(\sum_{i=N_D^w+1}^{N_D^w+N_I^w-1}x_i\right)^2\geq 0 \quad \forall\begin{bmatrix} x_{N_D^w+1}\\ \vdots \\ x_{N_D^w+N_I^w-1}\end{bmatrix}\in\mathbb{R}^{N_I^w-1} \\
\prod_{o\in S_\varepsilon^w}(\eta_o\varepsilon+1)\prod_{l\in S_I^w}(w_l+1)\prod_{m\in S_D^w}(\eta_m D+1)-C=0,\ 0<\eta_k\varepsilon<w_k<\eta_k D \qquad \forall k\in S_I^w \\
w_i=\eta_i\varepsilon \ \ \forall i\in S_\varepsilon^w,\ \ w_j=\eta_j D \ \ \forall j\in S_D^w
\end{array}\right\}\Leftrightarrow$$

$$\left\{\begin{array}{l}
\left(\frac{1}{\eta_k}+a\frac{B}{A}\left(\frac{1}{\eta_k}\right)^a(w_k)^{a-1}\right)(w_k+1)+\lambda C=0 \qquad \forall k\in S_I^w \\
\mu_i=\frac{1}{\eta_i}+a\frac{B}{A}\frac{1}{\eta_i}\varepsilon^{a-1}+\frac{\lambda C}{(\eta_i\varepsilon+1)}\geq 0 \qquad \forall i\in S_\varepsilon^w \\
\nu_j=\frac{-\lambda C}{(\eta_j D+1)}-\left(\frac{1}{\eta_j}+a\frac{B}{A}\frac{1}{\eta_j}D^{a-1}\right)\geq 0 \qquad \forall j\in S_D^w \\
\begin{bmatrix} E_{N_D^w+1}+E_{N_D^w+N_I^w} & E_{N_D^w+N_I^w} & \cdots & E_{N_D^w+N_I^w} \\ E_{N_D^w+N_I^w} & E_{N_D^w+2}+E_{N_D^w+N_I^w} & \cdots & E_{N_D^w+N_I^w} \\ \vdots & \vdots & \ddots & \vdots \\ E_{N_D^w+N_I^w} & E_{N_D^w+N_I^w} & \cdots & E_{N_D^w+N_I^w-1}+E_{N_D^w+N_I^w}\end{bmatrix} \ \textit{is psd on}\ \mathbb{R}^{N_I^w-1} \\
\prod_{o\in S_\varepsilon^w}(\eta_o\varepsilon+1)\prod_{l\in S_I^w}(w_l+1)\prod_{m\in S_D^w}(\eta_m D+1)-C=0,\ 0<\eta_k\varepsilon<w_k<\eta_k D \qquad \forall k\in S_I^w \\
w_i=\eta_i\varepsilon \ \ \forall i\in S_\varepsilon^w,\ \ w_j=\eta_j D \ \ \forall j\in S_D^w
\end{array}\right\}$$

O.E.Δ.

Chapter 4: Natural gas derived hydrogen in the presence of carbon fuel taxes and concentrated solar power

This work focuses on the incorporation of renewable energy resources into the natural gas-based production of hydrogen, via steam methane reforming (SMR). The novel concept of "energetically enhanced steam methane reforming" (EESMR) is introduced, which changes the endothermicity level of the SMR process through incorporation of carbon monoxide and steam into the SMR feed. Novel EESMR flowsheets are presented in which the aforementioned resources are internally generated and recycled, so as to create a natural gas-based hydrogen production system with methane as raw material and a hybrid (methane/solar) energy supply. The current worldwide carbon tax legislative environment is briefly reviewed, and its potential impact on SMR-versus-EESMR economic viability is quantified. A novel method for solution of linear parametric programming problems is proposed based on the concept of dimensionality reduction – this allows the analytic quantification of the optimum objective function value and associated optimum variable vector. Regions in carbon/renewable utility cost coefficient ratio space are identified, in which one technology is superior over the other. EESMR is shown to be preferable in the presence of significant levels of taxation on the use of natural gas as fuel.

Section 4.1: Introduction

Worldwide production of hydrogen is 50 million tons per year[1]. As can be seen in Figure 4.1, 96% of this production comes from fossil fuels, while only 1% comes from renewable resources.[2] Hydrogen has numerous uses (see Figure 4.2), as an industrial feedstock[1] (e.g., for methanol, ammonia, and subsequently fertilizer production), as an upgrading agent[2] (e.g., for converting heavier feed-stocks to lighter fuels in the refining industry), as gaseous fuel[3] (e.g. in

fuel cells for both electricity generation & hydrogen fueled vehicles), and as liquid fuel[4] (e.g. in space craft for propulsion).

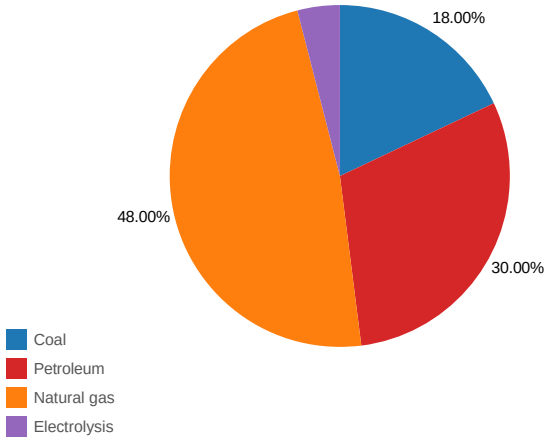

Figure 4.1: Worldwide Resources used for Hydrogen Production[1]

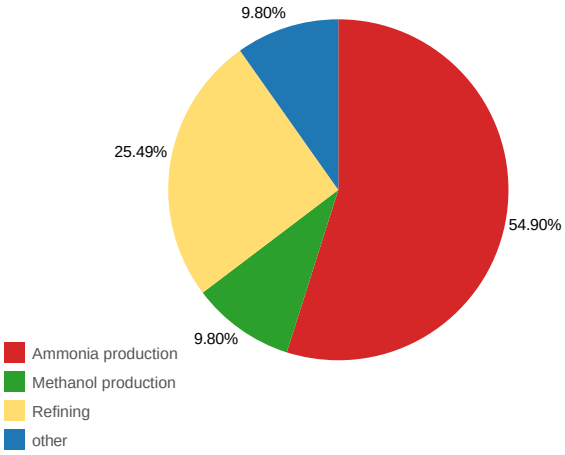

Figure 4.2: Worldwide Hydrogen Utilization[1]

Increasing the percentage of renewable energy used in hydrogen production is a major challenge, whose successful resolution can yield significant benefits, such as increased sustainability of the energy supply, and reduced carbon dioxide (CO_2) emissions to the atmosphere[5]. To better understand how this goal may be pursued, it is instructive to briefly

review hydrogen production methods.

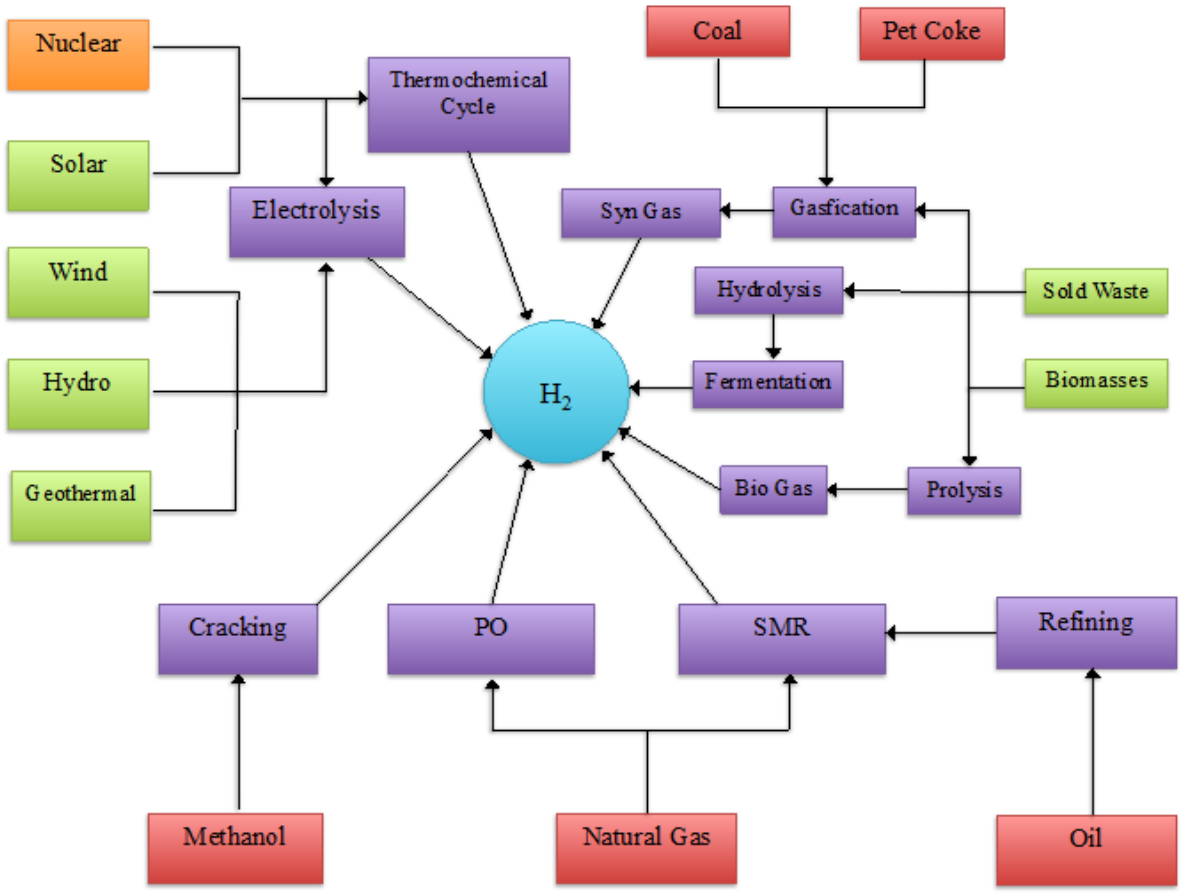

Figure 4.3: Hydrogen production methods and energy sources

The steam-coal-iron hydrogen production process, developed in the early 20th century, is one of the oldest commercial hydrogen production methods[6,7]. Over the past forty years, the evolution of hydrogen production technologies has culminated into processes with increased efficiency, enhanced profitability, and reduced environmental impact. Figure 4.3 illustrates the currently prevalent hydrogen production pathways, using a variety of technologies and energy resources. Electrolysis splits water to oxygen and hydrogen using electricity generated from nuclear or renewable energy sources (e.g., solar, wind, hydro and geothermal)[8]. Its main advantage is the high purity of the obtained hydrogen (which enables its utilization in fuel cells),

while its disadvantages include low efficiency, and consumption of a high-quality energy form (electricity). Biomass can be used to generate hydrogen either through a hydrolysis/fermentation combination, or through pyrolysis and/or gasification, whereby syngas and bio gas are first generated as raw material for subsequent hydrogen production[8]. Water-splitting thermo-chemical cycle based hydrogen production, utilizing either nuclear or concentrated solar energy, is a zero CO_2 emission process undergoing significant technological development, but yet to be commercialized[9]. Coal based hydrogen production is one of the most economically efficient methods of hydrogen production, but is burdened with high CO_2 emission rates.[9] Partial oxidation (POX) is a catalytic process in which oxygen is mixed with methane or low quality feeds (e.g. low value natural gas, coal, coke)[1,10], to generate hydrogen with no external heat input, but is faced with the major safety concern of the wide explosive range of the oxygen/hydrogen mixture.

Natural gas has become the main source of hydrogen, due to cost effectiveness, high hydrogen to carbon ratio, and wide availability.[10] Steam Methane Reforming (SMR) is the most commonly used process to produce hydrogen from natural gas[1,11].

The first steam reforming plant was built in the 1930s, by BASF and Standard Oil, as part of the Baton Rouge Refinery. During the early days of the 20th century BASF played a major role in the development and industrialization of the steam methane reforming (SMR) process. The process has been undergoing continuous technological development, which has led to more efficient catalysts, and improved reactor and separator designs. The process is highly endothermic and its external energy needs are typically supplied by burning a portion of the natural gas in a furnace[12]. BASF was the first to carry out the SMR in multiple reactor tubes within a heated furnace, where natural gas was burned to provide the aforementioned

endothermic load. The process operates near equilibrium (at 950-1,250 K and 5-30 bar[13]) and utilizes a nickel-alumina catalyst[13].

The aforementioned use of natural gas as both raw material and fuel in SMR based hydrogen production, suggests that a straightforward strategy to increase the percentage of renewable energy used in hydrogen production is to reduce or eliminate the use of natural gas as fuel in reforming. Past experience (see SO_x, NO_x emission reductions) indicates that technological developments are often coupled to the enactment of legislation. Worldwide carbon tax legislation is currently either being contemplated or enacted. Several categories of carbon related taxation are considered, with some focusing on carbon dioxide emissions (carbon emission taxes), and others focusing on taxing the "burning" of fossil fuels, while leaving untaxed their use as raw materials. Thus, in a world where fossil fuel “burning” is taxed, the SMR process will be partially taxed for its portion of natural gas used as fuel. The position put forward in this work, is that a means of reducing (or even avoiding) such taxation is to reduce the high temperature reformer’s endothermic load (or even to alter it to being exothermic). In this way the reformer fuel requirements will be reduced or eliminated. Of course, the transformation of methane to hydrogen still necessitates energy input. However, such energy input need not be provided at the high temperature conditions of the reformer, but rather at a lower temperature, where alternative, renewable energy sources may be brought to bear. Indeed, such a reconfiguration of the energy input would open the way for hybrid fossil-fuel/renewable designs of the SMR process, where the natural gas is used predominantly as raw material, while the renewable energy resource is used to meet the process energy needs. Such a potential renewable energy resource is concentrated solar power (CSP), whereby reflectors are used to concentrate the sun’s radiation and transform it to high temperature heat.[15] CSP is typically implemented in

solar trough, solar tower and solar dish configurations.[15] A variety of working fluids can be used, including molten salts and synthetic oils, and low operating cost energy can be delivered at a variety of temperature levels. According to the National Renewable Energy Laboratory, solar towers can currently deliver temperatures of 835K, and are expected to reach 920K by 2020. This is also confirmed by Poullikkas et al.[15], who states that CSP tower plants using molten salts can deliver temperatures around 820K. Similarly, solar troughs can currently deliver 720K, and are expected to reach 773K by 2020. It thus becomes apparent that hot utilities at 770K, and 420K, can be delivered by concentrated solar power (CSP) tower and trough plants.

The remainder of this section is structured as follows. First, the status of carbon tax legislation around the world is surveyed. The section's main idea is next presented, in a section where the basics of steam methane reforming (SMR) are first reviewed, and then transitioning a reformer from being endothermic to being exothermic is presented. Subsequently, the proposed energetically enhanced steam methane reforming process is presented, including alternative process designs with varying levels of endothermicity. Heat integration for each of these designs is then carried out, so that their real energy consumption needs are properly quantified. Energy cost rates for which the proposed process is superior to traditional reforming are then identified. Finally, the presented process is discussed and conclusions are drawn.

Section 4.2: Overview of carbon tax legislation

Legislation aiming to reduce Green House Gas (GHG) emissions is currently being contemplated and/or enacted around the world, including the Kyoto (1990s), Paris (2015) and Marrakesh (2016) international agreements on climate change. Two dominant forms of such legislations have emerged: carbon taxes and carbon cap-and-trade systems. Carbon tax is an explicit surcharge on carbon emissions, similar to the interest rate surcharge imposed on capital

lending by central banks. On the other hand, cap-and-trade systems establish overall carbon emission limits, against which emission permits are issued. The carbon price is determined by a market system, in which these emission permits are traded. The cap and trade system provides flexibility to emitters to adjust their operations to the regulatory landscape. However, such flexibility results in longer emission reduction periods compared to the carbon tax system. Close examination of the aforementioned carbon legislation initiatives reveals a differentiation between *combustion processes*, where fossil fuels are burned, and *non-combustion processes*, where fossil fuels are used as raw material. Combustion processes account for 68% of the global GHG emissions, while non-combustion processes (e.g. industrial processes) account for 7% of the global GHG emissions[16]. The most comprehensive carbon legislation worldwide is the EU emissions trading system (EU ETS), a cap-and-trade system established in 2005 as the world's largest carbon pricing program, with 2,000 million metric tons (MMT) of GHG emissions and an average price of $7 per ton of CO_2. EU ETS covers only 45% of the entire EU greenhouse gas (GHG) emissions[17], since it only covers carbon dioxide, nitrous oxide, and perfluorocarbon emissions; and it exempts emissions covered by regional carbon taxes, transportation generated emissions, and emissions below a threshold generation level. The structure of the system allows for an overall GHG emissions target to be met even if some individual countries fail to maintain their targets. Under the EU ETS legislative directive, a *broad interpretation* of combustion installations is defined as "All combustion installations that produce electricity, heat or steam, even if their main purpose is not energy production, but e.g. the production of ethylene or ammonia (e.g. naphtha crackers or ammonia plants)".[17] This broad interpretation is used in the following countries: Austria, Belgium, Denmark, Finland, Ireland, Latvia, Portugal and Sweden [18]. An alternative *medium interpretation* states: "All combustion installations that produce

electricity, heat or steam, with the purpose of energy production, including those that are process-integrated, e.g. a steam plant integrated in e.g. chemical industry is included, but process furnaces such as crackers in the petrochemical industry are excluded."[17]. This interpretation is used in Estonia, Germany, Lithuania, Luxembourg and the UK[18]. Finally, a *narrow interpretation* states: "Only combustion installations that produce electricity, heat or steam and supply that to third parties."[17] and is used in France, Italy and Spain[18]. The above three EU ETS interpretations make clear that within this EU legislation not all CO_2 emissions are equal. Indeed, CO_2 emissions not directly resulting from electricity, heat or steam generation may be excluded from regulation. Since the focus of this work is the use of natural gas in the production of hydrogen via steam reforming, it is instructive to examine the impact of carbon taxes on natural gas use. To this end, the UK exempts from carbon tax natural gas fed to reformers for the production of hydrogen[19]. Such exemption aligns with the aforementioned *medium interpretation* of the EU ETS system. Germany also does not tax fuels, such as natural gas, used in electricity & heat generation, while the Czech Republic and Italy tax such fuels, and Ireland only taxes the use of natural gas for Combined Heat and Power (CHP) Generation. However, Ireland does not tax natural gas, when it is used as a feed to the chemical and petrochemical industries. Since 2012, Japan also introduced a carbon tax of $2.89 per ton of CO_2 on fossil fuels, such as natural gas, burned within a chemical process.

It becomes apparent from the above, that as carbon tax legislation around the world evolves, the dual role of natural gas use in hydrogen production, as both fuel and raw material feed, may be significantly differentiated in an economic sense, namely natural gas as fuel may become expensive, while natural gas as raw material may remain cheap. In turn, this suggests that increased carbon taxing of the use of natural gas as fuel, but not as raw material, may require

that the steam methane reforming (SMR) process be redesigned, so as to account for potentially cost prohibitive increases in the use of natural gas as fuel. Such a redesigned SMR process, that reduces methane use as fuel, while maintaining its use as raw material will be here on out referred to as "Energetically Enhanced Steam Methane Reforming" (EESMR). The conceptual transition from the traditional SMR process, to the EESMR process is described below.

Section 4.3: Transitioning from traditional to energetically enhanced reforming

The refining industry consumes ever increasing amounts of hydrogen, mainly in its crude oil cracking-treating operations. In fact, the reduced hydrogen content of U.S crude oil reserves is creating situations where refinery hydrogen demand exceeds hydrogen supply. Currently, the preferred method for large scale hydrogen production is steam methane reforming (SMR) of natural gas. Traditional reformers are operated industrially near equilibrium conditions (at 950-1,250 K and 5-30 bar[13]) with a high endothermic heat load that is provided through the burning of natural gas and other fossil fuel resources. The SMR process involves the following three reactions[14]:

$CH_4 + H_2O \rightleftarrows CO + 3H_2$ (HHV 206 kJ/mol) (R_1)

$CO + H_2O \rightleftarrows CO_2 + H_2$ (HHV -41.15kJ/mol) (R_2)

$CH_4 + 2H_2O \rightleftarrows CO_2 + 4H_2$ (HHV 164.95 kJ/mol) (R_3)

According to Le Chatelier's Principle, the forward reactions (R_1) and (R_3) are favored at low pressures, (e.g. 1 bar), but kinetic considerations necessitate the use of high pressures (e.g. 5-25 bar), and steam to methane molar ratios (e.g. α=3:1) exceeding the stoichiometric value (α=2:1), to insure high levels of methane conversion (above 90%) at high temperatures. At

equilibrium conditions, (R_3) is linearly dependent on (R_1) & (R_2) and can thus be ignored.

Tables 4.1, 4.2, and 4.3 show the inlet and resulting outlet species molar flowrates, and associated heat load, of a traditional, isothermal, Steam Methane Reformer operating at equilibrium, at various temperatures, and at P=5 bar. These results are obtained using the UNISIM software package, utilizing the Peng Robinson thermodynamic model, and are confirmed using total Gibbs free energy minimization calculations. They indicate that for steam to methane inlet molar ratios above 3 (i.e. α>3:1), and at temperatures 1050 K and above, high (>90%) methane conversions are attained, and that highly endothermic loads are required (54-60 kJ/s).

Inlet (Kmol/hr)			Outlet (Kmol/hr)					T=950 K
CH_4	CO	H_2O	CH_4	CO	CO_2	H_2O	H_2	Heat Load (kJ/s)
1	0	2	0.357019	0.315989	0.326992	1.030027	2.255935	36.88944639
1	0	3	0.228872	0.314748	0.456381	1.772491	2.769766	43.60485157
1	0	5	9.15E-02	0.27291	0.635569	3.455952	3.361006	50.40256858
1	0	10	1.23E-02	0.167385	0.820331	8.191954	3.783477	53.52254265
1	0	15	2.94E-03	1.15E-01	8.82E-01	13.12095	3.873162	53.49859292
1	0	20	1.02E-03	8.71E-02	0.911884	18.08913	3.90883	53.32546527

Table 4.1: Equilibrium SMR Inlet/Outlet Conditions (P=5 bar, T=950K)

Inlet (Kmol/hr)			Outlet (Kmol/hr)					T=1050 K
CH_4	CO	H_2O	CH_4	CO	CO_2	H_2O	H_2	Heat Load (kJ/s)
1	0	2	0.111282	0.622987	0.265731	0.845552	2.931884	53.18640267
1	0	3	4.58E-02	0.547912	0.406315	1.639459	3.268995	55.93858188
1	0	5	1.14E-02	0.406976	0.581619	3.429786	3.547404	56.40386442
1	0	10	1.23E-03	0.235687	0.763078	8.238156	3.759374	55.29476117
1	0	15	2.99E-04	0.164639	0.835062	13.16524	3.834166	54.66161207
1	0	20	1.05E-04	0.126373	0.873522	18.12658	3.873206	54.30461295

Table 4.2: Equilibrium SMR Inlet/Outlet Conditions (P=5 bar, T=1050K)

Inlet (Kmol/hr)			Outlet (Kmol/hr)					T=1150 K
CH_4	CO	H_2O	CH_4	CO	CO_2	H_2O	H_2	Heat Load (kJ/s)
1	0	2	1.92E-02	0.773227	0.207618	0.811538	3.150152	59.81567777
1	0	3	6.35E-03	0.652679	0.340972	1.665376	3.321926	59.37056547
1	0	5	1.50E-03	0.489838	0.508666	3.49283	3.504178	58.10331219

1	0	10	1.72E-04	0.299659	0.700169	8.300003	3.699654	56.39202126
1	0	15	4.34E-05	0.215657	0.7843	13.21574	3.784169	55.61219775
1	0	20	1.57E-05	0.168418	0.831567	18.16845	3.83152	55.17142133

Table 4.3: Equilibrium SMR Inlet/Outlet Conditions (P=5 bar, T=1150K)

It is thus apparent that enhancing the energy consumption profile of the SMR process requires that the aforementioned endothermic heat loads be reduced. To this end, an Energetically Enhanced Process (EEP) is defined next.

Definition: *A Process is Energetically Enhanced, compared to its traditional counterpart, if its energy consumption at high temperatures is either reduced or eliminated, even if such reduction necessitates higher energy consumption at lower temperatures.*

Given the above definition, the task pursued in this work can then be framed as seeking an Energetically Enhanced Steam Methane Reforming (EESMR) process, which aims to improve the environmental and economic profile of the SMR process (possibly in the presence of carbon taxation), by reducing the SMR high temperature, endothermic heat load.

In our earlier work[20,21], we established that a reactor's heat load may be possible to reduce through the use of a reactor network. In particular, we established theoretically, and demonstrated through case studies, that if the universe of possible reactor networks contains either only endothermic or only exothermic units, then the energy consumption associated with carrying out a particular set of reaction tasks does not depend on the network structure[20]. On the other hand, if the universe of possible reactor networks contains both endothermic and exothermic units, then the energy consumption associated with carrying out a particular set of reaction tasks depends on the network structure and can be possibly reduced through the use of an appropriate network[21].

Close examination of the reactions taking place in the SMR quickly reveals that although the overall process is endothermic, one of the reactions, (R_2), taking place within the reactor is

exothermic. Indeed, the reaction ($CO + H_2O \rightarrow CO_2 + H_2$) has an exothermic heat of reaction of (-41.5kJ/mol CO), which is about one fourth and one fifth in magnitude respectively, of the endothermic heats of reaction of (R_3), and (R_1). In turn this suggests, that identifying conditions in the considered reactor universe which increase the energetic contribution of (R_2), to the reactor overall heat load, will identify reactors with a lower endothermic load. This can be accomplished by introducing significant amounts of CO, and H_2O in the reactor feed. To assess the impact of this decision on reactor performance, Tables 4.4 and 4.5 show the inlet and resulting outlet species molar flowrates, and associated heat load, of an EESMR operating at equilibrium, at various temperatures, and at P=5 bar. These results are again obtained using the UNISIM software package, utilizing the Peng Robinson thermodynamic model. They indicate that for a given steam to methane inlet molar ratio, as the inlet amount of CO increases, methane conversion decreases, and the reactor's endothermic heat load decreases to the point where it can reverse its nature and become exothermic. The same results also indicate, that for a fixed inlet amount of CH_4, as inlet amounts of CO, and H_2O are both increased, with H_2O in excess of CO, methane conversion increases exceeding values of 90%, and even reaching values of 99%. In particular, for CH_4:CO:H_2O = 1:3:5, methane conversion is 91% (99%), and the reactor's endothermic load is 40.12 kW (48.28 kW) at T=1050 K (T=1150 K). For comparison purposes, for CH_4:H_2O = 1:5, Tables 4.2 and 4.3 suggest that methane conversion is 99% (99.8%), and the reactor's endothermic load is 56.40 kW (58.10 kW) at T=1050 K (T=1150 K). This heat load reduction effect becomes even more pronounced at higher CO, and H_2O ratios to CH_4, whereby the EESMR may even become exothermic. Indeed, for CH_4:CO:H_2O = 1:15:15, methane conversion is 98%, and the reactor's exothermic load is -2.98 kW at T=1150 K.

Furthermore, equilibrium calculations for carbon formation have been carried out, using

Gibbs Free Energy minimization, and for the aforementioned steam/carbon ratios, there is no carbon formation for the EESMR conditions listed in Tables 4.4 and 4.5.

Inlet (Kmol/hr)			Outlet (Kmol/hr)					T=1050 K
CH_4	CO	H_2O	CH_4	CO	CO_2	H_2O	H_2	Heat Load (kJ/s)
1	0.1	2	0.120664	0.689744	0.289593	0.831071	2.927602	52.36622802
1	0.3	2	0.138726	0.825492	0.335782	0.802943	2.919605	50.78471633
1	0.5	2	0.155923	0.964114	0.379963	0.77596	2.912194	49.27696218
1	1	2	0.195553	1.32241	0.482036	0.713517	2.895376	45.79983088
1	3	2	0.317363	2.890938	0.791699	0.525665	2.839609	35.15185961
1	5	2	0.399228	4.60835	0.992422	0.406807	2.794736	28.06737944
1	10	2	0.515176	9.221342	1.263482	0.251695	2.717953	18.16189217
1	15	2	0.573886	14.03173	1.394386	0.179501	2.672727	13.20782496
1	20	2	0.608667	18.92147	1.469866	0.138801	2.643865	10.29330447
1	0.1	3	5.11E-02	0.60831	0.440633	1.610424	3.287462	55.27398792
1	0.3	3	6.18E-02	0.731588	0.506594	1.555224	3.321139	53.95868665
1	0.5	3	7.28E-02	0.857973	0.56926	1.503507	3.35096	52.66348619
1	1	3	0.100509	1.18621	0.713282	1.387227	3.411756	49.52510626
1	3	3	0.206342	2.63676	1.156898	1.049443	3.537873	38.57892730
1	5	3	0.294448	4.244058	1.461494	0.832954	3.578149	30.09447189
1	10	3	0.443844	8.646473	1.909683	0.53416	3.578152	16.37063044
1	15	3	0.531107	13.32415	2.14474	0.386368	3.551418	8.61421045
1	20	3	0.608667	18.92147	1.469866	0.138801	2.643865	3.76913664
1	3	5	9.43E-02	2.182369	1.723291	2.371048	4.440274	40.12149182
1	5	5	0.165924	3.619487	2.214589	1.951335	4.716816	30.86129469
1	10	5	0.330637	7.665991	3.003372	1.327265	5.011462	12.8703939
1	15	5	0.454346	12.08053	3.465127	0.989218	5.102091	0.626447093
1	20	5	0.544231	16.6931	3.762673	0.781558	5.129979	-7.901561803
1	5	10	4.73E-02	2.551045	3.401616	5.645722	6.259601	26.80974384
1	10	10	0.155172	5.909069	4.935759	4.219412	7.470244	5.155381023
1	15	10	0.282906	9.768743	5.948352	3.334554	8.099635	-12.6878066
1	20	10	0.405559	13.92542	6.669017	2.736542	8.45234	-27.37890321
1	10	15	7.61E-02	4.742091	6.181785	7.894338	8.953415	-1.95000895
1	15	15	0.169672	8.147716	7.682611	6.487061	10.17359	-22.38496694
1	20	15	0.279877	11.91671	8.803409	5.476468	10.96378	-40.17806354
1	15	20	0.103469	6.944181	8.95235	10.15112	11.64194	-30.52636747
1	20	20	0.19016	10.37335	10.43649	8.753667	12.86601	-50.36933256

Table 4.4: Equilibrium EESMR Inlet/Outlet Conditions (P=5 bar, T=1050K)

Inlet (Kmol/hr)	Outlet (Kmol/hr)	T=1150 K

CH_4	CO	H_2O	CH_4	CO	CO_2	H_2O	H_2	Heat Load (kJ/s)
1	0.1	2	2.10E-02	0.854596	0.224424	0.796555	3.161485	59.54221
1	0.3	2	2.46E-02	1.019072	0.256371	0.768187	3.182699	59.01547
1	0.5	2	2.80E-02	1.185686	0.286278	0.741758	3.202169	58.5142
1	1	2	3.63E-02	1.610381	0.353336	0.682948	3.244485	57.36209
1	3	2	6.32E-02	3.39136	0.545445	0.51775	3.355861	53.85461
1	5	2	8.25E-02	5.251157	0.66635	0.416144	3.418869	51.4984
1	10	2	0.112054	10.05412	0.83383	0.278224	3.497668	48.05649
1	15	2	0.128473	14.95162	0.919905	0.208568	3.534486	46.2101
1	20	2	0.138835	19.88902	0.972149	0.166685	3.555645	45.06446
1	0.1	3	7.09E-03	0.72384	0.369069	1.638023	3.347794	59.05877
1	0.3	3	8.62E-03	0.868712	0.422673	1.585942	3.396828	58.45718
1	0.5	3	1.02E-02	1.016727	0.473093	1.537087	3.442552	57.88297
1	1	3	1.42E-02	1.398772	0.587009	1.42721	3.544353	56.55399
1	3	3	3.06E-02	3.048572	0.920869	1.10969	3.829192	52.37502
1	5	3	4.53E-02	4.81665	1.138084	0.907183	4.002285	49.3993
1	10	3	7.28E-02	9.476178	1.451057	0.621708	4.232761	44.71424
1	15	3	9.07E-02	14.29072	1.618558	0.472164	4.346393	42.00291
1	20	3	0.103067	19.1742	1.722734	0.380333	4.413534	40.24246
1	3	5	1.15E-02	2.505102	1.483427	2.528043	4.449015	48.28266
1	5	5	2.03E-02	4.093203	1.886476	2.133846	4.825511	43.92312
1	10	5	0.04236	8.448592	2.509048	1.533313	5.381967	36.66148
1	15	5	0.060724	13.07359	2.865686	1.195038	5.683515	32.1399
1	20	5	7.52E-02	17.82781	3.096944	0.978302	5.871208	29.04316
1	5	10	5.31E-03	2.951882	3.04281	5.962497	6.026887	33.98685
1	10	10	1.68E-02	6.611587	4.371641	4.645132	7.321324	20.73264
1	15	10	3.09E-02	10.73965	5.22948	3.801393	8.136861	11.75248
1	20	10	0.04519	15.1248	5.830013	3.215177	8.694444	5.185292
1	10	15	8.12E-03	5.419378	5.572502	8.435619	8.548141	9.974855
1	15	15	1.77E-02	9.099499	6.882844	7.134814	9.829871	-2.98361
1	20	15	2.91E-02	13.12058	7.850295	6.178828	10.76293	-12.8308
1	15	20	1.08E-02	7.888105	8.101123	10.90965	11.06881	-14.017
1	20	20	1.94E-02	11.57884	9.401732	9.6177	12.34344	-26.8281

Table 4.5: Equilibrium EESMR Inlet/Outlet Conditions (P=5 bar, T=1150K)

As shown above, increased CO and H_2O content in the SMR feed can reduce the endothermic heat load of the reformer, while maintaining high methane conversions, thus leading to EESMR. In turn this suggests that EESMR can be considered as an alternative to methane partial oxidation (POX) that overcomes POX's safety shortcomings (O_2/H_2 mixtures have a wide

explosive range), while opening the door to the creation of H_2 production flowsheets utilizing both fossil fuel and renewable energy resources as high temperature and medium temperature hot utilities, respectively.

Implementation of this altered reforming mode requires the availability of significant amounts of carbon monoxide to be fed into the EESMR. The traditional SMR process does not typically generate such large amounts of carbon monoxide. Thus, realization of an EESMR flowsheet requires the use of a carbon monoxide generating technology. This can be accomplished incorporating a Reverse Water Gas Shift Reactor (RWGSR) operating at medium temperatures so that its energetic needs are met by energy sources different than methane combustion. For example, the RWGSR's heat load can be provided by renewable energy from concentrated solar power. To further establish the feasibility of EESMR and to develop a better appreciation of the circumstances under which it can become preferable over the traditional SMR process, complete flowsheet realizations of the SMR and EESMR processes are presented below.

Baseline (Traditional SMR process):

A traditional SMR-based hydrogen production flowsheet is shown in Figure 4.4, while its detailed material stream and energy flow information is provided in Tables 4.6 and 4.7.

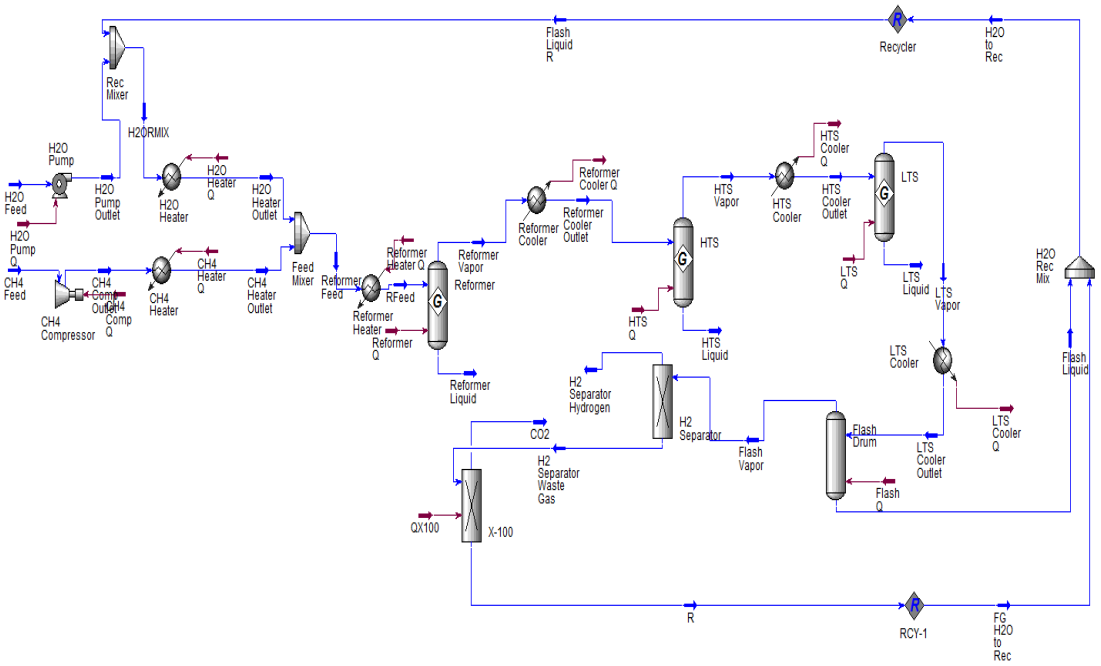

Figure 4.4: Baseline SMR design process flowsheet

Stream Name	T (K)	CH_4 (Kmol/hr)	CO (Kmol/hr)	CO_2 (Kmol/hr)	H_2O (Kmol/hr)	H_2 (Kmol/hr)
CH4 Feed	298	1	0	0	0	0
CH4 Comp Outlet	434	1	0	0	0	0
CH4 Heater Outlet	700	1	0	0	0	0
H2O Feed	298	0	0	0	2	0
H2O Pump Outlet	298	0	0	0	2	0
H2O Heater Outlet	700	0.021602	0.021574	0.000241	2.857964	0.44586869
Reformer Feed	700	1.021602	0.021574	0.000241	2.857964	0.44586869
Reformer Vapor	1145	0.021526	0.74728	0.274611	1.583518	3.72046619
Reformer Liquid	1145	0	0	0	0	0
Reformer Cooler Outlet	650	0.021526	0.74728	0.274611	1.583518	3.72046619
HTS Vapor	650	0.021526	0.20236	0.819531	1.038599	4.26538551
HTS Liquid	650	0	0	0	0	0
HTS Cooler Outlet	475	0.021526	0.20236	0.819531	1.038599	4.26538551
LTS Vapor	475	0.021526	0.021536	1.000355	0.857774	4.44621007
LTS Liquid	475	0	0	0	0	0
Flash Vapor	313	0.021526	0.021536	1.000114	0.083338	4.44620491
Flash Liquid	313	1.91E-10	3.08E-08	0.000241	0.774436	5.16E-06

H2 Separator Hydrogen	313	2.15E-07	2.15E-07	1E-05	8.33E-07	4.00158442
H2 Separator Waste Gas	313	0.021526	0.021535	1.000104	0.083337	0.44462049
Flash Liquid R	312	0.021602	0.021574	0.000241	0.857964	0.44586869
H2ORMIX	303	0.021602	0.021574	0.000241	2.857964	0.44586869
LTS Cooler Outlet	313	0.021526	0.021536	1.000355	0.857774	4.44621007
H2O to Rec	312	0.021602	0.021574	0.000241	0.857985	0.44586869
FG H2O to Rec	310	0.021602	0.021574	0	0.083549	0.44586353
RFeed	1140	1.021602	0.021574	0.000241	2.857964	0.44586869
CO2	310	0	0	1.000104	0	0
R	310	0.021526	0.021535	0	0.083337	0.44462049

Table 4.6: Baseline Design Material Stream Information

Stream	Energy Flow (kJ/s)
CH4 Comp Q	1.461
CH4 Heater Q	3.732
H2O Pump Q	5.281E-03
H2O Heater Q	47.70
Reformer Q	**60.68**
Reformer Cooler Q	29.68
HTS Cooler Q	10.04
Flash Q	0
HTS Q	-5.869
LTS Q	-2.020
LTS Cooler Q	18.38
Reformer Heater Q	24.43
QX100	-0.2663
QX	-0.7498

Table 4.7: Baseline Design Energy Flow Information

This baseline SMR design consists of the following reactor building blocks: Steam Methane Reforming (SMR), High Temperature Shift Reaction (HTSR) and Low Temperature Shift Reaction (LTSR). Each one of these reactors operates near equilibrium, and thus it is modeled as a Gibbs free energy minimization reactor in UNISIM. The overall flowsheet inlets are 1 kmol/hr CH_4, 2 kmol/hr H_2O and the overall flowsheet outlets are 4 kmol/hr H_2 and 1 kmol/hr CO_2. Following pumping to 5 bar, the H_2O stream is mixed with a H_2O recycle stream, and then heated to 1140K. The CH_4 stream is also compressed and heated to 5 bar and 1140K, and then mixed with the aforementioned H_2O stream to form the reformer feed, which features a

H_2O/ CH_4 molar ratio of 2.79. The reformer operating temperature and pressure are 1145K and 5 bar respectively, while its endothermic heat load is 60.68 kJ/s. The reformer outlet product is cooled to 650K and fed to a HTS reactor operating at 650K and 5 bar. The outlet product of the HTS reactor is in turn cooled to 475K, and then fed to an LTS reactor operating at 475K and 5 bar. The LTS reactor outlet stream is cooled to 313K, and then fed to a flash separation unit operating at 313K and 5 bar, where liquid H_2O is separated, from the non-condensable gases exiting the LTS, and then recycled back to the reformer inlet. The vapor outlet from the flash separation unit is fed to an H_2 separation unit, where high purity H_2 is extracted to generate one of the flowsheet products. The reduced content of H_2 in the CO_2 containing outlet of the H_2 separation unit, combined with the fact that the pressure of this stream remains at 5 bar, increases the partial pressure of H_2O in that stream. Given that the stream's temperature remains at 313K, thus keeping H_2O saturation pressure the same as at the outlet of the flash separator, some of the stream's H_2O content is liquefied and then removed in a second flash separation unit also operating at 313K and 5 bar. The condensed H_2O is mixed with the H_2O outlet from the first flash separator and recycled back to the reformer inlet, while the high purity CO_2 outlet of the second flash separator is the second of the flowsheet products.

The proposed EESMR hydrogen production flowsheet is shown in Figure 4.5, while detailed material stream and energy flow information (including minimum works for CO_2 and H_2 separation) for three alternative EESMR designs (all possessing the same flowsheet structure shown in Figure 4.5) are provided in Tables 4.8, 4.9, 4.10, and 4.11.

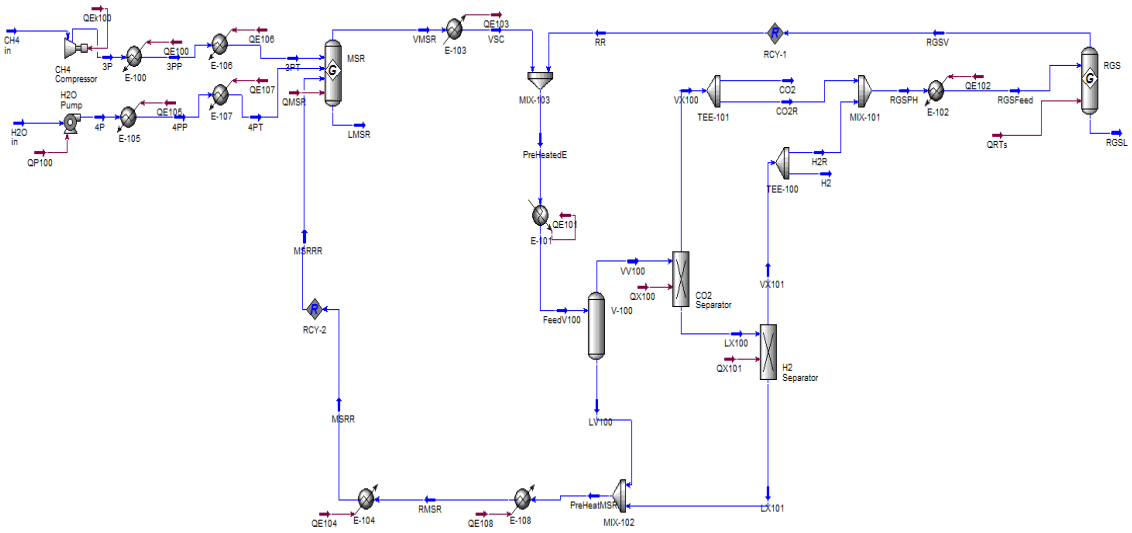

Figure 4.5: Proposed EESMR design process flowsheet

Stream	T(K)	CH_4 (Kmol/hr)	CO (Kmol/hr)	CO_2 (Kmol/hr)	H_2O (Kmol/hr)	H_2 (Kmol/hr)
VMSR	1145	0.026397	8.694545	7.1659	9.75486	10.21798
LMSR	1145	0	0	0	0	0
FeedV100	313	0.026397	14.76851	20.86554	15.68758	27.21948
VV100	313	0.026397	14.76847	20.85723	0.968653	27.21943
LV100	313	3.89E-10	3.51E-05	0.008307	14.71893	5.27E-05
LX100	313	0.026397	14.62079	0.208572	0.968653	27.21943
VX100	313	0	0.147685	20.64866	0	0
VX101	313	0	0	0	0	26.94723
LX101	313	0.026397	14.62079	0.208572	0.968653	0.272194
PreHeatMSR	313	0.026397	14.62082	0.216879	15.68758	0.272247
MSRR	1140	0.026397	14.62082	0.216879	15.68758	0.272247
MSRRR	1140	0.025292	14.64476	0.21679	15.70287	0.272187
CH4 in	298	1	0	0	0	0
H2O in	298	0	0	0	2	0
PreHeatedE	750	0.026397	14.76851	20.86554	15.68758	27.21948
H2	313	0	0	0	0	4
H2R	313	0	0	0	0	22.94723
CO2	313	0	0.007101	0.992899	0	0
CO2R	313	0	0.140583	19.65576	0	0
RGSPH	312	0	0.140583	19.65576	0	22.94723
RGSFeed	750	0	0.140583	19.65576	0	22.94723

RGSV	750	4.27E-47	6.078858	13.71748	5.938274	17.00896
RGSL	750	0	0	0	0	0
RR	750	4.27E-47	6.07396	13.69963	5.932724	17.0015
3P	459	1	0	0	0	0
3PT	1140	1	0	0	0	0
4P	298	0	0	0	2	0
4PT	1140	0	0	0	2	0
VSC	750	0.026397	8.694545	7.1659	9.75486	10.21798
3PP	700	1	0	0	0	0
4PP	700	0	0	0	2	0
RMSR	650	0.026397	14.62082	0.216879	15.68758	0.272247

Table 4.8: EESMR Design 1 Material Stream Information

Stream	T(K)	CH_4 (Kmol/hr)	CO (Kmol/hr)	CO_2 (Kmol/hr)	H_2O (Kmol/hr)	H_2 (Kmol/hr)
VMSR	1145	0.026665	7.363286	5.509576	7.424969	8.567012
LMSR	1145	0	0	0	0	0
FeedV100	313	0.026665	11.91044	15.40073	11.85905	21.7477
VV100	313	0.026665	11.91041	15.39481	0.755631	21.74766
LV100	313	3.8E-10	2.74E-05	0.005925	11.10341	4.07E-05
LX100	313	0.026665	11.79131	0.153948	0.755631	21.74766
VX100	313	0	0.119104	15.24086	0	0
VX101	313	0	0	0	0	21.53018
LX101	313	0.026665	11.79131	0.153948	0.755631	0.217477
PreHeatMSR	313	0.026665	11.79133	0.159873	11.85905	0.217517
MSRR	1140	0.026665	11.79133	0.159873	11.85905	0.217517
MSRRR	1140	0.026575	11.71386	0.159089	11.77537	0.216793
CH4 in	298	1	0	0	0	0
H2O in	298	0	0	0	2	0
PreHeatedE	750	0.026665	11.91044	15.40073	11.85905	21.7477
H2	313	0	0	0	0	4
H2R	313	0	0	0	0	17.53018
CO2	313	0	0.007754	0.992246	0	0
CO2R	313	0	0.11135	14.24861	0	0
RGSPH	312	0	0.11135	14.24861	0	17.53018
RGSFeed	750	0	0.11135	14.24861	0	17.53018
RGSV	750	3.19E-47	4.523872	9.83609	4.412522	13.11766
RGSL	750	0	0	0	0	0
RR	750	3.21E-47	4.547153	9.891155	4.434076	13.18069
3P	459	1	0	0	0	0
3PT	1140	1	0	0	0	0
4P	298	0	0	0	2	0

4PT	1140	0	0	0	2	0
VSC	750	0.026665	7.363286	5.509576	7.424969	8.567012
3PP	700	1	0	0	0	0
4PP	700	0	0	0	2	0
RMSR	650	0.026665	11.79133	0.159873	11.85905	0.217517

Table 4.9: EESMR Design 2 Material Stream Information

Stream	T(K)	CH_4 (Kmol/hr)	CO (Kmol/hr)	CO_2 (Kmol/hr)	H_2O (Kmol/hr)	H_2 (Kmol/hr)
VMSR	1145	0.016208	2.20857	1.41686	3.32024	4.46810
LMSR	1145	0	0	0	0	0
FeedV100	313	0.016198	2.63177	1.90997	3.72956	6.75248
VV100	313	0.016212	2.63357	1.91027	0.172844	6.75710
LV100	313	0	0	0.001021	3.55795	0
LX100	313	0.016210	2.60628	0.019100	0.172778	6.75463
VX100	313	0	0.026328	1.89067	0	0
VX101	313	0	0	0	0	6.687
LX101	313	0.016208	2.60636	0.019096	0.172787	0.067548
PreHeatMSR	313	0.016206	2.60631	0.020122	3.73079	0.067566
MSRR	1140	0.016206	2.60631	0.020122	3.73079	0.067566
MSRRR	1140	0.017043	2.60306	0.020159	3.71597	0.067773
CH4 in	298	1	0	0	0	0
H2O in	298	0	0	0	2	0
PreHeatedE	750	0.016198	2.63177	1.90997	3.72956	6.75248
H2	313	0	0	0	0	4
H2R	313	0	0	0	0	2.687
CO2	313	0	0.013734	0.986266	0	0
CO2R	313	0	0.012590	0.904110	0	0
RGSPH	312	0	0.012592	0.904247	0	2.68716
RGSFeed	750	0	0.012592	0.904247	0	2.68716
RGSV	750	0	0.423203	0.493636	0.410611	2.27655
RGSL	750	0	0	0	0	0
RR	750	0	0.424827	0.494250	0.411658	2.28826
3P	459	1	0	0	0	0
3PT	1140	1	0	0	0	0
4P	298	0	0	0	2	0
4PT	1140	0	0	0	2	0
VSC	750	0.016208	2.20857	1.41686	3.32024	4.46810
3PP	700	1	0	0	0	0
4PP	700	0	0	0	2	0

RMSR	650	0.016206	2.60632	0.020122	3.73079	0.067566

Table 4.10: EESMR Design 3 Material Stream Information

Stream	Design 1 Energy Flow (kJ/s)	Design 2 Energy Flow (kJ/s)	Design 3 Energy Flow (kJ/s)
QMSR	**-0.8529**	**13.93**	**50.42**
QE101	510.8	390.7	103.3
QE104	153.4	119.3	32.52
QE102	189.0	140.2	14.47
QRTs	**62.46**	**46.41**	**4.319**
QE103	150.8	120.5	46.02
QEk100	1.770	1.770	1.770
QE100	3.422	3.422	3.422
QP100	5.298E-03	5.298E-03	5.298E-03
QE105	32.51	32.51	32.51
QX101	-4.957	-3.961	-1.227
QX100	-4.382	-3.244	-0.4167
QE106	8.367	8.367	8.367
QE107	9.903	9.903	9.903
QE108	281.7	214.9	64.63
QX100 W_{min}	25.477	20.535	3.529
QX101 W_{min}	17.565	14.375	3.661

Table 4.11: Energy Flow Information for all EESMR designs

This proposed EESMR flowsheet consists of the following reactor building blocks: Steam Methane Reforming (SMR), and Reverse Gas Shift Reaction (RGSR). Each one of these reactors operates near equilibrium, and thus it is modeled as a Gibbs free energy minimization reactor in UNISIM. The overall flowsheet inlets are 1 kmol/hr CH_4 and 2 kmol/hr H_2O, and the overall flowsheet outlets are 4 kmol/hr H_2 and 1 kmol/hr CO_2. Following H_2O pumping and CH_4 compression to 5 bar, both streams are heated to 1140K, are mixed with a CO/H_2O recycle stream also heated to 1140K, and are then fed to the reformer, creating a reformer feed with 18/15/1 $H_2O/CO/CH_4$ molar ratio for design 1, 14/12/1 $H_2O/CO/CH_4$ molar ratio for design 2, and 5/3/1 $H_2O/CO/CH_4$ molar ratio for design 3. The reformer operating temperature and pressure are 1145K and 5 bar respectively, as in the baseline design, while the reformer's heat load is now exothermic at -0.8529 kJ/s for design 1, endothermic at 13.93 kJ/s for design 2, and

endothermic at 50.42 kJ/s for design 3. The reformer product stream is cooled to 750K and mixed with the recycle stream from the RGSR. The resulting mixed stream is cooled to 313K, and then fed to an adiabatic flash separator operating at 5 bar and 313K. This separator's liquid product is H_2O, which contributes to the formation of a stream that is eventually recycled to the reformer, while its vapor product is fed to a CO_2 capture unit, where high purity CO_2 is extracted. The high purity CO_2 outlet of the CO_2 capture unit is then split into the high purity CO_2 product of the overall flowsheet, and a CO_2 stream fed to the RGSR. The CO_2 lean outlet of the CO_2 capture unit is fed into a H_2 separation process, where high purity H_2 is extracted. The high purity H_2 outlet of the H_2 separator is then split into the high purity H_2 product of the overall flowsheet, and a H_2 stream also fed to the RGSR. The H_2 lean outlet of the H_2 separator is then mixed with the aforementioned flash separator's liquid H_2O outlet, and recycled to the reformer to contribute to the high H_2O, CO content of the reformer feed. The CO_2 and H_2 streams split from the corresponding high purity outlets of the CO_2 capture and H_2 separation units respectively, are mixed and then heated to 750K, so they can be fed to the reverse gas shift reactor (RGSR) operating at 5 bar and 750K. The RGSR has an endothermic heat load of 62.46 kJ/s for design 1, an endothermic heat load of 46.41 kJ/s for design 2, and an endothermic heat load of 4.319 kJ/s for design 3, and its outlet stream is recycled to the inlet of the aforementioned adiabatic flash H_2O separator.

The economic feasibility of the overall EESMR processes on an operating cost basis is related to its energetic expenditures, which are: hot/cold utility requirements (assessed through the presented pinch analysis), the works of compressing natural gas and water feed to the overall process (which are identical in all considered flowsheets and thus not elaborated on), and the works of separation for the CO_2 and H_2 processes (considered to be met through renewable

electricity) and do not affect the impact of carbon taxes that is the focus of this work.

Section 4.4: Heat Integration

The energetic assessment of the above presented baseline SMR and proposed EESMR flowsheets (designs 1, 2, and 3) requires that heat integration of all energy resources and demands be carried out. To this end, the traditional heat integration method of pinch analysis is employed[22]. In particular, since the use of multiple hot and cold utilities is considered, the pinch analysis based minimum utility cost problem for the above-mentioned flowsheets is solved[22,23].

In this study we consider that the high-temperature utility cost is directly correlated to the use of methane as fuel. If no high-temperature utility is consumed, then no CO_2 is emitted by natural gas burning. Of course all designs (both SMR and proposed EESMR ones) emit the same amount of carbon (in the form of CO_2) contained in the methane used as raw material. The CO_2 sequestration characteristics of the various processes are thus differentiated from the SMR to the EESMR designs by the extent of each design's high-temperature utility use. High (low) high-temperature utility use implies high (low) CO_2 emissions related to CH_4 burning. The CO_2 emissions related to CH_4 use as raw material are identical for all SMR and EESMR designs.

Given that the potential carbon taxation legislative environment is at best uncertain, a novel method is proposed below to solve the aforementioned minimum utility cost problem parametrically, namely considering that the cost coefficients of the considered utilities are unknown parameters, and the minimum utility cost solution is identified as a function of these cost coefficients. The general mathematical formulation of this parametric minimum utility cost problem is presented in equation (1).

$$
\left\{
\begin{array}{l}
\min\limits_{\{Q_{HUi}\}_{i=1}^{N_{HU}},\{Q_{CUi}\}_{i=1}^{N_{CU}},\{\delta_i\}_{i=0}^{N_I}} \sum\limits_{i=1}^{N_{HUC}} C_{HUCi}Q_{HUCi} + \sum\limits_{i=1}^{N_{CUC}} C_{CUCi}Q_{CUCi} \\
s.t. \\
Int.j: \delta_{j-1} + \sum\limits_{i=1}^{N_{HPV}} \lambda_{HPVi,j}\left(mC_p\right)_{HPVi}\left(T_{H,j-1}-T_{H,j}\right) + \sum\limits_{i=1}^{N_{HPC}} \lambda_{HPCi,j}Q_{HPCi} + \sum\limits_{i=1}^{N_{HUC}} \lambda_{HUCi,j}Q_{HUCi} = \\
\qquad \delta_j + \sum\limits_{i=1}^{N_{CPV}} \lambda_{CPVi,j}\left(mC_p\right)_{CPVi}\left(T_{C,j-1}-T_{C,j}\right) + \sum\limits_{i=1}^{N_{CPC}} \lambda_{CPCi,j}Q_{CPCi} + \sum\limits_{i=1}^{N_{CUC}} \lambda_{CUCi,j}Q_{CUCi} \quad \forall j = 1, N_I \\
\qquad Q_{HUCi} \geq 0 \;\; \forall i = 1, N_{HUC}, \;\; Q_{CUCi} \geq 0 \;\; \forall i = 1, N_{CUC}, \;\; \delta_j \geq 0 \;\; \forall j = 1, N_I, \;\; \delta_0 = 0, \;\; \delta_{N_I} = 0
\end{array}
\right\} \quad (1)
$$

Where $\{\delta_i\}_{i=0}^{10}$ are the cascading heat loads in the temperature interval diagram;

$\left\{\lambda_{HPVi,j}\right\}_{i=1,\,j=1}^{N_{HPV},N_I}$, $\left\{\lambda_{HPCi,j}\right\}_{i=1,\,j=1}^{N_{HPC},N_I}$, $\left\{\lambda_{HUCi,j}\right\}_{i=1,\,j=1}^{N_{HUC},N_I}$, $\left\{\lambda_{CPVi,j}\right\}_{i=1,\,j=1}^{N_{CPV},N_I}$, $\left\{\lambda_{CPCi,j}\right\}_{i=1,\,j=1}^{N_{CPC},N_I}$, $\left\{\lambda_{CUCi,j}\right\}_{i=1,\,j=1}^{N_{CUC},N_I}$

and $\left\{\left(mC_p\right)_{HPVi}\left(T_{H,j-1}-T_{H,j}\right)\right\}_{i=1,\,j=1}^{N_{HPV},N_I}$, $\left\{Q_{HPCi,j}\right\}_{i=1,\,j=1}^{N_{HPC},N_I}$, $\left\{Q_{HUCi,j}\right\}_{i=1,\,j=1}^{N_{HUC},N_I}$, $\left\{\left(mC_p\right)_{CPVi}\left(T_{C,j-1}-T_{C,j}\right)\right\}_{i=1,\,j=1}^{N_{CPV},N_I}$, $\left\{Q_{CPCi,j}\right\}_{i=1,\,j=1}^{N_{CPC},N_I}$, $\left\{Q_{CUCi,j}\right\}_{i=1,\,j=1}^{N_{CUC},N_I}$ are flag and heat loads in the jth interval of the ith stream with hot process varying (HPV), hot process constant (HPC), hot utility constant (HUC), cold process varying (CPV), cold process constant (CPC), and cold utility constant (CUC) temperature, respectively; and $\{C_{HUCi}\}_{i=1}^{N_{HUC}}$, $\{C_{CUCi}\}_{i=1}^{N_{CUC}}$ are the cost coefficients of the hot and cold utilities, respectively.

The collection of equality constraints labeled $Int.j$ are energy balances on all hot and cold streams available in the jth temperature interval. Temperature intervals are generated based on the temperatures of all process streams and utilities, with all cold stream temperatures increased by a specified $\Delta T_{\min}$. The inequalities are simply positivity constraints on all heat loads, and $\delta_0 = 0, \;\; \delta_{N_I} = 0$ state the considered flowsheet cannot accept heat from or expel heat to the environment.

The Temperature Interval Diagrams for the SMR baseline and EESMR designs 1, 2, 3 are shown in Figures 4.6 and 4.7, respectively. Tables 4.12, 4.13, and 4.14 contain stream

temperature heat load information for the SMR baseline, EESMR design 1, and EESMR designs 2/3, respectively, where all cold stream temperatures are uplifted by the considered minimum temperature difference $\Delta T_{\min} = 5K$.

Stream #	mC_p (kW/ K)	Energy Load (kW)	T_{in} (K)	T_{out} (K)	Intervals
1 (HPV)	0.05997	-	1145	650	3 4 5
2 (HPV)	0.0574	-	650	475	6
3 (HPV)	0.1135	-	475	313	7 8 9
4 (HPC)	-	2.0200	475	475	7
5 (HPC)	-	5.8689	650	650	6
6 (HPC)	-	0.7498	313	313	10
7 (HPC)	-	0.2663	313	313	10
8 (HUC)	-	Q_{HU1}	1200	1200	1
9 (HUC)	-	Q_{HU2}	770	770	4
10 (HUC)	-	Q_{HU3}	420	420	9
11 (CPV)	0.1202	-	303	700	5 6 7 8 9 10
12 (CPV)	0.0140	-	434	700	5 6 7
13 (CPV)	0.0555	-	700	1140	3 4
14 (CPC)	-	60.676	1145	1145	2
15 (CUC)	-	Q_{CU1}	298	298	11

Table 4.12: Stream temperature/energy load information for SMR baseline

	Design 1				
Stream #	mC_p (kW/ K)	Energy Load (kW)	T_{in} (K)	T_{out} (K)	Intervals
1 (HPV)	0.3819	-	1145	750	2 3 4
2 (HPV)	1.1688	-	750	313	5 6 7 8 9 10 11
3 (HPC)	-	22.5222	313	313	12
4 (HPC)	-	29.8593	313	313	12
5 (HPC)	-	0.8529	1145	1145	2
6 (HUC)	-	Q_{HUC_1}	1200	1200	1
7 (HUC)	-	Q_{HUC_2}	770	770	3

8 (HUC)	-	Q_{HUC_3}	420	420	9
9 (CPV)	0.0142	-	464	705	6 7
10 (CPV)	0.0190	-	705	1145	2 3 4 5
11 (CPV)	0.0809	-	303	705	6 7 8 9 10 11 12
12 (CPV)	0.0225	-	705	1145	2 3 4 5
13 (CPV)	0.8358	-	318	655	7 8 9
14 (CPV)	0.3131	-	655	1145	2 3 4 5 6
15 (CPV)	0.4313	-	317	755	4 5 6 7 8 9 10
16 (CPC)	-	62.4583	755	755	3
17 (CUC)	-	Q_{CUC_1}	303	303	12

Table 4.13: Stream temperature/energy load information for EESMR design 1

	Design 2		Design 3				
Stream #	mC_p (kW/ K)	Energy Load (kW)	mC_p (kW/ K)	Energy Load (kW)	T_{in} (K)	T_{out} (K)	Intervals
1 (HPV)	0.3051	-	0.1165	-	1145	750	3 4 5
2 (HPV)	0.8941	-	0.2364	-	750	313	6 7 8 9 10 11 12
3 (HPC)	-	18.3360	-	4.8879	313	313	13
4 (HPC)	-	23.7789	-	3.9458	313	313	13
5 (HUC)	-	Q_{HUC_1}	-	Q_{HUC_1}	1200	1200	1
6 (HUC)	-	Q_{HUC_2}	-	Q_{HUC_2}	770	770	4
7 (HUC)	-	Q_{HUC_3}	-	Q_{HUC_3}	420	420	10
8 (CPV)	0.0142	-	0.0142	-	464	705	7 8
9 (CPV)	0.0190	-	0.0190	-	705	1145	3 4 5 6
10 (CPV)	0.0809	-	0.0809	-	303	705	7 8 9 10 11 12 13
11 (CPV)	0.0225	-	0.0225	-	705	1145	3 4 5 6
12 (CPV)	0.6377	-	0.1918	-	318	655	8 9 10
13 (CPV)	0.2435	-	0.06637	-	655	1145	3 4 5 6 7
14 (CPV)	0.3200	-	0.03304	-	317	755	5 6 7 8 9 10 11
15 (CPC)	-	13.9309	-	50.42	1150	1150	2
16 (CPC)	-	46.4112	-	4.319	755	755	4
17 (CUC)	-	Q_{CUC_1}	-	Q_{CUC_1}	303	303	13

Table 4.14: Stream temperature/energy load information for EESMR designs 2/3

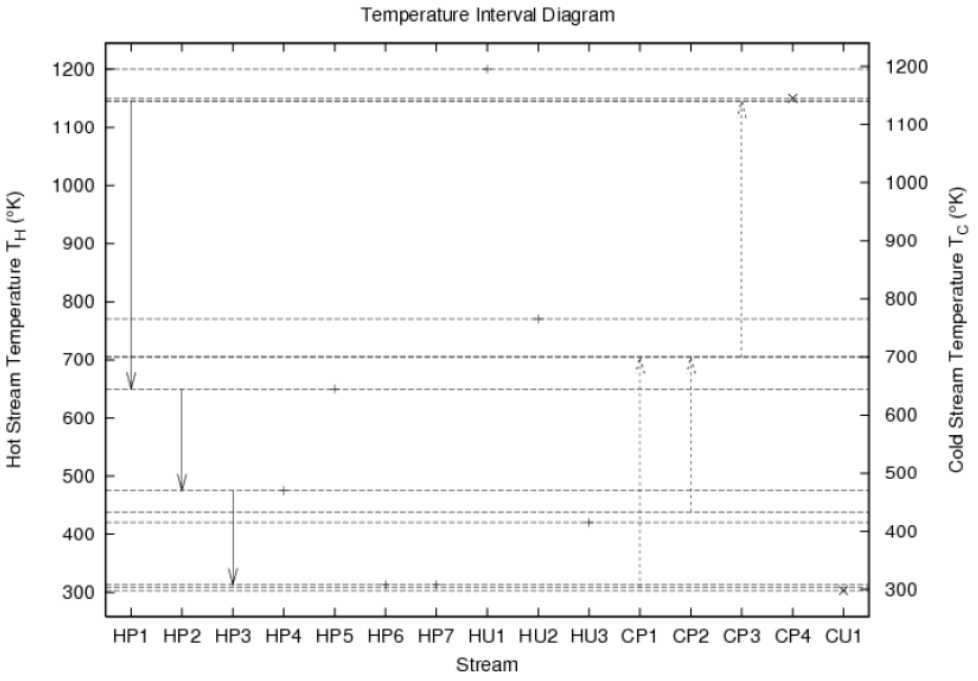

Figure 4.6: Temperature Interval Diagram for Baseline Design

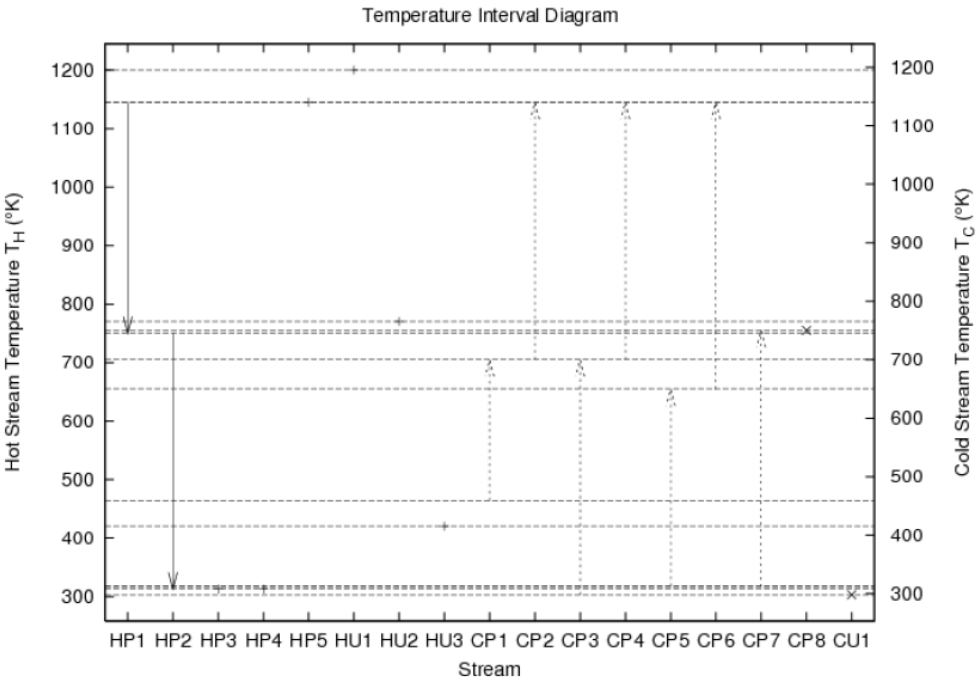

Figure 4.7: Temperature Interval Diagram for Designs 1, 2, and 3

The resulting parameter-dependent minimum utility cost formulations employ the restrictions $C_{HUC_1} \geq C_{HUC_2} \geq C_{HUC_3} \geq C_{CUC_1} \geq 0$. These inequalities reflect the progressively lower cost coefficients associated with energy loads exchanged at progressively lower temperatures (high temperature utilities cost more than lower temperature utilities).

The SMR baseline minimum utility cost formulation is given in equation (2).

$$\left\{\begin{array}{l} \nu_B \triangleq \min\limits_{Q_{HUC_1}, Q_{HUC_2}, Q_{HUC_3}, Q_{CUC_1}, \{\delta_i\}_{i=0}^{10}} C_{HUC_1} Q_{HUC_1} + C_{HUC_2} Q_{HUC_2} + C_{HUC_3} Q_{HUC_3} + C_{CUC_1} Q_{CUC_1} \\ s.t. \\ Int.1: Q_{HUC_1} = \delta_1 \\ Int.2: \delta_1 = \delta_2 + Q_{CPC_{14}} \\ Int.3: \delta_2 + \left(mC_p\right)_{HPV_1} \left(T_{H2} - T_{H3}\right) = \delta_3 + \left(mC_p\right)_{CPV_{13}} \left(T_{C2} - T_{C3}\right) \\ Int.4: \delta_3 + Q_{HUC_2} + \left(mC_p\right)_{HPV_1} \left(T_{H3} - T_{H4}\right) = \delta_4 + \left(mC_p\right)_{CPV_{13}} \left(T_{C3} - T_{C4}\right) \\ Int.5: \delta_4 + \left(mC_p\right)_{HPV_1} \left(T_{H4} - T_{H5}\right) = \delta_5 + \left(\left(mC_p\right)_{CPV_{11}} + \left(mC_p\right)_{CPV_{12}}\right)\left(T_{C4} - T_{C5}\right) \\ Int.6: \delta_5 + Q_{HPC_5} + \left(mC_p\right)_{HPV_2} \left(T_{H5} - T_{H6}\right) = \delta_6 + \left(\left(mC_p\right)_{CPV_{11}} + \left(mC_p\right)_{CPV_{12}}\right)\left(T_{C5} - T_{C6}\right) \\ Int.7: \delta_6 + Q_{HPC_4} + \left(mC_p\right)_{HPV_3} \left(T_{H6} - T_{H7}\right) = \delta_7 + \left(\left(mC_p\right)_{CPV_{11}} + \left(mC_p\right)_{CPV_{12}}\right)\left(T_{C6} - T_{C7}\right) \\ Int.8: \delta_7 + \left(mC_p\right)_{HPV_3} \left(T_{H7} - T_{H8}\right) = \delta_8 + \left(mC_p\right)_{CPV_{11}} \left(T_{C7} - T_{C8}\right) \\ Int.9: \delta_8 + Q_{HUC_3} + \left(mC_p\right)_{HPV_3} \left(T_{H8} - T_{H9}\right) = \delta_9 + \left(mC_p\right)_{CPV_{11}} \left(T_{C8} - T_{C9}\right) \\ Int.10: \delta_9 + Q_{HPC_6} + Q_{HPC_7} = \delta_{10} + \left(mC_p\right)_{CPV_{11}} \left(T_{C9} - T_{C10}\right) \\ Int.11: \delta_{10} = Q_{CUC_1} \\ Q_{HUC_1} \geq 0,\ Q_{HUC_2} \geq 0,\ Q_{HUC_3} \geq 0,\ Q_{CUC_1} \geq 0, \\ \delta_1 \geq 0,\ \delta_2 \geq 0,\ \delta_3 \geq 0,\ \delta_4 \geq 0,\ \delta_5 \geq 0,\ \delta_6 \geq 0 \\ \delta_7 \geq 0,\ \delta_8 \geq 0,\ \delta_9 \geq 0,\ \delta_{10} \geq 0 \end{array}\right. \quad (2)$$

Substitution of temperature/energy loads from Table 4.12, elimination of the cascading heat loads $\{\delta_i\}_{i=0}^{10}$, elimination of redundant constraints, and elimination of the cold utility heat load Q_{CUC_1}, leads to the simplified formulation shown in equation (3):

$$\nu_B\left(C_{HUC_1}, C_{HUC_2}, C_{HUC_3}, C_{CUC_1}\right) = -69.5172 C_{CUC_1} + \mu_B \quad (3)$$

where μ_B denotes the solution to the optimization problem (4).

$$\left\{\begin{array}{l} \mu_B \triangleq \min\limits_{Q_{HUC_1}, Q_{HUC_2}, Q_{HUC_3}, Q_{CUC_1}} \left(C_{HUC_1} + C_{CUC_1}\right) Q_{HUC_1} + \left(C_{HUC_2} + C_{CUC_1}\right) Q_{HUC_2} + \left(C_{HUC_3} + C_{CUC_1}\right) Q_{HUC_3} \\ \quad s.t. \\ \quad Q_{HUC_1} \geq 60.676 \\ \quad Q_{HUC_1} + Q_{HUC_2} \geq 70.3629 \\ \quad Q_{HUC_1} + Q_{HUC_2} + Q_{HUC_3} \geq 69.9323 \\ \quad Q_{HUC_1} \geq 0,\ Q_{HUC_2} \geq 0,\ Q_{HUC_3} \geq 0 \end{array}\right\} \quad (4)$$

Since $\left(C_{HUC_1} + C_{CUC_1}\right) \geq 0$, $\left(C_{HUC_2} + C_{CUC_1}\right) \geq 0$, $\left(C_{HUC_3} + C_{CUC_1}\right) \geq 0$, and $Q_{HUC_1} + Q_{HUC_2} \geq 70.3629$, then $Q_{HUC_3}{}^* = \max\left(0, 69.9323 - Q_{HUC_1} - Q_{HUC_2}\right) = 0$.

Then, since $C_{HUC_1} \geq C_{HUC_2}$, it then holds $Q_{HUC_1}{}^* = 60.676,\ Q_{HUC_2}{}^* = 9.6869$, which in turn implies $Q_{CUC_1}{}^* = 0.8457$. Thus,

$\nu_B\left(C_{HUC_1}, C_{HUC_2}, C_{HUC_3}, C_{CUC_1}\right) = \left\{60.676 C_{HUC_1} + 9.6869 C_{HUC_2} + 0.8457 C_{CUC_1}\right\}$, where

$\left\{Q^*_{HUC_1} = 60.676,\ Q^*_{HUC_2} = 9.6869,\ Q^*_{HUC_3} = 0,\ Q^*_{CUC_1} = 0.8457\right\}$

Similar arguments lead to expressions (5), (6), and (7) for the minimum utility costs for EESMR designs 1, 2, 3, respectively.

EESMR design 1

$$\nu_{D_1}\left(C_{HUC_1}, C_{HUC_2}, C_{HUC_3}, C_{CUC_1}\right) = 64.1071 C_{HUC_2} + 18.2784 C_{HUC_3} + 56.5807 C_{CUC_1} \quad (5)$$

where $\left\{Q^*_{HUC_1} = 0,\ Q^*_{HUC_2} = 64.1071,\ Q^*_{HUC_3} = 18.2784,\ Q^*_{CUC_1} = 56.5807\right\}$.

EESMR design 2

$$\nu_{D_2}\left(C_{HUC_1}, C_{HUC_2}, C_{HUC_3}, C_{CUC_1}\right) = 13.9309C_{HUC_1} + 51.9569C_{HUC_2} + 14.739C_{HUC_3} + 45.0519C_{CUC_1} \quad (6)$$

where $\left\{Q^*_{HUC_1} = 13.9309,\ Q^*_{HUC_2} = 51.9569,\ Q^*_{HUC_3} = 14.739,\ Q^*_{CUC_1} = 45.0519\right\}$

EESMR design 3

$$\nu_{D_3}\left(C_{HUC_1}, C_{HUC_2}, C_{HUC_3}, C_{CUC_1}\right) = 50.42C_{HUC_1} + 13.6909C_{HUC_2} + 7.0727C_{HUC_3} + 8.7692C_{CUC_1} \quad (7)$$

where $\left\{Q^*_{HUC_1} = 50.42,\ Q^*_{HUC_2} = 13.6909,\ Q^*_{HUC_3} = 7.0727,\ Q^*_{CUC_1} = 8.7692\right\}$

Considering $\left\{C_{HUC_1} \geq C_{HUC_2} \geq C_{HUC_3} \geq C_{CUC_1} \geq 0\right\}$, and normalizing with respect to C_{HUC_1}, yields $\left\{1 \geq \frac{C_{HUC_2}}{C_{HUC_1}} \geq \frac{C_{HUC_3}}{C_{HUC_1}} \geq \frac{C_{CUC_1}}{C_{HUC_1}} \geq 0\right\}$. Then, the regions in the 3-dimensional cost coefficient ratio space $\left\{\frac{C_{HUC_2}}{C_{HUC_1}}, \frac{C_{HUC_3}}{C_{HUC_1}}, \frac{C_{CUC_1}}{C_{HUC_1}}\right\}$ where each of the four aforementioned designs has lower utility cost than all the others are:

Region D_1, where Design 1 has the lowest cost is defined in equation (8); its vertices are shown in Table 4.15 and is shown in Figure 4.8. Similar computations lead to the computation of the vertices for regions D_2 (which turns out to be empty), D_3 , and B , where design 2, design 3, and baseline design have the lowest minimum utility cost, respectively. The vertices of all these regions are also shown in Table 4.15, and the regions D_3, B are also illustrated in Figure 4.8.

$$D_1 \triangleq \left\{ \begin{array}{l} \left[\frac{C_{HUC_2}}{C_{HUC_1}}, \frac{C_{HUC_3}}{C_{HUC_1}}, \frac{C_{CUC_1}}{C_{HUC_1}} \right] \in \mathbb{R}^3 : 0 \overset{1}{\leq} \frac{C_{CUC_1}}{C_{HUC_1}} \overset{2}{\leq} \frac{C_{HUC_3}}{C_{HUC_1}} \overset{3}{\leq} \frac{C_{HUC_2}}{C_{HUC_1}} \overset{4}{\leq} 1 \\ -60.676 + \left(64.1071 - 9.6869\right) \frac{C_{HUC_2}}{C_{HUC_1}} + 18.2784 \frac{C_{HUC_3}}{C_{HUC_1}} + \left(56.5807 - 0.8457\right) \frac{C_{CUC_1}}{C_{HUC_1}} \overset{5}{\leq} 0 \\ -13.9309 + \left(64.1071 - 51.9569\right) \frac{C_{HUC_2}}{C_{HUC_1}} + \left(18.2784 - 14.739\right) \frac{C_{HUC_3}}{C_{HUC_1}} + \left(56.5807 - 45.0519\right) \frac{C_{CUC_1}}{C_{HUC_1}} \overset{6}{\leq} 0 \\ -50.42 + \left(64.1071 - 13.6909\right) \frac{C_{HUC_2}}{C_{HUC_1}} + \left(18.2784 - 7.0727\right) \frac{C_{HUC_3}}{C_{HUC_1}} + \left(56.5807 - 8.7692\right) \frac{C_{CUC_1}}{C_{HUC_1}} \overset{7}{\leq} 0 \end{array} \right\} \quad (7)$$

	Region B			Region D_1			Region D_3		
	$\frac{C_{HUC_2}}{C_{HUC_1}}$	$\frac{C_{HUC_3}}{C_{HUC_1}}$	$\frac{C_{CUC_1}}{C_{HUC_1}}$	$\frac{C_{HUC_2}}{C_{HUC_1}}$	$\frac{C_{HUC_3}}{C_{HUC_1}}$	$\frac{C_{CUC_1}}{C_{HUC_1}}$	$\frac{C_{HUC_2}}{C_{HUC_1}}$	$\frac{C_{HUC_3}}{C_{HUC_1}}$	$\frac{C_{CUC_1}}{C_{HUC_1}}$
1	1	1	0	0	0	0	0.9259	0.9259	0
2	0.9259	0.9259	0	1	0	0	0.8182	0.8182	0
3	1	0.8840	0	0.8182	0.8182	0	1	0.8840	0
4	1	1	1	1	0.0003	0	1	0.0003	0
5	0.5398	0.5398	0.5398	0.4607	0.4607	0.4607	0.5398	0.5398	0.5398
6	1	0.4169	0.4169	1	0.0001	0.0001	0.4607	0.4607	0.4607
7							1	0.4169	0.4169
8							1	0.0001	0.0001

Table 4.15: List of vertices for lowest-cost regions B, D_1, D_3

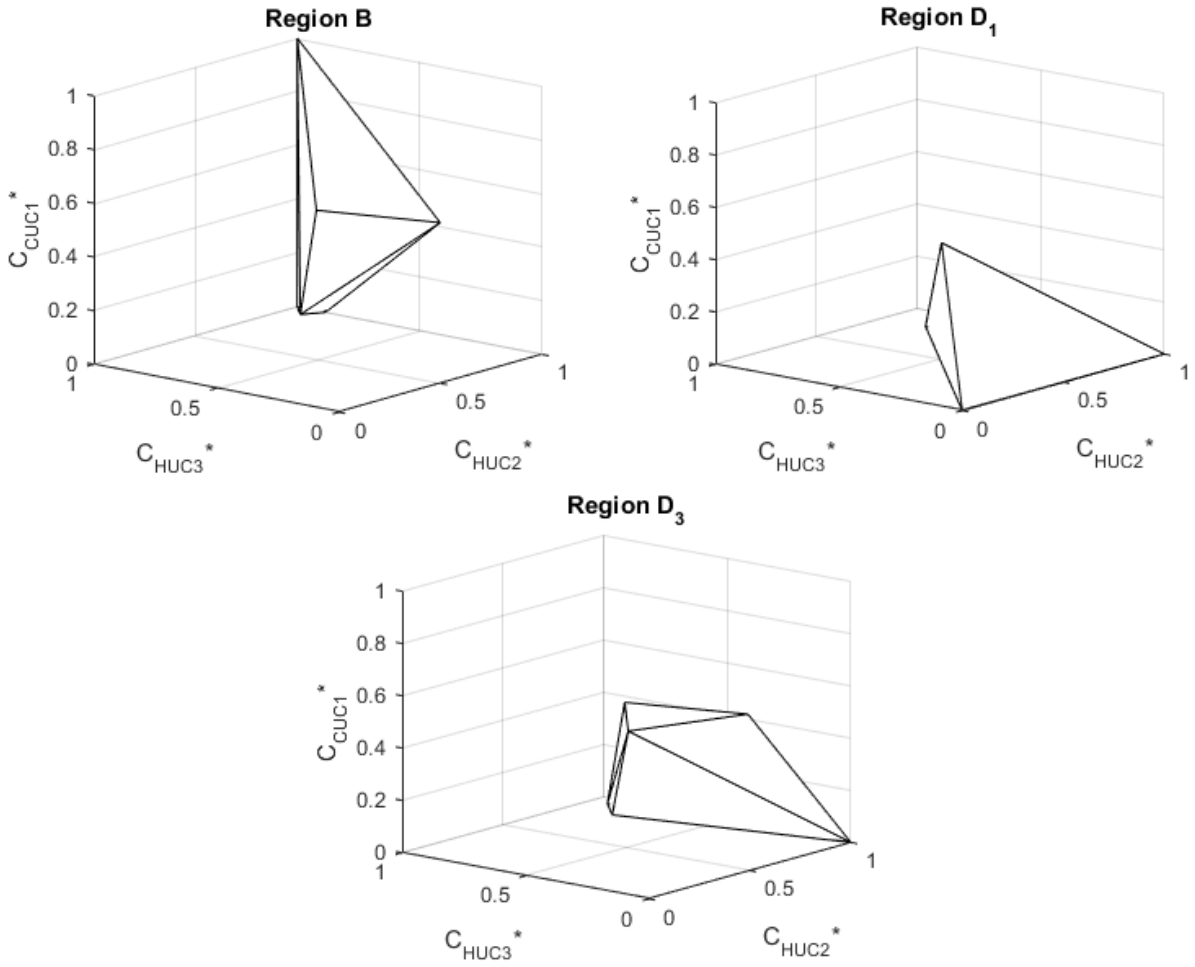

Figure 4.8: Identified lowest-cost regions

Section 4.5: Discussion and conclusions

A novel energetically enhanced steam methane reforming process (EESMR) has been proposed, and several EESMR designs were developed. The process uses carbon monoxide to provide some (or even all) of the endothermic load of reforming natural gas, thus reducing to any desirable degree the high temperature heat load required to be provided to an SMR process. The required CO can be provided through recycling and transformation of carbon dioxide to monoxide through a reverse gas shift process. Converged flowsheets are developed and heat integrated, that demonstrate the feasibility of this EESMR process. By reducing the high temperature heat loads needed by the SMR process, one can reduce the amount of natural gas

burned to meet the reformer's energetic needs. Instead, the carried-out heat integration suggests that the EESMR process heating needs at 1200K can be effectively supplemented by using concentrated solar power provided at 770K and 420K. In addition, the EESMR generates CO_2 at higher purity than the conventional SMR, thus enabling CO_2 sequestration.

In a carbon tax legislative environment, in which burned natural gas is taxed, while natural gas used as raw material is not, the EESMR process can become economically preferable from a utility cost viewpoint. To accurately quantify the utility cost coefficient prices for which either the traditional SMR or one of three EESMR designs are preferable, regions in cost coefficient ratio space are quantified over which each design has lower minimum utility cost than all the others.

The obtained regions suggest the following:

SMR (baseline) is preferable when the medium and low temperature hot utilities cost similarly to the high temperature hot utility.

EESMR design 1 (exothermic reforming) is preferable when the low temperature hot utility, and the cold utility cost significantly less than the high temperature hot utility.

EESMR design 2 (slightly endothermic reforming) is never preferable.

EESMR design 3 (slightly less endothermic reforming than baseline) is preferable when the medium temperature hot utility costs similarly to the high temperature hot utility, and the cold utility costs significantly less than the high temperature hot utility.

The above suggest that EESMR can become a preferable method of hydrogen production in a world where natural gas burning is heavily taxed.

Notation

C: Cost coefficient ($/kJ)

C_p: Heat capacity (kJ/K)

$Int.j$: The jth temperature interval

m : Mass (kg)

Q : Heat load (kJ/s)

T : Temperature (K)

$W_{\min}$: Minimum work of separation (kJ/s)

Greek letters

δ_i : Cascading heat load from the ith temperature interval (kJ/s)

λ : A flag whose value is 1 (0) if a particular heat load is available (not available) in a temperature interval

μ : Optimal value of reduced-dimensionality heat integration problem

ν : Optimal value of heat integration problem

Subscripts

B: Baseline case

C: Cold stream

CPC: cold process stream with constant temperature

CPV: cold process stream with varying temperature

CUC: cold utility stream with constant temperature

D_i : The ith design case

H: Hot stream

HPC: hot process stream with constant temperature

HPV: hot process stream with varying temperature

HUC: hot utility stream with constant temperature

I: Temperature interval

Section 4.6: References

1. Zakkour, P.; Cook, G. CCS Roadmap for Industry: High-purity CO2 sources. Sectoral Assessment-Final Draft Report. Global Technology Roadmap for CCS in Industry 2010,

2. El Azzeh, S.; Sarshar, M.; Fayaz, R. Hydrogen Economy and the Built Environment. World Renewable Energy Congress-Sweden; 8-13 May; 2011; Linköping; Sweden. 2011; pp 1986–1995.

3. Kendall, K. Hydrogen and fuel cells in city transport. International Journal of Energy Research 2016, 40, DOI: 10.1002/er.3290.

4. Stephens, J.; Cartagena, W. Liquid Hydrogen Propellant Tank Sub-Surface Pressurization with Gaseous Helium. 2015

5. Dincer, I.; Acar, C. Review and evaluation of hydrogen production methods for better sustainability. international journal of hydrogen energy 2015, 40, DOI: 10.1016/j.ijhydene.2014.12.035

6. Messerschmitt, A. Verfahren zur Erzeugung von Wasserstoff durch abwechselnde Oxidation und Reduktion von Eisen in von außen beheizten, in den Heizraeumen angeordneten Zersetzern. German Patent DE 1911, 266863.

7. Hacker, V.; Fankhauser, R.; Faleschini, G.; Fuchs, H.; Friedrich, K.; Muhr, M.; Kordesch, K. Hydrogen production by steam–iron process. Journal of Power Sources 2000, 86, DOI: 10.1016/S0378-7753(99)00458-9.

8. Gardner, D. Hydrogen production from renewables. Renewable Energy Focus 2009, 9, DOI: 10.1016/S1755-0084(09)70036-5.

9. Riis, T.; Hagen, E. F.; Vie, P. J.; Ulleberg, Ø. Hydrogen Production and Storage–R&D Priorities and Gaps. IEA Hydrogen Implementing Agreement (HIA) 2006,

10. on Energy, B.; Council, E. S. N. R.; on Engineering, D.; Council, P. S. N. R.; of Engineering, W. N. A. The hydrogen economy: Opportunities, costs, barriers, and R&D needs; National Academies Press, 2004.

11. Metz, B.; Davidson, O.; De Coninck, H.; Loos, M.; & Meyer, L. IPCC special report on carbon dioxide capture and storage. Intergovernmental Panel on Climate Change, Geneva (Switzerland). Working Group III, 2005.

12. Christiansen,L.J. Use of modeling in scale-up of steam reforming technology. Catalysis Today 2016, 272, DOI: 10.1016/j.cattod.2016.03.007.

13. Xu, J.; Froment, G. F. Methane steam reforming, methanation and water-gas shift: I. Intrinsic kinetics. AIChE Journal 1989, 35, DOI: 10.1002/aic.690350109.

14. Lopez, J. A. P.; Manousiouthakis, V. I. Natural gas based hydrogen production with zero carbon dioxide emissions. international journal of hydrogen energy 2011, 36, DOI: 10.1016/j.ijhydene.2011.07.061.

15. Poullikkas, A. Economic analysis of power generation from parabolic trough solar thermal plants for the Mediterranean region: A case study for the island of Cyprus. Renewable and sustainable Energy reviews 2009, 13, DOI: 10.1016/j.rser.2009.03.014 .

16. https://www.iea.org/publications/freepublications/publication/CO2EmissionsFromFuelCombustionHighlights2015.pdf

17. https://ec.europa.eu/clima/sites/clima/files/docs/factsheet_ets_en.pdf

18. http://www.ecofys.com/files/files/ecofys_2004_analysisnationalallocationplansets.pdf

19. https://www.gov.uk/government/publications/excise-notice-ccl13-climate-change-levy-reliefs-and-special-treatments-for-taxable-commodities/excise-notice-ccl13-climate-change-levy-reliefs-and-special-treatments-for-taxable-commodities

20. Ghougassian, P., Manousiouthakis, V. I., " Attainable Composition, Energy Consumption and Entropy Generation Properties for Isothermal/Isobaric Reactor Networks", *Industrial & Engineering Chemistry Research*, 52, January 2013, DOI: 10.1021/ie301158m.

21. Minimum Entropy Generation for Isothermal Endothermic/Exothermic Reactor Networks, Paul G. Ghougassian and Vasilios Manousiouthakis, AIChE, 2014, DOI: 10.1002/aic.14598

22. Posada, A., Manousiouthakis, V., “Heat and power integration of methane reforming based hydrogen production”, Industrial & Engineering Chemistry Research, Vol.44, No. 24, November 2005, DOI: 10.1021/ie049041k

23. Holiastos, K., Manousiouthakis, V. I., “Minimum hot/cold/electric utility cost for heat exchange networks”, Computers & Chemical Engineering, Vol. 26, No. 1, Jan. 2002, DOI: 10.1016/S0098-1354(01)00726-8.